Convention on Long-range Transboundary Air Pollution

emep

Co-operative programme for monitoring and evaluation of the long-range transmission of air pollutants in Europe

STATUS REPORT 4/2004

Transboundary particulate matter in Europe

Status report 4/2004

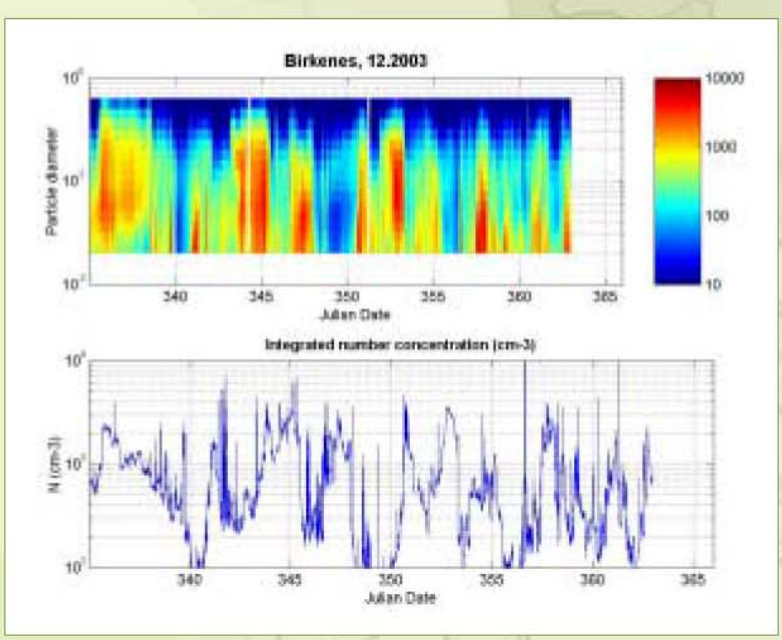

ccc & msc-w & ciam

NILU: EMEP Report 4/2004
REFERENCE: O-98134
DATE: AUGUST 2004

EMEP Co-operative Programme for Monitoring and Evaluation of the Long-Range Transmission of Air Pollutants in Europe

Transboundary particulate matter in Europe Status report 2004

Joint
CCC & MSC-W & CIAM
Report 2004

Norwegian Institute for Air Research
P.O. Box 100, NO-2027 Kjeller, Norway

D N M I
Norwegian Meteorological Institute
P.O. Box 43 Blindern, NO-0313 Oslo, Norway

IIASA – International Institute for Applied Systems Analysis
Schlossplatz 1, AT-2361 Laxenburg, Austria

Edited by Kjetil Tørseth

List of Contributors

Wenche Aas[1]	Leonor Tarrasón[2]	Markus Amann[3]	Les White[4]
Anne-Gunn Hjellbrekke[1]	Svetlana Tsyro[2]	Janusz Cofala[3]	Paul Makar[5]
Mihalis Lazaridis[1]	David Simpson[2]	Chris Heyes[3]	Philippe Thunis[6]
Chris Lunder[1]	Vigdis Vestreng[2]	Zbigniew Klimont[3]	Christoph Wehrli[7]
Jan Schaug[1]	Heiko Klein[2]	Wolfgang Schöpp[3]	
Karl-Espen Yttri[1]	Jan Eiof Jonson[2]		

[1] EMEP Chemical Coordinating Centre
[2] EMEP Meteorological Synthesizing Centre – West
[3] EMEP Centre for Integrated Assessment Modelling
[4] Les White Associates
[5] Environment Canada
[6] Joint Research Centre (JRC-EI)
[7] Physikalisch-Meteorologisches Observatorium Davos

Contents

Page

Executive Summary

The previous EMEP joint report on Particulate matter presented in 2003 (EMEP Report 4/2003) presented a critical discussion of the information on aerosols currently available from EMEP's observational data, its modelling results, and the emission inventories. Several strengths and shortcomings were identified and specific recommendations were given for future improvements. Special emphasis was given to the interlinking of monitoring and modelling results, and to evaluate to what extent the available observations suffice for validating the EMEP model. Further, tasks for improving both the emission compilation, the model development and the observational programme was identified.

The objective of this report is to present an updated assessment of the particulate matter concentrations in 2002 using observations and model results, and by applying improved emission inventories. Also, an initial outlook into projections of particulate matter level in the future is presented. As regards the monitoring and modelling activities are concerned, emphasis has been made on presenting recent developments in our capabilities.

Measurements of PM_{10} within EMEP were taken up at two more sites in 2002 compared to the preceding year. The total number of sites is, however, small and the sites cover a rather small part of Europe, 36 PM_{10} and 19 $PM_{2.5}$ sites. None of the EMEP sites exceeded the PM_{10} annual limit value for the protection of human health, set by EU in the first Daughter Directive. The corresponding 24-hour limit was slightly exceeded at a site in northern Italy in 2002. Several sites measured relative high $PM_{2.5}$ masses compared to the corresponding PM_{10} masses indicating a large fraction of fine particles. No limit value has been set for $PM_{2.5}$ mass in EU. $PM_{2.5}$ standards from the United States EPA exist, however, and a site in Austria could have been in conflict with this standard.

Preliminary results from a unique carbon measurement campaign, which took place between 1st July 2003 and 1st July 2003 at 14 sites in 13 European countries, are presented. Elemental carbon (EC) was estimated to account for 1–5% of the PM_{10} mass on an annual basis. In general the concentration of EC increased from summer to winter. Organic matter (OM), estimated using a factor multiplied with OC (organic carbon), account for 13–45% of the PM_{10} mass. At the Scandinavian and the Slovakian sites the summertime concentrations of OC were found to be a factor 1.4–1.6 higher than those recorded during winter, possible due to biogenic OC and PBAP (Primary Biological Aerosol Particles). For the other sites the concentration of OC increases by a factor 1.2–2.7 from summer to winter. Most likely this can be explained by increased emissions from residential heating (coal, oil and wood) and traffic during winter (cold starts) as for EC.

Particle number distribution measurements is presented from southern Norway (Birkenes), from Crete (Finokalia) and onboard a vessel cruising in the eastern Mediterranean. The particle numbers are considerably lower in winter than in summer at Birkenes, maybe due to higher biogenic activity in spring and summer but it can also be explained by seasonal changes in air masses and lower rate of incoming solar radiation in winter. Diurnal variations were observed and most of

the nucleation events were characterized by a sharp increase of nuclei mode number concentration around noon. In Greece the concentrations of ultrafine particles (< 30nm) were highest during the winter while the concentrations of the 100–300 nm size fraction were higher during the summer. Comparing the winter and summer periods the nucleation events were observed more frequently in winter than in the summer. This is probably due to the lower concentration of PM_1 and PM_{10} observed in the winter period.

There is also a chapter presenting a characterization of particulate matter including Saharan dust in eastern Mediterranean. These studies show that there is a consistent pattern of geographical variability in Europe with lower concentrations of particulate matter in the far north and higher concentrations in southern countries. This is due to natural emissions of unsaturated hydrocarbons (including isoprene) that are highly reactive, and high emissions of anthropogenic gaseous and aerosol pollutants in southern Europe. Furthermore, the Mediterranean region is characterized by North African desert dust besides sea spray.

The aerosol load from surface to the top of the atmosphere as expressed through the aerosol optical depth is discussed. The report presents AOD data from Ny-Ålesund (NO), Jungfraujoch (CH) and Hohenpeißenberg (DE). During March and September when all three sites had valid monthly averages, the Arctic AOD at 500 nm were about three to four times higher than the high altitude averages from Jungfraujoch and about one half to one third of the Hohenpeißenberg.

Following the recommendations from the evaluation of EMEP Unified model by TFMM Workshop in Oslo last year and in preparation of the revision of the National Emission Ceilings Directive, there has been a considerable effort to update and review the emission data used as basis for scenario analysis and impact calculations. In particular, the spatial distribution of the emissions used as input to the Unified EMEP model has been thoroughly revised and a new methodology for allocating emissions by sector has been proposed and tested. The new methodology relies on validated official gridded sector GS data reported from the Parties and on ancillary information on population, large point source (LPS) intensities and locations, traffic patterns, agricultural activities and land-use. An important advantage of the new methodology is that it guarantees the consistency throughout Europe of emissions from different pollutants from the same emission sources. For the first time since CEPMEIP emissions where introduced in EMEP modelling, the distribution of primary PM emissions is now generally consistent with the emissions of PM gaseous precursors.

Initial tests to check the validity of the new emission distribution have produced reassuring results for the gridding of traffic emissions and the distribution of gaseous precursors for PM. The new distribution of emissions has been shown to generally improve the spatial correlation of modelled results with observations of gaseous PM precursors. However the largest uncertainties still remain associated with primary PM emissions. Also information on the chemical speciation of the primary PM emissions provides mixed results when used by the model. For example, with the new emission data, model calculated elemental carbon (EC) is in average 49% lower than measured. The spatial correlation between calculated and measured EC is good (0.88). However, the temporal correlation coefficients

between modelled and measured EC concentrations vary broadly. Further validation of PM emissions is in progress but the initial results indicate that further efforts should be made to improve the quality of PM emission data, especially those related to sources from production processes and agriculture.

The other main short-term recommendation from the TFMM workshop to Review and Evaluate the Unified EMEP Model was to analyse further the possible contributions to the undetermined PM mass, that is, the part of PM mass that is observed but not explained by modelling approaches. In particular, the recommendation was to investigate the how much of the un-determined PM mass could be particle-bound water and how important the contribution from organic aerosols could be. Chapter 3 and Chapter 4 respectively report on the modelling progress under these two subjects.

The EMEP models, as most other state-of-art models, underestimate observed ambient concentrations of particulate matter. This is because the scientific understanding of processes and sources relevant to PM is still under development. In 2002, the aerosol model underestimates $PM_{2.5}$ and PM_{10} concentrations by 42% and 50% respectively. The model underestimation of observed PM concentrations could be partly due to particle-bound water present in measurements with gravimetric methods, but which is not accounted for in the model previous versions. The new model version includes particle-bound water as an output variable that allows estimates of the contribution of particle-bound water to PM mass. It is estimated that the aerosol water content in gravimetrically measured $PM_{2.5}$ and PM_{10} mass is 20% to 35% on average. Accounting for particle water in model calculated PM improves the correspondence between model results and observation: the model underestimation of $PM_{2.5}$ and PM_{10} decreases to 19% and 33% respectively and, interestingly, the temporal correlation increases at the most of stations. This would explain about half of the underestimation of modelled results in comparison with observation, the un-determined PM mass. However, there are caveats to this estimate as no verification of this particle-bound water content is presently available.

The understanding of secondary organic aerosol (SOA) has been undergoing rapid change for several years now. Increasing evidence for polymerisation and other reactions within aerosol would suggest that even more SOA should be formed than given in the standard models. Even though most SOA modules in use today are based upon the same framework, they may still give very different results to one another. Differences can be of more than a factor of ten. Therefore, it is currently impossible therefore to assign much certainty to the results of any SOA model.

Nevertheless, it is instructive and important to apply our best-available theories in order to begin the iterative process of matching model-results and observations, a process which will ultimately lead to better models and which should generate further ideas for the type of measurements which can be used to decide between competing theories. With the increasing number of measurements from for example the NILU EC/OC campaign, the EU CARBOSOL project (http://www.vein.hu/CARBOSOL), or from national projects, there is some hope of evaluating a model against observations in a semi-empirical way. Initial

conclusions on the comparison of model results from observations suggest that: a) a model with no SOA and current emissions strongly underpredicts OC across Europe; b) adding a 'standard' SOA module gives much more OC in summer (even too much at some sites - not shown); c) the SOA-model underestimates OC in wintertime probably both because missing primary anthropogenic organic aerosol (POC) and missing SOA. Work is in progress to compare more closely the EMEP model results with available measurements and propose possible ways to reconciliate the modelled sources and the observations.

Finally, this report presents a first perspective on the likely future development of emissions and air quality in Europe in absence of further legal measures to control emissions. While this assessment brings together for the first time a wide range of updated information on economic development, energy policies, emission inventories, atmospheric dispersion and impacts of air pollution, it has to be considered as provisional since information in all these fields needs further refinement and validation. Of particular urgency is the further improvement and validation of emission estimates for the countries that are not included in the Clean Air For Europe (CAFE) program of the Commission of the European Union. However, despite the large number of outstanding improvements in detail, the overall picture at the European scale as presented in this report is unlikely to change dramatically. Thus, a preliminary conclusion would suggest that the full implementation of the present legislation on emission controls will lead to significant reduction of emissions in the future. However, these improvements are not likely to fully eliminate all negative impacts of air pollution within the time period analysed in this report.

1. Measurements of particulate matter

by Anne-Gunn Hjellbrekke, Mihalis Lazaridis, Chris Lunder, Jan Schaug, Christoph Wehrli, Karl Espen Yttri and Wenche Aas

1.1 Measurements of PM mass (PM_{10}, $PM_{2.5}$ and SPM) in 2002

Measurements of PM_{10} were taken up at two more sites in 2002 compared to the preceding year, at Montelibretti (IT1) and Stará Lesná (SK4). Table 1.1 gives the annual values of particulate matter in air, mostly daily samples, from 2002. The location of sites as well as more statistics and metadata have been given by Hjellbrekke (2004). Plots with annual averages of PM_{10} and $PM_{2.5}$ are given together with the modelling results in Chapter 3 (Figure 3.1). A comparative large amount of fine particles in the PM_{10} mass occurred at several sites.

It should be noted that in addition to the fairly small PM_{10} EMEP network, a much larger network with rural stations, urban background sites as well as measurements in hotspots is run in Europe in the European Union (EIONET; http://www.eionet.eu.int/) and data collected in the AIRBASE data base. The network, together with the 2001 results, was presented in last year's measurement report (Kahnert, 2003).

Table 1.1: Annual averages of particulate matter.

Code	PM_{10}	$PM_{2.5}$	SPM	Code	PM_{10}	$PM_{2.5}$	SPM
AT0002R	29.23	23.27	-	ES0013R	12.28	8.02	17.73
AT0004R	11.99	-	-	ES0014R	15.38	10.64	23.38
AT0005R	11.16	-	-	ES0015R	12.27	6.70	22.93
CH0001G	-	-	3.40	ES0016R	13.85	9.43	20.02
CH0002R	21.12	15.89	-	FI0017R	9.96	-	-
CH0003R	19.64	-	-	IE0031R	13.18	-	-
CH0004R	12.40	8.74	-	IT0001R	33.22	-	-
CH0005R	13.21	-	-	IT0004R	35.45	29.39	-
CZ0003R	20.74	-	-	NL0009R	22.89	-	-
DE0001R	20.17	-	-	NO0001R	7.43	5.75	-
DE0002R	19.49	14.85	-	NO0099R	16.49	6.83	-
DE0003R	9.90	7.64	-	PT0001R	14.27	-	-
DE0004R	16.01	12.30	-	SE0005R	-	-	-
DE0005R	12.30	-	-	SE0008R	-	-	-
DE0007R	16.38	-	-	SE0011R	-	-	-
DE0008R	11.96	-	-	SE0012R	8.88	-	-
DE0009R	18.84	-	-	SE0014R	-	-	-
ES0007R	21.40	10.31	38.65	SK0002R	-	-	-
ES0008R	18.54	10.13	27.94	SK0004R	18.95	-	-
ES0009R	10.80	6.98	17.23	SK0005R	-	-	34.85
ES0010R	18.90	12.90	35.47	SK0006R	-	-	14.76
ES0011R	15.95	12.45	24.91	SK0007R	-	-	23.27
ES0012R	14.64	8.15	21.36				

None of the EMEP sites exceeded the annual limit value for the protection of human health, set by EU in the first Daughter Directive. The corresponding 24-hour limit, was slightly exceeded in northern Italy at the Ispra site IT0004 (37 higher values in 2002).

No limit value has so far been set for $PM_{2.5}$ concentrations in EU. The revised $PM_{2.5}$ standards from the United States EPA is 15 $\mu g/m^3$ for annual arithmetic mean, allowing for an average of multiple community oriented monitors and averaged over 3 year. The corresponding standard for 24-hour averages is the 98^{th} percentile concentration not to exceed 65 $\mu g/m^3$, averaged over 3 years and maximum population oriented monitor in an area. The annual arithmetic average from the site Illmitz AT2, being 23.3 $\mu g/m^3$, was higher than the annual limit value in the US standard. The 98%-ile of the 24-hour $PM_{2.5}$ concentration from this site in 2002 was slightly higher than the corresponding US standard.

1.2 Preliminary results from the EMEP EC/OC campaign

The main focus of the campaign has been to address the level of carbonaceous material present in ambient aerosols at representative rural background sites in Europe. The dataset contain weekly concentrations of elemental carbon (EC), organic carbon (OC) and PM_{10} for 14 sites in 13 European countries for an entire year (2002.07.01–2003.07.01). Aerosol sampling has been performed using CEN approved or equivalent PM_{10} gravimetric samplers, collecting one 24h sample every week. Aerosols were collected on pre-heated quartz-fibre filters. After exposure the filters were sent back to NILU for analysis. An instrument that correct for charring during analysis has been used to quantify EC and OC for all samples collected using the Thermo Optical EC/OC method (Sunset laboratories Inc.).

The sampling sites are categorized into four different classes and are likely influenced by different major sources. This should be kept in mind when comparing the results from the different sampling sites. Table 1.2 gives an overview of the sampling sites included in the campaign, their site-category and the annual ambient concentration. Maps showing the EC and OC concentration are shown in Chapter 3 (Figure 3.15) together with modelled results.

Table 1.2: Annual ambient concentrations of EC, OM and PM_{10} and relative contribution of EC, OM, and the sum EC+OM to the PM_{10} concentration. Sampling period 2002.07.01–2003.07.01.

Site	Site category	EC [1] µg m^{-3}	OM [2] µg m^{-3}	PM_{10} µg m^{-3}	EC/PM_{10} %	OM/PM_{10} %	(EC+OM)/$_{PM10}$ %
Illmitz (AT02)	Rural Backgr.	1.11	11.13	30.9	3.6	36.1	39.7
Košetice (CZ03)	Rural Backgr.	1.16	9.08	25.0	4.6	36.4	41.0
Virolahti (FI17)	Rural Backgr.	0.40	4.16	11.0	3.6	37.8	41.4
Langenbrügge (DE02)	Rural Backgr.	0.70	8.61	26.1	2.7	32.9	35.6
Kollumerwaard (NL09)	Rural Backgr.	0.70	5.18	26.1	2.7	19.9	22.6
Mace Head (IE31)	Rural Backgr.	0.21	2.39	19.0	1.1	12.6	13.7
Braganca (PT01)	Rural Backgr.	0.87	8.20	19.4	4.5	42.2	46.7
Birkenes (NO01)	Rural Backgr.	0.16	2.33	7.4	2.1	31.4	33.5
Stara Lesna (SK04)	Rural Backgr.	0.89	8.64	19.2	4.6	44.9	49.5
Aspvreten (SE12)	Rural Backgr.	0.31	4.24	10.6	3.0	39.9	42.8
Penicuik (GB46)	Rural	0.60	3.06	14.3	4.2	21.3	25.5
Ghent (BE02)	Urban backgr.	1.98	6.59	37.0	5.4	17.8	23.2
S.P.C (IT08)	Urban backgr.	1.58	9.46	41.0	3.9	23.1	26.9
Ispra (IT04)	Near-city	2.04	12.64	42.0	4.9	30.1	35.0

1) To account for hydrogen and trace levels of other elements, concentrations of EC (µg C m^{-3}) have been multiplied by a factor of 1.1 for all sites.
2) OM is OC multiplied by a factor of 1.6. (urban background sites and the "Near-city") or 2.0 (background sites and the rural site)

1.2.1 Elemental carbon

The annual average of EC varies between 0.14–1.86 µg C m^{-3}. The lowest concentrations are in general observed at the sites in Scandinavia and at the British Isles, whereas the highest ones are reported for the sites in the in the central, eastern and southern parts of Europe (Figure 1.1). By multiplying the concentration of EC (µg C m^{-3}) by a factor 1.1, taking into account the presence of approximately 10% hydrogen as well as trace levels of other elements, EC was found to account for 1.1–5.4% of PM_{10} on an annual basis.

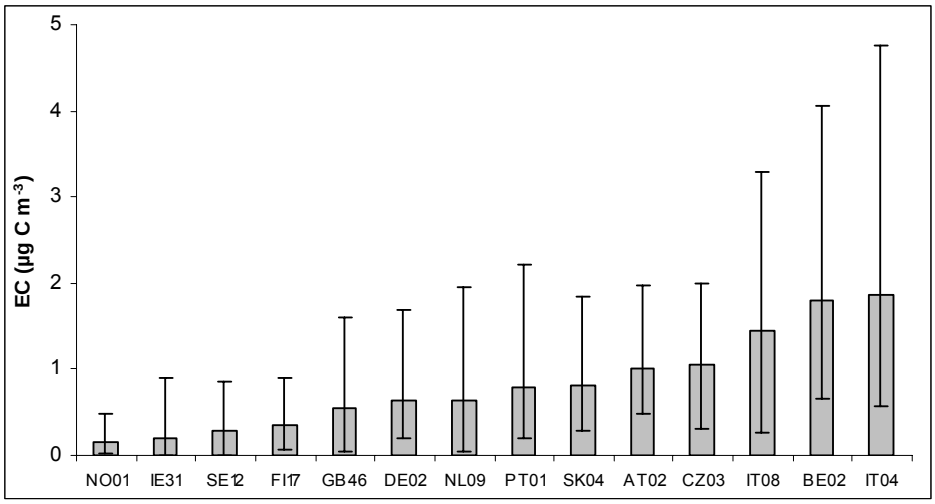

Figure 1.1: Annual mean concentration of EC including the 5% and 95% percentile. Sampling period 01.07.2002–01.07.2003.

Wintertime (October - March) concentrations of EC were found to be higher than those recorded during summer (April–September) except at the Norwegian site ($EC_{Winter}/EC_{Summer} = 0.95$). The highest ratio were observed at the sites in Germany, Netherlands and Italy (JRC), ratios between 2.1–2.5. The increased levels of EC found during winter may be explained by increased emission from residential heating (coal, oil and wood) and traffic during winter (cold starts) and possibly more frequent inversions.

1.2.2 Organic carbon

The annual average of OC varies between 1.17–7.90 µg C m^{-3}, highest concentration of OC in Italy and the lowest concentration in Norway, similar as seen for EC, Figure 1.2. In order to account for oxygen, nitrogen and hydrogen not included in the EC/OC analysis, the OC (µg C m^{-3}) concentration at the urban background sites and the "Near-city" site were multiplied by a factor 1.6. A factor of 2.0 was applied for the rural background sites and the rural site. Using these conversion factors, organic matter (OM) was found to account for 12.6–44.9% of PM_{10}.

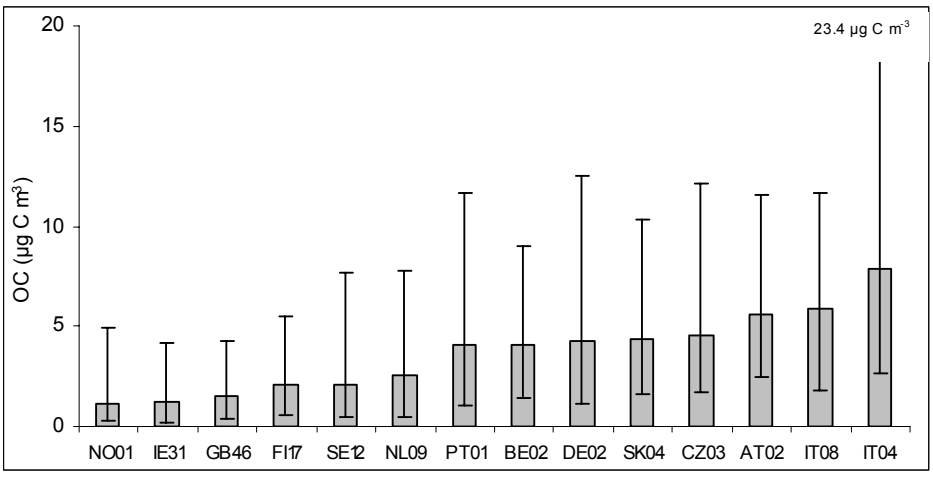

Figure 1.2: Annual mean concentration of OC including the 5% and 95% percentile. Sampling period 01.07.2002–01.07.2003.

At the three Scandinavian sites and at the site in Slovakia, the summertime (April–September) concentrations of OC were found to be a factor 1.4–1.6 higher than those recorded during winter. One possible explanation may be that this is due to biogenic OC and PBAP (Primary Biological Aerosol Particles) contributing to the OC fraction at these sites during summer. Together with low impact from anthropogenic derived OC. For the other sites the concentration of OC increases by a factor 1.2–2.7 from summer to winter. Most likely this can be explained by increased emissions from residential heating (coal, oil and wood) and traffic during winter (cold starts) as for EC.

The largest episodes for OC were 30.5 µg C m^{-3} and 36.3 µg C m^{-3} observed at Braganca (PT01) and Ispra (IT04) during winter. LC/MS analysis of selected samples from the Portuguese site has revealed quite high (>1 µg m^{-3})

concentrations of levoglucosan during late fall and winter. This finding indicates that wood burning for residential heating is an important source influencing this rural background site during the cold season. This also suggests that wood burning for residential heating can explain the maximum OC concentration reported for this site. The maximum concentration at Ispra is likely an episode of polluted air coming from the nearby city of Milan.

1.2.3 Total carbon

Total carbonaceous material, EC+OM, accounted for 13.7–49.5% of the PM_{10}. However, as much as 61.6% of PM_{10} could be accounted for by carbonaceous matter at the Portuguese site during winter. The lowest fraction of EC+OM in PM_{10} was found at Mace Head (IE31), not exceeding 15% in any season.

1.2.4 Ratios

The annual mean EC/TC ratios vary from 10% at IE31 to 31% at BE08, reflecting the relative impact of EC-rich sources. Rau (1989) reported EC/TC ratios between 0.14–0.27 for aerosols emitted from wood burning on conventional fireplaces, whereas traffic (primarily diesel vehicles) have EC/TC ratios as high as 0.6–0.7 (Williams et al., 1989). Aging of airmasses tend to lower the EC fraction of the aerosol as it is mixed with non-combustion particles, likewise will the EC/TC ratio decrease due to condensation of organic material from the gas phase. For the sites in Ireland, Norway and Sweden, low annual levels of EC are reflected in low EC/TC-ratios, whereas the sites BE08 and IT04 are typical examples of the opposite. Apart from the sites in Belgium and Portugal, EC accounts for a larger fraction of TC during winter than during summer. This can partly be explained by the general increase in concentration of EC during winter, In addition, also the wintertime reduction in OC reported for the sites in Finland, Norway, Slovakia and Sweden contributes to the higher EC/TC ratio during winter.

The EC/PM_{10} ratio is higher during winter than during summer except at the Belgian and the Portuguese sites. For the Scandinavian sites and the Slovakian site there is a profound increase in the OM/PM_{10} ratio from winter to summer (Finland and Sweden approx. 16-17%). As previously emphasized this can be due to biogenic OM and PBAP contributing significantly to these sites during the growth season. For the Portuguese site there is a significant decrease in the OM/PM_{10} ratio from winter to summer (26.5%). It has previously been suggested that this is due to high levels of OC emitted from wood burning for residential heating during the cold season. The seasonal variation for the OM/PM_{10} ratio has also an impact on the $(EC+OM)/PM_{10}$ ratio. For the sites in Finland, Slovakia and Sweden approximately 50% of PM_{10} can be accounted for by carbonaceous material, whereas at the Portuguese site over 60% of PM_{10} can be attributed to carbonaceous material during winter.

The annual mean TC/PM_{10} ratio varies from 4% at the Irish site to 27% at the Slovakian site (TC given in $\mu g\ C\ m^{-3}$). Disregarding the Irish site, the EC/TC ratio does not vary too much, only by a factor 2.7. However, this picture is somewhat misleading as only the carbon content of TC is accounted for.

1.2.5 Artefacts

Sampling of atmospheric aerosols for subsequent analysis of the carbonaceous content has proven to be challenging. Semi-volatile OC condensed onto particles trapped by the filter, might evaporate during continued sampling. This is known as a negative artefact. Semi-volatile OC is known to adsorb onto filter-material during sampling and is recognized as a positive artefact as the amount of OC on the filter increases although no particulate OC has been added (Turpin et al., 1994; McDow and Huntzicker, 1990). The positive artefact is enhanced by the fact that pre-baked quartz fibre filters are used for sampling. Pre-baking the filters will activate them and facilitate the adsorption of semivolatile OC to the filter surface.

The positive artefact can be more pronounced in areas with low levels of particulate OC as the difference between the Quartz-fibre filters capacity of adsorbing vaporous OC and the filter loading of particulate OC can be really small. This can be overcome by increasing the particulate OC loading on the filter either by increasing the sampling time or the sampling volume. The positive artefact has been shown to decrease as the filter face velocity increases (McDow and Huntzicker, 1990). This should be kept in mind when comparing concentrations of OC obtained from samplers operating at different filter face velocities.

1.3 Size distribution measurements Birkenes (NO01) in 2003

Particle mass is mostly determined by accumulation and coarse particles, whereas Aitken and nucleation particles make a negligible contribution to PM_{10}, $PM_{2.5}$, or even PM_1 mass. On the other hand, coarse particles contribute little to particle number densities. The main contribution to the particle number concentration comes from ultra fine particles UFP, i.e. nucleation and Aitken particles, and to a less extent from accumulation particles. A better characterisation of Aitken particles is needed to facilitate our understanding of adverse health effects of aerosols, and of the dynamic growth of Aitken particles to accumulation mode particles by heterogeneous chemical processes. Accurate prediction of aerosol number concentrations is important for estimating the indirect climate forcing of aerosols.

Few measurement data on particle number concentrations are available. One of the most extensive networks for measuring particle number distributions in Europe is a Nordic network comprising several Swedish and Finnish stations, and, since autumn 2002, the EMEP station at Birkenes. Here we present the results obtained with the new Differential Mobility Particle Sizer (DMPS) instrument installed at Birkenes, which measures aerosol size distributions in the diameter range between 19.0 nm and 643.2 nm.

Figure 1.3 and Figure 1.4 show time series of number size distributions (upper panel) and total number concentrations (lower panel) measured in December 2003 and July 2003, respectively. Particle numbers are considerably lower in winter than in summer, which is in nice agreement with published data from other Nordic background stations (Tunved et al., 2003). Potential explanation for the seasonal variation in particle number concentration might be a higher biogenic activity in

spring and summer, which produces larger amounts of organic vapours that contribute to the growth of aerosol particles by condensing onto existing particles, but can also be explained by seasonal changes in air masses, lower rate of incoming solar radiation and thus less new particle formation during the winter period and/or a higher rate of precipitation and overall cloudiness during the winter (Tunved et al., 2003).

Figure 1.5 presents a 9-day period in early spring characterized by repeated particle formation events. High particle number concentrations (lower panel) are correlated with the appearance of new small Aitken particles, most likely due to local nucleation events. Also the dynamic growth of the Aitken particles to accumulation size on the time scale of 1-3 days is observed.

Diurnal variations were observed and most of the nucleation events were characterized by a sharp increase of nuclei mode number concentration around noon (Figure 1.5). The frequency of nucleation events in 2003 at Birkenes has been shown to be largest around spring and summertime. This seasonal variation has been observed at similar sites (Tunved et al., 2003).

Figure 1.6 presents an episode dominated by long-range transport of aerosols. Only few occurrences of small Aitken particles can be observed. The most prominent feature in the upper panel is a distribution of particles between roughly 30 nm and 110 nm, which appears in the morning of Julian day 320 in 2002 and disappears in the morning of the following day. There is no appearance of smaller Aitken particles precedes the appearance of these aerosols. This leaves, in principle, two possible explanations. The aerosols may be primary particles that are locally emitted. However, as Birkenes is a regional background station far away from major emission sources, this is rather unlikely. It is more plausible that these particles are aged aerosols that originate from a more distant source region, and that these aerosols have undergone long-range transport in the atmosphere.

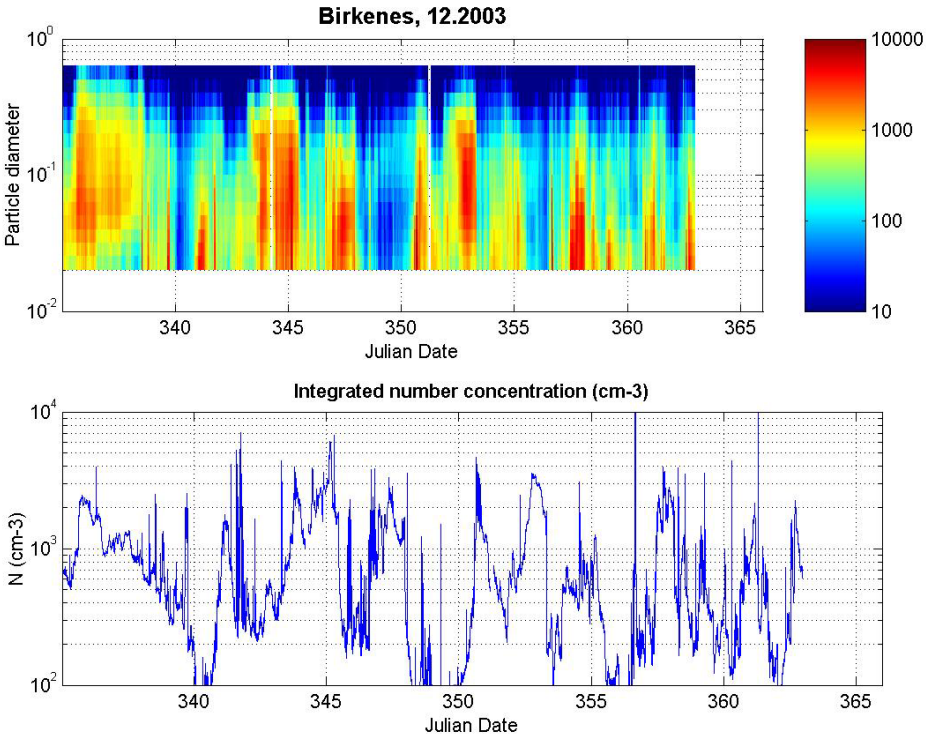

Figure 1.3: Spectral plot of aerosol number as a function of size distribution (μm) and Julian Day (upper panel) and time series of total number concentration (lower panel) at Birkenes in December 2003.

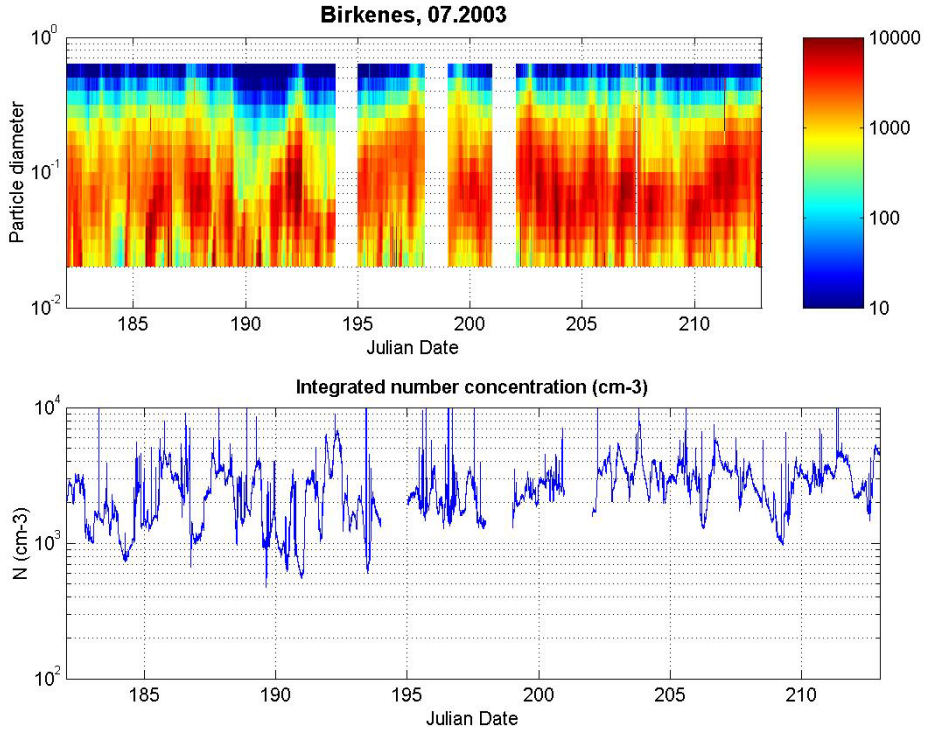

Figure 1.4: Spectral plot of aerosol number as a function of size distribution (μm) and Julian Day (upper panel) and time series of total number concentration (lower panel) at Birkenes in July 2003.

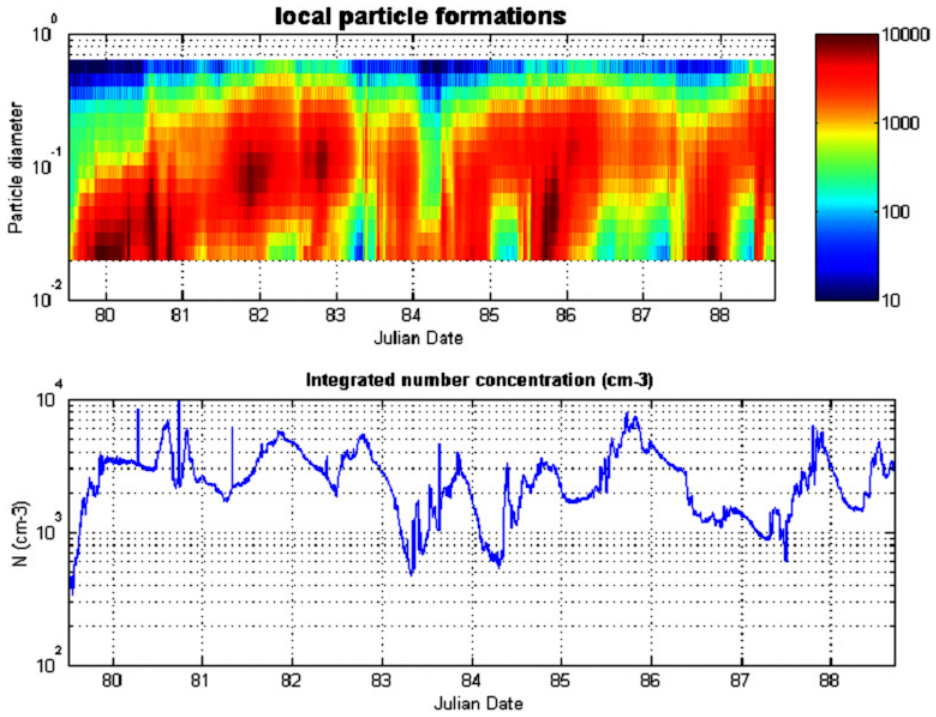

Figure 1.5: A 9-day period in early spring2003 with repeated local particle formations and diurnal variations.

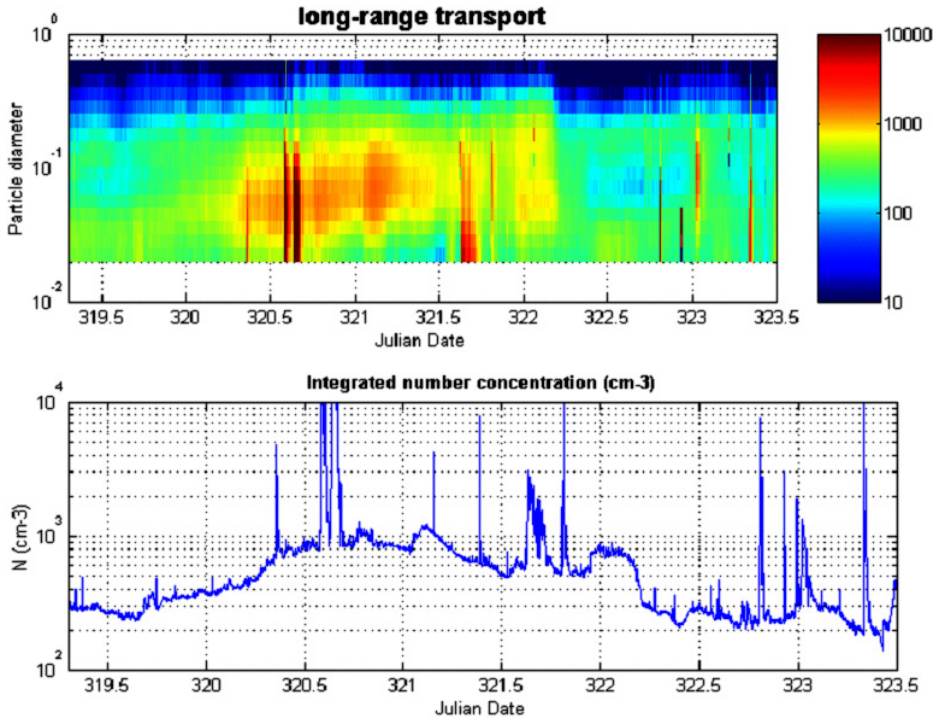

Figure 1.6: An episode of long-range transported aerosols which appears in the morning of Julian Day 320 in 2002 and disappears in the morning the following day.

1.4 Submicron particle number concentrations measured during summer 2000 and winter 2001 in the Eastern Mediterranean

One of the objectives of the European Union funded SUB-AERO project was the investigation of new particle formation and it's fate in the Mediterranean area under different meteorological conditions and seasons (summer and winter) including their chemical composition. During the project two field campaigns were carried out at the Finokalia sampling site (10.–31.7.2000 and 7.–14.1.2001) and one campaign aboard the vessel Aegeon cruising in the Mediterranean Sea (25.–29.7.2000). This work included also mass and chemical size distributions of atmospheric aerosol collected by a low pressure cascade impactor at the Finokalia sampling site on Crete island and aboard the scientific boat Aegeon. Finokalia (35º 19' N, 25º 40' E) is a coastal remote site eastward Heraklion on the top of a hill (elevation 130 m) facing the sea within the sector of 270º to 90º. Depending on the weather the air masses reaching the station originate from Europe to Africa.

Along with the characterization of the collected atmospheric particulate matter particle number concentration measurements were also performed using a Scanning Mobility Particle Sizer (SMPS) and an optical particle counter (PMS Las-X) both in summer and winter. Simultaneously, gaseous pollutants (NO_2, HONO, $HONO_2$, SO_2, O_3), temperature, humidity, and wind direction and velocity were monitored. The instruments were connected to the same sampling inlet located at about 4 m above the ground.

The concentrations of ultrafine particles (< 30n) were highest during the winter where the concentration varied mostly from 1.10^2 to 5.10^2 cm^{-3} with several peaks going up to about 1.10^4 cm^{-3}. Corresponding concentrations measured during the summer campaign varied mostly from 1.10^1 to 1.10^3 cm^{-3} with an average value of about 1.10^2 cm^{-3} at Finokalia and from about 1.10^1 to 1.10^2 cm^{-3} with average value about $5.10^1 cm^{-3}$ aboard Aegeon vessel. The particle concentrations for size fraction 30–100 nm (accumulation mode) were mostly around 1.10^3 cm^{-3} for all measurements but increased up to 5.10^3 cm^{-3} in the middle of the winter campaign followed by a decrease to 5.10^1 cm^{-3}. The concentrations of the 100–300 nm size fraction were higher during the summer ranging from 1.10^3 to 5.10^3 cm^{-3} aboard the boat and from 2.10^2 to 2.10^3 cm^{-3} at Finokalia. Corresponding concentrations measured during the winter varied from 1.10^2 to 1.10^3 cm^{-3}.

The particle distributions measured during the summer were typically monomodal with concentration maximum around 70–150 nm at Finokalia and around 100–220 nm aboard Aegeon. Number distributions measured during the winter were predominantly bimodal with modes around 40–100 and 120–220 nm, respectively. During the three nucleation events which were observed in the middle of the winter campaign another mode appeared at about 20 nm. Note that during the nucleation events the smaller mode fell down from about 80 nm to 40 nm while the higher mode has disappeared. Similar behaviour was observed during the summer (14–15 July 2004) where also a smaller mode at around 40 nm appeared in connection to an observed nucleation event. The evolution of nucleation event (10–11 January 2001) is shown in Figure 1.7.

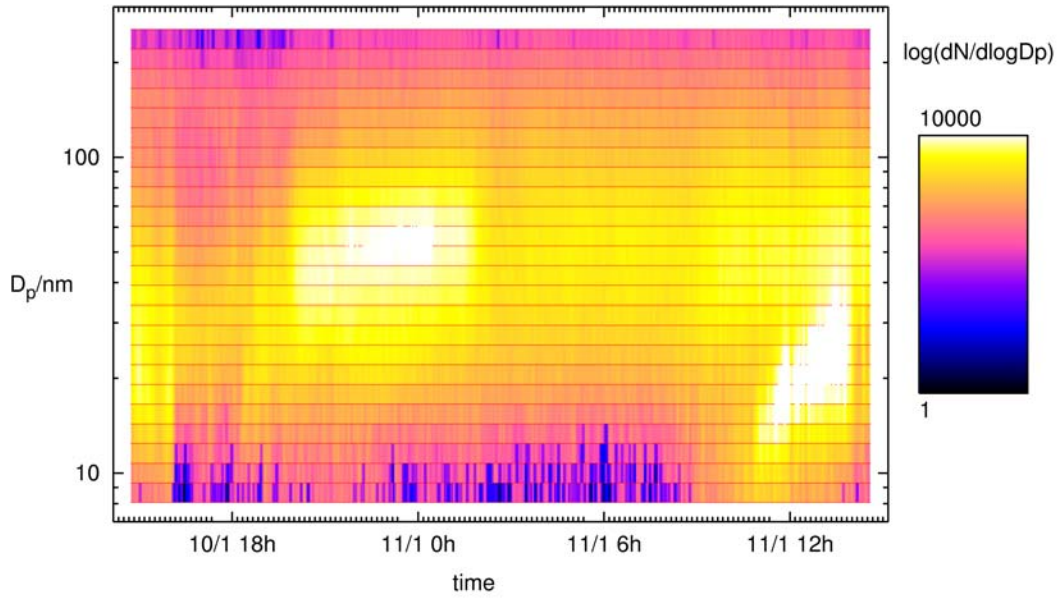

Figure 1.7: Evolution of a nucleation event at the Finokalia station during 10-11 January 2001.

Comparing the winter and summer periods the nucleation events were observed more frequently in winter (3 events during seven days) than in the summer (1 event during three weeks). This is probably due to the lower concentration of PM_1 and PM_{10} observed in the winter period (Smolík et al., 2003) resulting in lower coagulation scavenging of small nuclei and also due to higher biogenic emissions from plants and higher humidity which increase the driving force for the particle growth (Kulmala et al., 2004). It has to be noted also that both in winter and summer the nucleation events were accompanied by a decrease of the Aitken mode position down to about 40 nm.

1.5 Particulate matter characteristics in the Eastern Mediterranean – Saharan dust episodes

There is a consistent pattern of geographical variability in Europe with lower concentrations of particulate matter in the far north and higher concentrations in southern countries. This is due to natural emissions of unsaturated hydrocarbons (including isoprene) that are highly reactive, and high emissions of anthropogenic gaseous and aerosol pollutants in Southern Europe (Hoffman et al., 1997). Aerosol yields obtained from experimental measurements and theoretical estimates also indicate that highly non-linear aspects are involved in the production of organic aerosols. Furthermore, the Mediterranean region is characterized by a specific natural aerosol load, namely sea spray and North African desert dust. These natural particulate emissions are involved in heterogeneous reactions with anthropogenic gaseous pollutants and may modify the processes leading to gas-to-particle conversion (Millan et al., 1997; Rodriguez et al., 2002; Bardouki et al., 2003).

In the current study the focus is on the PM_{10} and $PM_{2.5}$ levels at the Acrotiri research monitoring station on the island of Crete (Greece) in a period between 2003 and 2004 and the influence of African dust outbreaks on the particulate

matter concentration. The work here presents one of the first studies of continuous aerosol monitoring at the Eastern Mediterranean.

Figure 1.8 shows the average daily values for PM_{10} during the measurement period. The average value for the whole period is 35.1 μg/m^3. There is a large variability of the PM_{10} values during the summer period with concentrations 80-90 μg/m^3. During the winter period the PM_{10} concentrations are in general lower and the variability smaller. However, on the 27/02/04 a major Saharan dust event lead to an average PM_{10} level of 193.2 μg/m^3. It is interesting to note that the PM_{10} levels in the evening between 9 and 12 p.m. reached 400 μg/m^3 with the highest value of 528 μg/m^3 around 11 p.m., which is a very high concentration even for typical Saharan dust episodes (Rodriguez et. al., 2001).

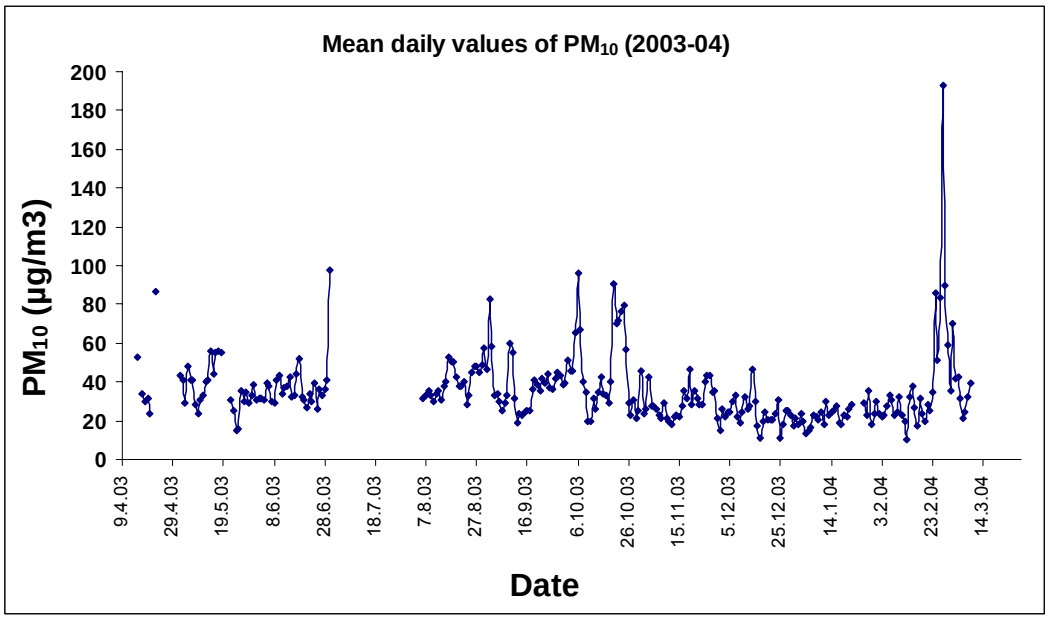

Figure 1.8: Daily average PM_{10} concentration at the Acrotiri research station.

The lowest observed PM_{10} value during the measurement period was on 13/02/04 (10 μg/m^3) where a large storm influenced the area. It is evident from the PM_{10} concentrations that the high aerosol concentrations occur during specific short time intervals (1-3 days) due to the influence of southern winds originating from Africa.

$PM_{2.5}$ measurements were started 10/03/04 and the average $PM_{2.5}$ concentration during from 10/03/04 to 31/05/04 is 26.3 μg/m^3. There are three periods in which the $PM_{2.5}$ concentration reached high values, which correspond to Saharan dust episodes in the area.

The transport from the Greek mainland and the European continent contributes significantly to the particulate matter levels in the area since the north winds are dominant during the year. However, the particulate matter concentration at the Acrotiri during the transport of air masses from the northern Europe is elevated but considerable lower than the high concentrations during the outbreaks of African dust.

The annual average PM_{10} standard of 40 μg/m^3 is not exceeded in the area. However, the EU 2010 annual average PM_{10} standard of 20 μg/m^3 is exceeded. Furthermore, the US-EPA annual average $PM_{2.5}$ standard of 15 μg/m^3 seems to be exceeded in the area. Since the Acrotiri station measures $PM_{2.5}$ levels from March 2004 only, no certain conclusion can, however, be drawn for the $PM_{2.5}$ annual average concentration.

1.6 Sun photometer measurements within WMO GAW during 2003

A global network of aerosol optical depth (AOD) observations started in 1999 in the frame of the Global Atmosphere Watch (GAW) program of the World Meteorological Organization (WMO). A World Optical Depth Research and Calibration Center (WORCC) was established in 1996 at PMOD/WRC.

Measurements of direct solar radiation in four narrow spectral bands centred at 862, 500, 412 and 368nm from the network stations are collected off-line at WORCC for centralized evaluation of aerosol optical depth on a monthly basis. Data quality control includes instrumental tests, like detector temperature, solar pointing staying within specifications, and automated cloud screening by two different algorithms. Final results are delivered as hourly averages after statistical tests to the World Data Centre for Aerosols (WDCA) in Ispra. Where atmospheric conditions permit, instruments are calibrated on-site, while for other sites they can be recalibrated by comparison to standard instruments maintained at WORCC, Davos.

By end of 2003, eight international stations were delivering data, 3 more stations have agreed to participate, but were, for lack of solar trackers, not yet operational. Here we compare the 2003 results from the Ny-Ålesund, Hohenpeißenberg and at Jungfraujoch. The three sites are all different with respect to aerosol optical depth and also aerosol concentrations at the measurement site. The data presented have been filtered with a tight cloud and tracking filter, daily averages represent at least 90, and monthly averages at least 360 quality controlled records.

At Ny-Ålesund the sun photometers has sun trackers that direct the photometers to the sun disc and leads the spectrometers to follow the sun across the sky during the day. The sun photometers are passive instrument that records the sun irradiance only, and they cannot carry out measurements during dark hours or during foggy or cloudy conditions. Fog and low clouds often occur in Ny-Ålesund, and this reduces the data completeness seriously at this site. The polar night at Ny-Ålesund lasts from 26th October to 16th February, the measurement season is therefore much shorter than at the sites. The observatory at Hohenpeißenberg is located in the southern part of Germany about 60 km southwest of Munich and some 20 km north of the rising Alpine mountain range. The observatory's altitude is, however, nearly 1000 m asl and the observatory is above the polluted surface layer much of the time. Given a clear sky, this sun photometer can be operated all year around. The aerosol load and surface concentrations are generally higher at Hohenpeißenberg than at the two other sites. The observatory at Jungfraujoch is located at about 3600 m asl and is frequently in the free troposphere above the boundary layer. The aerosol optical depth, as well as the particle concentration at the site, is therefore normally

extremely low permitting this site to be used for calibration of master sun photometers.

Figure 1.9 and Figure 1.10 compare the aerosol optical depth at 500 nm at the three sites by giving the monthly mean values and the daily averages respectively.

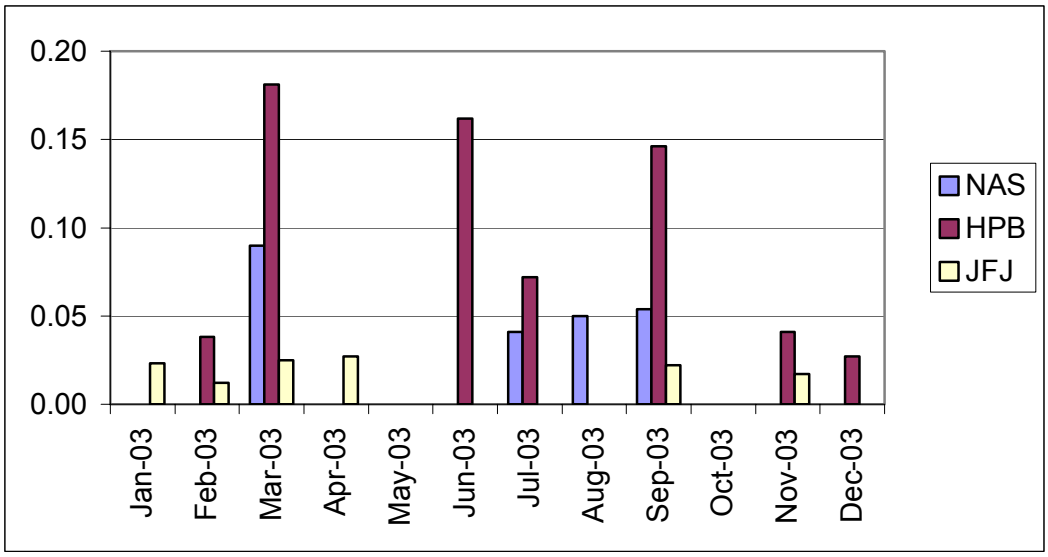

Figure 1.9: Monthly mean AOD at 500 nm measured at Ny-Ålesund (NAS), Hohenpeißenberg (HPB), and at Jungfraujoch (JFJ), applying a tight cloud and tracking filter.

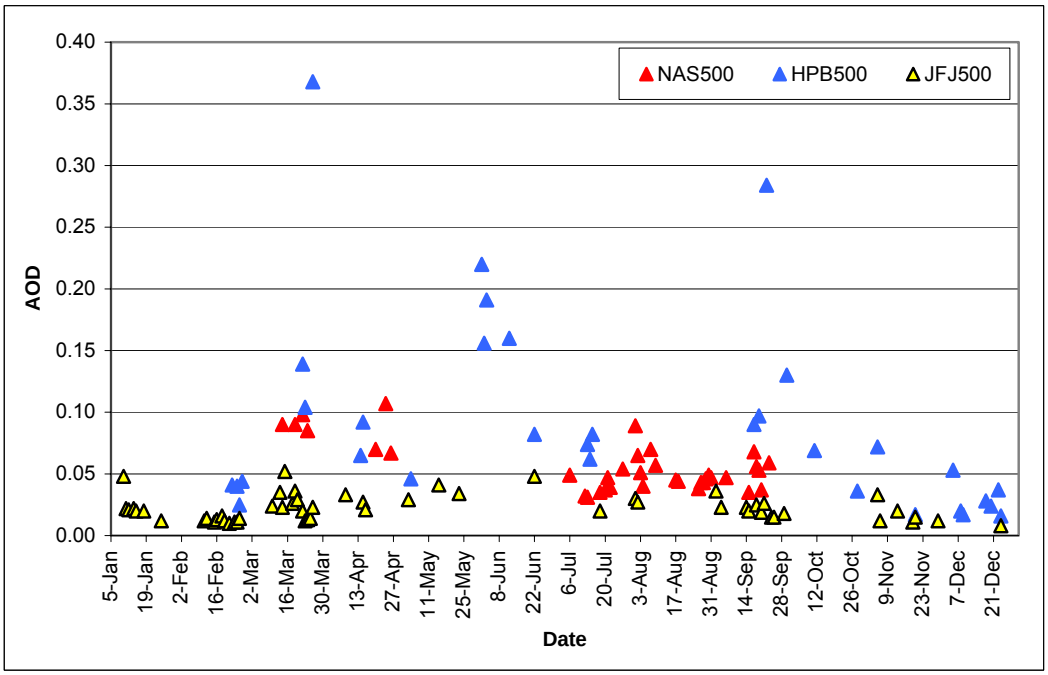

Figure 1.10: Daily averages of AOD at 500 nm measured at Ny-Ålesund (NAS), Hohenpeißenberg (HPB), and at Jungfraujoch (JFJ), applying a tight cloud and tracking filter.

The AOD at Hohenpeißenberg is about a factor of ten higher than at Jungfraujoch on one or two days in March and September, but during winter both observatories have very low and more equal aerosol optical depths. The Hohenpeißenberg monthly averages of AOD at 500 nm in Figure 1.9 were about 2-3 times higher than those at Jungfraujoch during November and February.

It is also evident from Figure 1.9 and Figure 1.10 that the optical depth at 500 nm in the Arctic at Ny-Ålesund generally was lower than that at Hohenpeißenberg, but much higher than at Jungfraujoch. During March and September when all three sites had valid monthly averages, the Arctic AOD at 500 nm were about three to four times higher than the high altitude averages from Jungfraujoch and about one half to one third of the Hohenpeißenberg monthly averages in 2003.

It should be noted that in order to obtain general and quantitative conclusion on the levels of the AODs at the three measurement sites, data from at least five years should be needed. This is particularly important when applying a tight cloud and tracking filter that, although including high quality data only, could exclude a large fraction of the measurements.

2. Emission distributions used for source-receptor calculations and CAFÉ scenario analysis

by Leonor Tarrasón, Heiko Klein, Philippe Thunis, Vigdis Vestreng and Les White

In preparation of the revision of the National Emission Ceilings Directive, there has been a considerable effort to update and review the emission data used as basis for scenario analysis and impact calculations. In particular, the spatial distribution of the emissions used as input to the Unified EMEP model has been thoroughly revised and a new methodology for allocating emissions by sector has been proposed and tested. This effort responds to the new challenges in environmental policies, where as effects are oriented towards population and the non-compliance areas become discrete, the proximity to sources becomes more important.

This chapter documents the emission data used in source-receptor calculations and scenario calculations carried out by EMEP/MSC- W this year and under the EU CAFÉ-BASELINE project. The data is characterised by national totals, sector distributions and by the spatial distribution of the emissions. Special attention has been given to the identify changes in the 2004 emission data with respect to emission estimates from previous years.

2.1 National Emission Totals

National emission totals used for 2002 model calculations are based on official submissions of the Parties to UNECE/EMEP. These data have been compiled and verified by national experts and have been revised as documented in Vestreng at al, (2004). National emission data are presented at the end of this chapter in Appendix Tables A1 to Table A4 for gaseous main pollutants and Tables A5 and A6 for primary particle emissions.

The tables contain also scenario projections for 2010 and 2020 as provided by IIASA in April 2004. These estimates, referred to as IIASA_April2004 scenario estimates, are very similar to those used for MSC_W source-receptor calculations (referred to as IIASA_March2004) and are those used for the EURODELTA project. The scenario values differ somewhat from those presented in Chapter 5 (Amann et al., 2004), which correspond to new updates by IIASA_May2004. This continuous update in scenario estimates reflects the progress of work under the CAFÉ BASELINE project and new estimates are expected again by the end of August (IIASA_August2004).

Emission totals over the whole EMEP domain remain almost constant in 2002 with respect to 2001, both for main compounds and particulate matter primary emissions. Changes in emissions are below 1% for all compounds, although the reported changes can be more significant for individual countries and regions. We have distinguished the *European Union* (EU25) from *EMEP Eastern Europe*

(EEE[1]) and *Other Areas*, the later group including Iceland, Norway and Switzerland. Europe (*Total*) corresponds to all anthropogenic emissions inside the EMEP domain. For the European Union, we have distinguished EU15 member states previous to the 2004 extension from the new member states that are included under EU10+ in order to highlight significant differences between these countries, when occurring. Figure 1 shows the changes in national totals for 2002 with respect to 2001 for these different regions. There is a general decrease in the emissions of all compounds for most regions, except in Eastern European countries, where emissions of most components increase in average with respect to 2001. Changes considered by region are generally below 5%. The only exception is for *Other Areas*. The reason for larger changes in *Other Areas* is that this group includes only 3 countries, so that weighted average values are closer to individual country variations. The reported emission changes for individual countries can be larger than the regional weighted average. However, individual national changes do not normally exceed 20% and are generally below 10%. The only two exceptions are for VOC emissions from Armenia and for PM_{10} emissions from Switzerland, where reported emissions are about ½ of those reported in 2001. Emission changes from the later can be easily visualised in Figure 2.1, and they are the reason for the high PM_{10} changes calculated in *Other Areas.*

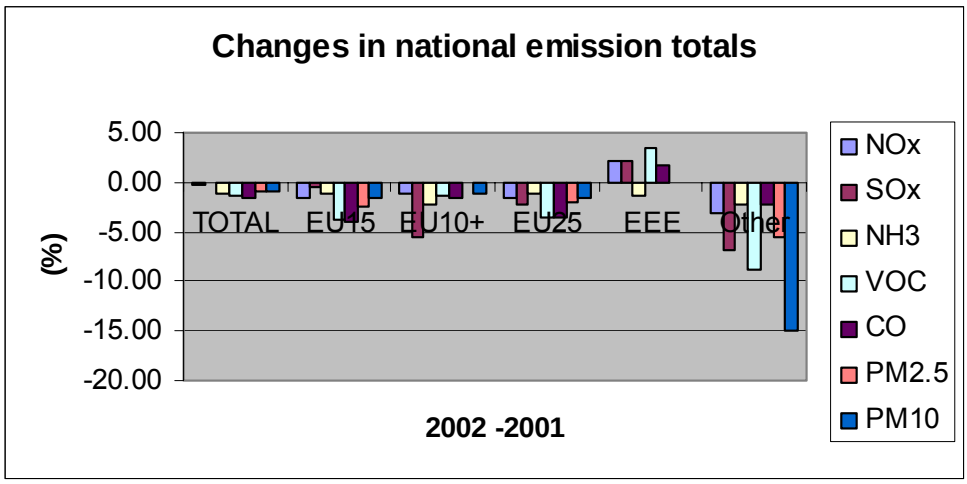

Figure 2.1: Percentage changes in national emissions of main compounds and primary particulate matter for different European regions. Negative values indicate decrease of emissions in 2002 with respect to 2001.

Figure 2.2 shows the decrease in reported emissions for different regions since 1990, for main compounds. Since 1990, emissions of sulphur dioxide are reported to have decreased by 49% in the EMEP area, the decrease of emissions being larger in EU25 (66%) than in Eastern European countries (42%). However, this

[1] EEE, EMEP Eastern Europe, has been defined to include: Albania, Armenia, Azerbaijan, Belarus, Bosnia and Herzegovina, Bulgaria, Croatia, Georgia, Kazakhstan, Republic of Moldova, Romania, Russian Federation, Serbia and Montenegro, The Former Yugoslavian Republic of Macedonia, Turkey and Ukraine.

decrease of sulphur emissions in EU25 has been achieved to a large extent because of stronger reductions in the new European Union member states (EU10+). For ammonia, the decrease of emissions in Western Europe since 1990 is generally smaller (7% in EU15, 3% for Other Areas) than in Eastern European countries (43% in EU10+, 33%in EEE). The new EU countries have reduced ammonia emissions far more effectively than the EU15 countries, bringing the average reduction for EU25 down by 15.5%.

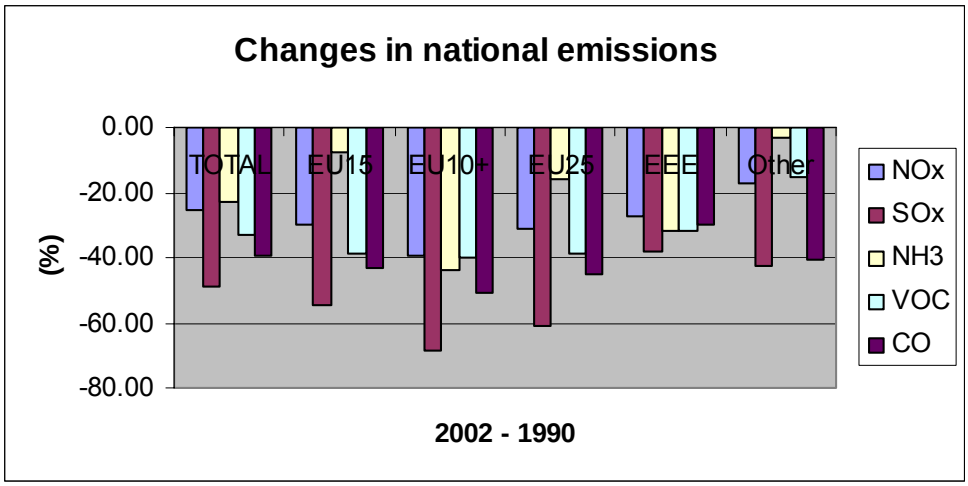

Figure 2.2: Percentage changes in national emissions of main compounds for different European regions. Negative values indicate decrease of emissions in 2002 with respect to 1990.

2.2 Sector distributions

The sector distributions used throughout this report for status calculations, scenario runs and source-receptor calculations with the Unified EMEP model have been revised by IIASA and are based on official submissions by the Parties and bilateral consultations with emission experts carried out under the EU CAFÉ_BASELINE project. The process is documented in Chapter 5 in this status report (Amann et al., 2004).

The NFR sector disaggregated data reported by the Parties and revised by IIASA has been the basis for the conversion to the levels used as input in the EMEP Unified model. For modelling purposes, the final aggregation levels by sector follow the SNAP code nomenclature at level 1.

Figure 2.3 shows aggregated sector distributions for SO_x, NO_x, NH_3, VOC, $PM_{2.5}$ and PM_{10} anthropogenic emissions. The data is presented for the five different area regions introduced in last section. In addition, emissions from ship traffic in sea areas are also presented as an independent group. All regions are represented with two different emissions columns: the column to the left shows the sector distribution used in 2003 (old) and the column to the right is the 2004 (new) estimate by IIASA. Emission values in Figure 2.3 correspond to year 2000. The picture shows the relative importance of the different regions and sectors to total

emissions. It is interesting to note that in 2000, emissions from EU15 dominate the emissions from the European Union for all pollutants. The European Union emissions of NO_x, NH_3, VOC and CO (not shown) are about twice as large as emissions from the rest of countries in EMEP (EMEP Eastern European countries, EEE). For SO_x and PM_{10} emissions, EU25 and EEE contribute similarly to the total EMEP emissions. For SO_x and NO_x, emissions from ship traffic are larger than those from the whole group of countries under EU10+, the new member states of the European Union.

Although differences between the old and new estimates can be significant for single sectors, the emission totals for all components agree within 3%. This justifies the use of the new sector distribution as a percent of total emissions. For model simulations for other years than 2000, we have used the new sector distribution as percent of the actual national emissions for the simulated year.

Figure 2.4 shows the percentage contribution of each sector to the total emissions. Again, the data is presented per component and for the five main regions. Both estimates identify the same main contributor sectors to total emissions of all pollutants, differences affect mainly on the relative importance of main contributor sector. Differences are generally larger for individual countries than for regions and groups of countries, as indicated also in Figure 2.4 where the largest differences between estimates are seen in the smaller group of countries, *Other areas*. Differences are largest for primary PM emissions than for the main gaseous components (also for CO that is not shown). The largest changes are related to ground-based sectors for primary PM emissions: residential combustion and traffic emissions, both in the vicinity of population centres. As the change in the emissions of PM with the new estimate is between source sectors that are co-located and emitted at the same height, we do not expect these differences to affect significantly the Unified EMEP model estimates.

More interesting are the changes that the new distribution introduces in sectors with relatively small contribution to total emissions. The new sector distribution resolves inconsistencies in the reporting from the countries. For example, countries report in different sectors emissions from machinery and off-road transport related to main activities like agriculture or fossil fuel extraction. While these emissions of should be reported in sector 8 (off-road transport and machinery), some countries report instead NO_x and CO emissions in sector 10 (agriculture and forestry) and sector 5 (fossil fuel extraction). These are now corrected in the IIASA sector distribution. Another example is related to the reports of VOC emissions in sector 10 (agriculture and forestry). Some countries include emissions of isoprenes and terpenes from forests as anthropogenic emissions. Other countries consider instead forest emissions as natural emissions and report these under nature (SNAP 11). The inconsistency in reporting VOC emissions has consequences for the model results as it might lead to a duplication of the VOC emissions from forests. This is because the Unified EMEP model calculates its own biogenic VOC emissions (Simpson et al., 1995) in a way that is consistent throughout the whole model domain and depends on the actual meteorological conditions of the simulated year. Duplication problems are now avoided by using IIASA new sector distributions.

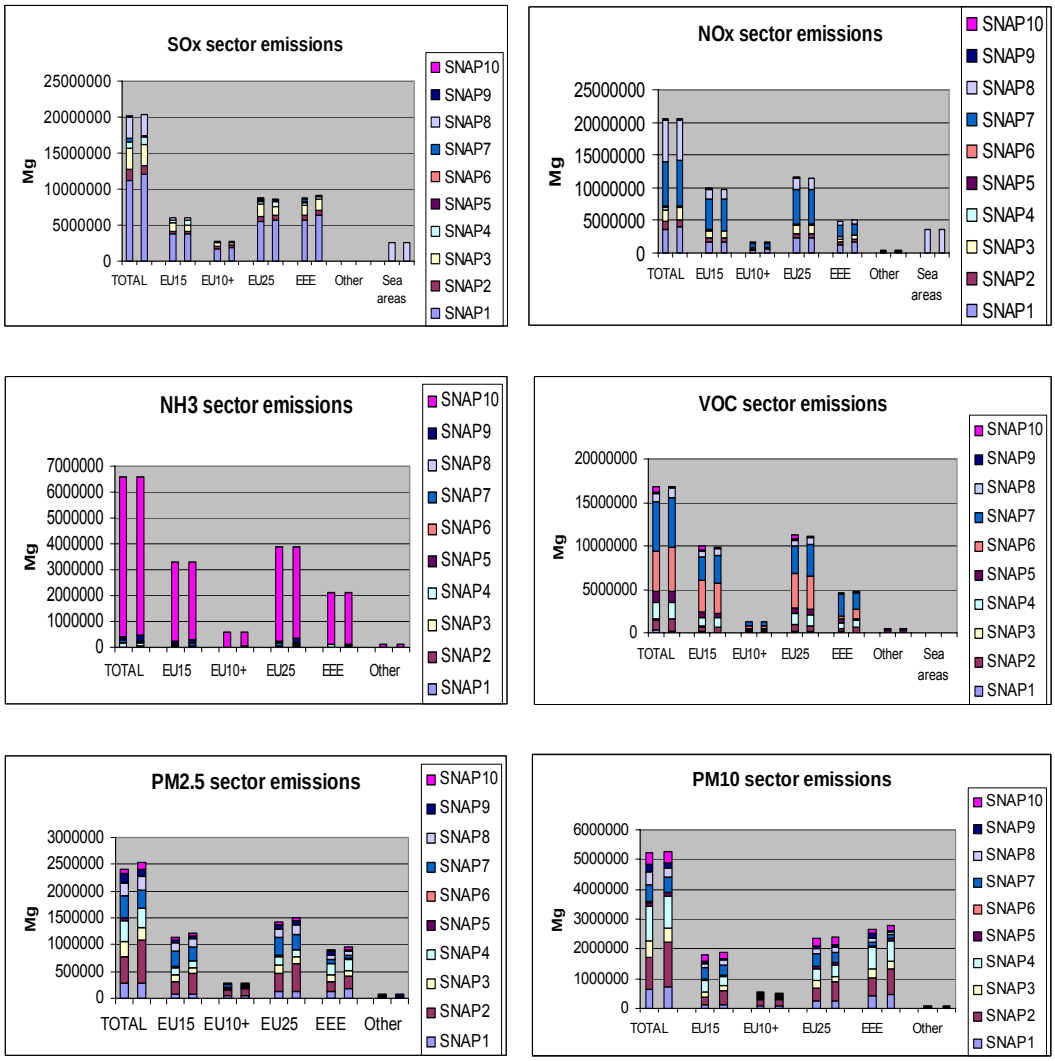

Figure 2.3: Sector emissions from anthropogenic sources aggregated at SNAP level 1 for different components and different regions over Europe (see text for further explanation).

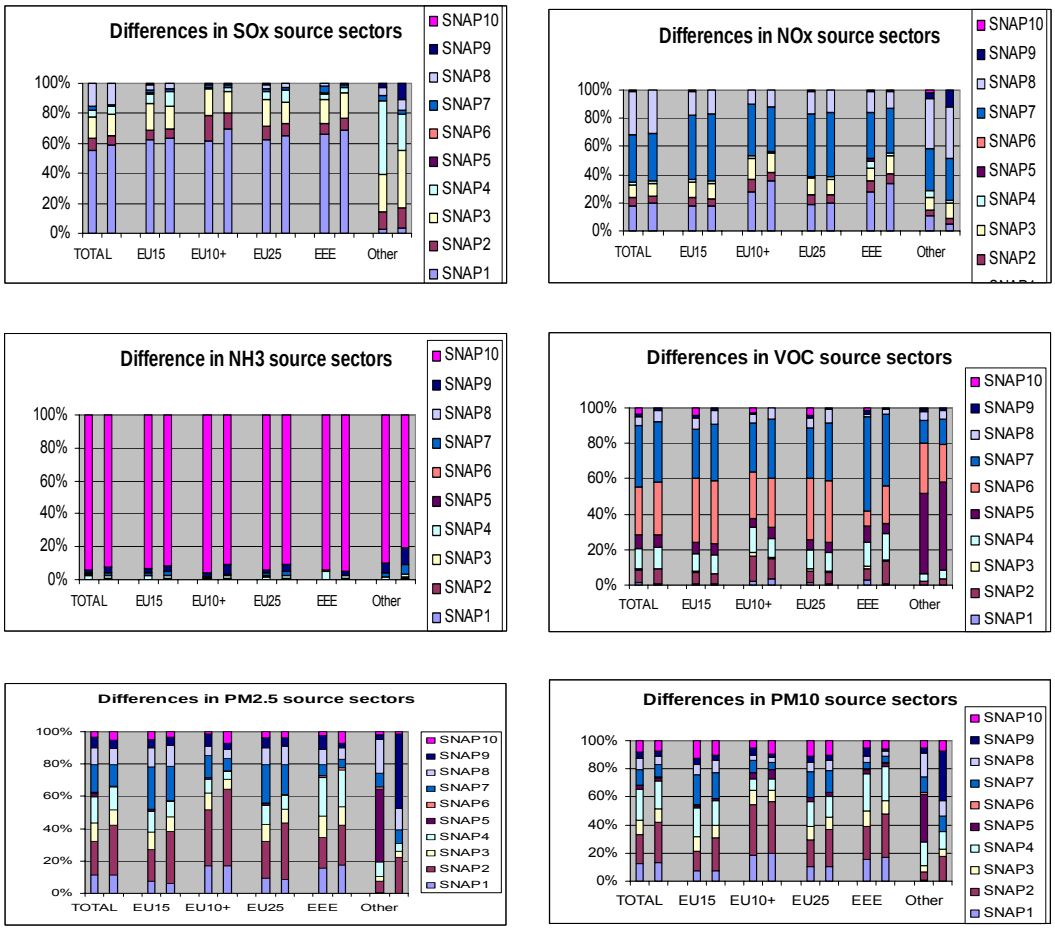

Figure 2.4: Differences in the relative contribution of the anthropogenic source sector to total emissions. In each graph, columns to the left are sector contributions used in 2003 EMEP results, the right columns are corrections made by IIASA under the CAFÉ BASELINE project and used as basis for 2004 EMEP/MSC-W results.

2.3 Spatial distribution of national sector emissions

The spatial distribution of emissions is a determining input for atmospheric transport and dispersion calculations. The modelled air concentrations and depositions are intrinsically linked to spatial location of the emissions. As the study of effects from air pollution becomes more oriented towards population and the areas non-compliance with existing international agreements become more discrete, the proximity to sources becomes more important. Thus, an accurate description of the spatial distribution of emissions is even more relevant at present.

The methodology to determine the spatial distribution of emissions used in EMEP/MSC-W modelling has been revised and updated in the past two years, in cooperation with CONCAWE and the JRC-EI through the CITY DELTA project. The new methodology has now been implemented and tested. In the following we describe the basic principles of the new methodology, present its results and compare them with previous estimates. At the end of this section, some illustrative

examples are presented on the significance of the spatial distribution of emissions for air pollution dispersion calculations.

2.3.1 Methodology used for gridding national sector emissions

The main requirements for the new methodology to provide the spatial distribution of the emissions are that the method can be applicable for the whole EMEP domain and that it should guarantee consistency among different compounds. The new methodology follows an aggregated sector approach, so that emissions over Europe from the same sector are distributed according to the same principles. This also guarantees consistency in the spatial distribution of the different pollutants as the same source can emit different compounds.

The sector information has been aggregated following SNAP level 1 because it is at this level of aggregation that most gridded information presently exists. For each sector, we have identified a series of ancillary information that can be used as indicators of the spatial distribution of the emission in the sector. The quality of the ancillary data and their appropriateness as indicators will determine the accuracy of the emission distribution. The new methodology is flexible on its implementation, so that more accurate information can be incorporated as it becomes available to the method. Table 2.1 gives an overview of the ancillary information used for gridding the emissions in each SNAP sector.

Table 2.1: Overview of the ancillary data used to derive the spatial distribution of sector emissions in the new 2004 methodology.

Sector aggregation	**Gridded according to following ancillary data (2004 methodology)**	**Notes**
SNAP 1: Energy Combustion	LPS information for NO_x, SO_x (IER) LPS from countries, when available	Both spatial positions and intensities are presently used
SNAP 2: Residential Combustion	Population (IIASA)	
SNAP 3: Industrial Combustion	50% Population (IIASA) 50% LPS NO_x, SO_x (IER, countries)	Only 4 countries have reported LPS data
SNAP 4: Production Processes	LPS NO_x, SO_x (IER, countries)	Both spatial positions and intensities are presently used
SNAP 5: Extraction Fossil Fuels	GS data for S5 for PM (TNO, CEPMEIP)	
SNAP 6: Solvent and Product Use	Population (IIASA)	
SNAP 7: Road Transport	GS data for S7 for NO_x, if available: or GS data for S7 for PM (TNO, CEPMEIP)	Only 11 countries have reported gridded sector data for NO_x
SNAP 8: Other Mobile Sources	GS data for S8 for NO_x, if available; or GS data for S8 for PM (TNO, CEPMEIP)	Only 11 countries have reported gridded sector data for NO_x
SNAP 9: Waste	XX% Population (IIASA) XX% LPS (IER, countries) XX% Agriculture (S10,TNO, CEPMEIP)	Fractions per country based in CEPMEIP information (see Table 2.3)
SNAP 10: Agriculture & Forestry	GS data in S10 for PM (TNO, CEPMEIP)	

Information on Large Point Source (LPS) locations and emission intensities is used for identifying the position of emissions from sector 1 and sector 4, for all countries. It is also considered that 50% of the emissions from combustion in industry (sector 3) can be allocated to iron, steel and non-ferrous metal industry, thus also distributed according to the information on LPS. The LPS data used at present has been compiled by the University of Stuttgart (IER) and includes both SO_x and NO_x emissions. While LPS SO_x information is used to distribute SO_x emissions, all other gaseous compounds and primary particle emissions are distributed according to information on LPS NO_x. The main difference with respect to the gridding method described last year in Vestreng (2003) is that, in the new methodology, information on the actual intensity of the LPS is used to differentially distribute the sector emissions over a country. When LPS information is reported by the countries, it is checked for consistency with the information from IER and used as ancillary data to distribute emissions from sectors 1, 4 and 3. Table 2.2 provides an overview on national LPS data available in 2004. Only four countries have reported data on LPS and not for all components. The accuracy spatial distribution of sectors 1, 4 and 3 is expected to increase as better and more complete information on large point sources is made available. For example, we are aware that the present method introduces a systematic bias in the spatial distribution emissions in sector 4, as it locates production process emissions following energy combustion. We expect that this bias will be reduced when we are in position to use more refined LPS data that distinguishes between sector emissions and includes all different compounds. Other sources of ancillary data that could be used in the future are information from the EPER database and further LPS data from national reports.

Table 2.2: Overview of official information on Large Point Sources (LPS)[2] reported to UNECE/EMEP and available in 2004.

Country code	CO	NH_3	NMVOC	NO_x	SO_x	PM_{10}	$PM_{2.5}$	Total components
CZ – Czech Republic	1		1	1	1			4
ES – Spain	1	1		1	1			4
MK – TFYR of Macedonia	1			1	1			3
SI – Slovenia	1		1	1	1			4
Total no. countries	4	1	2	4	4	0	0	15

Information on Population (POP) numbers and distribution is a good indicator for emission sources in the surroundings of urban centres. Therefore, population data is used supporting information to distribute emissions from residential sources (sector 2) and emission from solvent and other product use (sector 6). Population is also used to map 50% of sector 3 emissions, as it can be used as a good indicator of the location of electricity and heat production. The population data presently used has been provided by IIASA and therefore it has the additional advantage to be consistent with the data used in the evaluation of impact from air pollution in human health.

[2] LPS are sources over the following yearly intensities: 500 Mg for SO_x, 500 Mg for NO_x, 500 Mg for CO, 10 Mg for NMVOC, 1 Mg for NH_3 and 50 Mg for PM.

Information from the CEPMEIP project (TNO) for PM emissions has been tested for different sectors and found to be a good ancillary indicator for emissions from road traffic (sector 7), other mobile sources (sector 8) and agricultural sources (sector 10) when no other information is available. TNO has used mostly population and to a limited extent also roadmap information to establish the spatial distribution of sectors 7 and 8. Emissions from agriculture are distributed based on farm activity data at high spatial resolution and land use information. Since the information compiled by TNO for the CEPMEIP project (CEPMEIP, 2002) focuses on particulate matter, the activity data is mostly related for poultry farms. The extrapolation of these emission distribution data to other pollutants, introduces a bias for ammonia emissions that we know are mostly related to dairy and pig farms. We hope to be able to correct for this bias in follow-up versions of the gridding methodology, for instance by using FAO statistics and land-use information.

Information on national gridded sector emissions (GS) should be reported every five years to the CLRTAP. However, very few countries report gridded sector emissions. In 2004, only 12 countries have reported gridded sector data and not for all pollutants. When countries have reported GS data, we have compared the official reports with the results of the methodology explained above. The result of the comparison has generally been reassuring for both cases. However, it showed that the national GS data for road traffic emissions and other mobile source generally reproduced better the roadmap network in the country than TNO S7 and S8 data. For this reason, when countries have reported GS data for NO_x (11 countries), that data is used instead of TNO data to consistently derive sector 7 and sector 8 emission distributions for all other pollutants.

The method to map emissions from waste treatment and disposal is necessarily more complex than for other sectors since the activities in sector 9 can include both waste incineration in urban areas and open burning of agricultural waste. In three countries, Azerbaijan, Norway and the United Kingdom, emissions in this sector include also flaring activities in oil platforms although it is an open question whether the emissions should be allocated in sector 9 or rather in sector 5. Population is used as an indicator to distribute waste incineration sources in the country. The distribution of emissions from open burning of agricultural waste is based on the distribution of sector 10. The proportion of sources to either one waste category varies from country to country. We have used CEPMEIP (2002) data on waste activities detailed at SNAP level 2 to determine that proportion of waste emissions. The results are summarised in Table 2.3, where the recommended height of the emissions is also established. For population related waste, low height sources correspond to open waste and high sources correspond to incinerators.

The method summarized in Table 2.1, Table 2.2 and Table 2.3 has been applied to all countries that have not reported gridded sector data for all components. If a country has reported GS data for a component, we compare the reported gridded sector (GS) data with our method results. If there are no obvious inconsistencies, the officially reported GS sector data is directly used. Table 2.4 provides an overview of the countries that have reported in the last four years GS data that has been seen to be used directly in EMEP model applications.

Table 2.3: Overview of indicators used for the spatial distribution of emissions from Sector 9, waste treatment and disposal related activities in each country.

	PERCENTAGE FROM AGRICULTURE related waste	Height of agriculture related emissions	PERCENTAGE FROM POPULATION related waste	Height of population related emissions (High= Incinerators, Low=Open waste)	PERCENTAGE FROM FLARING (Oil and Gas Production)	Height of LPS related emissions
AL	75%	Low	25%	Low	0%	High
AM	50%	Low	50%	Low	0%	High
ASI	50%	Low	50%	Low	0%	High
AT	0%	Low	100%	High	0%	High
AZ	25%	Low	20%	Low	55%	High
BA	50%	Low	50%	Low	0%	High
BE	0%	Low	100%	High	0%	High
BG	75%	Low	25%	Low	0%	High
BY	100%	Low	0%	Low	0%	High
CH	0%	Low	100%	High	0%	High
CY	75%	Low	25%	Low	0%	High
CZ	100%	Low	0%	Low	0%	High
DE	0%	Low	100%	High	0%	High
DK	25%	Low	75%	High	0%	High
EE	100%	Low	0%	Low	0%	High
ES	50%	Low	50%	High	0%	High
FI	50%	Low	50%	Low	0%	High
FR	0%	Low	100%	High	0%	High
GB	0%	Low	90%	High	10%	High
GE	50%	Low	50%	Low	0%	High
GR	75%	Low	25%	Low	0%	High
HR	75%	Low	25%	Low	0%	High
HU	60%	Low	40%	High	0%	High
IE	0%	Low	100%	Low	0%	High
IS	0%	Low	100%	Low	0%	High
IT	0%	Low	100%	High	0%	High
KZ	100%	Low	0%	Low	0%	High
LT	100%	Low	0%	Low	0%	High
LU	0%	Low	100%	High	0%	High
LV	100%	Low	0%	Low	0%	High
MD	100%	Low	0%	Low	0%	High
MK	100%	Low	0%	Low	0%	High
NL	0%	Low	100%	High	0%	High
NO	0%	Low	0%	High	100%	High
PL	25%	Low	75%	Low	0%	High
PT	25%	Low	75%	Low	0%	High
RO	75%	Low	25%	High	0%	High
RU	75%	Low	25%	Low	0%	High
SE	0%	Low	100%	High	0%	High
SI	60%	Low	40%	Low	0%	High
SK	50%	Low	50%	High	0%	High
TR	25%	Low	75%	Low	0%	High
UA	100%	Low	0%	Low	0%	High
YU	75%	Low	25%	Low	0%	High

Table 2.4: Overview of official submissions on the spatial distribution of sector emissions (gridded sector data, GS) available in 2004.

Country code	CO	NH_3	NMVOC	NO_x	SO_x	PM_{10}	$PM_{2.5}$	Total components
AT - Austria	1	1	1	1	1	1	1	7
CH- Switzerland	1	1	1	1	1			5
DE- Germany	1	1	1	1	1			5
DK- Denmark	1	1	1	1	1	1	1	7
ES - Spain	1	1	1	1	1			5
FI - Finland	1	1	1	1	1	1	1	7
GB - United Kingdom	1	1	1	1	1	1		6
LT- Lithuania	1	1	1	1	1			5
NL - Netherlands	1	1	1	1	1			5
NO- Norway	1	1	1	1	1			5
RU - Russian Federation		1						1
SE - Sweden	1	1	1	1	1			5
Total no. countries	11	12	11	11	11	4	3	63

2.3.2 Results and differences with respect to previous years

The new methodology to distribute sector emissions in the EMEP domain has been used in all calculations by the EMEP Unified model carried out in 2004. In the following, we highlight differences in the spatial distribution of emissions with respect to estimates from previous years. It should be noted that the comparison is carried out for two estimates using the exactly the same sector totals and the same total national emissions, so that the differences presented in this section correspond only to the spatial distribution of emissions.

Sector 1

The distribution of sources from power plants and energy combustion has changed significantly in Italy, particularly around Milan area; in France around Paris; in Portugal, Ireland and Belgium. The largest differences however are in Eastern European countries: Croatia, Romania, Serbia and Montenegro, Czech Republic, Slovenia, Slovakia, Poland, Belarus, Ukraine and the Russian Federation. Figure 2.5 shows the distribution and extent of the changes in spatial distribution of power combustion sources with respect to previous years. The figure shows ratios between the old and the new spatial distribution of sources. Red areas indicate places where emissions were assumed significantly higher (by a factor of 5) last year than in the present 2004 estimate. Black points correspond to areas with significantly higher emissions with the present 2004 allocation methods. Blue depicts areas with no significant changes in the spatial distribution of emissions, usually relating either to areas where there exist official reports of gridded sector data or to regions outside the UNECE domain where even ancillary data is difficult to find.

Figure 2.5a) shows changes in emissions of sulphur dioxide. Since sector 1 is the predominant sector for SO_x emissions, changes in the spatial distributions of this sector are particularly relevant for the total SO_x emissions. For other compounds, however, the map of changes looks similar to Figure 2.5a). This is because

changes in NO_x distributions are in this case similar to SO_x and the distribution of CO and VOC emissions from energy combustion have been distributed in the new methodology to be consistent with NO_x emissions, so that the ratio of NO_x/VOC and NO_x/CO remains constant. In the future we might change this, as information from Large Point Sources is updated per component.

The largest difference in the spatial distribution of sector 1 with respect to other components is for PM emissions. For PM_{10} and $PM_{2.5}$, the distribution of combustion sources was before based on TNO-CEPMEIP distributions while now they are based on reported GS and the LPS data either from IER or directly reported by the countries. This secures that primary PM emissions are now distributed consistently with the emissions of the gaseous precursors of PM. Since 95% of PM_{10} emissions from combustion sources is in the fine mode, the changes in Figure 2.5b) are also representative for $PM_{2.5}$.

The reason for changes illustrated in Figure 2.5a) and Figure 2.5b) is the update in the methodology applied to distribute the emissions form energy combustion. Last year, a method was used to re-distribute the emissions from sector 1 according to the position of Large Point Sources, but the emissions were still homogenously distributed among the different LPS in each country. The updated methodology used this year, redistributes all emissions in the sector according to information on the actual intensities of emissions from each LPS. This means that the new distribution of sector 1 differentiates emissions within the countries according to the extent of each individual LPS.

Sector 2

Residential combustion has been gridded according to population for all compounds, as we expect these emissions to occur in urban centres. Differences with previous calculations are evident from Figure 2.6a) in Portugal, Italy, France, Ireland, Slovenia, Poland, Belarus, Czech Republic, Slovakia, Slovenia, Hungary, Romania, Ukraine and the Russian Federation. All these countries have not reported GS data, but in the former methodology the distribution of emissions from this sector was made according to the sector share of reported gridded totals emissions. The use of gridded total emissions even though they are reported by the countries gives rise to inconsistencies. An example is shown in Figure 2.6a) concerning the large changes (red points) in Sicily (Italy). The maximum SO_2 emission area from Italy is situated in Sicily, corresponding to Mount Etna volcanic emissions. In the old methodology, sector emissions were distributed according to grid totals, scaled by the share of each sector to national totals. As a result, a significant part of Italy's residential combustion emissions were placed in Sicily. The new methodology is more correct as it allocates the emissions of sector 2 in urban centres, following population. This is done so even if countries have reported gridded emission totals.

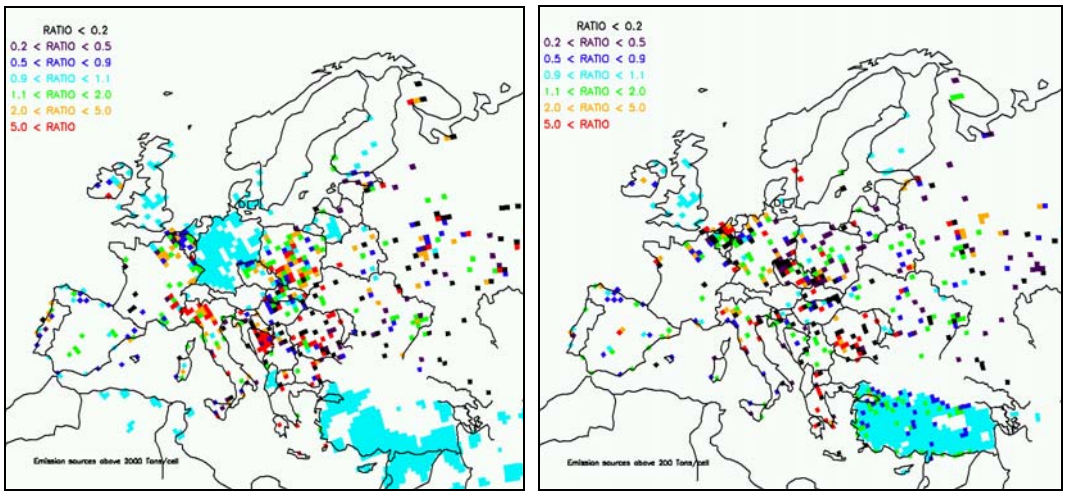

Figure 2.5: Energy Combustion. Differences in the distribution of sector 1 emissions with the new grid methodology: a) SO_x (left panel) and b) PM_{10} (right panel). See text for further explanation.

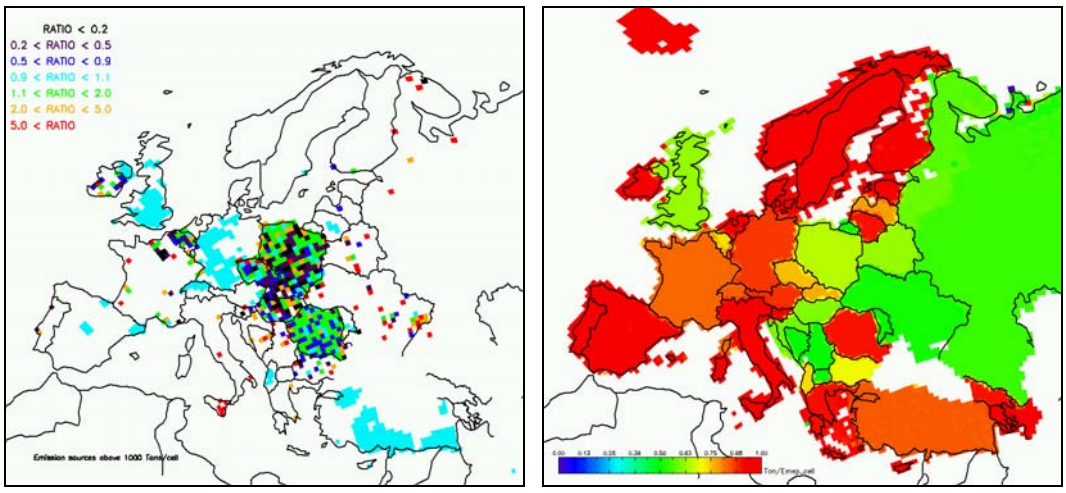

Figure 2.6: Residential Combustion. a) Differences in the spatial distribution of sector 2 SO_x emissions due to the new gridding methodology (left panel). b) Ratio $PM_{2.5}/PM_{10}$ illustrating the consistency of the PM emission in sector 2 (right panel). See text for further explanation.

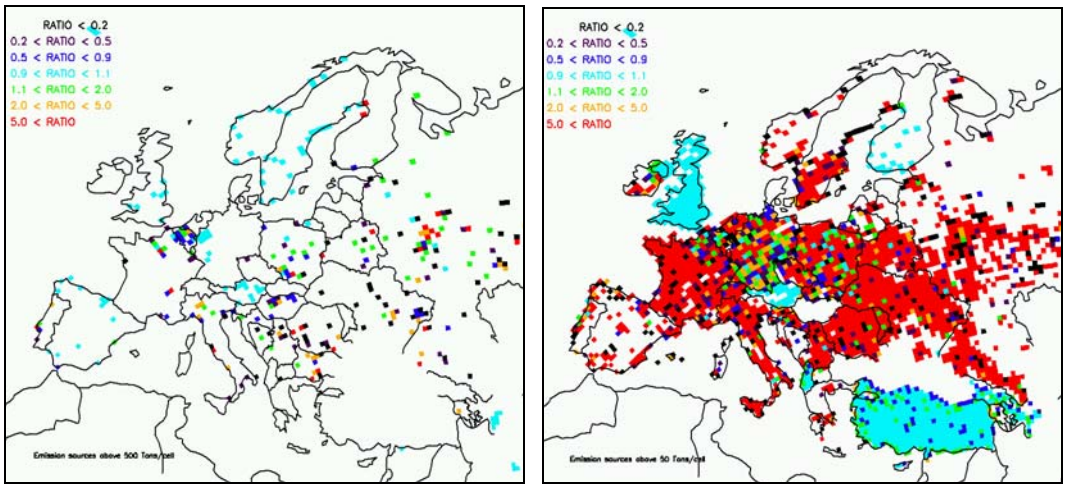

Figure 2.7: Production Processes. Differences in the distribution of sector 4 emissions with the new grid methodology: a) NO_x (left panel) and b) PM_{10} (right panel). See text for further explanation.

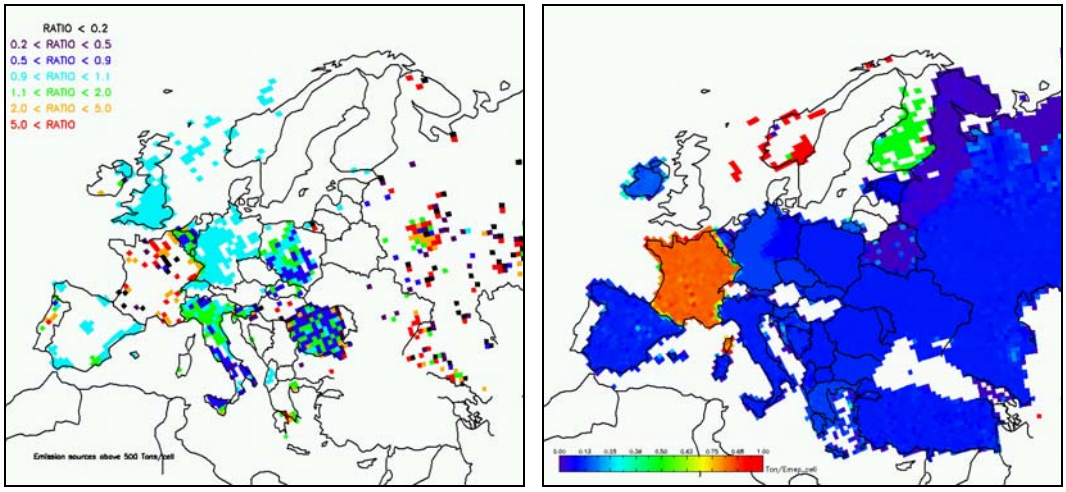

Figure 2.8: Extraction and Distribution of Fossil Fuels. a) Differences in the distribution of Sector 5 emissions with the new grid methodology for VOC (left panel) and b) Ratio $PM_{2.5}/PM_{10}$ illustrating the consistency of the PM emission in sector 5 (right panel). See text for further explanation.

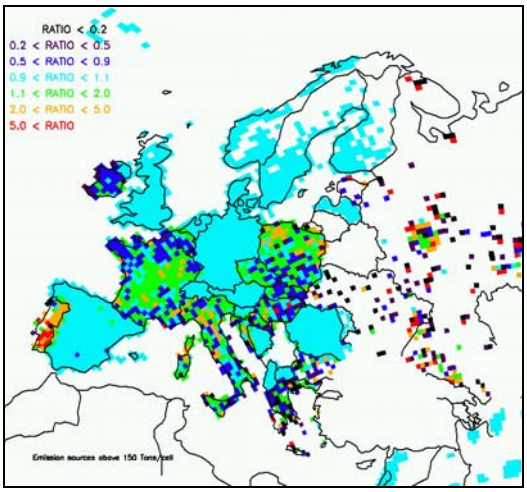

Figure 2.9: Solvents and Product Use. Differences in the distribution of sector 6 emissions with the new grid methodology for VOC emissions. See text for further explanation.

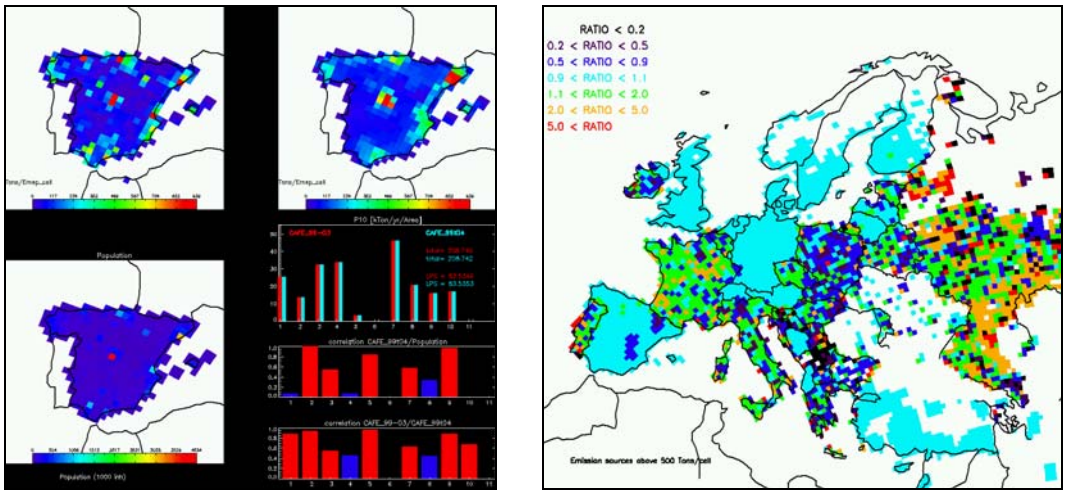

Figure 2.10: Road transport. a) Illustration of methods used to distribute PM_{10} emissions from road traffic in Spain, following TNO S7 data or NO_x GS7 reported emissions b) Differences in the distribution of sector 7 emissions with the new grid methodology for NO_x emissions (right panel). See text for further explanation.

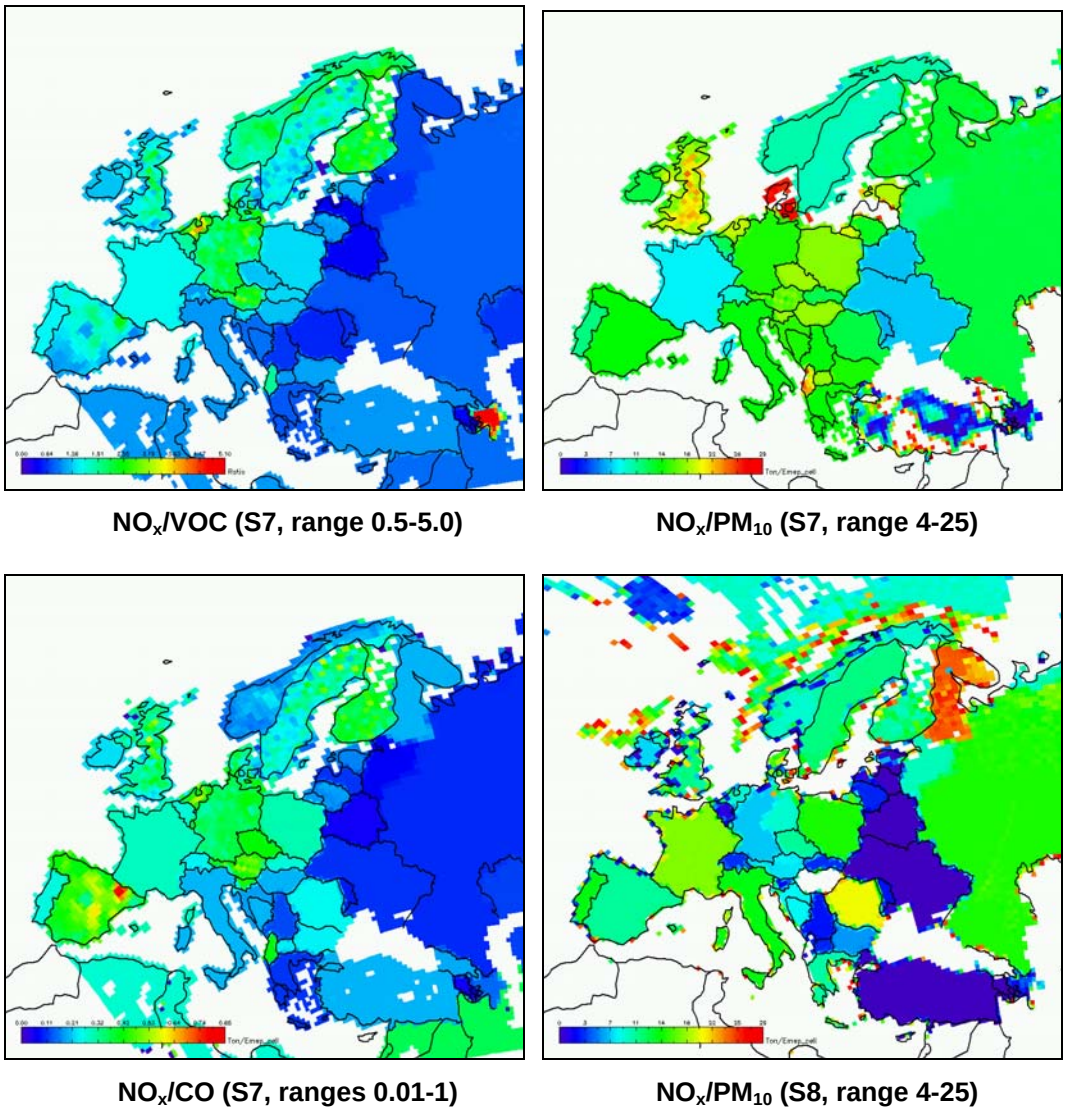

NO_x/VOC (S7, range 0.5-5.0) **NO_x/PM_{10} (S7, range 4-25)**

NO_x/CO (S7, ranges 0.01-1) **NO_x/PM_{10} (S8, range 4-25)**

Figure 2.11: Indicator ratios used to test the consistency of the emissions from different compounds for traffic sector 7 and sector 8. See text for further explanation.

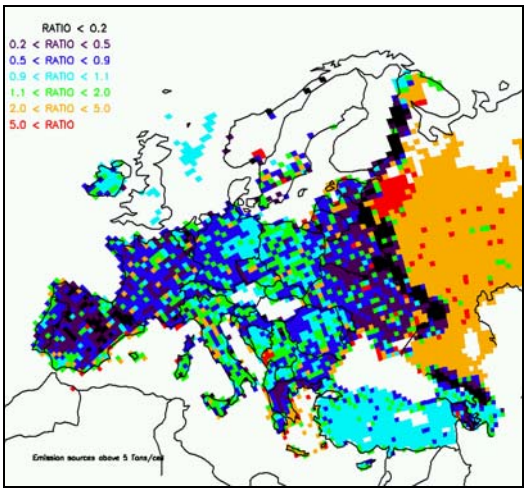

Figure 2.12: Waste. Differences in the distribution of sector 9 emissions for PM_{10} with the new grid methodology. See text for further explanation.

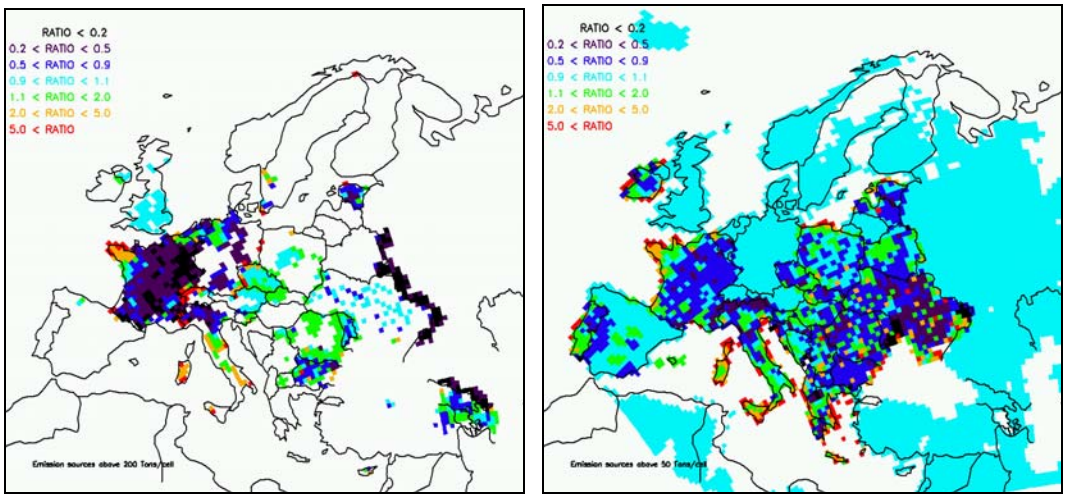

Figure 2.13: Agriculture & Forestry. Differences in the distribution of sector 10 emissions with the new grid methodology for a) PM_{10}-TNO S10 update (left panel) and for b) NH_3 emissions (right panel) and. See text for further explanation.

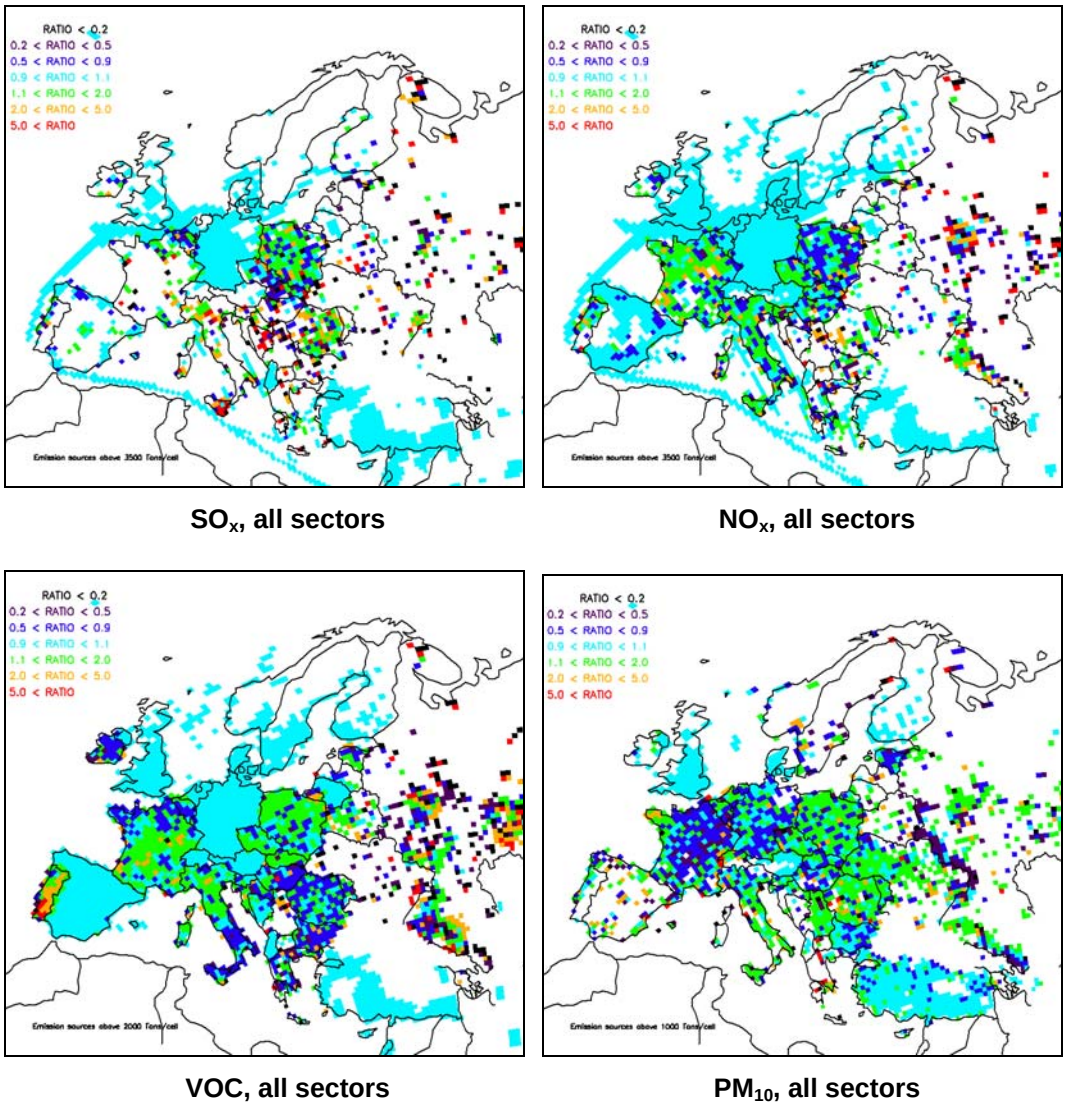

SO_x, all sectors **NO_x, all sectors**

VOC, all sectors **PM_{10}, all sectors**

Figure 2.14: Differences in the distribution of SO_x, NO_x, VOC and PM_{10} emissions for all sectors with the new grid methodology. See text for further explanation.

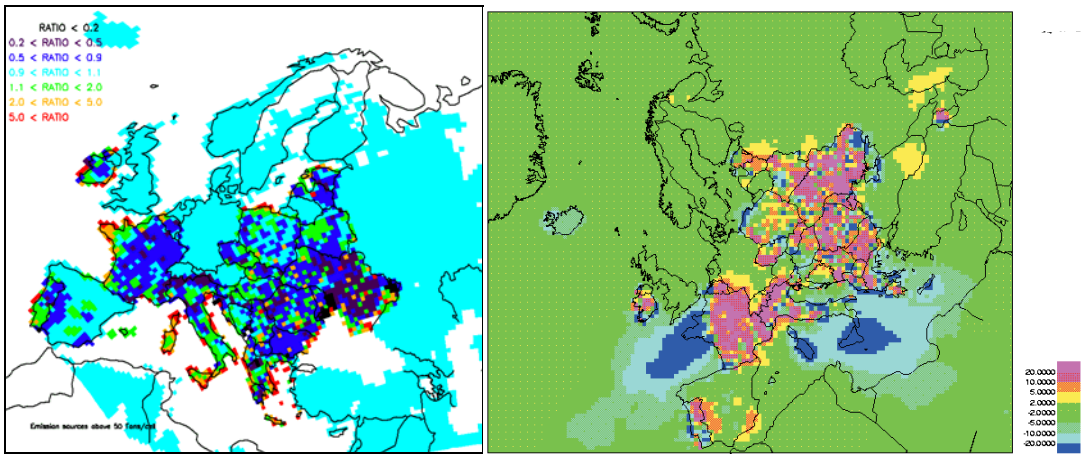

Figure 2.15: Comparison of emission distribution changes in ammonia emissions from S10 (left panel) and the corresponding changes in air concentrations of NH_3+NH_4 in air (right panel) from EMEP model calculations in Fagerli (2004).

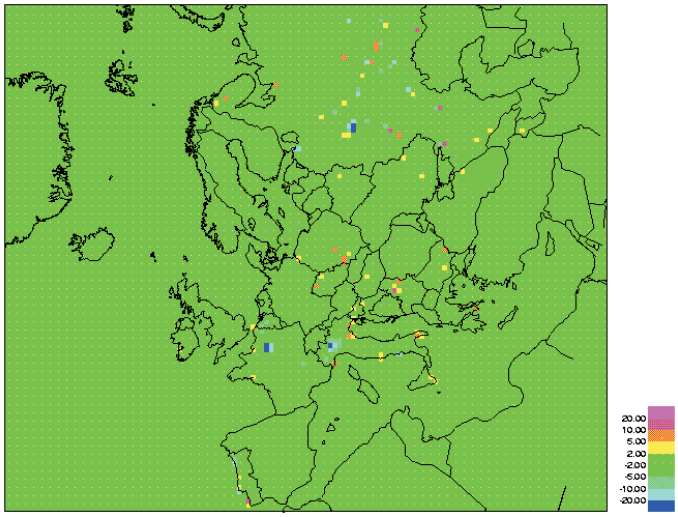

Figure 2.16: Percentage changes in yearly mean ozone concentrations due to changes in the distribution of emissions using the new gridding methodology. See text for further explanation.

For PM, emissions from sector 2 follow also population distribution and are consistent with the gaseous pollutants. To analyse the consistency of the PM emissions across Europe we have checked the ratio between $PM_{2.5}$ and PM_{10}. The $PM_{2.5}/PM_{10}$ ratio from sector 2 emissions gives an indication of the relative importance of combustion of gas, oil, wood and coal burning for residential purposes in each country. We can expect a larger fraction of $PM_{2.5}$ in gas and oil burning, and a larger content of fly ash (PM_{10}) in wood and coal burning. Therefore, we can expect a lower ratio in Eastern European countries that in Western European countries. The results of the test depicted in Figure 2.6b) show an average ratio of 0.5 in Eastern European countries and of 0.95 in Western European countries, as expected for sector 2.

Sector 3

The same type of differences in the spatial distribution of sector 1 and sector 2 are found also in the distribution of industrial combustion sources. Changes affect the same countries as in Figure 2.5 and Figure 2.6, and for the same reasons as explained above: the new methodology makes a consistent use of ancillary data for all components and countries that have not reported GS data, it does no longer use gridded totals information and it explicitly uses information on LPS intensities instead of only their locations.

Sector 4

Figure 7 shows differences in the spatial distribution of emissions from non-combustion production processes. The differences respond to the present use the total information on LPS, allocating also the intensities, and not only positioning as it was done before. However, the methodology used still needs to be refined for emissions from this sector: we are allocating non-combustion processes according to energy combustion information and this can give rise to inaccuracies. It is important to compile more detailed ancillary data from LPS (IER, country reports, EPER) so that it includes also sector emission information.

Emissions from production processes are less significant for total SO_x, NO_x emissions than for PM_{10} and $PM_{2.5}$. However, it is for PM emissions that we found the largest differences between the two gridding methods (see Figure 2.7b)). The reason for the largest differences for PM_{10} (and $PM_{2.5}$) data is that the old methodology used TNO-CEPMEIP data while we are now using NO_x LPS data from IER or countries. TNO-CEPMEIP included a series of area sources in this production sector that are now concentrated in LPS areas. As mention above, it is difficult to say how accurate is the new description of sector 4 sources because of the ancillary data used has its obvious limitations. Figure 2.7b) shows, for example, that the new methodology misplaces cement factories in Spain while the TNO-CEPMEIP distribution seemed to be more in line with the actual source distribution. How important these problems are for the modelled concentrations fields of PM matter, needs to be investigated further.

Sector 5

Sector 5 emissions are related to mining and fuel extraction. Emissions from this sector are significant for VOC and PM. We do not expect emissions from NO_x and SO_x and NH_3 reported in this sector and only low values of CO emissions from oil fields. Figure 2.8 shows the differences in the distribution of VOC emissions due to the use of the new methodology. The new methodology uses gridded sector emissions for sector 5 from TNO-CEPMEIP emissions of PM to distribute the VOC, thus securing the consistency of the emission spatial distribution among pollutants. In the old method, distribution of pollutant emissions in sector 5 was done according to gridded total distributions. The old methodology systematically located VOC emissions close to urban centres. This was because the main contributors to VOC emissions are solvent and paint industry and transport emissions, all of them normally situated around city/urban centres and adjacent roads. Figure 2.8a) shows that the new methodology consistently moves VOC emissions from sector 5 away from city centres.

PM emissions from sector 5 are mostly due to dust fugitive emissions from mining and are dominantly in the coarse mode. Only a small fraction of the PM emissions from sector 5 are emitted as $PM_{2.5}$. Again, the analysis of the ratio between $PM_{2.5}$ and PM_{10} is a good test of the consistency of PM emissions reported in both modes. The average value for $PM_{2.5}/PM_{10}$ emissions from sector 5 over Europe is 0.15. Figure 2.8b) identifies France, Finland and Norway as outliers in the estimated PM emissions for sector 5. Bilateral discussions with national emission experts from these countries are further required to clarify the possible inconsistencies.

Sector 6

Emissions from solvents and product use generally represent about 30% of the total VOC emissions. Emission from this sector are located in the new methodology according to population, and therefore systematically moved towards urban centres. The differences with the old methodology that located these emissions according to grid total emissions are shown in Figure 2.9. Since about 40% of VOC emissions originate from traffic (both road and off-road), gridding by total emissions involved systematic biases that are now corrected. We do not expect any significant contribution to emissions from other pollutants in this source sector.

Sector 7

The present methodology to allocate emissions from road traffic uses reported gridded sector data for NO_x for distributing all other pollutant emissions in this sector. However, only 11 countries have reported gridded sector emissions from NO_x. For countries that have not reported the gridded sector data for NO_x, TNO-CEPMEIP emission distribution for PM_{10} in sector 7 are used instead as tracers of the road traffic distributions. Figure 2.10 shows examples on the changes in the gridded emission distribution when using different methods.

The upper left panel in Figure 2.10a) shows the distribution of PM_{10} emissions from sector 7 with TNO-CEPMEIP. It can be seen these emissions are spatially correlated with population by comparing with the population map in the lower left panel. The upper right panel in Figure 2.10a) shows the spatial distribution of PM_{10} emissions using official gridded sector 7 data for NO_x (NO_x GS7) to allocate the emissions. The NO_x GS7 method is not highly correlated with population as indicated in the lower left panel in Figure 2.10a). In fact, the distribution of PM_{10} emissions using the official NO_x GS7 data corresponds much better to the distribution of traffic volumes and roadmaps from Spain. The same applies to all other pollutants: NO_x GS7 is better indicator to grid road transport emissions than the TNO S7 method that relates PM in traffic more to population than the actual roadmaps. Still, only 11 countries have reported gridded sector NO_x, so the TNO-CEPMEIP distributions have been generally used. Despite its limitations, the use of the new method is more adequate than the previous use of gridded total data, as illustrated for NO_x in Figure 2.10b).

The reason for the superiority of the new method is that about 30% of NO_x emissions are related to combustion and not only to traffic emissions. The old method distributed traffic emissions according to gridded total data and could

therefore erroneously locate traffic emissions in areas with power plants. Such erroneous distribution of NO_x emissions in some particular areas gave rise to inconsistencies with VOC emissions and had consequences for the calculation of ozone concentrations. The new method avoids this type of inconsistencies and secures that emissions from the same sources are distributed equally for all pollutants.

To test the robustness of the new method and check the consistency of the results, we have calculated the ratios between NO_x, PM_{10}, VOC and CO all from road traffic emissions and compared these to COPERT III and European Auto Oil vehicle fleet/activity data for year 2000.

The first ratio analysed is NO_x/VOC. This ratio is significantly affected by the proportion of diesel-powered vehicles (e.g., heavy duty vehicles or diesel passenger cars) in the overall road transport fleet. A higher presence of diesel will tend to increase the ratio of NO_x to VOC. For the mix of vehicle technologies in the EU in year 2000, COPERT results indicate a range of between 4.5 (100% Diesel) and 0.75 (100% Gasoline). The upper left panel in Figure 2.11 shows the values of the NO_x/VOC ratio when applying the new methodology for gridding emissions. There are interesting variations in the ratios within European countries that have reported emission GS data indicating the differences on the type of vehicles circulating in different roads. Averaged values over EU15 are 1.1-2.0 and about 0.8-1.3 in EU10+, corresponding well with COPERT estimates.

In Eastern Europe, the situation is different as the vintage of the vehicles is old thus lowering the NO_x/VOC ratio in EEE countries down to 0.5 (typical of pre-catalyst passenger cars). Armenia appears to be a special case, with NO_x/VOC ratios up to 5, which could be due to a dominating presence of old diesel trucks in the country.

The next ratio analysed and compared to COPERT results is NO_x/PM_{10}. The ratio NO_x/PM_{10} is again indicative of the type of vehicle and type of fuels used. Gasoline cars generate NO_x emissions but little PM_{10} (at least in terms of mass)[3] while for diesel vehicles both PM_{10} and NO_x are emitted. Consequently, the overall NOx/PM10 ratio will be higher in situations with a larger proportion of gasoline powered vehicles in the overall fleet. The vintage of the vehicles also a role, since older heavy duty diesel technology, of the type still present in Eastern Europe; emit significantly emissions of PM_{10}.

Typical NO_x/PM_{10} ratios in Western Europe are about 20; somewhat higher in countries with lower percentages of diesel vehicles (like the United Kingdom, where the ratio is about 25) and lower for countries with high penetration of diesel vehicles (like Spain, with 15; and France with 11). The old diesel vehicles from Armenia and other Eastern European countries tend to emit significantly more PM_{10} (but not NO_x) and the ratios can then be about 4, according to COPERT. In the Russian Federation, a combination of use of old vintage gasoline cars and

[3] In many cases, the mass emissions of particulate matter from gasoline powered vehicles are ignored in determining overall emissions from road transport. For example COPERT III does not provide an emission correlation for particulates from gasoline vehicles.

smaller old diesel trucks could explain a NO_x/PM_{10} ratio of about 15. The right upper panel in Figure 2.11 shows the results for the emission estimates used in EMEP that correspond well with the COPERT estimates.

The last ratio analysed is NO_x/CO, which again is indicative of the type of vehicles and fuels used in a country and should be consistent with the other two ratios. Diesel vehicles emit considerably less carbon monoxide than gasoline cars. Typical ratio values in EU25 according to COPERT are $NO_x/CO=1$ (100% diesel) and 0.1 for (100% gasoline). The values derived from EMEP are lower but show the higher values in countries where diesel powered vehicle are more dominant, and lower values in countries where this is not so.

In Eastern Europe, the vintage of the cars is older. For old gasoline cars (pre-catalyst), COPERT estimates a significantly lower NO_x/CO ratio, down to 0.05. The values in EMEP in Eastern Europe are consistent with this low ratio, consistent with the NO_x/VOC and NOx/PM10 ratios that already indicated a high presence of old gasoline vehicles. The only inconsistency is in Armenia. The NO_x/VOC ratio in Armenia was very high which indicated a generalised use of old diesel trucks in the country. According to COPERT, the NO_x/CO ratio for old diesel trucks should be around 2. However, Armenia reports NO_x/CO of 0.02, more in line with other Eastern European countries. Bilateral discussions with national experts should help to clarify these values.

In general, the ratio values derived from EMEP emissions correspond well with COPERT estimates. An overview of the comparison between COPERT estimates and the ratio values derived from EMEP emissions is given in Table 2.5 for road transport emissions.

Table 2.5: Summary comparison of COPERT and EMEP derived estimates for pollution emission ratios from road traffic.

	NO_x/VOC	NO_x/PM_{10}	NO_x/CO
EU 15 - COPERT	1.1-2.0	10-25	0.3-0.4
EU 15 – EMEP use	1.1-3.0	8-25	0.1-0.5
EU10+ - COPERT	0.8-1.3	8-15	0.2-0.4
EU10+ – EMEP use	0.6-1.2	8-25	0.2-0.5
EEE -COPERT	0.5-0.75	4-10	0.05-1 (2)
EEE – EMEP use	0.5-0.8 (5)	4-15	0.01-0.3
Expected ranges	0.5-5.0	4-25	0.01-2

Sector 8

The methodology to distribute emissions of off-road traffic and machinery is the same as for road traffic emissions. If countries have reported gridded sector information for NO_x, the distribution is used as basis for distributing the other pollutants, otherwise PM_{10} information from CEPMEIP (sector 8) is used. The resulting differences between the new and old methodology resemble those for sector 7 and therefore are not shown. Emissions from ship traffic are included in

this sector but the present methodology does not imply any changes in the spatial distribution of shipping sources. Both the spatial distribution and the intensity of international sources in sector 8 require a careful re-evaluation as there are identified inconsistencies in the reporting of these emissions from the countries. However such re-evaluation is beyond the purpose of this study.

As for traffic emissions, we have calculated NO_x/VOC, NO_x/PM_{10} and NO_x/CO ratios and compared them to COPERT results in order to check the consistency of the results. For emissions in sector 8, we expect a more generalised use of diesel in off-road transport than in road traffic emissions. Thus, we expect lower values in the ratio NO_x/PM_{10} in all countries than those calculated for sector 7. The lower right panel in Figure 2.11 shows the ratio NO_x/PM_{10} in sector 8. Comparing this with the upper right panel in Figure 2.11, we see that the ratio decreases in general, as expected. It is interesting to note the anomalies in port areas and also in Turkey. Turkey is the only country where the new methodology has not been applied consistently because of lack of ancillary information. Further efforts should be dedicated in the short term to fully include Turkey in the new gridding methodology. The high NO_x/PM_{10} ratios in port areas are another example of the inconsistencies in international shipping data in sector 8 and require, as already mentioned, a special separate study.

Sector 9

This is the sector where the new methodology has introduced the largest variations with respect to previous year's estimates. The contribution from waste treatment and disposal to emission totals is below 5% for most gaseous emissions, and about 5% for primary PM emissions. Consequently, the change from a gridded total scaling approach to the new methodology has introduced significant changes in most countries, even though the influence of such changes in the distribution of total emissions will be small. The new methodology uses population as indicator to distribute waste incineration in urban areas and agricultural activities from CEPMEIP as indicator for agricultural waste. In addition, some few countries include flaring activities in this sector. The resulting changes between the two methods are presented in Figure 2.12. A significant feature in this picture, presently under bilateral discussion with TNO, is that agricultural activities from the Russian Federation are moved with the new methodology towards the European borderline. Further refinement of sector 9 gridded distribution will depend on the availability of ancillary data and/or national information on gridded sector data.

Sector 10

In the new methodology, emissions from agricultural sources are re-arranged according to TNO-CEPMEIP data for sector 10 which in turn is based on farming activities and land-use information. We do not expect emissions of other gases than NH_3 emitted in this sector, as explained in section 2 above when discussing IIASA's revised sector distribution. Ammonia emissions from agriculture are mainly related to dairy and pig farms while for PM, about 2/3 of all emissions originate in this sector from poultry farms. This difference can give rise to a systematic bias in the spatial distribution of ammonia emissions but such bias is considered to be small, as in most countries farming activities areas are

collocated. The advantage of the new method is that it can be applied to the whole of Europe and that is guarantees the consistency of primary PM emissions and gaseous precursors.

In 2004, TNO elaborated a new estimate of the spatial distribution of agricultural emissions (Visschedijk, pers. comm.) for use as ancillary data in the new gridding methodology. The new TNO S10 estimate differs considerably from previous estimates in France, Italy and the Russian Federation, as illustrated in Figure 2.13a). In particular, for the Russian Federation, official gridded data for NH_3 is available to EMEP and the distribution of agricultural sources differs with the new TNO S10 but is more in agreement with previous CEPMEIP distributions. For NH_3, the spatial distribution of emissions follows the reported data in the Russian Federation and therefore, no changes are made in this country with respect to the previous distributions (Figure 2.13b). However this implies that PM_{10} and NH_3 emissions are not consistent in Russian Federation, especially along its borders with other Eastern European countries. As already mentioned, the updates in S10 emission distributions are presently under discussion and we trust that bilateral discussions with TNO will provide a solution and an explanation for the Russian Federation emissions.

2.3.3 Significance of the new spatial distribution methods for the calculation of air concentrations and depositions

Initial tests with the Unified EMEP model have been carried out to determine the significance of the new spatial distribution of emissions in the model results. The model has been run twice, with the same sector and national emission totals but using the old spatial distribution in the first run and the new spatial distribution in the second run. Work is in progress to analyse the differences and initial results are presented in Chapter 5 in the status report on acidification, eutrophication and ground level ozone (Fagerli, 2004). Here, only some preliminary conclusions are summarised.

The spatial differences in the sum of all sectors are driving the changes in the model results. The individual sector distributions affect the model calculations mostly through the related height of emissions to the atmosphere. Figure 2.14 shows the spatial differences for all sectors for SO_x, NO_x, VOC and PM_{10}. Since 95% of ammonia sources originate from agriculture-related activities, the spatial differences for all sectors for NH_3 correspond well to the changes illustrated in Figure 2.13. To facilitate the comparison, spatial distribution changes for ammonia emissions and ammonia and ammonium concentrations in air are depicted in Figure 2.15. As for all other studied primary pollutants, the concentration changes for NH_3+NH_4 spatially correspond with the emissions changes.

The largest differences in the spatial distribution of emissions are for primary PM. This is because there are considerable changes in the spatial distribution of emissions from source sectors that contribute significantly to the total emissions of PM mass, namely sectors 4, 7 and 10. For gaseous emissions, the contribution of sources from sectors 4 (production processes) and 10 (agriculture and forestry) are generally below 12-14%, for primary PM emissions the contribution of these two sectors to total emissions is 20% for $PM_{2.5}$ and 30% for PM_{10}. While the

changes in the distribution of sources from road traffic are an obvious improvement in the new methodology, there are recognised limitations in the new methodology results for sector 4 and sector 10. The implications of these are presently under evaluation.

The initial study is presented in EMEP Status report 1/2004 (Fagerli, 2004) for gaseous compounds indicates that the changes in the air concentrations of pollutants due to the proposed re-distribution of emissions can be significant. For annual averages of SO_2 and NH_3+NH4 concentrations in air changes can be over 20%. For nitrate and sulphate, the changes in some areas can be up to 10-20%. For ozone, changes become more significant in the vicinity of cities. For example, the changes in VOC and NO_x emission distributions around Paris and Milan, imply changes in the mean ozone concentrations up to 20% (see Figure 2.16). This is most relevant for population impact studies.

It will be difficult to validate the changes in the emission distribution through comparison of model results with observations, because the most significant changes are in Eastern Europe, that is, in areas where there are few available monitoring results. However, the initial analysis of the derived concentrations indicates that the new spatial emission generally improves the spatial correlation of modelled results with observations. Further work will continue in this direction but the initial results are reassuring for the validity of the new emission gridding method.

2.4 Conclusions

All model calculations, source-receptor studies and scenario analysis carried out in 2004 with the Unified EMEP model use the same basic assumptions on the spatial distribution of emission sources. All calculations have also assumed the same basic sector distribution per pollutant and per country. The basic national sector distribution has been revised and updated by IIASA through bilateral discussions with the Parties. Scenario runs and source-receptor calculations have used the 2010 and 2020 national projections developed by IIASA under the EU CAFÉ_BASELINE project (see Chapter 5 in this report, Amann et al., 2004). Status calculations for 2002 and model runs for previous years have used national emission totals as reported by the Parties and revised by MSC-W in co-operation with ETC/ACC (Vestreng et al., 2004).

Changes on national emission totals in 2002 are small with respect to 2001. For all main components and primary particle emissions, national emission changes in the EMEP domain are below 1%. For individual countries and components, changes in the national emissions are generally below 20%. For sector distributions, the adopted new distribution introduces the largest changes in ground-based sectors for primary PM emissions: residential combustion and traffic emissions, both in the vicinity of population centres. The new sector distribution resolves a series of identified inconsistencies in the sector allocation of emissions reported by the countries.

Significant changes with respect to previous calculations especially concern the spatial distribution of the emissions. A new methodology has been applied that ensures consistency in the location of sources for different pollutants across the

whole EMEP domain. For the first time since CEPMEIP emissions where introduced in EMEP modelling, the distribution of primary PM emissions is now generally consistent with the emissions of PM gaseous precursors.

The new methodology relies on validated official gridded sector GS data reported from the Parties and on ancillary information on population, large point source (LPS) intensities and locations, traffic patterns, agricultural activities and land-use. Differences in the spatial distribution of emissions are considerable for all source sectors and can be well above a factor of 5 in single areas. Countries that have not reported consistent gridded sector GS information are those more affected by the changes in spatial distribution of emissions derived from the new methodology. Changes are most significant in France, Italy, Ireland, Portugal and the Eastern European countries.

The main reasons for the differences are that the new methodology: a) makes a consistent use of ancillary data on for all components and countries that have not reported GS data, b) it does no longer use gridded totals information and c) it explicitly uses information on LPS intensities instead of only their locations. The generalized use of official gridded total information in the old methodology introduced considerable inconsistencies among pollutants and had consequences for the model derived air concentrations and depositions. Recognised examples are the imbalances in the distribution of NO_x and VOC emissions in urban areas that area now corrected with the new methodology

To check the validity of the new methodology and the robustness of the results we have identified a series of relevant pollutant ratios and tested them against independent emission estimates. In particular, for traffic emissions, the comparison of the derived NO_x/VOC, NO_x/PM_{10} and NO_x/CO ratios with COPERT results has been reassuring for the gridding of traffic emissions.

Initial tests with the Unified EMEP model have been carried out to determine the significance of the new spatial distribution of emissions in the model results and its validity in comparison with observations. In general, the new spatial distribution can imply up to 20% changes in the modelled concentrations and depositions. Although it is difficult to validate the changes in the emission distribution since the most significant changes are in Eastern Europe or in areas where there are few available monitoring, the initial analysis of the derived concentrations indicates that the new distribution of emissions generally improves the spatial correlation of modelled results with observations.

The accuracy of the new methodology depends on the quality of the ancillary data used to distribute the emissions. It is intended to continue updating and improving such information in the future, especially concerning non-combustion sources in sector 4 and agricultural activities in sector 10, where the present methodology has recognised limitations. In the process of updating the ancillary information, co-operation with national experts will be essential and we hope that the presentation of this new methodology will also encourage the national elaboration of gridded sector data.

3. Model assessment of particulate matter in Europe in 2002

by Svetlana Tsyro

3.1 Introduction

In line with recommendations specified in the last year PM report (EMEP Report 4/2003) and given by the workshop of Task Force on Measurements and Modelling to Review and Evaluate the Unified EMEP Model, held 3-5 November 2003 in Oslo, further efforts have been made in 2003-2004 to improve model calculations of particulate matter (PM). In this chapter, the most recent model calculation results and their validation is presented with emphasis on the progress made since last year with respect to PM model results.

Model assessment of concentrations of particulate matter in 2002 has been made using the latest version of EMEP model and applying improved emission inventories. Our calculations show that in 2002, regional PM_{10} concentrations exceeded the 24-hour limit value of 50 $\mu g/m^3$ for the protection of human health (EU first Daughter Directive) in more than 35 days in several locations.

This chapter also presents the evaluation of model performance with respect to PM_{10} and $PM_{2.5}$ concentrations against observation data. Moreover, calculated PM chemical composition and the concentrations of individual aerosol components are validated with available measurements. Although the amount and quality of PM observations has been progressively increasing, available PM measurement data is still insufficient for proper evaluation of the model performance, both with respect to its geographical coverage and appropriate completeness (e.g. PM chemical speciation). In particularly, the need for co-located and concurrent measurements of PM components is highlighted.

Responding to the TFMM recommendation, the particular attention in this chapter is given to the following issues:

Particle-bound water in PM

The EMEP models, as most other state-of-art models, underestimate observed ambient concentrations of particulate matter. This is because the scientific understanding of processes and sources relevant to PM is still under development. In 2002, the aerosol model underestimates $PM_{2.5}$ and PM_{10} concentrations by 42% and 50% respectively. The model underestimation of observed PM concentrations could be partly due to particle-bound water present in PM measurements with gravimetric methods, but which is not accounted for in the model previous versions. The new model version calculates the water content of $PM_{2.5}$ and PM_{10} for specific conditions required for filters equilibration (20ºC temperature and 50% relative humidity) that allows estimating the contribution of particle-bound water to PM mass. It is calculated that aerosol water content in gravimetrically determined $PM_{2.5}$ and PM_{10} mass is 20% to 35% on average. However, there are caveats to this estimate as no verification of this water content is presently available. Accounting for particle water in model calculated PM has been shown

to improve the correspondence between model results and observation: the model underestimation of $PM_{2.5}$ and PM_{10} decreases to 19% and 33% respectively and, interestingly, the temporal correlation increases at the most of stations.

Improved PM emissions

The main recent improvements of $PM_{2.5}$ and PM_{10} emission data concern their spatial distribution and sector disaggregation (see Chapter 1 in this report), and also chemical speciation of $PM_{2.5}$ emissions based on work by Kupiainen et al. (2004). The effect of improved PM emissions on $PM_{2.5}$ and PM_{10} concentrations is initially analysed here, focussing on calculated concentrations of elemental carbon (EC). Using the new emission data, model calculated EC is on average 49% lower than measured EC. One of the reasons is that the model calculates fine EC as IIASA emissions of EC in PM_1 have been used, while no data on coarse EC emissions was available. The spatial correlation between calculated and measured EC is good (0.88). However, the temporal correlation coefficients between modelled and measured EC concentrations vary broadly. The validation of PM emissions is in progress, but the initial results indicate that further efforts should be made to improve the quality of PM emission data. In particular, distribution of PM emissions between different sectors needs further analysis. Also, the work should be continued on describing the chemical speciation of PM emissions.

3.2 Concentration distribution of $PM_{2.5}$ and PM_{10} in 2002

As indicated by WHO Task Force on Health, fine PM mass is (still) an appropriate indicator for assessing health effects, even though toxicology suggests a particular importance of heavy metals, certain organic compounds (e.g. PAHs), endotoxins and ultra fine (UF) particles. Also, the coarse fraction of PM is linked to some morbidity endpoints, probably independent of fine PM (Schneider, 2004). Therefore, assessment of the concentration levels and composition for both $PM_{2.5}$ and PM_{10} is presented in this report.

Calculations presented in this report have been performed with the latest version of the EMEP aerosol model, which is a part of the EMEP Eulerian Unified model system. The description of the model and documentation on its recent development can be found in Simpson et al. (2003) and EMEP Status report 1/2004 (Fagerli et al., 2004). The updated and reviewed emission data has been employed in the model calculations. The national total emissions of aerosol gaseous precursors and primary PM_{10} and $PM_{2.5}$ used in the calculations are as reported in Chapter 1 in this report. Furthermore, the recently developed by IIASA emission inventory for fine OC and EC has been used to describe the chemical composition of $PM_{2.5}$ emissions (Kupiainen et al. 2004).

The geographical distribution of annual mean concentrations of PM_{10} and $PM_{2.5}$ in 2002, as calculated with the EMEP aerosol model and measured at EMEP sites, is presented in Figure 3.1 (upper and middle panels). In addition, mean PM_{10} concentrations obtained during NILU coordinated OC/EC campaign are shown in the lower panel in Figure 3.1. Within this campaign (Chapter 1.2), PM_{10} concentrations were measured one day a week in the period from 1 July 2002 to 1 July 2003.

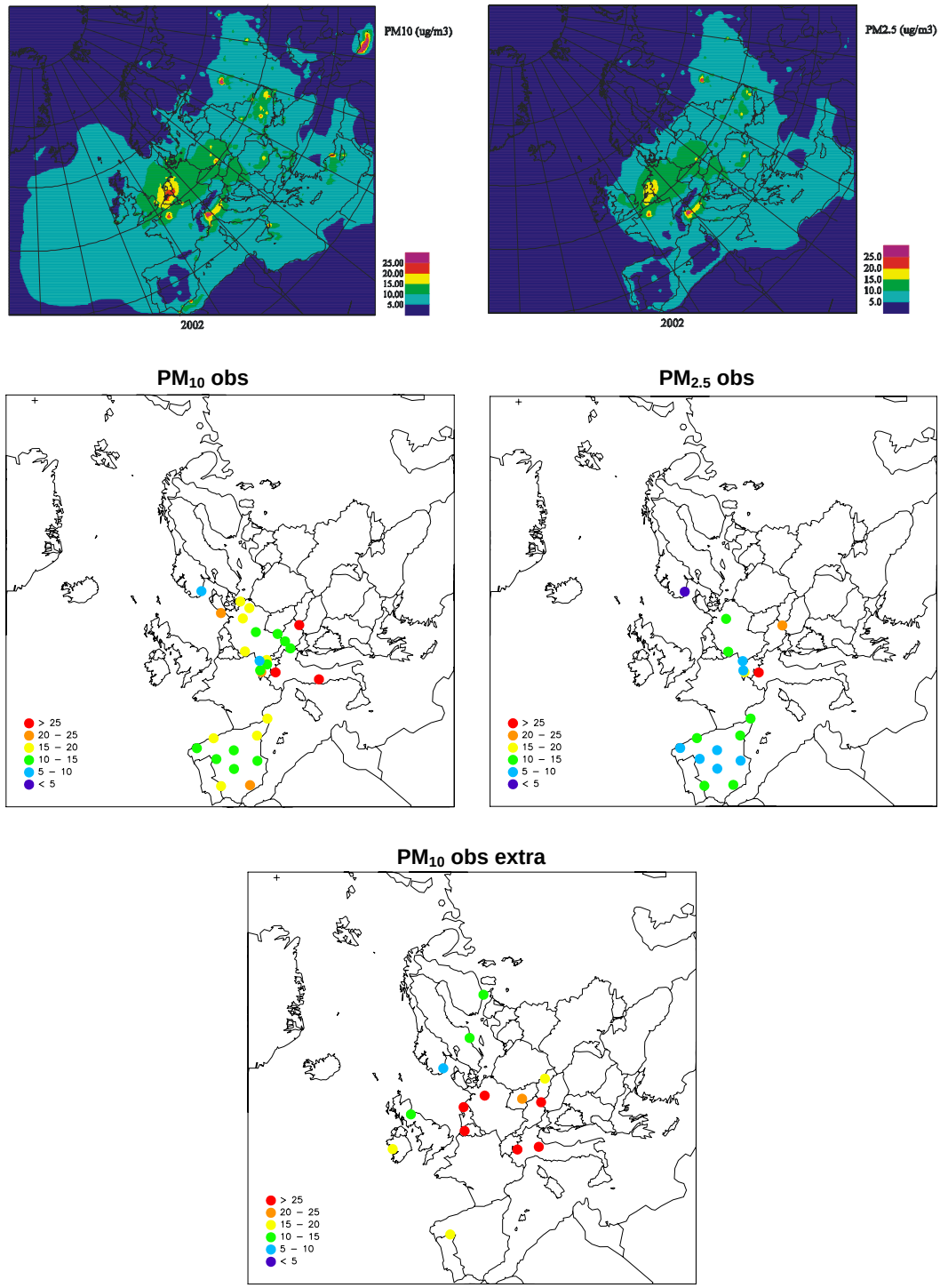

Figure 3.1: Model calculated (upper panel) and observed (middle panel) annual mean concentrations of PM_{10} and $PM_{2.5}$ in 2002; and mean PM_{10} concentrations collected one day a week from July 2002 to June 2003 within the EMEP OC/EC campaign.

Model results and observations agree that the highest average PM_{10} and $PM_{2.5}$ concentrations in 2002 occurred in the Netherlands and Northern Italy. Figure 3.1 reveals that the model calculates PM_{10} and $PM_{2.5}$ concentrations lower than observed mostly everywhere, with the greatest underestimation found in Spain, Italy and Switzerland. It should be pointed out that except for the contributions of sea salt and sulphate aerosols formed from DMS emissions from the seas, the model only accounts for the anthropogenic fraction of PM, whereas ambient PM may include significant natural contributions (e.g. carbonaceous aerosols and mineral dust). Moreover, please, note that the calculated PM_{10} and $PM_{2.5}$ concentrations plotted in Figure 3.1 do not take into account the content of particle-bound water (henceforth referred to as dry PM_{10} and $PM_{2.5}$ concentrations), whereas the measured PM concentrations are likely to include aerosol water. Several plausible reasons for the discrepancy between model results and observations will be discussed in the following sections.

Figure 3.2 shows for each grid cell a number of days with calculated for 2002 PM_{10} concentrations exceeding the limit value of 50 µg/m^3. According to the EU Council Directive 1999/30/EC, this 24-hour value is not to be exceeded more than 35 times a calendar year. Even though the model underestimates PM_{10} concentrations, our calculations show the number of exceedance days for PM_{10} close to and above 35 in several locations (in Paris, North Italy, the Netherlands, Moscow area and some places in Poland).

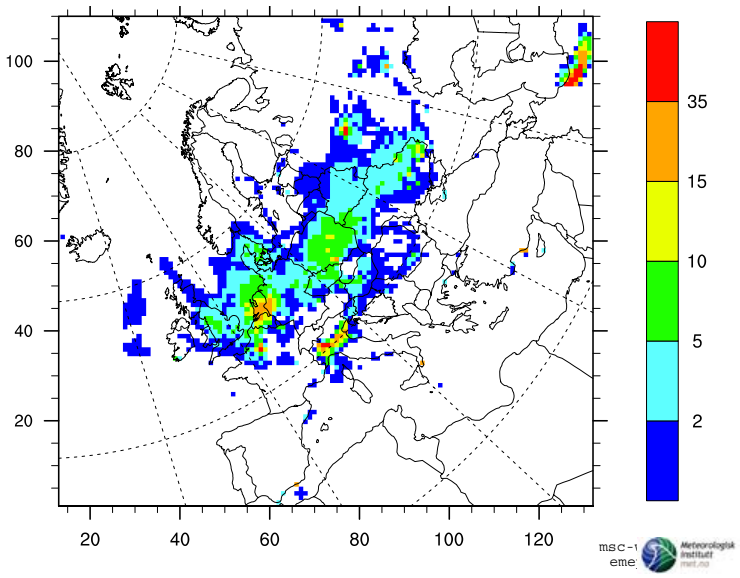

Figure 3.2: Number of days with calculated PM_{10} concentrations exceeding 50 µg/m^3 in 2002.

3.3 Contribution of different components (sources) to European $PM_{2.5}$ concentrations

Model calculated $PM_{2.5}$ includes primary $PM_{2.5}$ ($PPM_{2.5}$) directly emitted from the anthropogenic sources and secondary inorganic aerosols (SIA) formed in the atmosphere from gaseous precursors originating from SO_2 and NO_2 emissions.

Maps in Figure 3.3 show calculated distributions of annual mean concentrations of primary $PM_{2.5}$ and fine SIA, along with the individual SIA components sulphate (SO_4^{2-}), nitrate (NO_3^-) and ammonium (NH_4^+) in 2002. The model calculations suggest that SIA is the largest contributor to $PM_{2.5}$ mass practically all over Europe. Exceptions are the areas of high primary $PM_{2.5}$ concentrations associated with major sources of PM emissions. Among SIA components, SO_4^{2-} is a clearly prevailing aerosol at most of the places, except in the Netherlands, Belgium and adjacent parts of France and Germany, where NO_3^- and NH_4^+ appear to also be important SIA contributors.

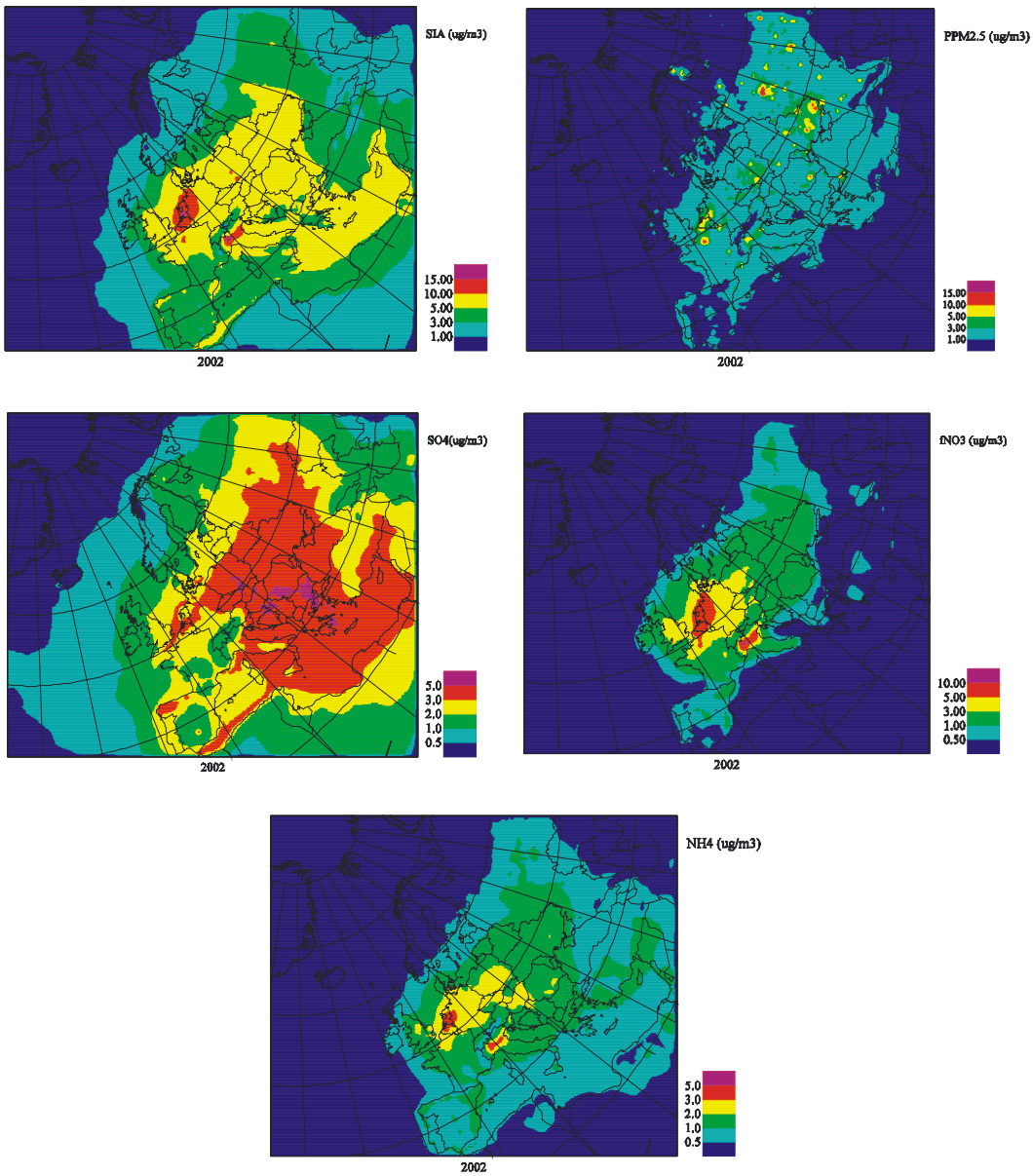

Figure 3.3: Model estimated concentrations of primary anthropogenic PM_{10} (PPM), secondary inorganic aerosol (SIA) and of the individual SIA components: sulphate (SO_4^{2-}), nitrate (NO_3^-) and ammonium (NH_4^+) in 2002.

3.4 Evaluation of aerosol model performance for PM mass

3.4.1 Annual mean aerosol concentrations (regional gradients)

Model calculated annual mean PM_{10} and $PM_{2.5}$ concentrations are plotted in Figure 3.4 versus measured values. In 2002, PM measurements from 6 countries were available to EMEP: at 26 sites for PM_{10} and 17 sites for $PM_{2.5}$. The model underestimates observed PM_{10} concentrations by a factor of 1.5 at German sites and by factor of 2-2.5 at all other sites. Model underestimation of measured $PM_{2.5}$ concentrations is smaller, within a factor of 2 for all the sites. In general, the model manages to give a realistic picture of PM_{10} and $PM_{2.5}$ regional distribution with the spatial correlation coefficients of 0.56 and 0.78 respectively. However, calculated PM_{10} and $PM_{2.5}$ gradients in Germany and Switzerland appear to be smaller than observed gradients.

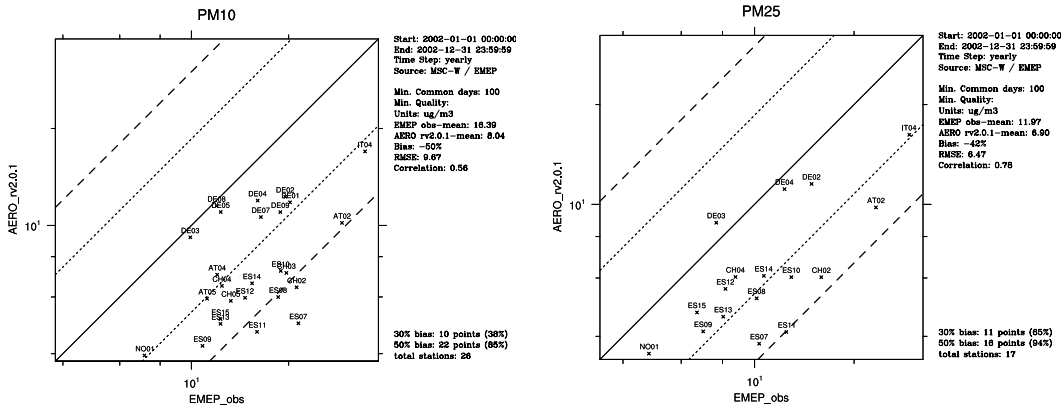

Figure 3.4: Scatter-plots for model calculated vs. EMEP measured PM_{10} and $PM_{2.5}$ in 2002.

Figure 3.5 compares calculated SIA concentrations with measurements at those EMEP stations, where concentrations of secondary inorganic components, namely SO_4^{2-}, NO_3^- and NH_4^+, were measured concurrently. The scatter-plot shows that the model tends to overestimate measured SIA concentrations close to major emission areas and to underestimate the long-range transported SIA. On the whole, the model performance for SIA is rather good, with the bias of 18 % and the spatial correlation coefficient of 0.87. These verification results for SIA cannot explain the discrepancy between modelled and observed PM concentrations, especially because among those sites with SIA measurements PM_{10} and $PM_{2.5}$ is only measured at Birkenes (NO01).

Figure 3.5 also shows scatter-plot for calculated versus observed SO_4^{2-} aerosol at EMEP sites with PM_{10} measurements. It can be noticed that similar to the scatter-plot for $PM_{2.5}$ and PM_{10}, SO_4^{2-} underestimation by the model is larger at Spanish and Swiss stations. Then, underestimation of NH_4^+ concentrations by the model can be anticipated at the same stations, but no NH_4^+ measurements for verification of results were available at those sites. Measurements of NO_3^- were also unavailable at those sites. Therefore we can only conjecture that model underestimation of $PM_{2.5}$ concentrations in Spain and Switzerland can to some extent be explained by its underestimation of sulphate and ammonium.

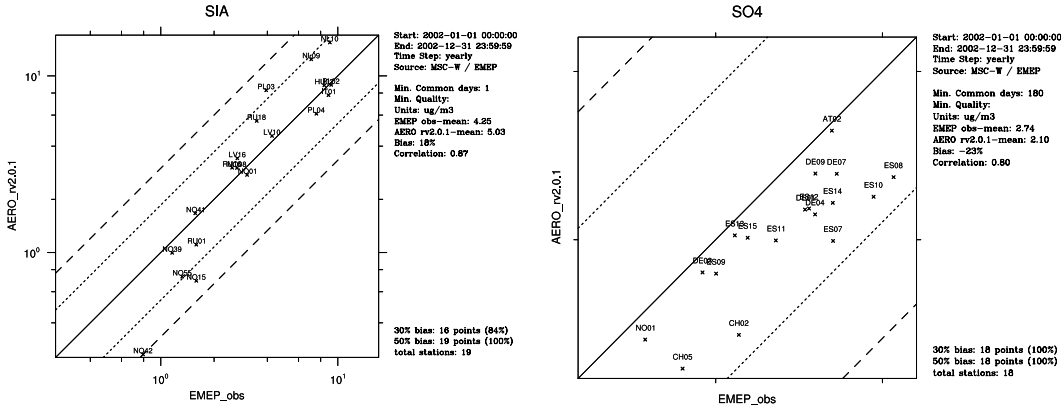

Figure 3.5: Scatter-plots for model calculated vs. measured SIA at all EMEP sites and SO_4^{2-} in EMEP sites with PM_{10} measurements in 2002.

Scatter-plots for calculated versus measured NO_3^- and NH_4^+, including all EMEP stations where observations were available (Figure 3.6), indicate a rather good model performance for those components. However, notice that none of the sites in Figure 3.6 has also measurements of PM concentrations.

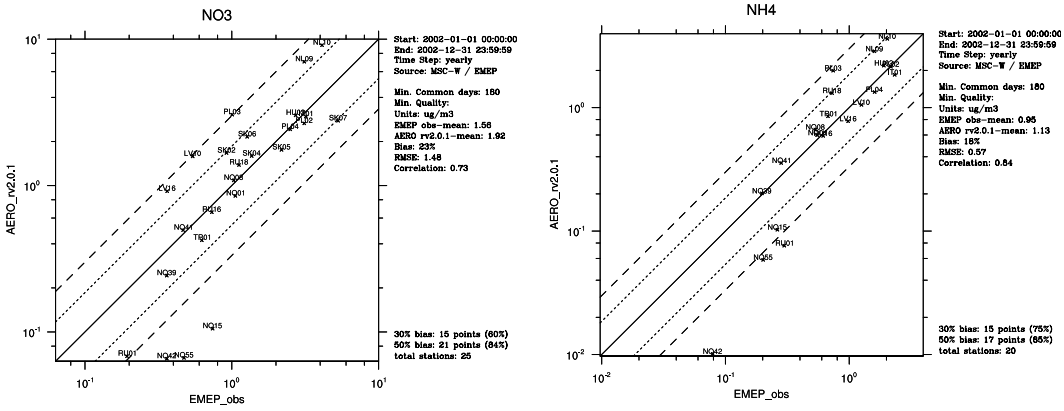

Figure 3.6: Scatter-plots for NO_3^- and NH_4^+, model calculated vs. measured at EMEP sites in 2002.

In summary:

- Annual mean concentrations of $PM_{2.5}$ and PM_{10} are underestimated by the aerosol model by 42 and 50% respectively, when dry calculated PM mass is compared with measurements. The spatial correlation coefficients between calculated and measured $PM_{2.5}$ and PM_{10} are 0.78 and 0.50.

- The general model performance for SIA is fairly good, but the lack of co-located and concurrent measurements of the individual aerosol components hampers the elucidation of model underestimation of $PM_{2.5}$ and PM_{10} concentrations.

- The main reason of model underestimation of PM is that the model still does not include some uncertain aerosol sources and processes; among those are

secondary organic aerosol (SOA) formation, wind soil erosion and dust particles mobilisation.

- The model appears to calculate too small horizontal PM gradients, in particularly in Germany and Switzerland. This can probably be because of the uncertainties in primary PM emissions and/or unaccounted PM sources.

3.4.2 Seasonal variation of aerosol concentrations

The calculated versus measured monthly time-series of particle concentrations in 2002 are presented in Figure 3.7. It is evident from Figure 3.7 that the model underestimation of observed concentrations of $PM_{2.5}$ and especially PM_{10} is largest in summer. Smaller underestimation of $PM_{2.5}$ and PM_{10} in the cold period is partly because the model overestimates SIA in that period (from November through March), which to some extent compensates for its PM underestimation. The SIA overestimation is largely due to model overestimation of winter NO_3^- concentrations.

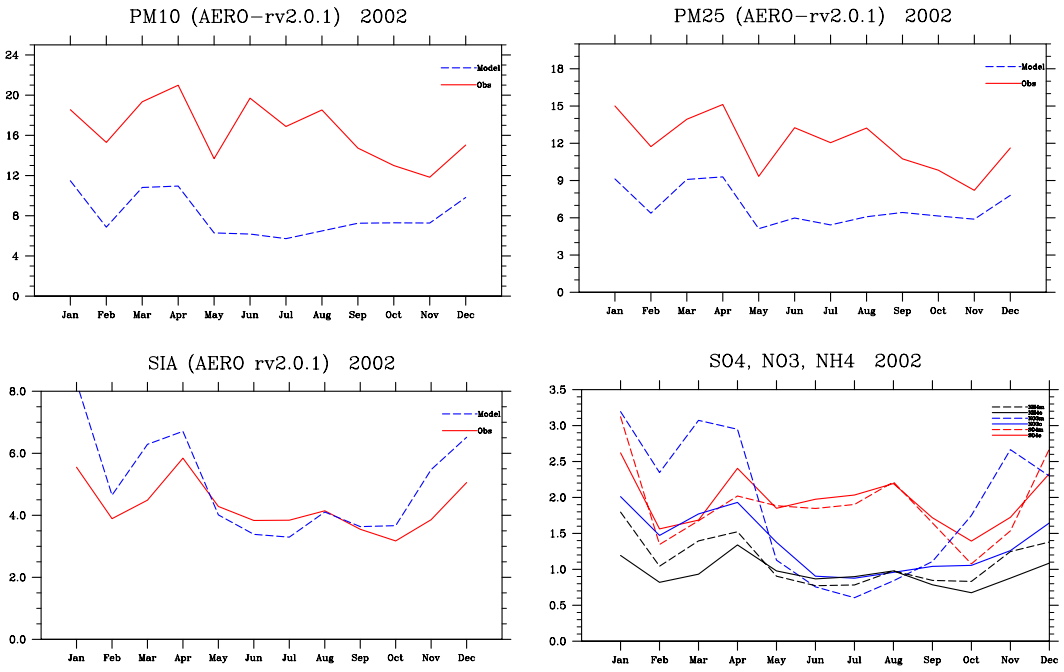

*Figure 3.7: Monthly time-series of calculated (dashed blue) and measured (solid red) PM_{10}, $PM_{2.5}$, SIA ($SO_4^{2-}+NO_3^-+NH_4^+$) and individual concentrations of SO_4^{2-}, NO_3^- and NH_4^+ *), averaged over all EMEP sites where measurements were available. *) SO_4^{2-} is represented with red, NO_3^- with blue and NH_4^+ with black lines; model – dashed lines.*

In summer months, model underestimation of measured $PM_{2.5}$ and PM_{10} is believed to be related to model's not accounting for secondary organic aerosol (SOA) and primary biogenic particles, which are expected to have a summer maximum. Moreover, ambient PM_{10} can also have an appreciable contribution from natural mineral dust, not considered by the model. The potential sources of mineral dust are agricultural fallow lands, especially in arid/semi-arid areas. The

role of wind blown and re-suspended dust in PM mass varies greatly spatially and temporally and it is a large challenge to quantify this contribution. In addition, Saharan dust intrusions contribute to the dust concentrations in Mediterranean countries. Even though those intrusions are rather intermittent (maybe 7-10 major dust outbreak events a year with a duration 2-7 days in Spain), they can significantly increase the average PM_{10} level.

On average, the model performance with respect to both $PM_{2.5}$ and PM_{10} is better in spring and autumn, when the spatial correlation coefficients are quite high (0.58–0.87) and RSME is smallest (Table 3.1). For PM_{10}, the spatial correlation between calculated and measured concentrations is lowest in winter. This is because the model does not manage to represent the situation at mountain stations: 3 German and 2 Swiss sites, where too high PM_{10} levels are calculated. This appears to be the main reason for too small calculated annual mean PM_{10} gradients, as pointed at above. Effect of mountain stations on the model performance statistics in winter is less pronounced for $PM_{2.5}$ just because only two elevated sites measured $PM_{2.5}$ in 2002. In summer, the negative bias is the largest and the correlation is relatively low for both $PM_{2.5}$ and PM_{10}.

Table 3.1: Averaged over EMEP sites with measurements, seasonal performance statistics of the aerosol model for PM_{10} and $PM_{2.5}$ in 2002.

		Obs. mean	Mod. mean	Bias (%)	RSME	Correlation
PM_{10}	winter	16.62	9.17	-44	13.39	0.29
	spring	18.00	9.35	-48	9.42	0.71
	summer	18.32	6.19	-66	12.81	0.46
	autumn	13.20	7.29	-44	7.57	0.58
$PM_{2.5}$	winter	13.17	7.77	-40	11.05	0.60
	spring	12.74	7.81	-38	5.63	0.87
	summer	13.04	5.92	-54	7.85	0.41
	autumn	9.57	6.17	-35	5.19	0.79

Bias is calculated as (Mod.mean – Obs.mean)/Obs.mean; RMSE (root mean square error) is calculated as $1/N\ (\Sigma\ (\text{mod-obs})^2)^{1/2}$

3.4.3 Particle-bound water in $PM_{2.5}$ and PM_{10}

It was pointed out that the EMEP aerosol model, similarly to the most of state-of-art aerosol models, systematically underestimates observed PM concentrations. Undoubtedly, model accurate calculation of the individual aerosol constituents is a prerequisite for adequate representation of atmospheric PM concentrations. On the other hand, available measurements on the chemical characterization of PM_{10} and $PM_{2.5}$ (e.g. Putaud et al., 2003; Yttri, 2003; Zappoli et al., 1999) reveal that full chemical PM mass closure is rarely achieved. That means there is a difference between gravimetrically measured PM mass and the sum of all identified aerosol components. The mass fraction not identified by chemical analysis can comprise as much as 30-40% of gravimetric PM_{10} or $PM_{2.5}$ mass. The unaccounted PM mass can partly be due to non-C atoms in organic aerosols and/or due to sampling

and measurement artefacts. Moreover, a considerable part of the unaccounted PM mass is likely to consist of water associated with particles.

Filter-based gravimetric methods are recommended by the EMEP measurement manual and employed for determining PM_{10} mass at EMEP sites. The manual requires that dust-loaded filters should be equilibrated at 20°C (± 1) and 50% relative humidity (± 5) for 48 hours before they are weighed, both prior to the sample collection and after sampling. However, equilibration of filters does not necessarily remove all particle-bound water. A number of experimental studies revealed that particle can contain 10-30% of water in mass at the relative humidity of 50% (e.g. Winkler and Junge, 1972; Neusüβ et al., 2002; Schwela et al., 2002). Thus, gravimetrically measured particle mass does not necessarily represent dry PM_{10} and $PM_{2.5}$ mass (i.e. the sum of all PM components, excluding aerosol water). This is thought to be one of the reasons for model under-prediction of gravimetrically measured PM, if calculated dry PM_{10} and $PM_{2.5}$ concentrations are compared with observations.

The mass of particle-bound water in PM_{10} and $PM_{2.5}$ has been calculated with the aerosol model for the specific conditions of samples equilibration (20°C and 50% RH). Particle water content is determined by the mass fraction and the type of mixture of soluble PM constituents, which in our calculations was SIA and sea salt. According to model simulations, the annual mean water content in gravimetrically measured PM_{10} mass varies between 0.5 $\mu g/m^3$ in Scandinavia and 6.5 $\mu g/m^3$ in the Netherlands and Belgium, while for $PM_{2.5}$ it varies between 0.3 and 5 $\mu g/m^3$. The particle water constitutes from 20 to 35% of model calculated annual mean PM_{10} and $PM_{2.5}$ concentrations, which is in a general agreement with existing experimental data. However, the comprehensive validation of calculated particle water content against observations is not currently feasible due to the lack of appropriate measurements.

The calculations suggest that the particle water in PM_{10} and $PM_{2.5}$ can explain from 30 to 80 % of the unaccounted PM mass, when compared with data on PM chemical composition available at 6 stations (1 in Norway (NO01)), 2 in Austria (Puxbaum et al., 2003) and 3 in Spain (Querol, *personal commun.*) (see Table 3.2 and Figure 3.8, Figure 3.11, Figure 3.12). More results and tests on particle-bound water are presented in the paper recently submitted to the Atmospheric Chemistry and Physics Journal (Tsyro, 2004). These results as well as available experimental evidences suggest that the particle water should be accounted for in model calculated PM_{10} and $PM_{2.5}$ when evaluating against gravimetrically measured PM mass.

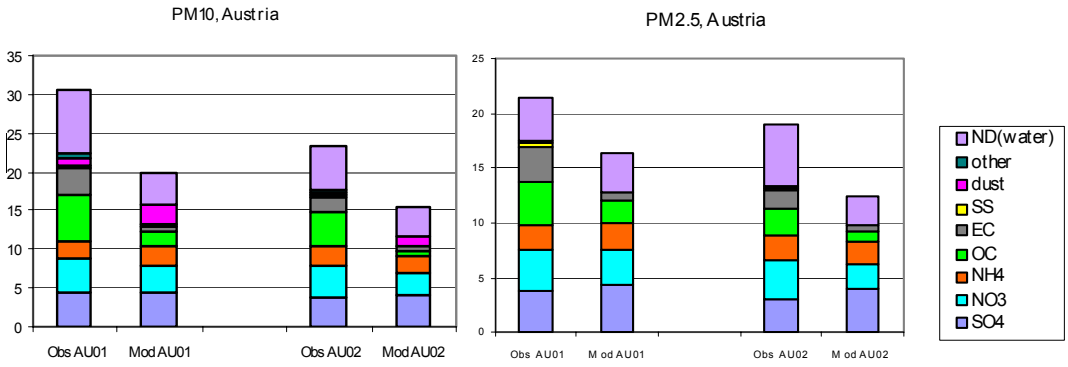

Figure 3.8: Measured and modelled chemical composition of PM_{10} and $PM_{2.5}$ at Austrian sites in Wien (AU01) and Streithofen (AU02) in the period 1.01 – 31.05.2000. The purple colour denotes unaccounted (Not Determined) PM fraction in measurements and particle water in model calculations. Unit: $\mu g/m^3$.

Annual and monthly mean PM concentrations

Scatter-plots in Figure 3.9 compares calculated annual mean wet, i.e. including particle water, PM_{10} and $PM_{2.5}$ concentrations with EMEP measurements. The model still underestimates observed PM_{10} and $PM_{2.5}$ concentrations, but the biases of -33 % and -19 % respectively are considerably smaller compared to the results for dry PM (Figure 3.4). As expected, the spatial correlation between modelled and measured PM_{10} and $PM_{2.5}$ has not improved.

The monthly time-series (Figure 3.10) show that accounting for particle-bound water in calculated PM improves the correspondence between calculated and observed PM_{10} and $PM_{2.5}$ concentration values with respect to that for calculated dry PM concentrations.

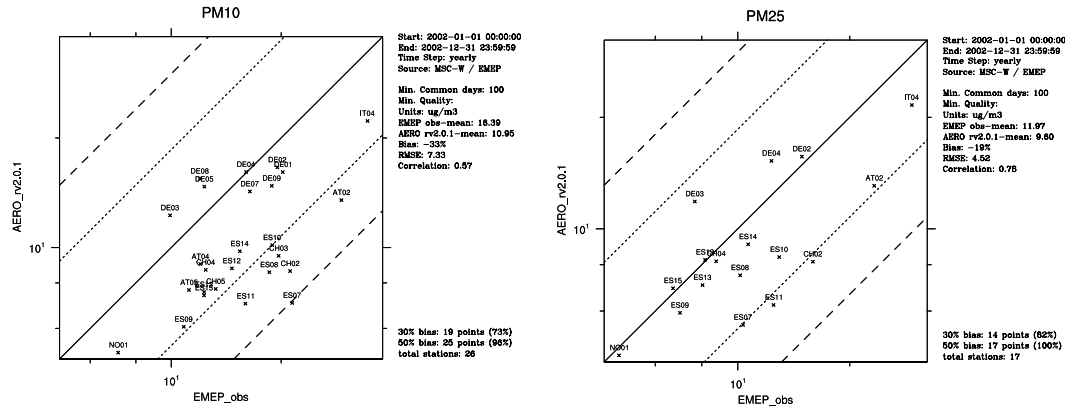

Figure 3.9: Scatter-plots for model calculated wet PM_{10} and $PM_{2.5}$ concentrations vs. EMEP measurements in 2002.

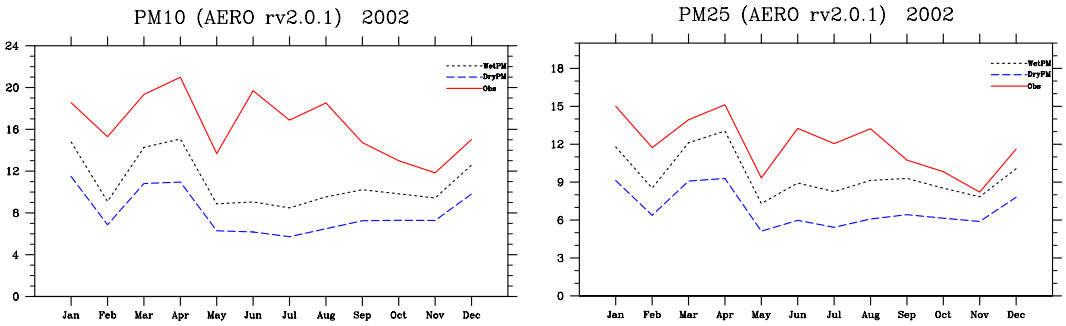

Figure 3.10: Monthly time-series of calculated dry (dashed blue), calculated wet (dotted black) and measured (solid red) PM_{10} and $PM_{2.5}$ concentrations, averaged over all EMEP sites where measurements in 2002 were available.

Daily PM concentrations

Accounting for particle-bound water in calculated PM mass has resulted in a certain improvement of modelled daily $PM_{2.5}$ and PM_{10} as compared with EMEP measurements (Table 3.2 and Table 3.3). Calculated wet PM_{10} and $PM_{2.5}$ concentrations are closer to the measured PM values. It is interesting to note that the temporal correlation has also slightly improved at most of the stations.

Table 3.2: Model performance statistics for calculated dry and wet $PM_{2.5}$ compared with measurements at EMEP sites in 2002 (- elevated over 900 m sites)*

		Obs.mean	Mod.dry	Corr.dry	Mod.wet	Corr.wet
DE02	Langenbrügge/Waldhof	14.85	11.53	0.61	15.67	0.62
DE03	Schauinsland *	7.64	8.81	0.27	11.85	0.34
DE04	Deuselbach	12.30	11.11	0.51	15.26	0.56
CH02	Payerne	15.89	6.03	0.45	8.15	0.44
CH04	Chaumont	8.74	6.04	0.36	8.17	0.42
AT02	Illmitz	23.27	9.79	0.58	13.07	0.59
IT04	Ispra	29.39	16.22	0.44	21.58	0.43
NO01	Birkenes	5.75	3.55	0.65	4.55	0.67
ES07	Viznar	10.31	3.80	0.52	5.50	0.52
ES08	Niembro	10.13	5.21	0.52	7.49	0.53
ES09	Campisabalos	6.98	4.14	0.45	5.93	0.50
ES10	Cabo de Creus	12.90	6.03	0.49	8.39	0.49
ES11	Barcarrota	12.45	4.12	0.59	6.23	0.56
ES12	Zarra	8.15	5.56	0.64	8.25	0.67
ES13	Penausende	8.02	4.59	0.55	7.05	0.59
ES14	Els Torms	10.64	6.09	0.47	9.08	0.49
ES15	Risco Llano	6.70	4.72	0.39	6.91	0.41

Table 3.3: Model performance statistics for calculated dry and wet PM_{10} compared with measurements at EMEP sites in 2002 (- elevated over 900 m sites).*

		Obs.mean	Mod.dry	Corr.dry	Mod.wet	Corr.wet
DE01	Westerland/Wenningsted	20.17	11.8	0.62	15.3	0.63
DE02	Langenbrügge/Waldhof	19.49	12.28	0.60	16.43	0.61
DE03	Schauinsland *	9.90	9.18	0.25	12.21	0.32
DE04	Deuselbach	16.01	11.95	0.42	16.04	0.48
DE05	Brotjacklriegel *	12.30	11.01	0.10	14.66	0.13
DE07	Neuglobsow	16.38	10.62	0.55	14.12	0.57
DE08	Schmüke *	11.96	11.51	0.18	15.39	0.22
DE09	Zingst	18.84	11.00	0.57	14.44	0.59
CH02	Payerne	21.12	6.43	0.42	8.55	0.43
CH03	Taenikon	19.64	7.12	0.42	9.45	0.42
CH04	Chaumont	12.40	6.49	0.34	8.62	0.39
CH05	Rigi	13.21	5.83	0.34	7.64	0.38
AT02	Illmitz	29.23	10.18	0.56	13.47	0.56
AT04	St. Koloman	11.99	7.03	0.31	8.98	0.35
AT05	Vorhegg *	11.16	5.93	0.38	7.61	0.44
IT01	Montelibretti	33.22	11.11	0.38	14.69	0.40
IT04	Ispra	35.45	16.98	0.47	22.17	0.47
NO01	Birkenes	7.43	3.95	0.57	4.95	0.58
ES07	Viznar *	21.40	4.97	0.49	6.66	0.48
ES08	Niembro	18.54	6.00	0.47	8.25	0.46
ES09	Campisabalos *	10.80	4.23	0.33	5.98	0.38
ES10	Cabo de Creus	18.90	7.23	0.43	9.59	0.40
ES11	Barcarrota	15.95	4.68	0.67	6.66	0.65
ES12	Zarra	14.64	5.97	0.49	8.66	0.53
ES13	Penausende	12.28	4.95	0.46	7.42	0.51
ES14	Els Torms	15.38	6.61	0.41	9.64	0.45
ES15	Risco Llano	12.27	5.12	0.26	7.31	0.28

At all of the stations, the model performance for $PM_{2.5}$ is somewhat better than for PM_{10} (smaller underestimations and higher correlations). The lowest model performance is found at elevated German (DE03, DE05 and DE08) and Swiss (CH03 and CH05) sites. This is largely because the model does not quite manage to represent winter $PM_{2.5}$ and PM_{10} concentrations at mountain sites, when the sites are in free troposphere, whereas in other seasons model results for those sites are quite good. However, this does not seem to be the case for modelled PM concentrations at Spanish mountain sites (ES07 and ES09), probably because a larger scale mountain area on the Iberian Peninsula is better resolved in the model. In fact, at most of the Spanish sites, the model performance appears worse in summer months (larger underestimation and somewhat lower temporal correlation).

Summarising, accounting for particle water in modelled PM_{10} and $PM_{2.5}$ has been shown to improve the general agreement between calculated and measured PM concentrations. However, model calculated aerosol water needs to be verified against observations. At present, the lack of measurement data on particle-bound water hampers the validation of model calculations of particle water content. This

represents the major caveat to using the model estimates of particle water in policy-related EMEP model calculations of PM.

3.4.4 Validation of model calculated chemical composition of $PM_{2.5}$ and PM_{10}

Particulate matter, being a complex mixture of many different pollutants, is contributed to by many different sources. In view of the recommendation of WHO Task Force on Health to use $PM_{2.5}$ as an indicator for particle related health effects, the focus of model development work is currently on achieving full assessment of the anthropogenic fraction of $PM_{2.5}$. Information on the chemical composition of $PM_{2.5}$ and PM_{10} is essential for source allocation of particulate concentrations and for consequent development and evaluation of emission control strategies. Such information is also potentially important to facilitate the assessment of the adverse toxicological effects of specific components on the human's health.

Furthermore, to facilitate the further progress in PM modelling, verification of individual PM components is necessary. Thus, the availability of measurements of $PM_{2.5}$ and PM_{10} chemical speciation for model evaluation is crucial for its development and improvement. Scatter-plots and time-series comparing calculated $PM_{2.5}$ and PM_{10} concentrations with observations reveal that the model currently underestimates PM concentrations, but they do not explain what causes the underestimation. On the other hand, ostensibly correctly predicted by the model PM concentrations can be the result of error compensation. Therefore, to determine the causes of discrepancy between model and measurement results and to ensure that the right results on PM concentrations are obtained for fair reasons, verification of the individual PM constituents is needed. This need requires co-located and concurrent measurements of all main components of $PM_{2.5}$ and PM_{10} and ultimately the complete information on PM chemical speciation.

In this section, the further validation of model calculated PM chemical composition is presented, as more measurements on PM chemical speciation have become available. Within the EMEP monitoring network, concentrations of PM_{10} and its main components were measured only at Birkenes in 2001-02. Furthermore, data on $PM_{2.5}$ and PM_{10} chemical speciation at two sites in Austria and three sites in Spain were made available to EMEP/MSC-W (Table 3.4). Evaluation of model results against those measurements is presented here.

Modelled calculated and measured chemical composition of PM_{10} and $PM_{2.5}$ at those sites, averaged over all days with measurements, are compared in Figure 3.11 and Figure 3.12. Purple bar parts represent both the unaccounted mass in measured $PM_{2.5}$ and PM_{10} and the model calculated particle water. The comparison of calculation results and observations suggests some causes of model underestimation of PM_{10} and $PM_{2.5}$ concentration. While secondary inorganic aerosols are calculated by the model with acceptable accuracy at the most of sites, large discrepancies between calculations and observations are found for carbonaceous aerosol (OC and EC). At all of the sites, EC and especially OC concentrations are considerably underestimated by the model. Please, note that the model considered only fine EC and OC from anthropogenic primary PM_1 emissions (Kupiainen et al. 2004). Moreover, concentrations of mineral dust are also underestimated by the model at Spanish sites.

Table 3.4: Overview of the stations with measurements on PM chemical speciation.

Country	Station	Station code	Coordinates	Measurement period	Resolution
Norway	Birkenes (EMEP)	NO01	58°23' N 8°15' E	1.01-31.12.2001 1.01-31.12.2002	Inorganics-daily OC/EC - weekly Inorganics-daily, OC/EC-day a week
Austria (*)	Wien (urban) Streithofen (rural)	AU01 AU02	48°13'N 16°21'E 48°16'N 15°56'E	1.06.1999 -31.05.2000	Daily Daily
Spain (**)	Monagrega (rural) Bemantes (rural) Montseny (rural)		40°57'N 0°17'W 20°15'N 8°11'W 41°46'N 2°21'E	24.03.99-29.06.00 8.01-27.12.2001 22.03-29.08.2001	PM_{10}- 2 days a week $PM_{2.5}$- 1 day a week

(*) Puxbaum et al. (2003); (**) Rodriguez et al. (2002); Sources: Spanish Ministry of Science and Technology Spanish Ministry of Enviroment (Querol, *person. commun.*)

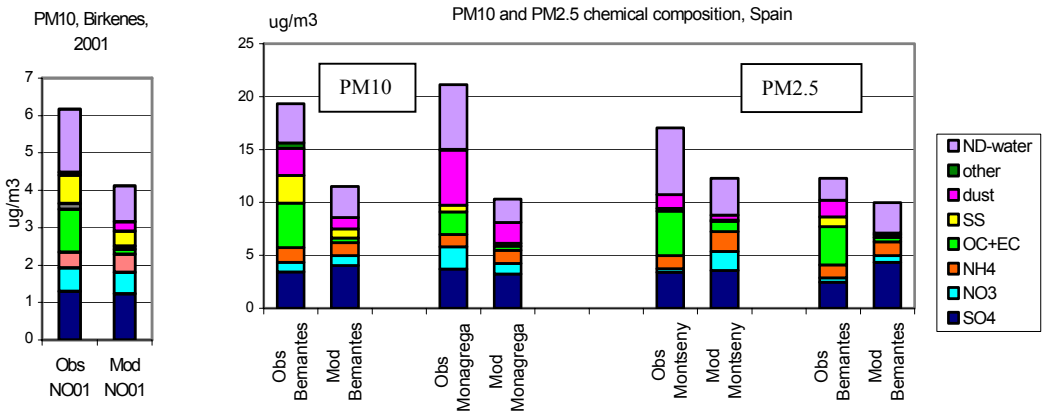

Figure 3.11: Model calculated and measured chemical composition of PM_{10} at Birkenes (2001), Bemantes (08.01-27.12.2001) and Monagrega (1.01.1999-31.07.2000) and $PM_{2.5}$ at Montseny (22.03-29.08.2002) and Bemantes (08.01-27.12.2001). Concentrations are averaged over days with measurements.

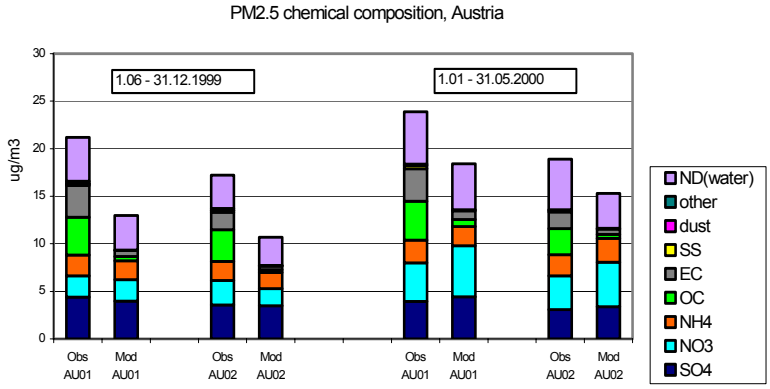

Figure 3.12: Model calculated and measured chemical composition of $PM_{2.5}$ in Wien (AU01) and Streithofen (AU02) in 1999 and 2000.

Validation of PM chemical composition against EMEP data at Birkenes (NO01)

The time-series in Figure 3.13 compare model calculated daily concentrations of PM_{10}, $PM_{2.5}$, coarse PM and the individual aerosol components with measurements at Birkenes (Norway) in 2002. The overall performance of the model with respect to almost all of PM components is encouragingly good.

The model manages to calculate daily $PM_{2.5}$ quite well as compared to observations: the average underestimation is 25% and the correlation coefficient is 0.65. The model underestimation of PM_{10} concentrations at Birkenes is greater (45%) and the correlation of 0.57 is lower than for $PM_{2.5}$. The underestimation of both $PM_{2.5}$ and especially PM_{10} is more pronounced in warm period.

The temporal correlation is fairly good for most of the PM constituents: 0.76-0.78 for SIA components (SO_4^{2-}, NO_3^- and NH_4^+) and 0.6 for sea salt. The lowest correlation coefficients are found for mineral dust and carbonaceous particles, which are still the most uncertain components in the model.

Concentrations of EC and OC were measured in both $PM_{2.5}$ and PM_{10} with a weekly time resolution. It should be noted that only carbonaceous particles from anthropogenic fine (in PM_1) EC and OC emissions developed recently by IIASA (Kupiainen et al., 2004) have been considered here, while also coarse EC and OC can be emitted by the anthropogenic sources (e.g. non-exhaust emissions from traffic, production processes, agriculture). However, model calculated EC concentrations are higher than the measured values, what indicates that further work on the improving and validating of EC emissions is needed. The model considerably underestimates measured EC concentrations. This is mainly caused by that the model does not account for SOA (contributing largely to fine PM) and primary biogenic organic aerosols (contributing mainly to coarse PM). The correlation between weekly averaged calculated and observed EC and OC concentrations is rather poor.

Furthermore, the model underestimates sea salt aerosol concentrations expressed as the sum of measured Na^+, Cl^- and Mg^{2+} concentrations. This can to some extent explain the model underestimation of PM_{10} and, in particularly, of coarse PM, sea salt particles being found largely in the coarse mode. The remaining part of underestimated coarse PM mass is probably associated with mineral dust.

Time-series of calculated and measured "mineral dust" concentrations in Figure 3.13 should be only considered provisional as both calculations and measurements do not include all dust components. Only anthropogenic fraction of mineral dust is currently included in the model. The chemical speciation of mineral dust is not resolved in the model as no appropriate information on the chemical composition of dust emissions is available at the moment. Model calculated bulk concentrations of anthropogenic dust are compared with the sum of measured concentrations of Ca^{2+} and K^+. These components represent only a (minor) fraction of ambient mineral dust, while the main components of natural dust, Si and Al, were not measured. Given the crudeness of comparison, the correlation coefficient of 0.39 indicates that some of the dust contributors are described fairly in the model.

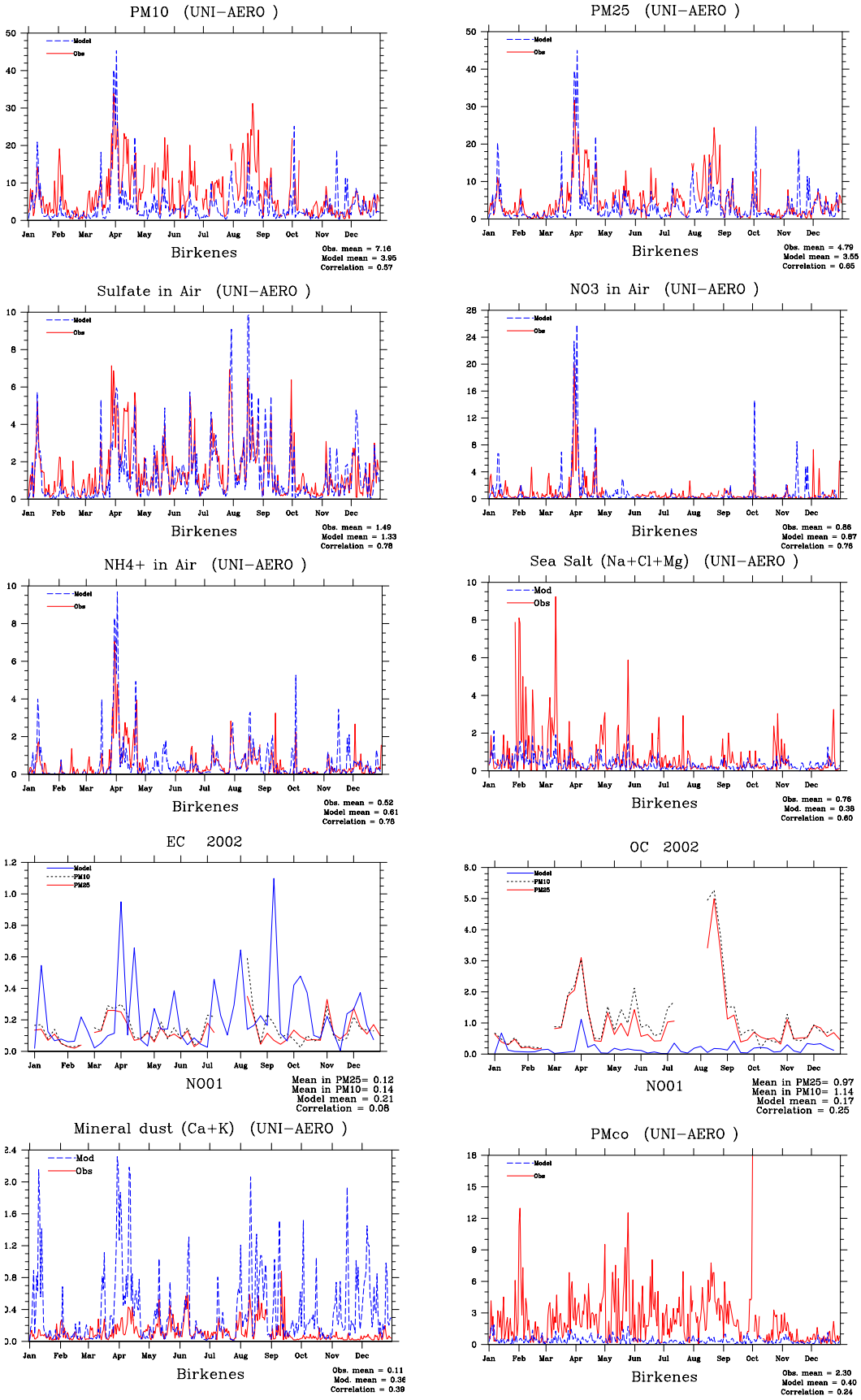

Figure 3.13: Daily time-series for 2002 of model calculated and measured concentrations of PM_{10}, $PM_{2.5}$ and coarse PM and individual aerosol components at Birkenes (NO01).

Validation of PM chemical composition against Austrian data

Measurements of the chemical composition of $PM_{2.5}$ and PM_{10} at two Austrian sites have been made available to EMEP/MSC-W from AUPHEP project (Puxbaum et al., 2003). The sites are: an urban background site in Wien (AU01) and a rural site in village Streithofen (AU02), ca. 30 km west of AU01 (Table 3.5). Puxbaum et al. (2003) estimated that the background particles contribute with at least 70% to urban PM_{10} concentrations in AU01. On the other hand, PM_{10} concentrations at AU02 were found to be to some extent influenced by the Wien plum during easterly flow. The urban plum enhanced the average rural PM_{10} to 23.7 μg/m^3 compared to 20.5 μg/m^3 at the regional background site Illmitz.

EMEP station AT02 (Illmitz) is situated relatively close to Streithofen site. Therefore, the main findings from the evaluation of model results with measurements at Streithofen can probably be used for explaining the model results at AT02 (about a factor of 2-2.5 underestimation of measured $PM_{2.5}$ and PM_{10}). The mean values of calculated and measured at AU01 and AU02 concentrations of PM and its components and correlation coefficients are summarised in Table 3.5. It should be pointed out that daily measurements of were available for $PM_{2.5}$ components, while only monthly averages for PM_{10} components.

Encouragingly good temporal correlation between calculated and measured concentrations (0.54–0.69) are found for all $PM_{2.5}$ components (except Na^+ in 1999).

Averaged over the measurement period, model calculated $PM_{2.5}$ and PM_{10} concentrations are about 40% and 60% lower than respective measured values. Calculated concentrations of SIA components are on average in a good agreement with measurements. It can be noticed that fine NO_3^- is somewhat overestimated, while NO_3^- mass in PM_{10} is underestimated in the model results. This indicates that the ratio between fine and coarse NO_3^- is not quite correctly represented by the model. This is because in the current version of the aerosol model, coarse NO_3^- only forms on sea salt aerosols, but not on dust particles, thus resulting in too little fraction of coarse NO_3^- far-off from the sea.

Model calculated concentrations of OC and EC are considerably lower than measured values. It can be seen from Table 3.5 that the model underestimation of OC is larger in PM_{10} than in $PM_{2.5}$. This is because in the model all OC, which in the current model version is primary anthropogenic OC, is assumed to be emitted in the form of fine particles, whereas a significant fraction (about 30%) of OC in PM_{10} was found to be in the coarse mode at the Austrian sites. The coarse OC was to a certain level attributed to primary biogenic organic aerosol (Puxbaum et al., 2003), which is not included in the model. Similarly, only fine anthropogenic EC is currently calculated with the model.

From mineral components, only Ca^{2+}, K^+ and Mg^{2+} were analysed which represent only a fraction of total dust mass (because of the large distant from the sea magnesium at those sites is assumed to originate from dust sources). Therefore, even though the model only includes anthropogenic fraction of dust, it

overestimates the sum of measured concentrations of mineral components. Other important dust components (i.e. Al, Si, Fe) were not analysed and probably contribute to the unaccounted PM mass at those sites. It should be pointed out that the unaccounted PM fractions, in particularly for PM_{10}, are rather large at both sites. Table 3.5 also includes model calculated mass of particle water in $PM_{2.5}$ and PM_{10}.

Table 3.5: Validation of model calculated PM_{10} and $PM_{2.5}$ components against observations at Austrian sites (June 1999-May 2000)

Site		PM	SO_4^{2-}	NO_3^-	NH_4^+	OC*)	EC*)	Na	Dust (**)	ND/ water
AU01-PM_{10} (monthly)	**Obs**	30.68	4.53	4.16	2.46	5.73	3.47	0.2	1.1	8.6
	Mod	10.72	4.61	3.41	2.23	0.45	0.58	0.05	3.16	4.12
AU02-PM_{10} (monthly)	**Obs**	23.71	3.84	4.13	2.56	4.22	1.95	0.14	0.44	6.0
	Mod	11.12	3.41	3.24	2.09	0.37	0.46	0.05	1.45	3.4
AU01-$PM_{2.5}$	**Obs 99**	20.89	4.37	2.27	2.19	3.97	3.32	0.07	-	3.54
	Mod 99	11.18	3.96	2.25	2.01	0.46	0.61	0.01		3.65
	Obs 00	23.67	3.94	4.06	2.39	4.09	3.46	0.09	-	4.39
	Mod 00	16.67	4.43	5.36	3.02	0.74*)	0.92*)	0.03		4.48
	Corr 99	0.65	0.52	0.69	0.67	0.68	0.64	0.26	-	0.22
	2000	0.64	0.54	0.63	0.67	0.59	0.67	0.48		0.42
AU02-$PM_{2.5}$	**Obs 99**	17.23	3.56	2.60	1.99	3.32	1.85	0.07	-	1.32
	Mod 99	8.66	3.48	1.75	1.70	0.29	0.38	0.01		2.99
	Obs 00	19.23	3.06	3.56	2.22	2.76	1.75	0.07	-	3.4
	Mod 00	12.68	3.37	4.59	2.49	0.44	0.54	0.03		3.6
	Corr 99	0.55	0.50	0.68	0.65	0.51	0.63	0.12	-	0.03
	2000	0.69	0.55	0.64	0.65	0.43	0.69	0.65		0.60

(*) Model calculated fine EC and OC; (**) In measurements represented by sum $Ca^{2+}+K^+ +Mg^{2+}$.
"-"- unavailable from model calculations

Validation of PM chemical composition against measurements in Spain (Source: Spanish Ministry of Science and Technology and Spanish Ministry of Enviroment; Rodriguez et al. (2002); Querol, *person. commun*.)

At three Spanish stations (Table 3.6), $PM_{2.5}$ concentrations are underestimated by the model ca. by a factor of 1.8 and PM_{10} concentrations by factors from 2.2 to 2.6. Calculated concentrations of SIA components and also Na^+ are on the whole in a satisfactory agreement with observations. The temporal correlation coefficients for these aerosols are between 0.45 and 0.88 at all three sites, except for fine SIA at Montseny, where a very poor correlation is found for NO_3^- and NH_4^+.

According to the work by Rodriguez et al. (2002), NO_3^- prevails as ammonium nitrate (NH_4NO_3) in the cold season and thus is largely in fine mode. Conversely, the coarse nitrate formed on sea salt and dust particles (i.e. in the form of $NaNO_3$ and $Ca(NO_3)_2$) appears to predominate in the warm season. The model underestimates mineral dust concentrations in Spain (see discussion below) and somewhat underestimates the concentrations of sea salt aerosol (Na^+). This can probably explain the model underestimation of NO_3^- mass in PM_{10} (Monagrega)

and overestimation of fine NO_3^- in $PM_{2.5}$ in Montseny, which is most pronounced in summer. On the other hand, NO_3^- formation at Bemantes (at the North Atlantic coast) is apparently more influenced by sea salt aerosol than by mineral dust. Therefore, model calculated NO_3^- concentrations at Bemantes are in a better agreement with observations.

Table 3.6: Validation statistics for model calculated PM_{10} and $PM_{2.5}$ chemical components at Spanish sites.

Site		PM	SO_4^{2-}	NO_3^-	NH_4^+	TC *)	Na	Dust	ND/ water
Monagrega PM_{10} -1999	**Obs**	19.63	3.82	1.91	1.29	2.07	0.22	4.68	5.37
	Mod	7.69	3.28	0.76	1.15	0.36	0.19	1.95	2.10
	Corr.	0.36	0.64	0.75	0.58	0.43	0.46	-0.01	
Monagrega PM_{10} -2000	**Obs**	22.45	3.58	2.29	1.07	2.16	0.36	5.76	6.89
	Mod	8.49	3.17	1.26	1.33	0.43	0.34	1.97	2.32
	Corr.	0.33	0.59	0.56	0.54	0.54	0.78	-0.05	
Bemantes PM_{10}	**Obs**	19.31	3.45	0.89	1.4	4.19	1.10	2.58	3.7
	Mod	8.59	4.04	0.93	1.24	0.42	0.88	1.07	2.94
	Corr.	0.61	0.75	0.71	0.82	0.64	0.79	0.26	
Bemantes $PM_{2.5}$	**Obs**	13.29	3.47	0.41	1.21	3.61	0.32	-	2.07
	Mod	7.68	4.33	0.64	1.32	0.42	0.23	-	2.89
	Corr.	0.84	0.88	0.80	0.85	0.72	0.43	-	
Montseny $PM_{2.5}$	**Obs**	17.06	3.42	0.32	1.23	4.21	0.15		6.31
	Mod	9.01	3.58	1.81	1.85	0.97	0.12	-	3.45
	Corr.	0.28	0.34	-0.27	0.03	0.42	0.32	-	

*) Total Carbon. Only fine fraction of TC is calculated with the model "-" means unavailable from model calculations

Moreover, the model significantly underestimates observed concentrations of total carbon (OC+EC). The primary reason for that is not accounting for secondary organic aerosol in the model. Also uncertainties associated with primary EC and OC emissions affect the model results, which is intended for further analysis. On the other hand, the temporal correlation between calculated and measured TC is comparable to that for inorganic components (0.42–0.72), suggesting a reasonable description of emission distribution and atmospheric transport of primary OC and EC.

Concentrations of mineral dust, particularly in PM_{10}, are greatly underestimated by the model. Concentrations of dust particles can episodically be significant due to wind soil erosion and outbreaks of Saharan dust in Spain. Mineral dust particles especially contribute to the coarse aerosol fraction. The very poor correlation between calculated dust concentrations, with only anthropogenic fraction being considered, and measurements indicates the importance of allowing also for natural sources of mineral dust in PM_{10} in Spain.

As it is seen in Figure 3.10, dust mass in $PM_{2.5}$ is underestimated by the model less than dust mass in PM_{10}. Figure 3.14 exemplifies that most of the episodes with enhanced PM_{10} concentrations were associated with the days when Saharan

dust events were reported in 1999 (pointed to by arrows). In addition to the mineral load, the Saharan dust may also have anthropogenic fraction, i.e. aerosols from biomass combustion and nitrates, which have been emitted in Northern Africa or re-circulated from Europe (Rodriguez et al., 2002 and references therein).

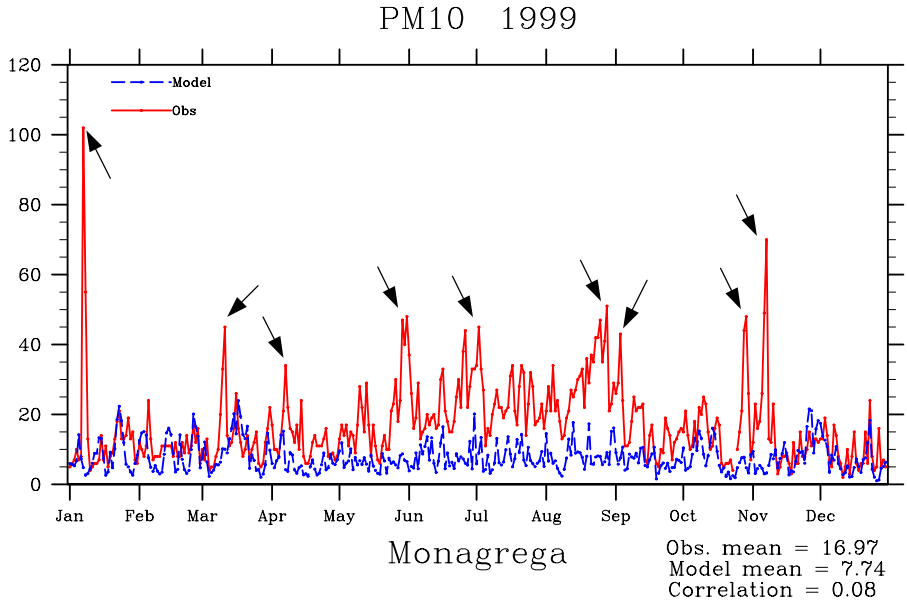

Figure 3.14: Calculated and measured PM_{10} at Monagrega, Spain: arrows indicate episodes with Saharan dust intrusion.

In summary, comparison of calculated PM chemical composition with limited measurement data available indicates the following:

- In general, model calculated concentrations of secondary inorganic aerosols, SO_4^{2-}, NO_3^- and NH_4^+, are in satisfactory agreement with observation; calculated concentrations of sea salt compare reasonably well with observations, but somewhat underestimated;

- The model considerably underestimates carbonaceous particles, especially OC (see also OC/EC verification and discussion below), which is one of the main reasons for model underestimation of observed $PM_{2.5}$ and PM_{10};

- Model underestimation of mineral dust episodes in particularly affected areas (like in Spain and other Mediterranean countries) can also contribute to PM_{10} underestimation. Besides, dust particles affect nitrogen and sulphate chemistry;

- Significant fractions of $PM_{2.5}$ and PM_{10} mass remain unidentified in measurements, what complicates the explanation of discrepancy between model results and measurements. As discussed in the previous section, model calculated particle water in $PM_{2.5}$ and PM_{10} can explain some part of the unaccounted PM mass, but thorough verification of calculated particle-bound water with observations is needed.

3.4.5 Model validation for individual aerosol components

SIA

In addition to results on SIA performance shown in the previous sections in this report, model validation with respect to SO_4^{2-}, NO_3^- and NH_4^+ against EMEP measurements is examined profoundly in EMEP Report 1/2004. The overall conclusion is that the model is able of calculating SIA components with satisfactory accuracy.

EC and OC

Model calculated EC and OC concentrations have been compared with measurements from OC/EC campaign coordinated by NILU. Concentrations of EC and OC were measured one day a week in the period of 1 July 2002–1 July 2003 at 15 sites around Europe. It should be highlighted that verification of calculated EC concentrations against observations can effectively be used for validating primary PM emissions. While measurements distinguishing between primary and secondary OC are no available, EC appears to be the only component which can be used to evaluate the quality of PM emission data at present. In the current calculations, the emission inventory for fine OC and EC (i.e. in PM_1 emissions) developed at IIASA has been employed (Kupiainen et al., 2004). Based on these data, OC and EC fractions in $PM_{2.5}$ emissions have been derived for each of the SNAP 1 sectors. Furthermore, also coarse carbonaceous particles can be emitted (e.g. in traffic non-exhaust emissions, production processes, agriculture, residential heating). However, as no appropriate data on the chemical composition of coarse PM emissions were available, all coarse PM emissions are currently assumed to consist of mineral dust. Thus, model calculated concentrations of EC and OC actually represent only the fine fraction, and are expected to be an underestimate of observed EC and OC.

Figure 3.15 presents modelled and observed geographical distribution of EC and OC concentrations in Europe. The measured concentrations are shown as averages over the whole measurement campaign period (1.07.2002–1.07.2003), while the calculated concentrations are annual means in 2002. The model manages to reproduce the main features of observed distribution pattern of EC and OC, with highest values in the northern Italy and Belgium and lowest values in Northern Europe. Yet, the model underestimates measured concentrations of EC and in particularly OC (please, keep in mind that the calculated EC and OC represents the fine aerosol fraction).

This can be better seen in the scatter-plots of calculated versus measured EC and OC concentrations averaged over the period 1.07–31.12.2002 (Figure 3.16). Rather good spatial correlation between model results and observations is seen for both EC and OC (0.88 and 0.86). The model tends to underestimate EC concentrations at most of the sites. High calculated EC concentrations at NO01 (Birkenes) are due to the significant contribution of EC emissions from the flaring on Norwegian oil platforms. When considering OC results, it should be kept in mind that model calculated OC does not represent all atmospheric organic aerosol, but only its anthropogenic primary fraction. Therefore, OC concentrations are considerably under-predicted by the model.

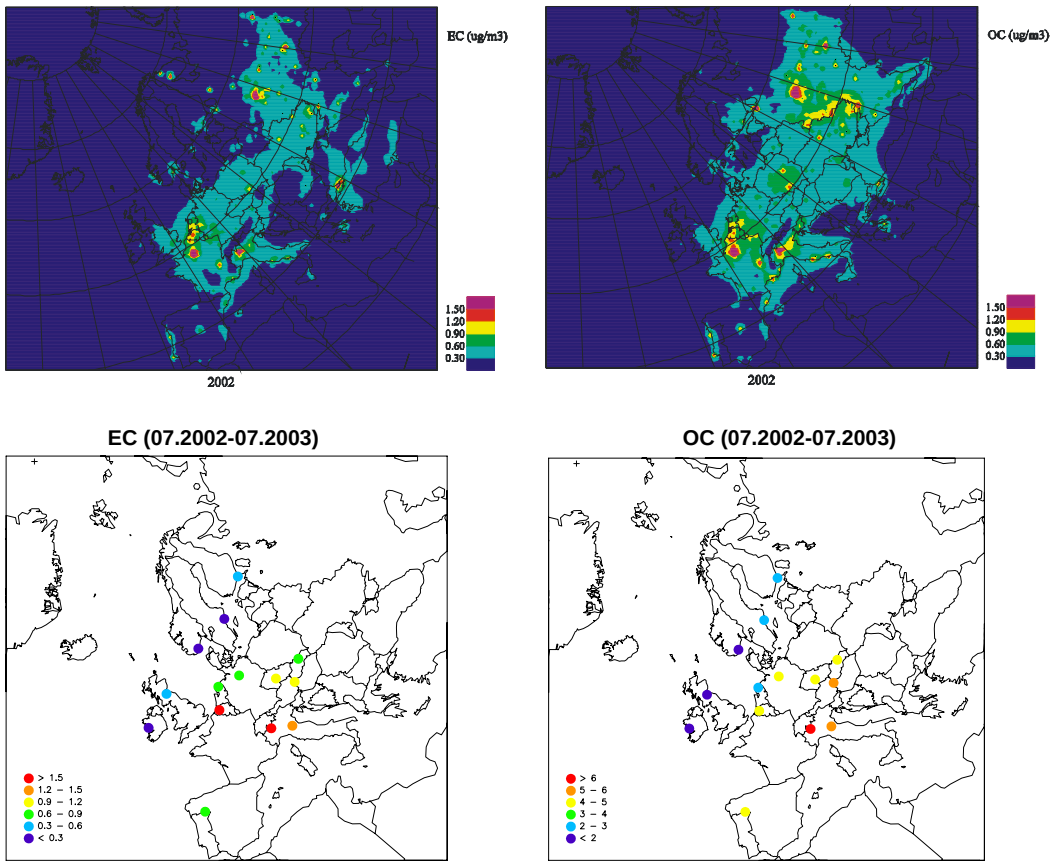

Figure 3.15: Maps of EC and OC concentrations: model calculated 2002 annual mean[*)] *(upper panel) and measured, averaged over the campaign period (lower panel)* [**)].

[*)] *Fine EC and OC from the model;* [**)] *Be aware of different colour scale in the legends for OC model results and observations.*

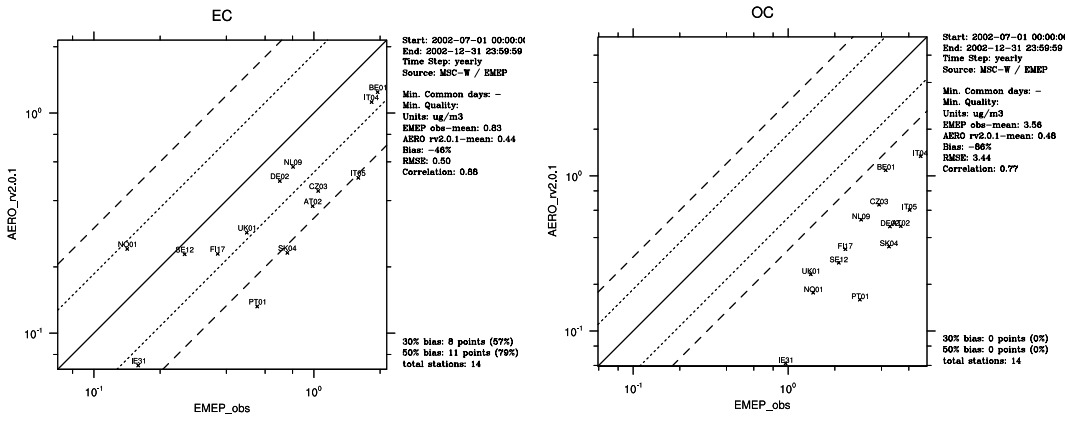

Figure 3.16: Scatter-plots of model calculated[*)] *versus measured EC and OC averaged over the period from July to December 2002 (measurements were taken one day a week during NILU coordinated OC/EC campaign).* [*)] *Fine EC and OC.*

Time-series of calculated versus measured EC concentrations are given in Appendix. The temporal correlation between calculated and measured EC concentrations vary rather broadly: from rather good (0.4-0.78) at 5 of 14 sites (DE02, IE31, IT04, IT05, FI17, NL09, PT01) to somewhat lower (0.26-0.36) at 4 sites (CZ03, SE12, SK04, NO01), to the poorest (0.06-0.16) at Illmitz (AT02), Penicuik (UK) and Gent (BE).

As it was already discussed, OC concentrations are considerably underestimated by the model, as the aerosol model does not account for secondary organic and primary biogenic aerosol. However, the temporal correlation between calculated and measured OC is fairly good, even better than for EC at some sites. The work on developing and testing parameterisations for SOA formation is successively progressing and some initial results are presented in the next chapter.

The validation of PM emissions has just started, but the initial results indicate that further efforts should be made to improve the quality of PM emission data. In particular, distribution of PM emissions between different sectors needs further analysis. Also, the work should be continued on describing the chemical speciation of PM emissions.

Sea salt

Sea salt particles represent a natural component in ambient aerosols. Nevertheless, they have to be properly accounted for in the model in order to achieve a full PM mass closure. Besides, sea salt affects the chemistry and transport of sulphate and nitrate as coarse SO_4^{2-} and NO_3^- aerosols form on sea salt particles.

Model calculated concentrations of sodium (Na^+) originated from sea salt aerosol have been compared with Na^+ measurements from 7 Norwegian and 3 Danish sites in 2001 and 2002. The scatter-plots in Figure 3.17 show that the model tends to underestimate measured Na^+ concentrations at all of the sites except for Spitsbergen (NO42). The spatial correlation between modelled and observed Na^+ concentrations in these years is quite good (0.84 and 0.72).

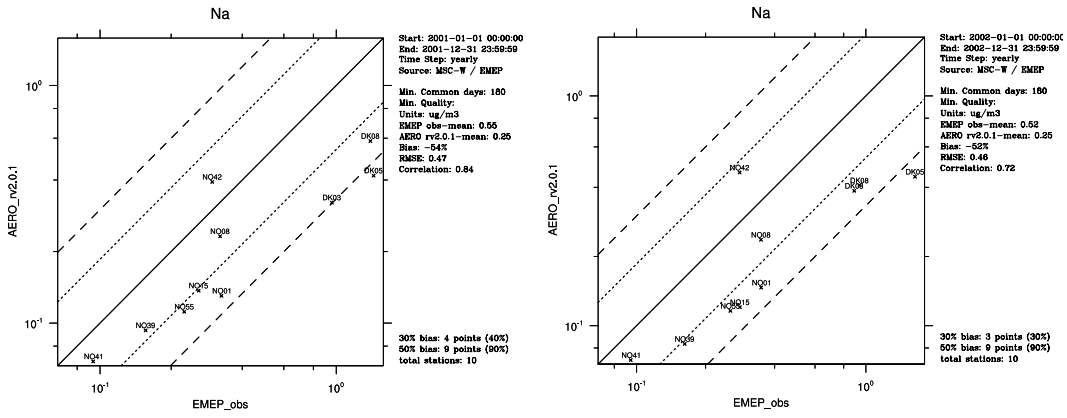

Figure 3.17: Scatter-plots of calculated versus measured Na^+ concentrations in 2001 and 2002.

Model underestimation of Na^+ at some stations is thought to result from the rather large gradients of sea salt in coastal areas (and thus large sub-grid concentration variability), which was not accurately enough resolved with the EMEP model.

The temporal correlation coefficients between calculated and measured daily Na^+ are also quite good, mostly between 0.4 and 0.7. The best agreement between model and observation results was found at Skreådalen (NO08), Tustervatn (NO15) and Anholt (DK08) in 2001 and 2002, and the worst at Spitsbergen (NO42) and Tange (DK03) in 2002. Some examples of time-series, given in Figure 3.18, show that the model manages to capture most of the sea salt episodes.

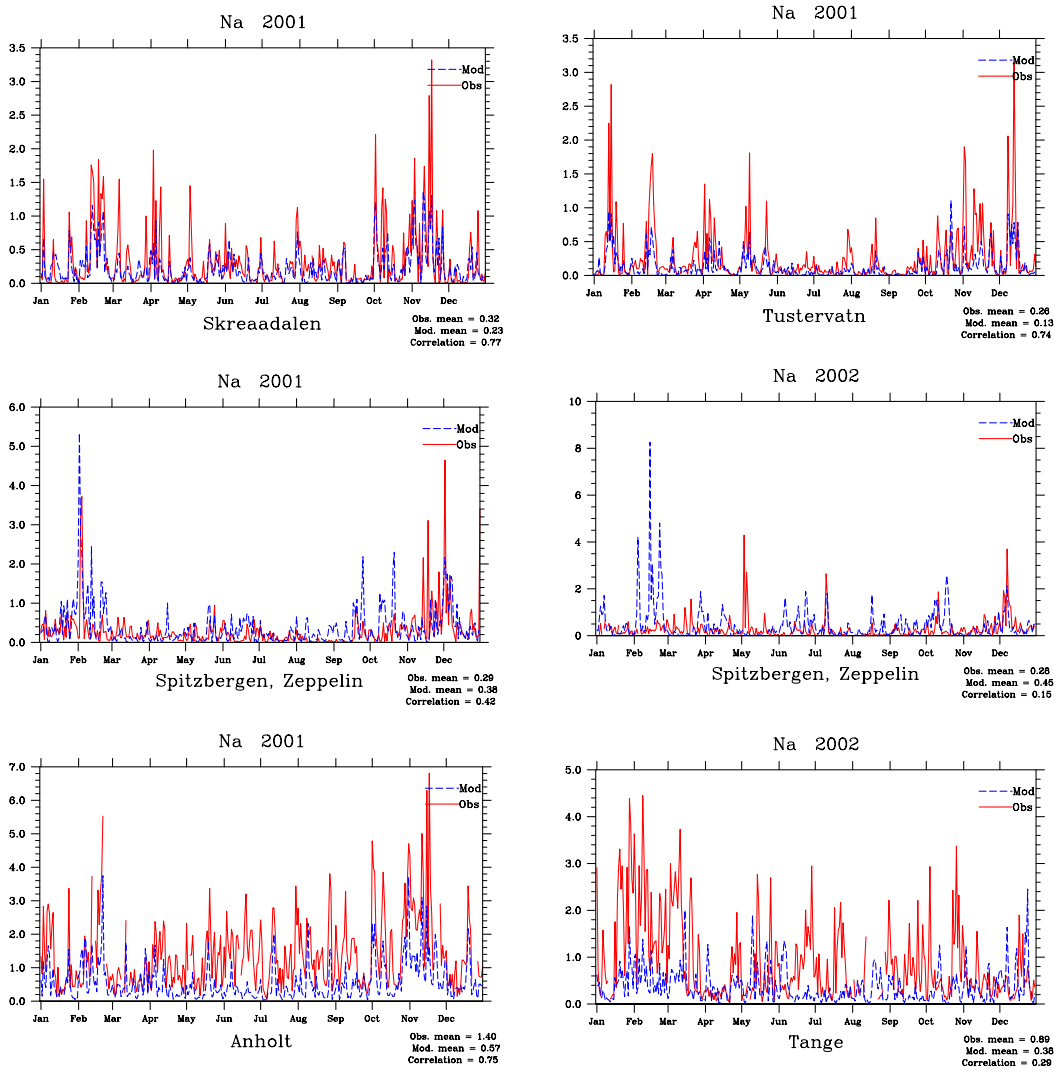

Figure 3.18: Time-series of calculated vs. measured Na^+ concentrations in 2001 and 2002 (selected stations).

Concluding the discussion on the results for different aerosol components, model calculations of SIA (SO_4^{2-}, NO_3^- and NH_4^+) are generally in a satisfactory agreement with observations. Overall concentrations of EC and particularly OC are considerably underestimated by the model. Concentrations of mineral dust are underestimated in the areas where the contribution of natural dust sources (wind

soil erosion, desert sand storms) to PM mass is significant. Sea salt aerosol is generally calculated rather well, though tends to be underestimated by the model.

Furthermore, uncertainties in calculated concentrations of EC, primary OC and anthropogenic mineral dust are to a large degree related to the uncertainties in PM emissions and their chemical composition. Secondary organic carbon and natural mineral dust is not yet included in the aerosol model. The work on developing and testing of the parameterisation of SOA formation is on-going (see Chapter 3). Moreover, the work on implementation in the model of wind blown dust and accounting for the effect of African dust is in good progress. And finally, accounting for particle water in calculated $PM_{2.5}$ and PM_{10} has been shown to improve the correspondence between the model results and observation. With particle water included, calculated $PM_{2.5}$ concentrations can account for around 80% of the measured $PM_{2.5}$ mass.

Following the recommendation from the evaluation of the EMEP model by TFMM Workshop (November 2003, Oslo), our efforts are presently focused on completion of the full mass closure for $PM_{2.5}$ and $PM_{10,}$ which is essential for the source apportionment and evaluation of policy options. The particular attention in the model development will be given to achievement of the full assessment of the anthropogenic fraction of $PM_{2.5}$. It has been shown that the EMEP model is able to calculate the regional component of main anthropogenic PM fractions (sulphate, nitrate, ammonium, some primary components) with the accuracy sufficient for the assessment of the outcome of different control measures. In its present form, the model should not be use in studies requiring the analysis of total PM mass, but it may be applied for analysis of the effects of identified emission changes.

3.4.6 Particle number

WHO Task force on Health indicated that ultra fine particles (those smaller than 0.1 μm in diameter) are expected to induce more severe (toxicological) health effects as they are able to penetrate deeper in the respiratory system, in the gas-exchange region of the lungs. UF particles contribute negligibly little to fine PM mass and thus have to be described by their number concentrations. Experimental evidences show that the particle number concentration does not necessarily correlate to particle mass. In other words, large number concentrations may occur in the areas with relatively moderate levels of PM mass and conversely.

Regional modelling of particle number concentration and size distribution involves far more uncertainties than calculation of particle mass and also particle composition. The largest uncertainties in calculated particle numbers are presently associated with the lack of information on the size disaggregation of anthropogenic PM emissions. Furthermore, sound description of aerosol dynamics processes in the model becomes crucial for accurate calculation of particle number, whilst it is much less important for PM mass calculations. At present, validation of model results on particle number concentrations is hampered by rather limited measurement data available.

Particle number concentrations calculated with the latest version of the aerosol model have been compared with measurements at four Nordic sites (Figure 3.19).

The data was collected within a framework of the Swedish ASTA research program in a close co-operation with University of Helsinki.

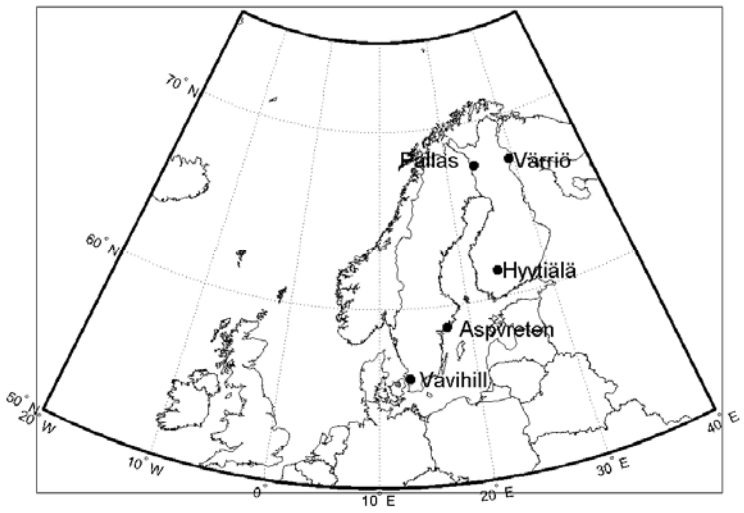

Figure 3.19: Location of the sites with measurements of particle number concentrations (from Tunved et al., 2003).

The measurement data set included hourly averaged number concentrations of particles with diameters in the range from 3-10 nm to ca. 0.5 μm, collected in the period from 1 June to 31 December 2000. To facilitate comparison with model calculations, the measured number concentrations were disaggregated in three sizes bins: nucleation (diameters smaller than 0.02 μm), Aitken (diameters between 0.02 and 0.1 μm) and small accumulation (diameters between 0.1 and 0.5 μm). The following conclusions can be drawn from examination of the time-series of calculated versus measured particle number concentrations.

Nucleation particles (Figure 3.20). At present, the model fails to describe properly the formation of new particle by nucleation. The model does not manage to capture the occurrence of nucleation events. At southern pair of the sites (Hyytiälä and Aspvreten), the model often fails to predict the onset of nucleation and greatly underestimates the number of nucleated particles. Conversely, at northern pair of the sites (Värriö and Pallas) the model tends to over-predict the frequency of nucleation bursts and the number of nucleated particles. The larger numbers of nucleation particles measured at Hyytiälä can also be because particles from as small as 3 nm in diameter were detected, while at the other sites the lower detection particle sizes were 7 to 10 nm.

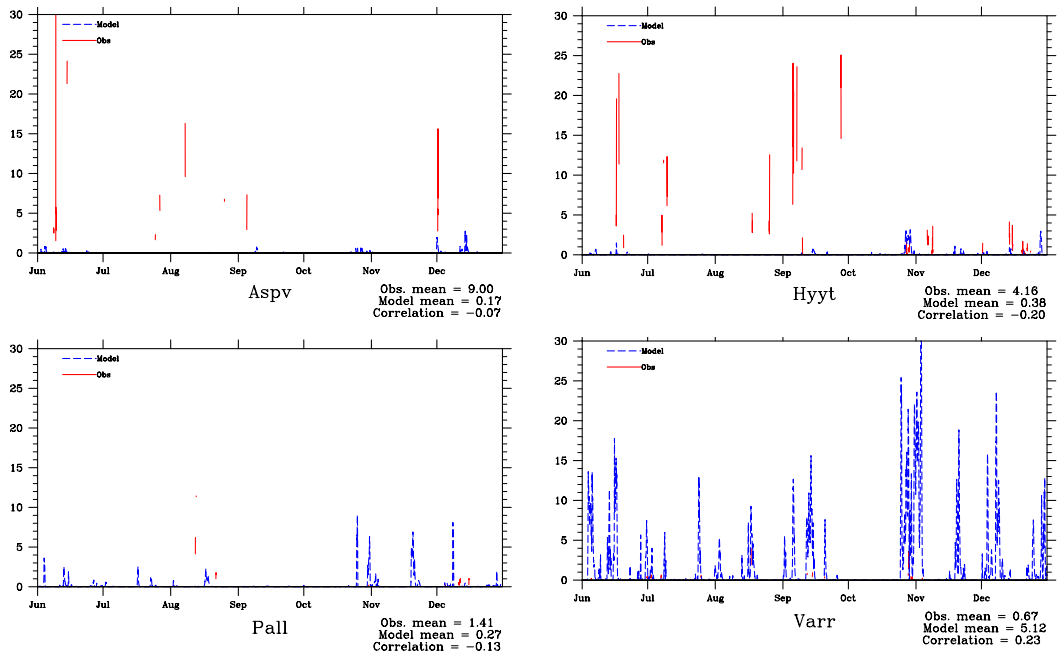

Figure 3.20: Model calculated (red) and measured (blue) hourly number concentration of nucleation particle: June-December 2000.

Aitken particles. Given the lack of appropriate information, rather crude assumption on PM emission size distribution is used in the EMEP aerosol model, as described in EMEP Report 1/2003 Part I. Model estimated levels of Aitken number concentrations are on average reasonably close to observations at the four stations. However, the seasonal variation of Aitken particle numbers predicted by the model differs from the measurements: modelled number of Aitken particles is higher in late autumn and winter following the seasonal variation of emissions in the model, whereas measurements show somewhat larger Aitken particle densities in summer.

When the whole period is considered, very poor correlations between calculated and measured number concentrations of Aitken particles are found for both hourly and daily concentrations (Figure 3.21). The failure of the model to describe the temporal evolution of Aitken particle number is probably due to its inadequate description of or/and not accounting for all important processes and sources (likely of local character), which determine the particle number. For example, much better correlation of calculated Aitken numbers with observations is found at Hyytiälä in the period from November to December, when nucleation events were not observed. While from June to September, when nucleation bursts occurred and the grown nucleation particles probably contributed to Aitken particle number, the correlation is very poor (Figure 3.21). Also at Värriö and Pallas (but not Aspvreten), better correlations between calculated and observed Aitken number concentrations were found for October through December months, yet at those sites it cannot be explained by the effect of nucleation alone.

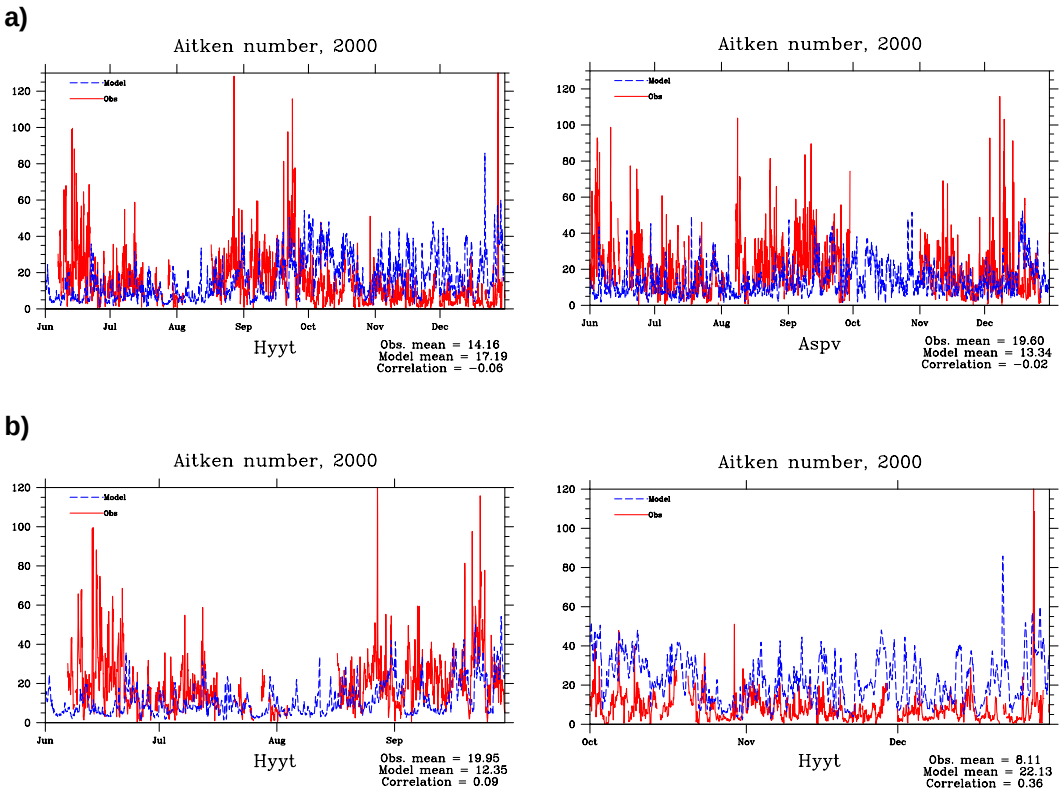

Figure 3.21: Hourly number concentrations of Aitken particles, calculated (blue) and measured (red), (a) for the period of 1 June–31 December 2000 at Hyytiälä and Aspvreten and (b) at Hyytiälä in warm and cold months.

Accumulation (<0.5 µm) particles. The model performs much better with respect to accumulation particle number concentrations. This is probably because the number of accumulation particles is to a larger degree determined by the emissions and transport and less affected by aerosol dynamics (sub-grid scale processes), and thus are less stochastic. Averaged over the period 1.06.-31.12.2000, model calculated number concentrations of accumulation particle are rather close to the observations (Figure 3.22). Similarly to results for Aitken particles, the model calculates greater number concentrations of accumulation particles in winter than in summer, whereas the observations show the opposite. The correlation coefficients at all four sites are between 0.13 and 0.43 for hourly and between 0.12 and 0.55 for daily number concentrations.

Particle total volume (Figure 3.23). The total volume of dry particles has been derived from model and measurement results assuming particle density of 10^3 kg/m^3. The model underestimates the particle integrated volume from measurements, but the correlation between modelled and measured particle volume is fairly good (0.42-0.54 for hourly and 0.51-0.64 for daily volume averages).

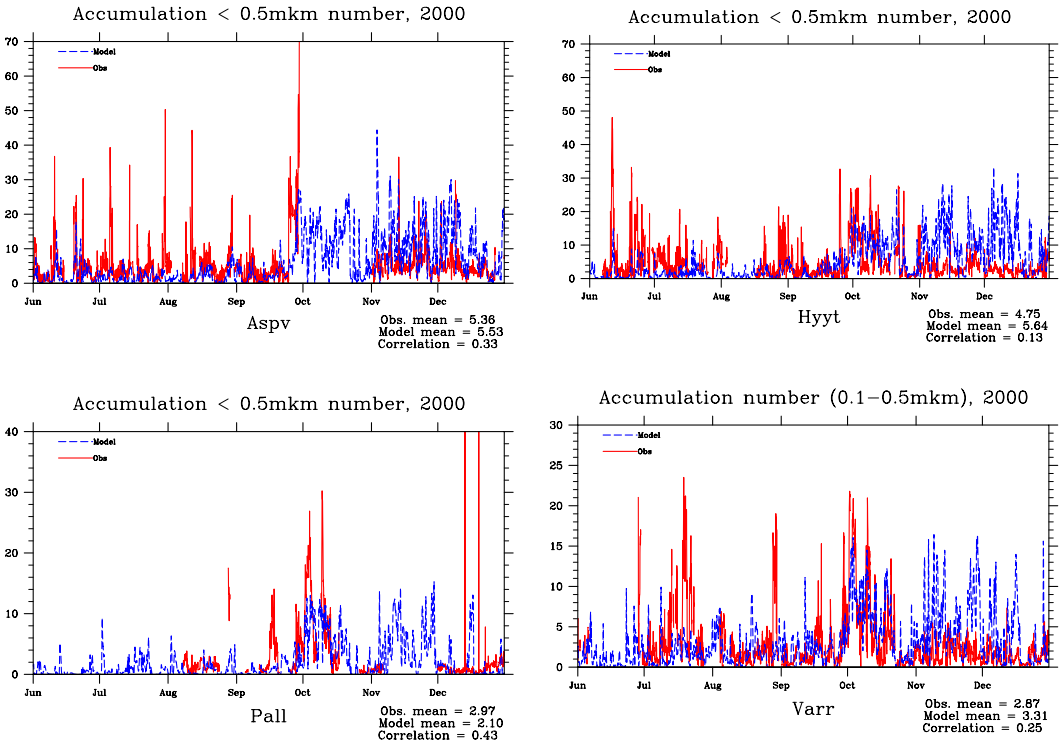

Figure 3.22: Hourly time-series of number concentration of accumulation particles, calculated (blue) and measured (red), at Aspvreten, Hyytiälä, Pallas and Värriö. 1 June–31 December 2000.

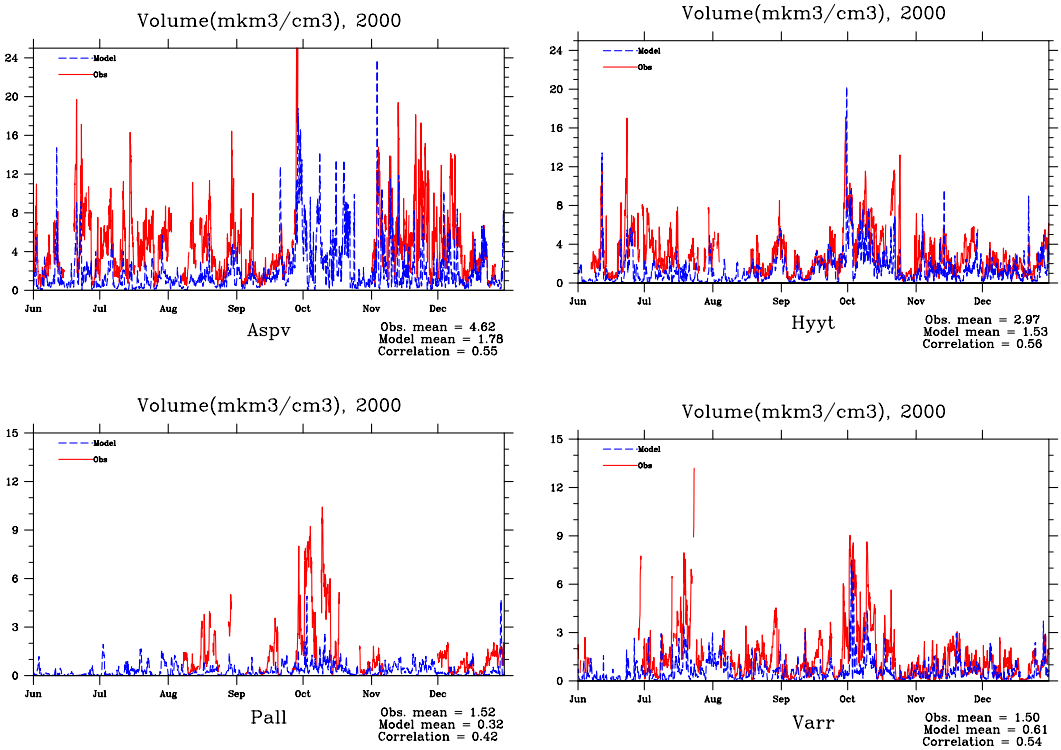

Figure 3.23: Hourly time-series of particle integrated volume, calculated (blue) and measured (red), at Aspvreten, Hyytiälä, Pallas and Värriö. 1 June–31 December 2000.

Acknowledgements

Measurements on PM chemical composition were made available to us from the Austrian AUPHEP project and from the databases of the Spanish Ministry of Science and Technology Spanish Ministry of Environment. Special thanks are due to Xavier Querol for providing us with the measurements in Spain and the assistance in understanding the data.

4. Modelling SOA and OC in Europe

by David Simpson and Paul Makar

4.1 Introduction

Our understanding of secondary organic aerosol (SOA) has been in a state of great flux for several years now. Important new results appear at regular intervals. Most current models, including EMEP, build upon the framework developed by Pankow (1994a,b); Odum et al. (1997), based upon gas-particle partitioning theory. This theory provides a quantitative explanation for the wide range of aerosol yields previously observed by different experiments. Recently, as new analytical techniques have become available, chemists have succeeded in identifying a significant proportion of the actual compounds in both the gas and aerosol phases of smog-chamber reactants (e.g. Kamens and Jaoui, 2001). Kinetic models can now be constructed which show rather good success in predicting the extent and composition of aerosol formation from such important precursor compounds as α-pinene under a wide range of conditions (Kamens et al., 1999; Kamens and Jaoui, 2001; Andersson-Sköld and Simpson 2001).

However, these successes apply mainly to smog-chambers (SCs), where conditions are usually very far removed from those of the ambient atmosphere. Differences include temperature and relative humidity in SCs, and especially concentration levels, which are often far from ambient levels. Additionally, SCs provide by design a rather simple mixture of gases, usually derived from the degradation of one main VOC species. A consequence of this is that the reaction products in SCs condense onto an aerosol phase, which is derived from this species. In the ambient atmosphere it is very likely that the SOA will condense onto pre-existing aerosol. The latter will be a very complex mixture of compounds which are derived from primary emissions and SOA condensation, and where aerosol-phase chemical reactions among these species may well have generated complex non-volatile compounds.

Most recently, a number of papers have recognised the role of various heterogeneous mechanisms for forming aerosols, in which the species, which condense onto an aerosol, undergo further reactions to form species of much lower volatility. These new findings have included experimental production of aerosols from species, which were previously not thought to be involved in SOA production (Jang et al., 2002; Kalberer et al., 2004; Limbeck et al., 2003. Additionally observations of ambient aerosol have provided good evidence for the existence of complex compounds such as polymers, or humic-like substances (e.g. Gelencsér et al., 2003; Hoffer et al., 2004).

From the above, it is obvious that attempting to use models to predict the formation and composition of SOA in ambient atmospheres is a very uncertain activity. Nevertheless, it is instructive and important to apply our best-available theories in order to begin the iterative process of matching model-results and observations, a process which will ultimately lead to better models and which should generate further ideas for the type of measurements which can be used to

decide between competing theories. This chapter briefly describes some preliminary modelling work undertaken within EMEP MSC-W, aiming to understand the extent to which current SOA theories are consistent with measurements. This work is currently in-progress and more details will be presented in a future publication.

4.2 The EMEP model

The model used in this work is an extended version of the EMEP MSC-W Unified 3-D model (Simpson et al., 2003a). This model has been thoroughly evaluated and found to perform well for both gases (e.g. O_3, NO_2), and inorganic particulates (e.g. sulphate, nitrate). For details, see Simpson et al. (2003b) and Fagerli et al. (2003).

The SOA model used here extends the chemical mechanism of the standard EMEP model with the inclusion of emissions of biogenic terpene emissions (represented as α-pinene) and a number of organic aeorsol components:

- POC: Primary emissions (anthropogenic)
- ASOA: Anthropogenic SOA (from aromatics)
- BSOA: Biogenic SOA (from terpenes)
- BGND: Background OC (mix of POC/BSOA)

For α-pinene the detailed gas/particle scheme of Andersson-Sköld and Simpson (2001) is used. This scheme, an extension of that presented in Kamens et al. (1999) was found to perform very well when compared to smog-chamber data over a wide range of concentrations. For aromatics a simpler 2-product scheme is used, with the representative species 3-methyl-2,5-furandione, tolualdehyde, following Ansari and Pandis (2000). Gas/Particle partitioning is applied in a similar manner to that used in Andersson-Sköld and Simpson (2001), but with vapour pressures calculated as a function of chemical structure and temperature using a Lee-Kessler approach.

The anthropogenic primary OC (POC) consists of two classes, (1) fossil-fuel combustion emissions; and (2) wood-burning from residential combustion. The fossil-fuel combustion is represented by heavy alkane and acid species such as tetracosane, heneicosane and hexadecanoic acid. The surrogates used to represent emissions from from wood-combustion include the very low-vapour pressure compounds levoglucosan and guaiacyl acetone, as well as benzoic acid and palmitic acid (e.g. Schauer et al., 2001, see e.g.). A 'background' OC concentration level of 1 $\mu g/m^3$ (near the surface) is also assumed throughout the model domain, consisting of a mixture of the VOC compounds from all other sources.

4.3 Model Results

Figure 4.1 shows the modelled annual average OC concentration, obtained for the year 2002 with the above model setup. The results clearly show a broad maxima of OC in Northern Europe and particularly Finland and Northern Russia. The reason for this distribution is made clear in Figure 4.2, which shows the very large percentage contribution of BSOA to this total. It is clear that the BSOA contribute

very much more OC than anthropogenic sources. Indeed, even the 'background' OC we have assumed in this modelling work is a bigger contributor to total OC levels than ASOA in many regions, and notably in western areas, accounting for most of the difference between the BSOA contribution and 100% (not shown).

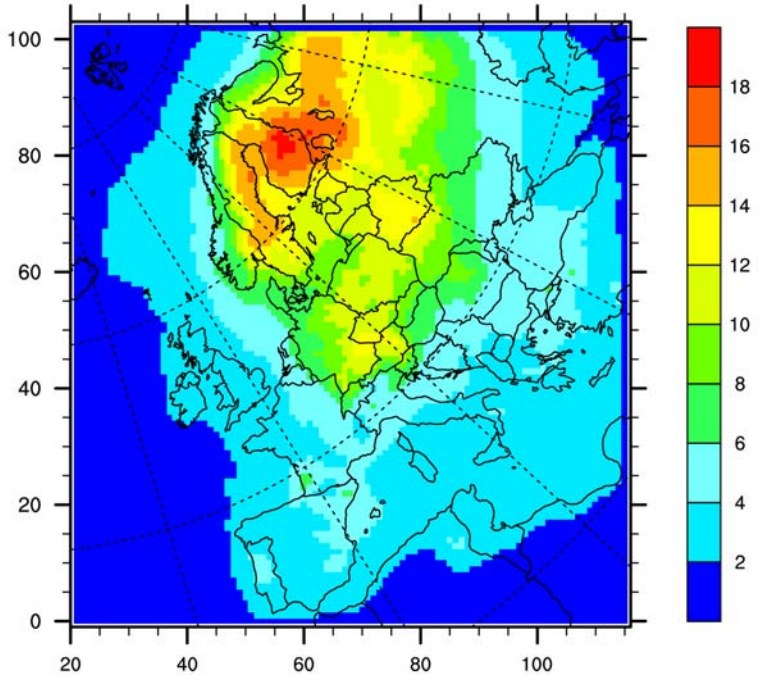

Figure 4.1: Modelled Organic Carbon (μg/m^3) over Europe, year 2002.

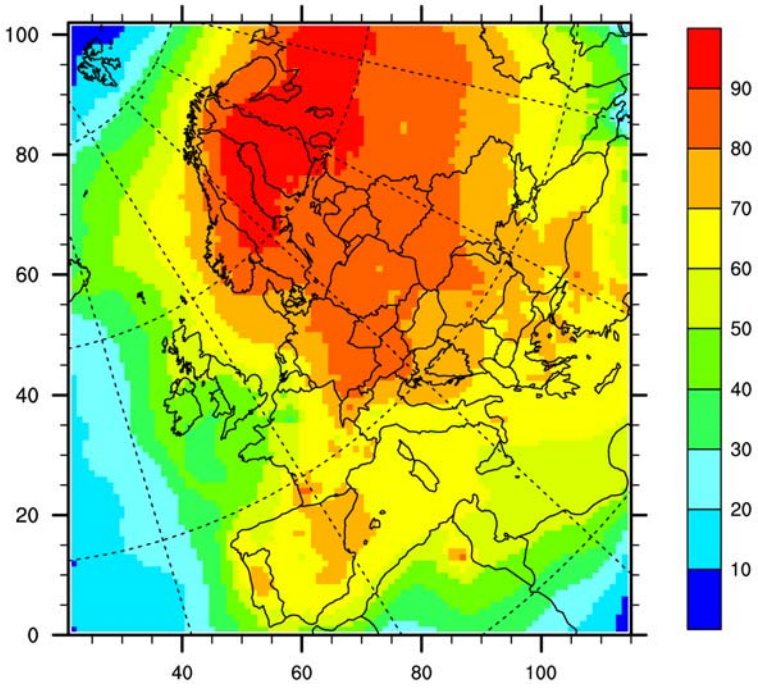

Figure 4.2: Percentage contribution of biogenic sources (BSOA) to OC.

4.4 Seasonal contributions

Figure 4.3 illustrates the seasonal variation of the model results for a location in Hungary, K-Puszta. For each source (ASOA which includes POC; BSOA; BGND=background, OIL=fossil-fuel, WOOD=wood combustion) the monthly OC values are plotted. This plot clearly shows the strong summer maximum produced by the BSOA component, produced by the strong summertime maxima in their emissions (Simpson et al., 1995). In contrast, all the anthropogenic sources have OC maxima in wintertime, presumably reflecting their temporal emission pattern and the fact that OC condensation is increased in cold temperatures.

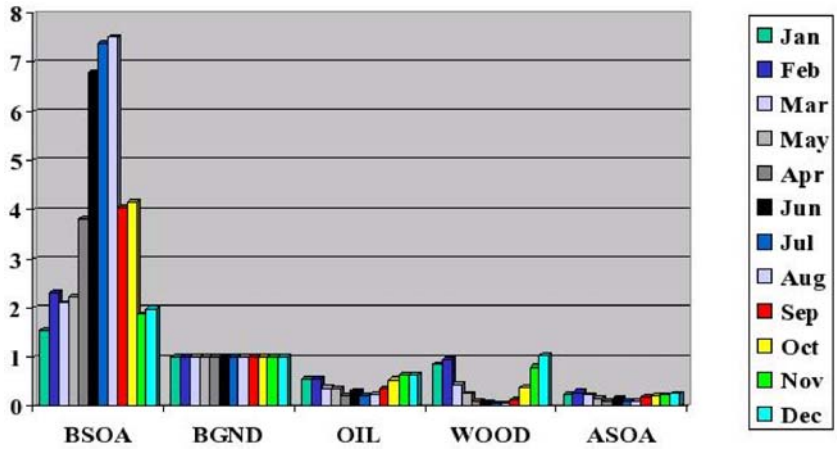

Figure 4.3: Seasonal variations in modelled OC from different sources. See text for source explanations.

4.5 Comparison with measurements

Figure 4.4 shows a comparison of the modelled OC against measurements made at the Austrian site Illmitz as part of the OC/EC campaign (Kahnert, 2003). Two modelled values are shown. The 'mod-POC' gives the contribution of modelled primary emissions of OC. The 'Mod-OC' gives the total model estimate of OC levels, including SOA. In general the levels of modelled and observed OC are quite similar at this site, especially considering the large uncertainties discussed above. However, one discrepancy is obvious and appears also in all other comparisons we have performed: the observations show large OC values in winter and do not show the clear seasonal cycle that the model results would suggest. The underprediction of winter-time OC may have a number of explanations (e.g. underestimation of POC emissions, insufficient ASOA production) and is currently under investigation.

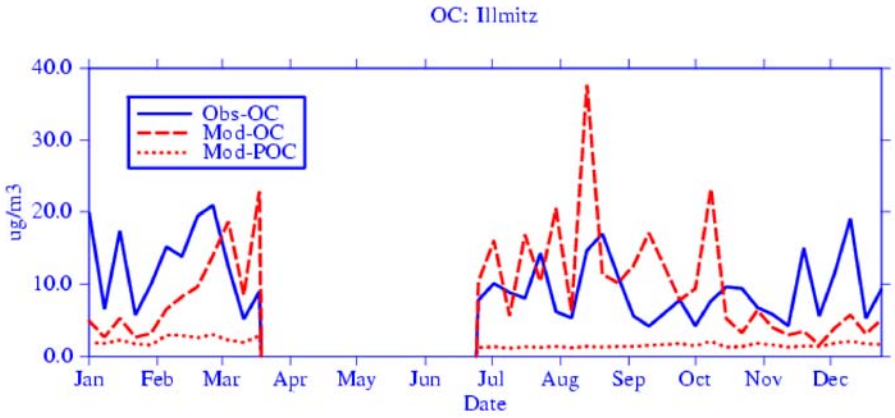

Figure 4.4: Modelled versus observed OC concentrations at Illmitz (Austria). Data are from 2002 for the July-Dec values and 2003 for the Jan-March values. See text for explanation of lines.

4.6 Discussion and conclusions

We have presented a very brief overview of the results of an extended version of the EMEP model, designed for studies of SOA formation over Europe. This work is in-progress, and so the results presented here are preliminary. However, this work and related studies conducted over several years suggest that:

- A model with no SOA and current emissions strongly underpredicts OC across Europe
- Adding a 'standard' SOA module gives much more OC in summer (even too much at some sites - not shown)
- The SOA-model predicts strong summer maxima in OC which are not reported
- Seems likely that the missing OC in winter-time results from both SOA and missing POC.

It should be noted again that SOA theories are undergoing rapid change. Increasing evidence for polymerisation and other reactions within aerosol would suggest that even more SOA should be formed than given in the standard models.

In fact, even though most SOA modules in use today are based upon the same framework as discussed above, they may still give very different results to one another. Pun et al. (2003) dramatically illustrated the importance of some of these uncertainties in a model study in the United States. Three SOA models, all representative of modern ideas and practice, were applied to the same model situation. The three models gave differences of more than a factor of ten in SOA.

It is currently impossible therefore to assign much certainty to the results of any SOA model. However, with the increasing number of measurements from for example the NILU EC/OC campaign, the EU CARBOSOL project (http://www.vein.hu/CARBOSOL), or from national projects, there is some hope of evaluating the model against observations in a semi-empirical way. As an interesting example, Szidat et al. (2004) used carbon-isotopes to estimate the

proportion of the organic aerosol over Zurich (Switzerland) coming from modern carbon (mainly BSOA) compared to fossil-fuel carbon. They found that between 59-80% of daytime OC could be assigned to modern biogenic sources. In future studies we will more closely compare the EMEP model results with these measurements and work towards a reconciliation of the modelled sources and the observations.

Acknowledgements

This work was supported by the EU project CARBOSOL and EMEP.

5. An initial outlook into the future development of fine particulate matter in Europe

by Markus Amann, Janusz Cofala, Chris Heyes, Zbigniew Klimont, Wolfgang Schöpp, Jan Eiof Jonson, David Simpson and Leonor Tarrason

5.1 Introduction

This chapter presents the initial results of a baseline assessment of future air quality in Europe by bringing together the recently updated analysis tools: improved emission estimates of the RAINS model, results from the Eulerian EMEP model and novel approaches to estimate impacts of air pollution on human health and ecosystems. The analysis combines recent information on expected trends in energy consumption, transport, industrial and agricultural activities with validated databases describing the present structure and technical features of the various emissions sources in all countries of the present EMEP modelling domain. It considers the penetration of already decided emission control legislation in the various Member States in the coming years and thereby outlines a likely range for the future emissions of air pollutants up to 2020. In a further step, the analysis sketches the resulting evolution of air quality in Europe and quantifies the consequences on the effects of air pollution on human health and vegetation using a range of indicators.

For the 25 Member States of the European Union, the analysis incorporates the findings of the draft baseline scenario of the Clean Air Programme for Europe as of May 2004. For the other countries in the EMEP model domain which are not Member States of the European Union this report presents the initial analysis conducted by CIAM on national emission estimates and emission projections, relying on internationally available material. While the model estimates for EU Member States have been discussed with national experts, validation for the non-EU countries is outstanding.

This report presents the general assumptions and findings of the analysis conducted to date. Obviously, all calculations are carried out at a national and sectoral level, and consequently all assumptions and results are available for each country in the EMEP model domain. It is, however, beyond the scope of this report to present this detailed information. Instead, the interested reader is invited to explore detailed results with the Internet version of the RAINS model, which can be freely accessed at http://www.iiasa.ac.at/web-apps/tap/RainsWeb/.

5.2 Methodology

5.2.1 The RAINS model

The analysis builds on the Regional Air Pollution Information and Simulation (RAINS) model, which describes the pathways of pollution from its anthropogenic driving forces to the various environmental impacts. In doing so, the model compiles for all European countries databases with the essential information on all aspects listed above and links this data in such a way that the

implications of alternative assumptions on economic development and emission control strategies can be assessed.

The RAINS model developed by the International Institute for Applied Systems Analysis (IIASA) combines information on economic and energy development, emission control potentials and costs, atmospheric dispersion characteristics and environmental sensitivities towards air pollution (Schöpp et al., 1999). The model addresses threats to human health posed by fine particulates and ground-level ozone as well as risk of ecosystems damage from acidification, excess nitrogen deposition (eutrophication) and exposure to elevated ambient levels of ozone. These air pollution related problems are considered in a multi-pollutant context (Figure 5.1), quantifying the contributions of sulphur dioxide (SO_2), nitrogen oxides (NO_x), ammonia (NH_3), non-methane volatile organic compounds (VOC), and primary emissions of fine ($PM_{2.5}$) and coarse (PM_{10}-$PM_{2.5}$) particles (Table 5.1). The RAINS model also includes estimates of emissions of relevant greenhouse gases such as carbon dioxide (CO_2) and nitrous oxide (N_2O). Work is progressing to include methane (CH_4) as another direct greenhouse gas as well as carbon monoxide (CO) and black carbon (BC) into the model framework.

A detailed description of the RAINS model, on-line access to certain model parts as well as all input data to the model can be found on the Internet (http://www.iiasa.ac.at/rains).

The RAINS model and its scientific basis are presently being reviewed by a team of experts to judge the scientific credibility of the model approach. The review team is expected to present its finding in the course of 2004.

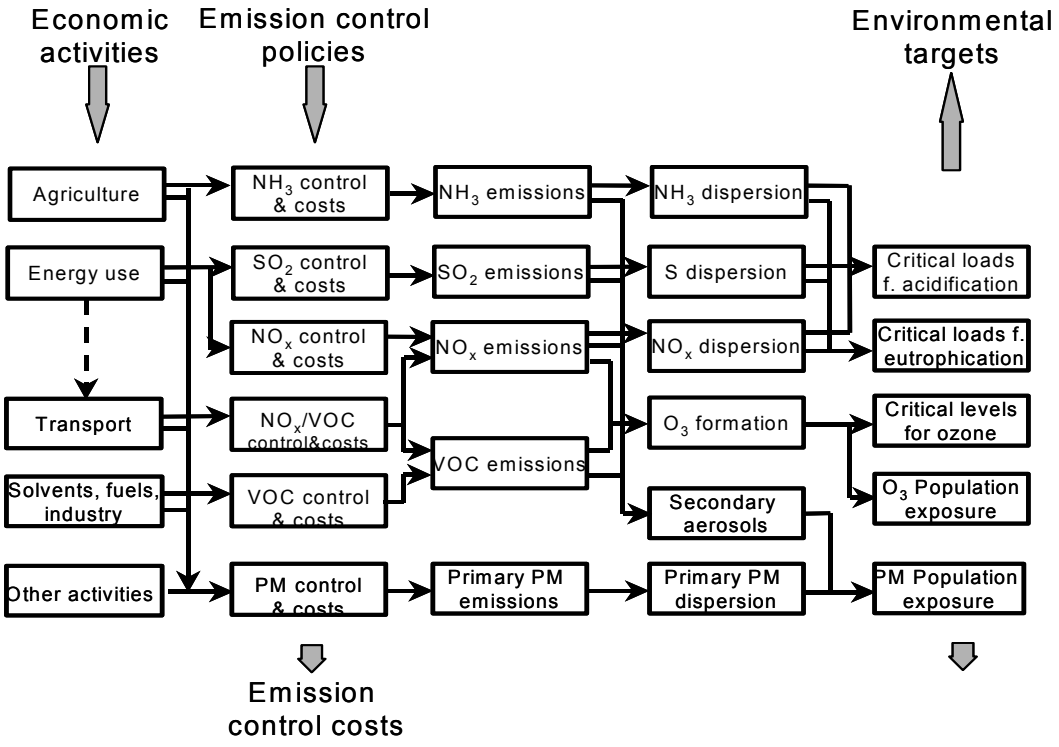

Figure 5.1: Flow of information in the RAINS model.

Table 5.1: Multi-pollutant/multi-effect approach of the RAINS model.

	Primary PM	SO_2	NO_x	VOC	NH_3
Health impacts:					
- PM	√	√	√	√	√
- O_3			√	√	
Vegetation impacts:					
- O_3			√	√	
- Acidification		√	√		√
- Eutrophication			√		√

5.2.2 The baseline energy projection

For the Member States of the European Union the analysis adopts the baseline energy projection of the 'European energy and transport – Trends to 2030' outlook of the Directorate General for Energy and Transport of the European Commission (CEC, 2003) as a starting point. This projection does not assume any further climate measures beyond those already adopted in 2002.

Even in absence of further policies to curb CO_2 emissions, the projection expects production of fossil primary energy within the EU to continue to decline throughout the period to 2020, after peaking in the period 2000-2005. Renewable sources of energy are likely to receive a significant boost as a result of policy and technology progress. Despite the evidence of some saturation for some energy uses in the EU, energy demand is expected to continue to grow throughout the outlook period though at rates significantly smaller than in history.

The EU energy system remains dominated by fossil fuels over the next 25 years and their share rises marginally from its level of just under 80 percent in 1995. The use of solid fuels is expected to continue to decline until 2010 both in absolute terms and as a proportion of total energy demand. Beyond 2015, however, due to the power generation problems that will ensue from the decommissioning of a number of nuclear plants, and the partial loss of competitiveness of gas based generation due to higher natural gas import prices, the demand for solid fuels is projected to increase modestly. Spurred by its very rapid penetration in new power generation plant and co-generation, gas is by far the fastest growing primary fuel. Its share in primary energy consumption is projected to increase from 20 percent in 1995 to 26 percent in 2010. The share of oil in primary consumption is projected to be relatively stable over the period to 2020.

Under baseline assumptions, the technology of electricity and steam generation improves leading to higher thermal efficiency, lower capital costs and greater market availability of new generation technologies. The assumed improvement, however, is not spectacular and no technological breakthrough occurs during the projection period in the baseline scenario. The use of electricity is expected to expand by 1.7 percent per year over the projection period and its growth is expected to be especially rapid in the tertiary and in the transportation sector. Total power capacity requirements for the EU increase by some 300 GW in the 1995-2020 period and a similar amount of new capacity will be required for the

replacement of decommissioned plants. Thus the EU is projected to build 594 GW of new plants over 1995-2020 in order to cover its growing needs and replace the decommissioned plants.

The use of traditional coal and oil plants is expected to decline very rapidly. Due to the decommissioning of older plants, there is a modest decline in the capacity of nuclear plants while nearly half of the thermal plant currently utilised by independent producers is also expected to be scrapped. These declines in capacity are more than made up from the dramatic increase in gas turbine combine cycle plants and small gas turbines. These increase by nearly 10 times over the projection period to exceed 380 GW or almost 45 percent of the total installed capacity by 2020.

The rising share of fossil fuels will lead to an increase in the carbon intensity of the EU energy system. Together with the modest increase in energy demand, this will lead to an increase in CO_2 by 16 percent in the 1995-2020 period. In absolute terms, the increase in emissions originated from combustion of natural gas more than make up for the sharp decline in emissions resulting from the decline in the use of solid fuels. Energy intensity improvements act in favour of moderating the rise of CO_2 emissions, but the overall carbon intensity does not improve (Table 5.3, Table 5.5).

For the other countries in the model domain, energy projections reflect national perspectives that have been communicated to international bodies (e.g., UN/ECE 1997) and CIAM at different points in time. These projections are in principle the same as used for the preparation of the Gothenburg Protocol (Table 5.4, Table 5.6). Table 5.2, Figure 5.2 and Figure 5.3 summarize the evolution of primary energy consumption up to 2020 that has been used for the draft baseline assessment.

The energy projections that have been used for the baseline air quality assessment imply an increase of CO_2 emissions relative to the year 2000 over the entire EMEP domain (Table 5.7, Figure 5.4). Overall, CO_2 emissions are projected to increase by seven percent in 2010 and by 14 percent in 2020 (12 percent in the EU-25 and 20 percent in the non-EU countries).

Table 5.2: Total primary energy consumption (on TPES basis, PJ/year).

	2000	2005	2010	2015	2020
Albania	86	100	101	124	139
Austria	976	1093	1167	1239	1319
Belarus	1181	1452	1430	1425	1459
Belgium	2428	2475	2557	2636	2660
Bosnia and Herzegovina	244	259	279	299	319
Bulgaria	793	744	734	758	792
Croatia	421	440	454	471	487
Cyprus	99	109	120	130	140
Czech Republic	1679	1685	1712	1755	1772
Denmark	835	826	828	842	870
Estonia	189	203	201	203	196
Finland	1391	1458	1564	1578	1595
France	11051	11922	12326	12801	13222
Germany	14214	14508	14562	14433	14331
Greece	1217	1392	1535	1630	1699
Hungary	1049	1091	1122	1155	1181
Ireland	597	690	751	785	822
Italy	7498	7502	7764	7922	8085
Latvia	135	152	163	177	188
Lithuania	302	275	281	318	351
Luxembourg	152	178	198	205	215
Malta	36	42	48	52	53
Netherlands	330	361	349	336	323
Norway	3186	3242	3381	3473	3591
Poland	1031	1084	1161	1195	1252
Portugal	3780	3739	4012	4312	4614
Republic of Moldova	1069	1104	1248	1362	1484
Romania	1546	1598	1746	1897	1981
Russian Federation*	14044	16891	16835	16760	16962
Serbia and Montenegro	583	650	696	743	791
Slovakia	760	702	733	798	859
Slovenia	267	288	304	309	317
Spain	5044	5510	6009	6447	6776
Sweden	2061	2246	2308	2329	2345
Switzerland	1163	1183	1224	1253	1322
The FYR of Macedonia	121	131	139	148	155
Ukraine	6592	6856	6910	6955	6986
United Kingdom	9532	9617	9720	9997	10435
Total	97683	103800	106674	109252	112088

* within the EMEP domain.

Table 5.3: Primary energy consumption by fuel for the EU-25 (PJ).

	2000	2010	2015	2020
Brown coal	2576	2541	2321	1906
Hard coal	8066	6646	6182	6054
Other solids	3709	3813	4016	4093
Heavy fuel oil	5310	4568	4204	4029
Middle distillates	10415	10856	11590	12220
Gasoline	10360	10720	10837	10913
Natural gas	17846	20672	23092	25301
Renewable	215	419	818	986
Hydropower	1065	1061	1112	1149
Nuclear	9949	10610	10267	10019
Total	69510	71907	74438	76671

Table 5.4: Primary energy consumption by fuel for the non-EU countries (PJ).

	2000	2010	2015	2020
Brown coal	1013	979	975	941
Hard coal	2051	2279	2166	2099
Other solids	1382	1563	1544	1484
Heavy fuel oil	2575	2885	2830	2783
Middle distillates	2224	2534	2741	2947
Gasoline	1918	1981	2150	2326
Natural gas	13509	16002	16128	16157
Renewable	5	8	14	27
Hydropower	984	977	998	1020
Nuclear	2582	2644	2604	2663
Total	28244	31852	32148	32446

Table 5.5: Energy consumption by sector for the EU-25 (PJ).

	2000	2010	2015	2020
Power generation	14927	15271	14801	14638
Industry	18044	17721	18472	19102
Households	17306	18276	19343	20204
Transport	14941	16332	17323	18081
Non-energy use	4330	4449	4677	4863
Total	69548	72049	74616	76889

Table 5.6: Energy consumption by sector for the non-EU countries (PJ).

	2000	2010	2015	2020
Power generation	4446	4822	4684	4523
Industry	6717	7400	7721	8056
Households	13509	16002	16128	16157
Transport	989	985	1011	1047
Non-energy use	2582	2644	2604	2663
Total	28244	31852	32148	32446

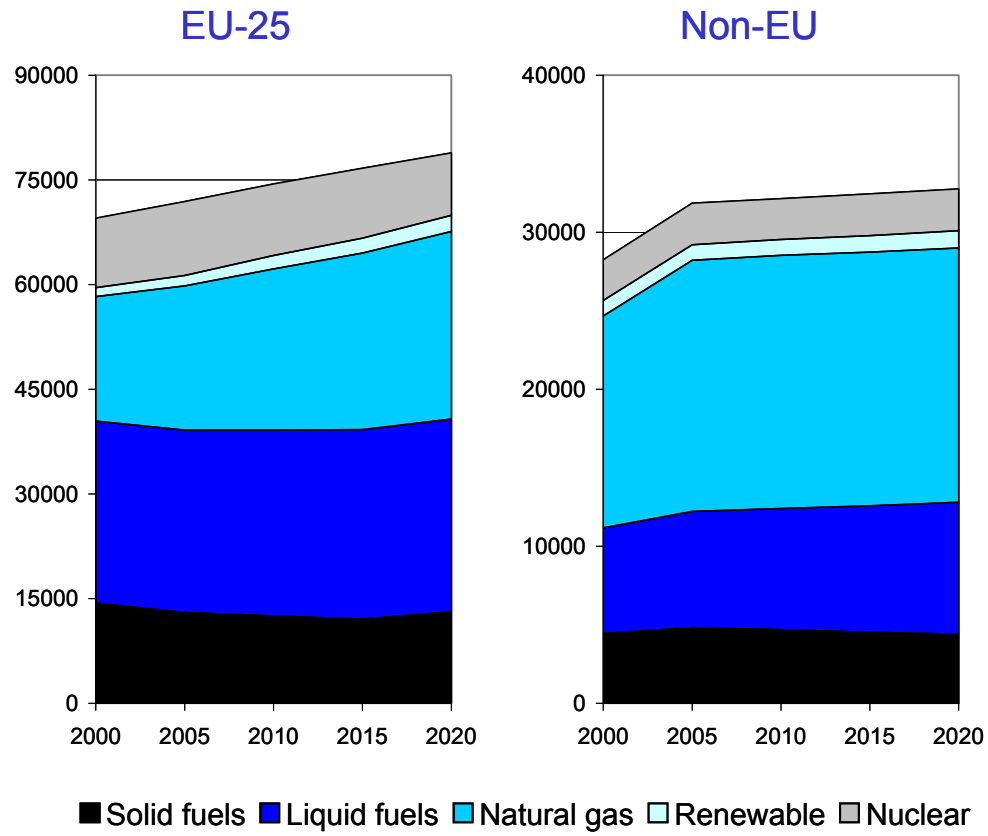

Figure 5.2: Energy use by fuel (in PJ/year).

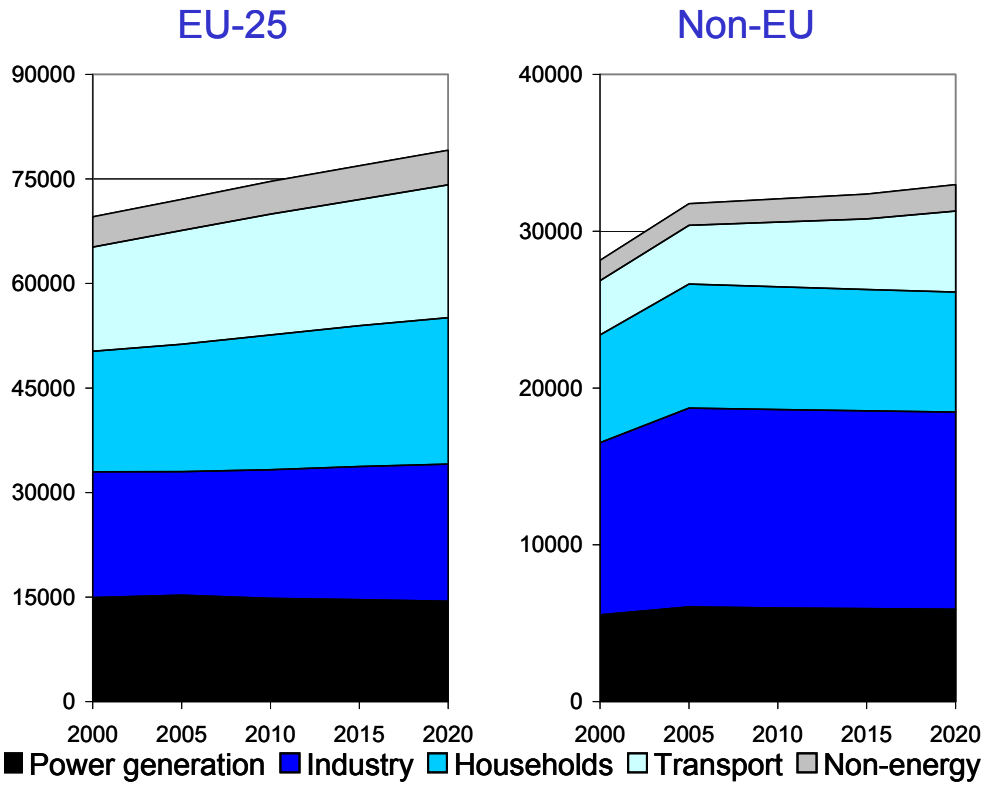

Figure 5.3: Energy use by sector (in PJ/year).

Table 5.7: Total national CO_2 emissions resulting from the energy baseline projection. RAINS calculations including CO_2 emissions from non-energy use of fuels and cement and lime production, in Mt CO_2.

	2000	2005	2010	2015	2020
Albania	4	5	5	6	7
Austria	61	64	64	66	70
Belarus	74	91	88	87	90
Belgium	125	124	125	129	137
Bosnia and Herzegovina	21	24	26	28	31
Bulgaria	47	49	51	52	54
Croatia	23	25	25	26	27
Cyprus	8	8	9	10	10
Czech Republic	123	108	104	105	104
Denmark	55	51	49	49	48
Estonia	15	16	16	15	15
Finland	68	71	68	72	73
France	413	433	447	459	491
Germany	904	920	945	943	1003
Greece	97	110	118	121	126
Hungary	59	63	64	68	71
Ireland	43	48	50	51	53
Italy	467	458	468	475	486
Latvia	7	8	9	10	11
Lithuania	12	13	17	20	22
Luxembourg	9	11	13	13	14
Malta	3	3	4	4	4
Netherlands	23	25	24	23	22
Norway	180	179	189	194	201
Poland	36	39	43	45	47
Portugal	313	308	321	335	352
Republic of Moldova	70	71	79	85	93
Romania	94	95	104	111	115
Russian Federation*	785	950	949	947	963
Serbia and Montenegro	50	59	70	81	92
Slovakia	40	35	41	45	49
Slovenia	15	16	17	17	18
Spain	302	314	329	351	370
Sweden	70	78	79	82	94
Switzerland	49	50	52	53	57
The FYR of Macedonia	11	12	13	14	15
Ukraine	400	417	419	420	421
United Kingdom	567	545	541	551	587
Total	5641	5895	6039	6166	6442

* within the EMEP domain.

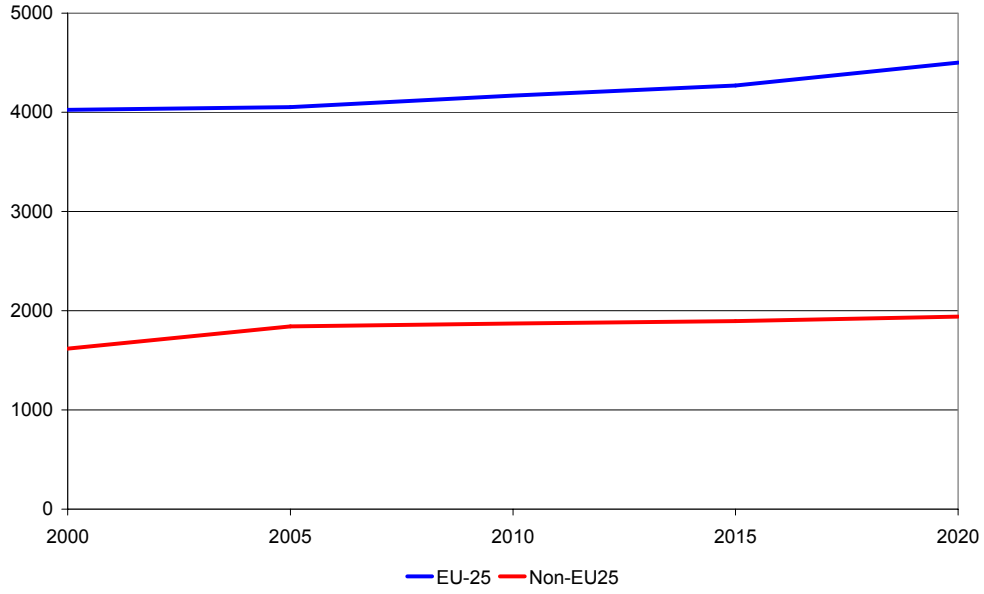

Figure 5.4: CO_2 emissions of the two baseline energy projections (in Mt CO_2).

5.3 Emission projections

5.3.1 Sulphur dioxide (SO_2)

With improved information on country-specific data, the RAINS model reproduces national emission estimates for SO_2 with only minor discrepancies, basing its calculations on reported activity levels (energy consumption, agricultural activities), country-specific emission factors and application rates of emission control measures (Figure 5.5). For the EU-15, the RAINS estimate deviates by 0.3 percent and for the New Member States by 0.8 percent.

Important discrepancies remain for Greece and Luxembourg, where the RAINS model estimates higher emissions than the national reports, and for Portugal and Slovakia, where RAINS estimates are lower than the numbers given in the official inventories. For Luxembourg, the larger RAINS estimate is a consequence of the fact that RAINS calculates emissions for all fuel sold in a country, while the numbers reported by Luxembourg refer only the fuel consumed within the country. For the other countries, resolution of the discrepancies requires further national information, especially if countries reported different emission figures to different organizations over time.

Estimates for non-EU countries need further validation, pending on the availability of documented national emission inventories.

Based on the representation of the base year inventory, the RAINS model projects the future fate of emissions based on the changes in the volumes of emission generative activities (as given by the energy projection) and the penetration of emission control legislation. For SO_2, the baseline scenario assumes all source-specific emission control legislation applicable in each country, but does not consider caps on total national emissions imposed by the National Emission Ceilings directive or the Gothenburg Protocol. Thus, further measures that could

possibly be under considerations in individual countries in order to meet emission ceilings, but which are not yet laid down in legislation, are excluded from consideration.

The baseline projections suggest SO_2 emissions to significantly decrease in the future. Compared to the year 2000, SO_2 emissions over the whole EMEP domain are expected to decline by 33 percent in 2010 and by 48 percent in 2020 for the baseline projection (Figure 5.6, Table 5.8).

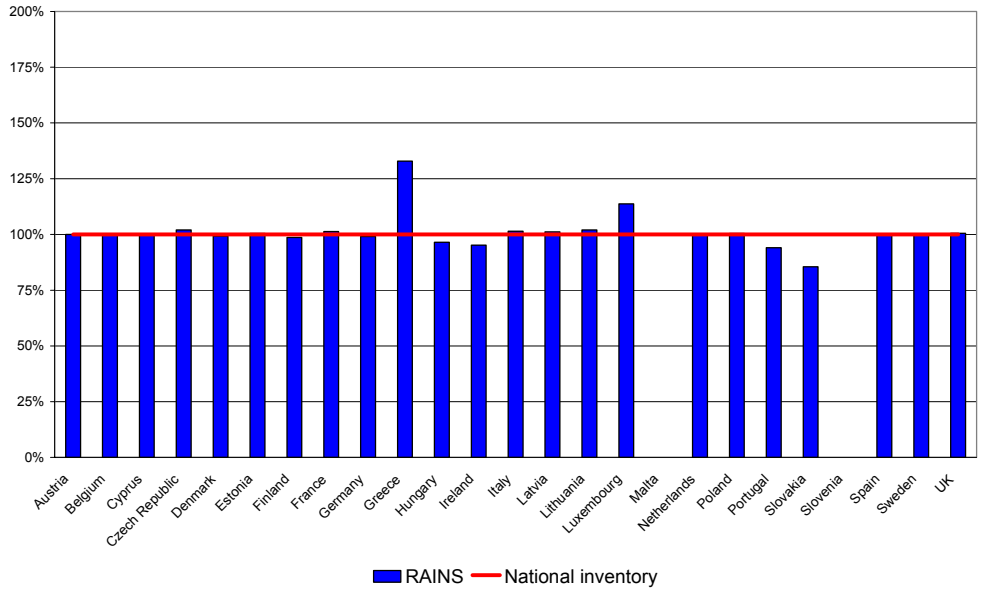

Figure 5.5: Comparison of national emission inventories for SO_2 with the RAINS estimates (for the year 2000).

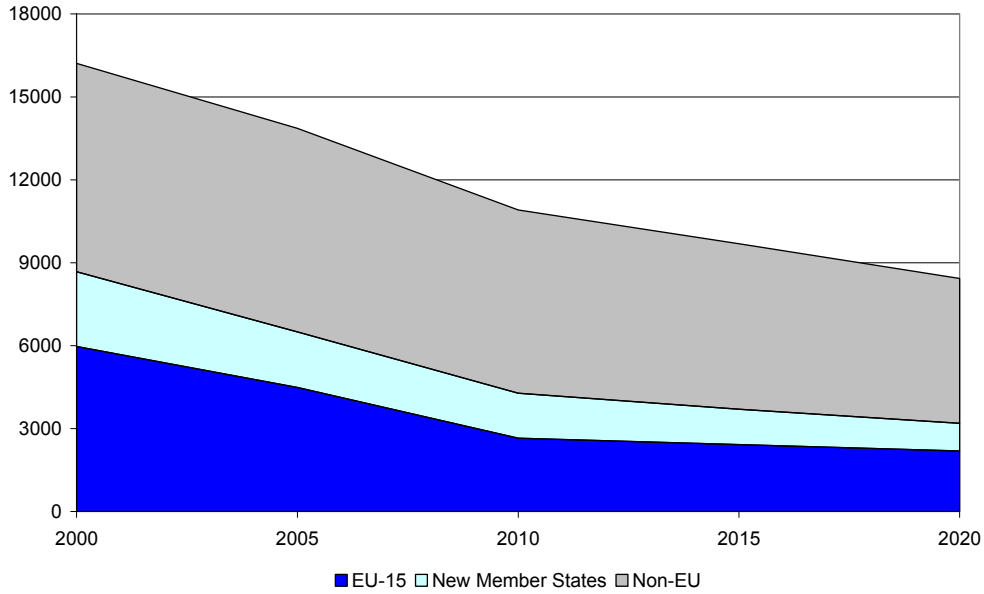

Figure 5.6: Development of SO_2 emissions in the EMEP region (kt SO_2).

Table 5.8: SO_2 emissions estimated by the RAINS model for the baseline scenario (kt).

	2000	2005	2010	2015	2020
Albania	32	32	30	30	31
Austria	31	29	25	24	24
Belarus	351	409	349	304	295
Belgium	186	148	105	99	97
Bosnia and Herzegovina	420	427	411	395	380
Bulgaria	1313	1071	979	934	828
Croatia	108	75	69	67	65
Cyprus	57	18	18	19	10
Czech Republic	249	175	126	93	70
Denmark	29	23	18	16	14
Estonia	91	68	44	18	11
Finland	82	73	63	63	62
France	649	569	404	364	339
Germany	641	523	450	411	426
Greece	476	418	165	163	110
Hungary	487	398	262	147	95
Ireland	133	76	34	27	20
Italy	745	449	366	347	298
Latvia	16	13	11	10	9
Lithuania	40	31	33	31	25
Luxembourg	4	4	3	2	2
Malta	26	11	12	12	3
Netherlands	114	124	117	109	102
Norway	89	71	68	69	70
Poland	28	25	23	23	22
Portugal	1513	1176	1045	882	722
Republic of Moldova	251	165	103	93	87
Romania	838	686	668	585	405
Russian Federation*	2425	2743	2464	2239	2014
Serbia and Montenegro	396	341	277	221	167
Slovakia	124	61	54	46	38
Slovenia	97	61	22	21	19
Spain	1400	1098	416	397	350
Sweden	68	67	66	64	66
Switzerland	20	19	16	15	14
The FYR of Macedonia	90	87	82	77	72
Ukraine	1404	1328	1145	994	842
United Kingdom	1189	771	366	278	225
Total	16213	13863	10909	9689	8429

* within the EMEP domain.

5.3.2 Nitrogen oxides (NO_x)

Also for NO_x, the RAINS databases allow rather accurate reconstruction of the nationally reported emission inventories for the year 2000. For the EU-15 as a whole, the draft RAINS estimate deviates by only one percent, and by 0.3 percent for the New Member States (Figure 5.7). As for SO_2, the major discrepancies occur for Greece and Luxembourg. There are certain discrepancies with national estimates at the sectoral level, which are expected to be resolved in the forthcoming months.

The emission factors for mobile sources applied in the earlier RAINS calculations were entirely based on data developed within the Auto/Oil project. In contrast, the present RAINS implementation for the CAFE program incorporates information on country-specific emission factors for vehicles as provided by national experts, under the condition that sufficient supplementary documentation on the methodologies applied by countries was supplied, so that international consistency is maintained.

It should be mentioned that the RAINS estimates presented in this report reflect higher than expected real-life NO_x emissions from heavy duty trucks subject to EURO-II and EURO-III as pointed out by the ARTEMIS project. Thus, the RAINS estimates for mobile sources are higher than the numbers given in the national inventories of some countries, which do not yet include this recent information.

The RAINS computation of future NO_x emissions is based on the projected volumes of emission generating activities (as provided by the PRIMES energy projections), country-specific emission factors that capture the composition of emission sources in each country and the penetration of emission controls as prescribed by legislation.

For the assumed energy projection, NO_x emissions in the EMEP domain are expected to decline in 2010 by 20 percent compared to the year 2000 level and by 2020 by 35 percent (Table 5.9). For the EU-15, NO_x emissions are estimated to shrink by 29 percent in 2010 and by 47 percent in 2020. Largest decreases will result from the measures in the power generation sector (-39 percent in 2010) and for mobile sources (-33 percent in 2010). For the New EU Member States, NO_x emissions are computed to decline by 30 percent in 2010 and by 54 percent in 2020 (Figure 5.8).

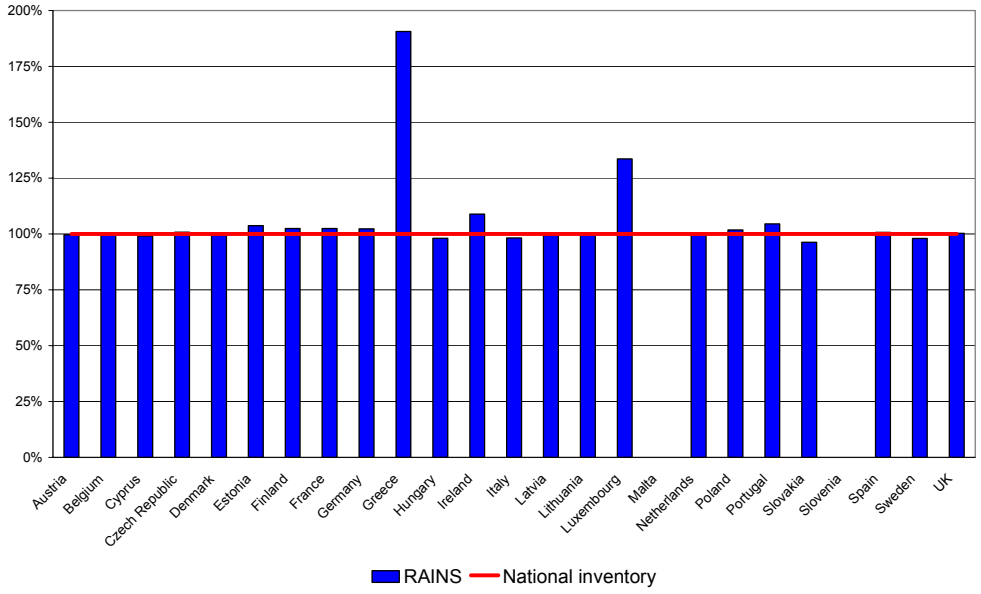

Figure 5.7: Comparison of national emission inventories for NO_x with the RAINS estimates (for the year 2000).

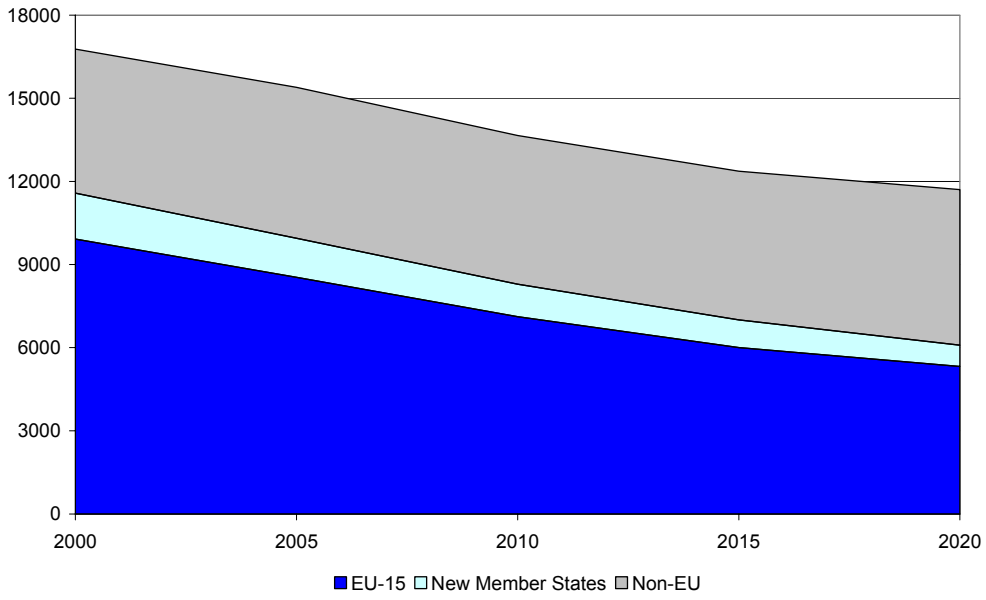

Figure 5.8: Development of NO_x emissions in the EMEP region (kt NO_x).

Table 5.9: NO_x emissions estimated by the RAINS model for the baseline scenario (kt).

	2000	2005	2010	2015	2020
Albania	23	16	22	25	28
Austria	218	212	180	174	150
Belarus	379	228	248	274	271
Belgium	400	416	334	282	227
Bosnia and Herzegovina	73	51	53	52	54
Bulgaria	303	225	191	184	147
Croatia	87	76	87	91	94
Cyprus	26	27	31	25	22
Czech Republic	487	336	295	241	187
Denmark	266	290	207	169	146
Estonia	73	40	37	37	28
Finland	276	236	214	183	151
France	1863	1640	1431	1254	1056
Germany	...	...	1643	1472	1178
Greece	325	331	329	303	276
Hungary	229	209	191	167	132
Ireland	107	116	128	107	94
Italy	1888	1784	1392	1206	1002
Latvia	88	52	36	38	31
Lithuania	129	73	49	47	41
Luxembourg	37	32	32	32	27
Malta	8	8	9	7	6
Netherlands	88	45	64	66	64
Norway	581	473	405	377	327
Poland	241	203	215	212	202
Portugal	1231	1136	844	723	616
Republic of Moldova	268	315	322	271	233
Romania	527	400	331	346	282
Russian Federation*	3713	2419	2535	2727	2758
Serbia and Montenegro	220	164	166	164	168
Slovakia	185	116	104	79	65
Slovenia	55	64	58	49	39
Spain	1137	1275	1303	1104	940
Sweden	333	292	247	224	194
Switzerland	165	131	101	90	74
The FYR of Macedonia	46	35	38	39	41
Ukraine	1739	1222	1146	1175	1184
United Kingdom	2879	2275	1755	1379	1119
Total	20692	16963	16772	15397	13656

* within the EMEP domain

5.3.3 Volatile Organic Compounds (VOC)

In comparison to SO_2 and NO_x, it is more difficult to reproduce nationally reported VOC emissions with internationally consistent sets on emission factors. Thus, the RAINS model shows larger discrepancies with national estimates, although the overall number for the EU-15 differs by not more than 0.16 percent, while for the New Member States the disagreement increases to five percent (Figure 5.9). Insufficient insight into the calculation methods applied in some countries makes it difficult to judge the quality of some of these national VOC inventories, so that for all following calculations caveats on the uncertainties of the emission inventories must be kept in mind.

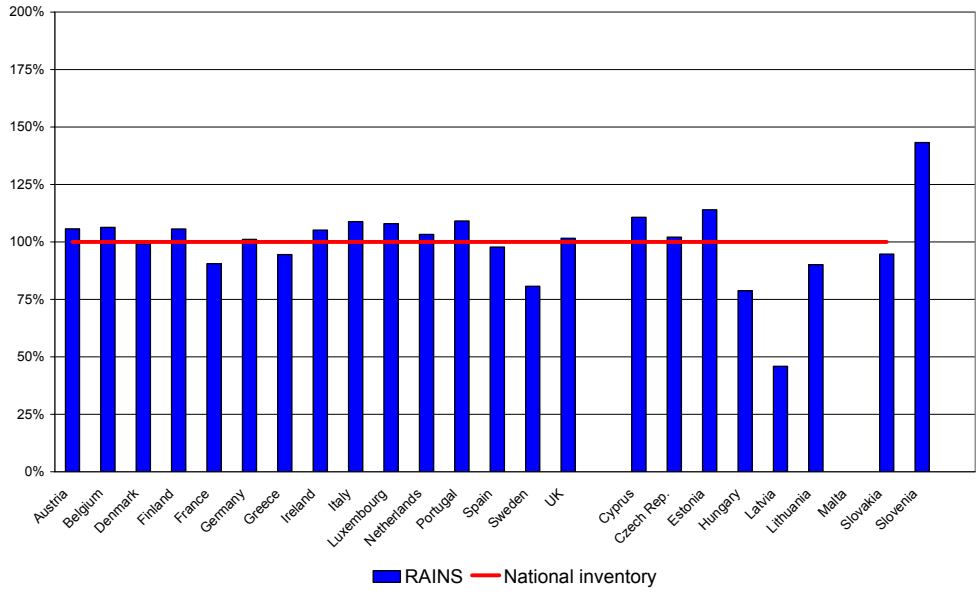

Figure 5.9: Comparison of national emission inventories for VOC with the RAINS estimates (for the year 2000)

Under the assumptions of the baseline scenario and with the emission control legislation currently in force, VOC emissions are expected to decrease in the region by 22 percent in 2010 and by 27 percent in 2020. Larger reductions are estimated for the EU countries (for 2010, 33 percent for the EU-15, while only 15 percent for the New Member States). The decline in emissions from mobile sources adds the largest contribution to the VOC decrease.

Table 5.10: VOC emissions estimated by the RAINS model for the baseline scenario (kt).

	2000	2005	2010	2015	2020
Albania	31	33	35	37	40
Austria	202	184	165	159	159
Belarus	232	264	262	259	268
Belgium	265	211	174	175	176
Bosnia and Herzegovina	41	42	45	48	51
Bulgaria	135	142	119	105	92
Croatia	105	107	106	108	108
Cyprus	16	12	9	9	9
Czech Republic	241	203	164	152	150
Denmark	135	104	91	86	86
Estonia	38	37	33	30	30
Finland	178	162	132	116	106
France	1562	1224	1025	943	937
Germany	1621	1301	1141	960	867
Greece	296	251	189	175	175
Hungary	152	123	100	93	88
Ireland	93	82	72	68	70
Italy	1647	1370	973	814	734
Latvia	33	31	25	18	16
Lithuania	64	55	50	44	42
Luxembourg	16	14	11	11	12
Malta	6	5	4	3	3
Netherlands	42	43	42	41	41
Norway	287	266	238	237	242
Poland	343	330	299	249	146
Portugal	590	517	454	429	418
Republic of Moldova	317	266	222	213	223
Romania	395	436	392	353	313
Russian Federation*	2689	2744	2759	2752	3012
Serbia and Montenegro	145	148	150	150	153
Slovakia	90	78	68	66	69
Slovenia	58	44	34	28	26
Spain	1131	1028	844	803	807
Sweden	245	212	175	168	168
Switzerland	142	122	102	96	96
The FYR of Macedonia	26	29	32	34	37
Ukraine	752	714	730	777	832
United Kingdom	1519	1108	903	854	863
Total	15881	14041	12371	11662	11664

* within the EMEP domain.

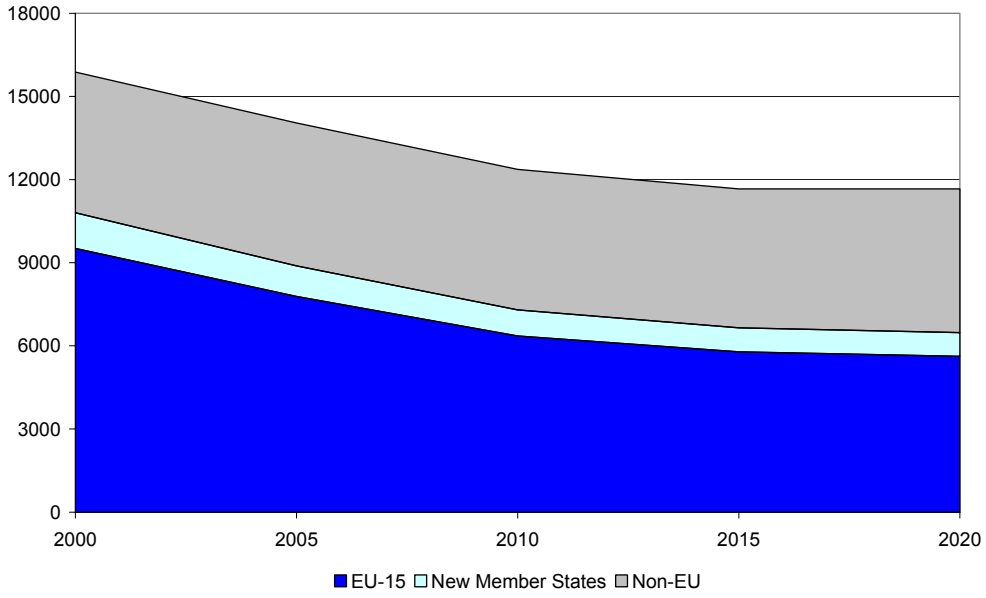

Figure 5.10: Development of VOC emissions in the EMEP region (kt VOC).

5.3.4 Ammonia (NH_3)

While the provisional databases in the RAINS model reproduce for the year 2000 total ammonia emissions of the EU-15 with only 0.8 percent difference to the national estimates, there are still large discrepancies for individual countries. Further national information is necessary to understand the reasons for the differences and to improve the model estimates (Figure 5.11).

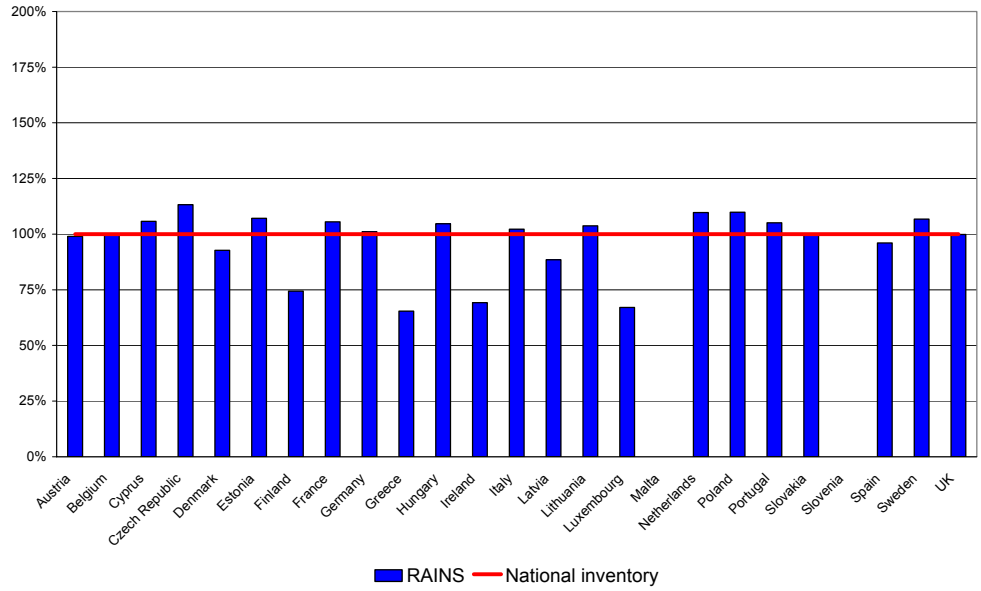

Figure 5.11: Comparison of national emission inventories for NH_3 with the RAINS estimates (for the year 2000).

For ammonia emissions, no specific control measures in addition to different national practices are assumed for the baseline projection. Slight increases of NH_3 emissions are calculated for the future (Table 5.11), mainly due to increased livestock projections for the non-EU countries (Figure 5.12).

Table 5.11: NH_3 emissions estimated by the RAINS model for the baseline scenario (kt).

	2000	2005	2010	2015	2020
Albania	22	24	26	26	26
Austria	54	57	56	55	54
Belarus	128	138	147	147	147
Belgium	81	80	79	78	76
Bosnia and Herzegovina	17	17	17	17	17
Bulgaria	92	107	124	124	124
Croatia	33	33	33	33	33
Cyprus	6	6	6	6	6
Czech Republic	66	65	63	63	64
Denmark	94	93	93	92	91
Estonia	10	10	11	12	12
Finland	38	38	38	37	37
France	727	743	732	716	701
Germany	638	636	624	614	606
Greece	55	54	54	52	52
Hungary	78	83	83	84	85
Ireland	129	133	131	127	123
Italy	434	426	421	411	402
Latvia	12	14	14	15	16
Lithuania	50	55	55	56	57
Luxembourg	5	4	4	4	4
Malta	1	1	1	1	1
Netherlands	36	40	45	45	44
Norway	159	157	154	152	150
Poland	29	28	27	27	27
Portugal	309	323	328	329	335
Republic of Moldova	67	69	69	68	67
Romania	223	253	285	285	285
Russian Federation*	714	764	835	835	834
Serbia and Montenegro	66	68	69	69	69
Slovakia	32	32	32	32	33
Slovenia	18	19	20	20	20
Spain	394	383	382	376	370
Sweden	51	52	51	49	48
Switzerland	66	65	63	61	61
The FYR of Macedonia	15	15	15	15	15
Ukraine	486	553	619	619	619
United Kingdom	309	329	320	312	307
Total	5745	5966	6125	6064	6018

* within the EMEP domain

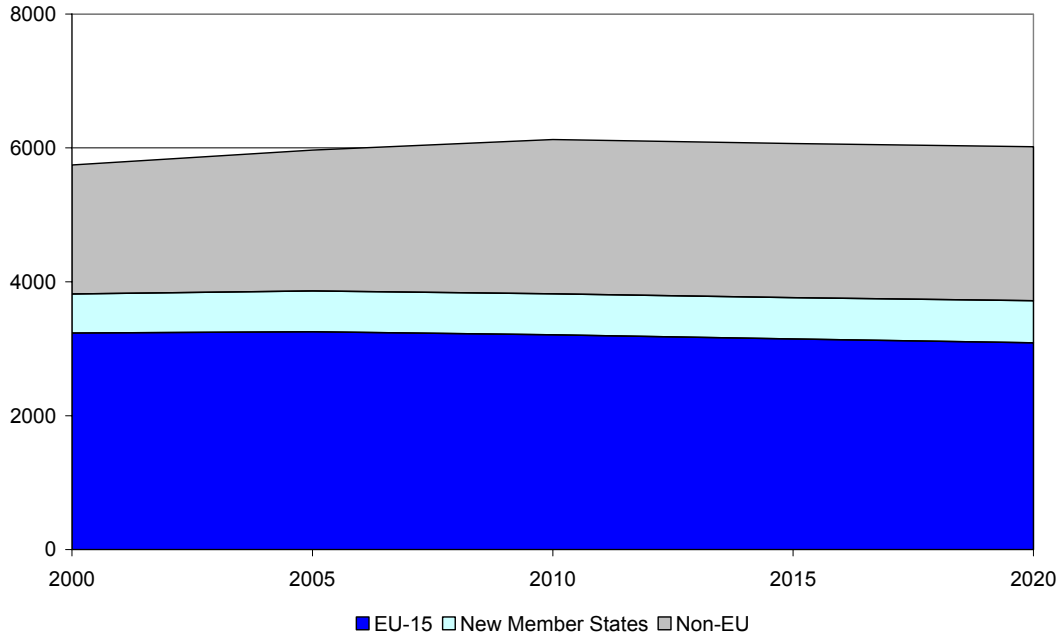

Figure 5.12: Development of NH_3 emissions in the EMEP region (kt NH_3).

5.3.5 Fine particulate matter (PM)

While the RAINS model applies a uniform and reviewed methodology using country-specific emission factors to compute primary emissions of fine particles, only few countries have reported national estimates. Thus, a comparison of the RAINS estimates with national figures is only possible to a limited extent (Figure 5.13, Figure 5.14). Generally, disagreements with the available estimates for PM are larger than for other pollutants. However, in absence of well-documented inventories for the majority of Member States, it is difficult to judge the quality of the RAINS calculations.

For the year 2000, RAINS estimates for the EU-15 about one third of the primary PM_{10} emissions (660 kt) to originate from industrial process emissions and other non-combustion sources. The transport sector contributes another 490 kt (including non-exhaust emissions), while wood combustion in small stoves is calculated to emit 360 kt. In the New Member States, the largest share of primary PM_{10} emissions was caused by the combustion of coal, mainly in the domestic sector.

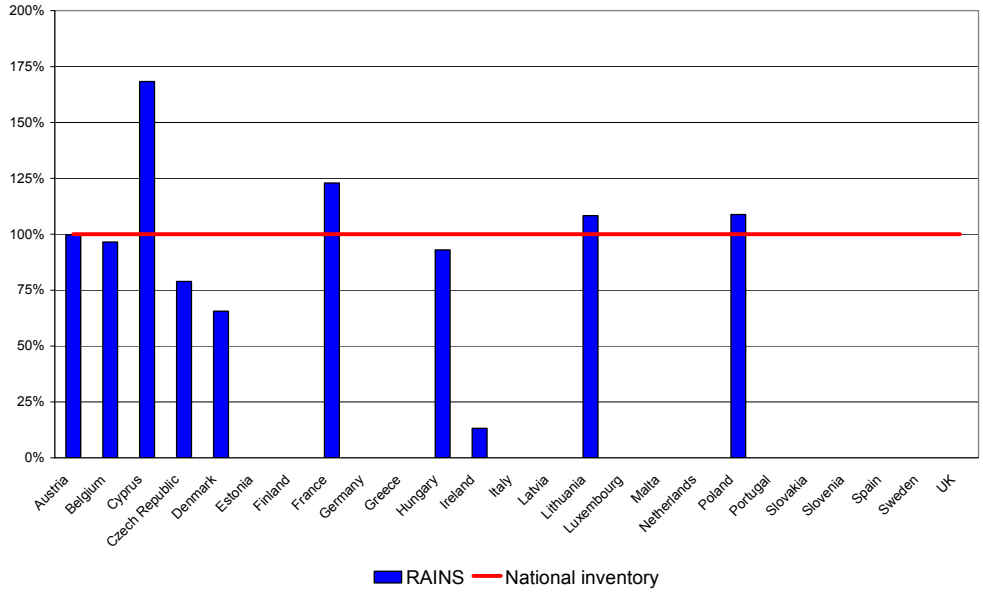

Figure 5.13: Comparison of national emission inventories for PM10 with the RAINS estimates (for the year 2000).

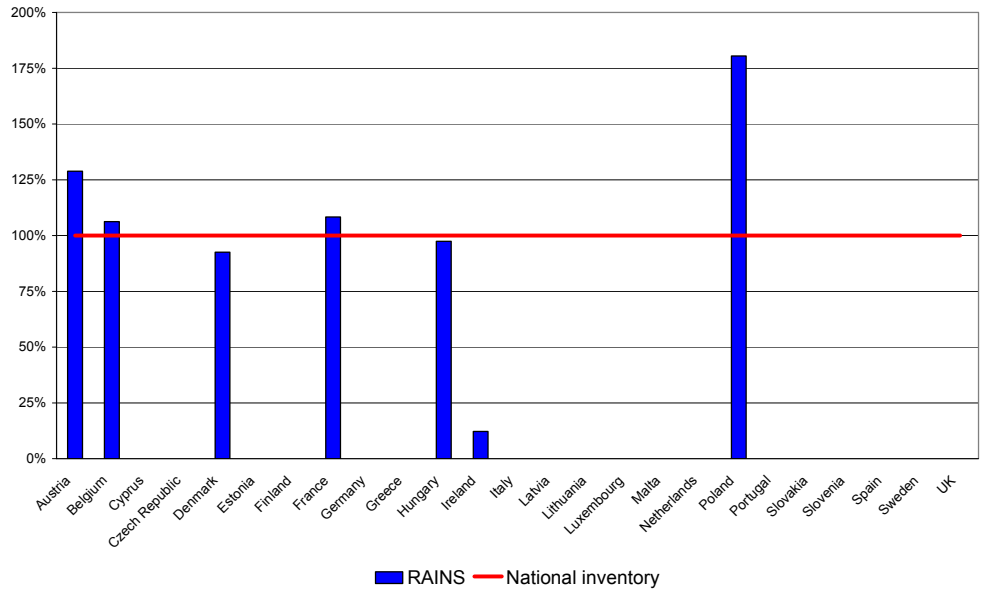

Figure 5.14: Comparison of national emission inventories for PM2.5 with the RAINS estimates (for the year 2000).

As a consequence of a structural changes and specific control measures, primary PM emissions are expected to decline in the coming years (Table 5.12, Table 5.13). Larger reductions are envisaged for $PM_{2.5}$ (-19 percent in 2010 and -26 percent in 2020) than for PM_{10} (-16 percent in 2010 and -22 percent in 2020). The major decline in PM emissions originates from stationary combustion of fossil fuels. Emissions from mobile sources (including non-exhaust emissions) show a declining trend too, but less steep than the stationary sources. For the EU-15, it is estimated that PM_{10} emissions decrease in the baseline scenario from

2000 to 2010 by approximately 25 percent and by more than 30 percent in the New Member States. For 2020, total primary PM10 emissions would be 32 percent lower in the EU-15 and 47 percent in the New Member States.

Calculations suggest a stronger decline in the fine fraction of PM, i.e., for $PM_{2.5}$. For the EU-15, primary emissions of $PM_{2.5}$ would under the assumptions of the baseline scenario be 29 percent below the year 2000 levels, and 40 percent in 2020. In the New Member States, $PM_{2.5}$ is calculated to decline by 31 and 49 percent, respectively (Figure 5.15).

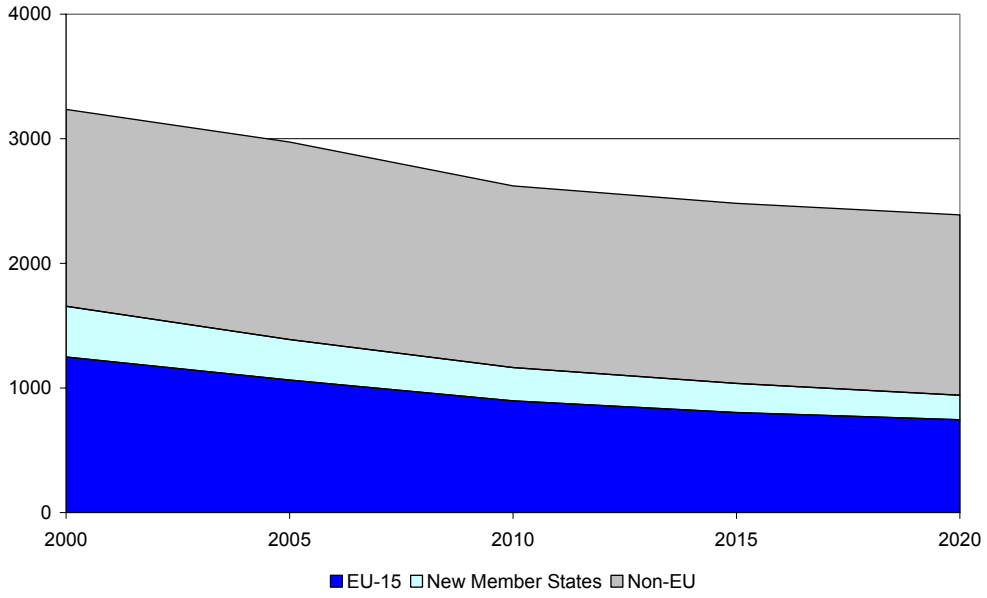

Figure 5.15: Development of $PM_{2.5}$ emissions in the EMEP region (kt $PM_{2.5}$).

Table 5.12: PM_{10} emissions estimated by the RAINS model for the baseline scenario (kt).

	2000	2005	2010	2015	2020
Albania	9	9	7	7	8
Austria	47	44	42	40	38
Belarus	56	58	49	43	41
Belgium	63	49	43	41	40
Bosnia and Herzegovina	48	45	37	35	34
Bulgaria	92	89	80	76	70
Croatia	29	23	20	21	21
Cyprus	5	5	5	5	5
Czech Republic	83	64	53	45	37
Denmark	34	30	28	26	24
Estonia	42	31	18	12	9
Finland	42	43	37	35	32
France	358	314	275	255	248
Germany	254	236	218	205	204
Greece	66	73	69	65	62
Hungary	86	55	39	38	37
Ireland	20	21	17	15	14
Italy	264	211	177	157	145
Latvia	10	9	8	7	6
Lithuania	20	19	18	17	15
Luxembourg	4	4	4	3	3
Malta	1	1	1	1	1
Netherlands	41	46	38	31	24
Norway	58	55	52	50	48
Poland	55	51	48	45	44
Portugal	299	239	206	182	155
Republic of Moldova	58	51	48	47	47
Romania	161	141	135	124	114
Russian Federation*	1382	1481	1388	1375	1371
Serbia and Montenegro	92	85	76	77	81
Slovakia	28	22	22	21	20
Slovenia	21	16	14	13	11
Spain	227	184	158	147	138
Sweden	40	34	30	28	27
Switzerland	15	14	13	12	12
The FYR of Macedonia	21	19	16	16	15
Ukraine	518	497	457	464	470
United Kingdom	202	164	132	116	114
Total	4850	4531	4074	3896	3789

* within the EMEP domain.

Table 5.13: $PM_{2.5}$ emissions estimated by the RAINS model for the baseline scenario (kt).

	2000	2005	2010	2015	2020
Albania	6	7	5	6	6
Austria	35	32	30	28	26
Belarus	36	38	34	31	29
Belgium	38	29	24	23	21
Bosnia and Herzegovina	20	19	17	16	16
Bulgaria	57	53	46	43	39
Croatia	19	16	14	15	15
Cyprus	3	3	3	3	3
Czech Republic	55	42	34	28	23
Denmark	23	20	18	16	15
Estonia	22	18	13	9	6
Finland	36	37	31	28	26
France	277	234	197	177	162
Germany	166	149	132	121	117
Greece	50	55	51	47	44
Hungary	60	38	27	25	24
Ireland	13	14	11	9	8
Italy	202	159	127	107	94
Latvia	7	7	6	5	4
Lithuania	17	16	14	14	12
Luxembourg	3	3	2	2	2
Malta	1	1	1	1	1
Netherlands	23	25	21	18	14
Norway	37	33	29	27	25
Poland	50	46	43	40	39
Portugal	211	173	146	127	104
Republic of Moldova	45	40	38	37	36
Romania	106	94	86	77	70
Russian Federation*	882	928	864	865	875
Serbia and Montenegro	44	42	39	40	42
Slovakia	18	15	14	13	13
Slovenia	15	12	10	9	7
Spain	163	130	107	96	87
Sweden	30	25	21	19	17
Switzerland	10	9	7	7	6
The FYR of Macedonia	9	9	8	8	8
Ukraine	315	299	273	280	288
United Kingdom	130	104	80	67	64
Total	3235	2974	2622	2481	2388

* within the EMEP domain.

5.4 Air quality and impacts

5.4.1 $PM_{2.5}$

The Eulerian EMEP model has been used to calculate changes in the anthropogenic contribution to ambient concentrations of $PM_{2.5}$ in Europe resulting from the changes in the precursor emissions (primary $PM_{2.5}$, SO_2, NO_x, NH_3).

However, at the moment, the scientific peers do not consider the modelling of total particulate mass of the EMEP model (and of all other state-of-the-art models) as accurate and robust enough for policy analysis. Thus, one should not base an integrated assessment on estimates of total PM mass concentrations.

The largest deficiencies have been identified in the quantification of the contribution of natural sources (e.g., mineral dust, organic carbon, etc.) and water. The quantification of secondary organic aerosols (SOA) is not considered mature enough to base policy analysis on. A certain fraction of SOA is definitely caused by anthropogenic emissions, but some estimates suggest that the contribution from natural sources might dominate total SOA. Clarification of this question is urgent to judge whether the inability of contemporary atmospheric chemistry models to quantify SOA is a serious deficiency for modelling the anthropogenic fraction of total PM mass.

In contrast, the modelling of secondary inorganic aerosols is considered reliable within the usual uncertainty ranges. This applies especially to sulphur aerosols. The lack of formal validation of the nitrate calculations is explained by insufficient monitoring data with known accuracy; the model performs reasonably well for other nitrogen-related compounds.

The validation of calculations for primary particles is hampered by insufficient observational data on PM composition. Primary particles comprise a variety of chemical species, some of which (e.g., organic aerosols) originate also from secondary particle formation. Work at EMEP is underway to use improved emission inventories of black carbon, which are themselves only in a research phase, to use black carbon monitoring data as a tracer for emissions of primary particles. In principle, however, modelling of the dispersion of largely non-reactive substances like primary particles is generally considered as a not too ambitious undertaking. Thus, with some further evidence from EMEP/MSC-W on the performance of the Eulerian model for black carbon, an integrated assessment could rely on EMEP's dispersion calculations for primary particles over Europe.

Thus, there are arguments that the present modelling capabilities allow quantification of the dispersion of (most of) the fine particles of anthropogenic origin. This permits calculating changes in PM concentrations over Europe due to changes in anthropogenic emissions, and to estimate the health impacts that can be attributed to anthropogenic emission controls. On the other hand, it is not possible to make any statements on the absolute level of PM mass concentrations, and subsequently not on the absolute health impacts of the total particle burden in the atmosphere. This limitation, however, does not seem to impose unbalanced restrictions on the overall analysis, since also the evidence from the available

epidemiological studies does not allow drawing conclusions about the total health impacts.

Modelled anthropogenic contribution to rural $PM_{2.5}$ concentrations (primary anthropogenic PM and secondary inorganic aerosols) have been calculated for the emissions of the year 2000 for the meteorological conditions of 1999 and 2003. The results show a substantial influence of the inter-annual meteorological variability on $PM_{2.5}$ concentrations, in particular 2003 appears as a especially extreme year with very high surface concentrations that still needs to be verified. Since at present model calculations are only available for these two years and no statement on the representativeness of these meteorological conditions has been made, the further calculations presented in this report use the mean meteorological conditions from these years as a basis.

As shown in Figure 5.16, the decline in emissions of primary particles as well as in the precursor emissions for secondary aerosols is calculated to lead to significant reductions of $PM_{2.5}$ concentrations throughout Europe. While the absolute levels given in the graphs cannot be directly compared with observations, the changes in $PM_{2.5}$ levels over time shown in this series of graphs should give a lower estimate of reductions in $PM_{2.5}$ levels that can be expected from the declines in emissions. It should be kept in mind, however, that in reality these changes will be masked by the inter-annual meteorological variability as indicated in above.

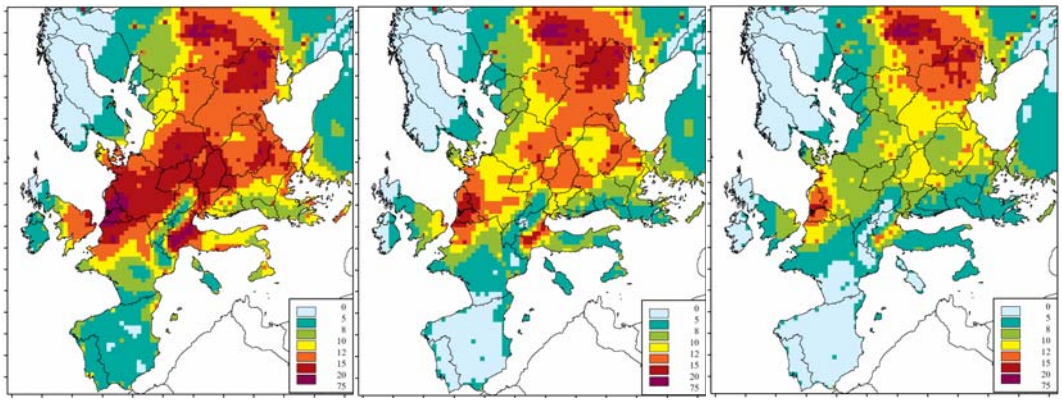

Figure 5.16: Identified anthropogenic contribution to modelled rural $PM_{2.5}$ concentrations (annual mean, $\mu g/m^3$) for the baseline emissions of the year 2000 (left panel), the year 2010 (centre panel) and for 2020 (right panel).

5.4.2 Losses in life expectancy due to anthropogenic $PM_{2.5}$

Based on a methodology described in Amann et al. (2004), the RAINS model estimates changes in the loss in statistical life expectancy that can be attributed to changes in anthropogenic emissions (ignoring the role of secondary organic aerosols). This calculation is based on the assumption that health impacts can be

associated with changes in $PM_{2.5}$ concentrations. Following the advice from the UN/ECE Task Force on Health, RAINS applies a linear concentration-response function and associates all changes in the identified anthropogenic fraction of $PM_{2.5}$ with health impacts. Thereby, no health impacts are calculated for PM form natural sources and for secondary organic aerosols. It transfers the rate of relative risk for $PM_{2.5}$ identified by Pope et al., 2002 for 500.000 individuals in the United States to the European situation and calculates mortality for the population older than 30 years. Thus, the assessment in RAINS does not quantify infant mortality. Awaiting results from the City-Delta project, the provisional estimates presented in this report assume $PM_{2.5}$ from primary emissions in urban areas to be 25 percent higher than in the surrounding rural areas.

Results from these provisional estimates are presented in Figure 5.17. The reductions of the baseline emissions will significantly reduce calculated losses in life expectancy in the European Union, although even in 2020 for large parts of the population life expectancy losses attributable to anthropogenic PM exceed six months.

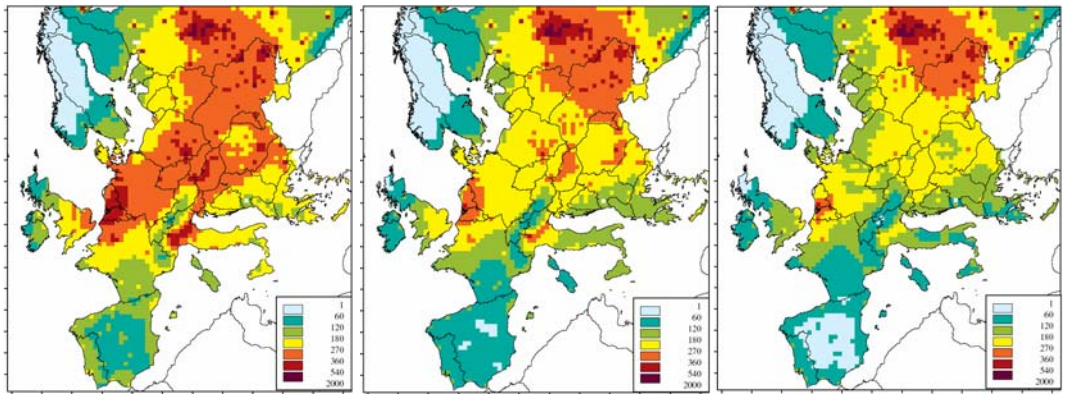

Figure 5.17: Loss in statistical life expectancy that can be attributed to the identified anthropogenic contributions to $PM_{2.5}$ (in days).

5.4.3 Ozone

The Eulerian EMEP model has also been used to calculate changes in ozone concentrations resulting from the emissions of the baseline scenario.

Following the findings of the WHO review of health impacts of particulate matter and ozone, the joint WHO/UNECE Task Force on Health at its 7th session (6-7 May 2004) has concluded to relate health impacts of ozone (premature mortality) with the maximum daily eight-hour mean concentrations taking into account the full year. Since the EMEP model results have not yet been evaluated along this metric, this report cannot present a health impact assessment for ozone.

Instead, Figure 5.18 presents the evolution of the excess ozone that is considered harmful for forest trees, using the AOT40 (accumulated ozone over a threshold of 40 ppb) as a metric. The updated manual for critical levels (UN/ECE, 2004)

specifies a no-effect critical level of 5 ppm.hours for trees. Related to this quantity, significant excess ozone is calculated for 2000 for large parts of the European Union. Baseline emission reductions will improve the situation, but will not be sufficient to eliminate the risk even by 2020.

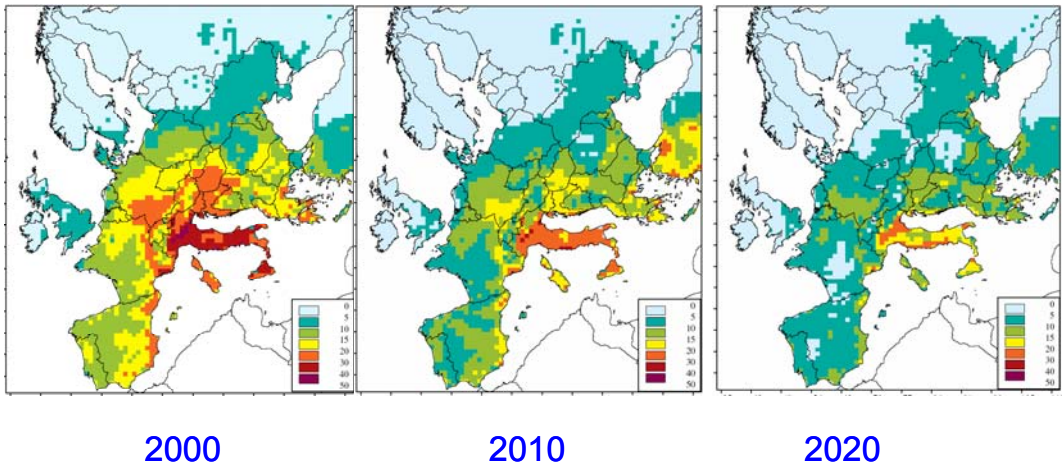

Figure 5.18: Rural AOT40 for forests (in ppm.hours) calculated for the baseline scenario, based on mean meteorological conditions of 1999 and 2003. The critical level for forest trees indicating a no-effect threshold is set at 5 ppm.hours.

5.4.4 Acid deposition

The baseline projections also suggest improvements in ecosystems protection against acid deposition. However, due to improved scientific insight which now allows reliable calculation of specific deposition rates for individual land use types (forests, open land, etc.), a systematic underestimation of deposition to forests that was inherent to earlier calculations could be removed. Thus, substantially larger quantities of sulphur and nitrogen deposition are now calculated for forest ecosystems than was calculated earlier, e.g., for the NEC directive.

Figure 5.19 displays the evolution of forest area over time receiving acid deposition above their critical loads (using the 2003 critical loads data). Obviously, the situation is expected to improve, but substantial areas are calculated to remain at risk. This is mainly due to the almost constant levels of ammonia emissions, which make ammonia to the dominating source of acidification in the future.

This calculation has to be considered as preliminary, and further analysis involving the scientific effects community will be necessary to provide a comprehensive interpretation of these results. In a similar way, further analysis will be able to assess acidification of aquatic ecosystems.

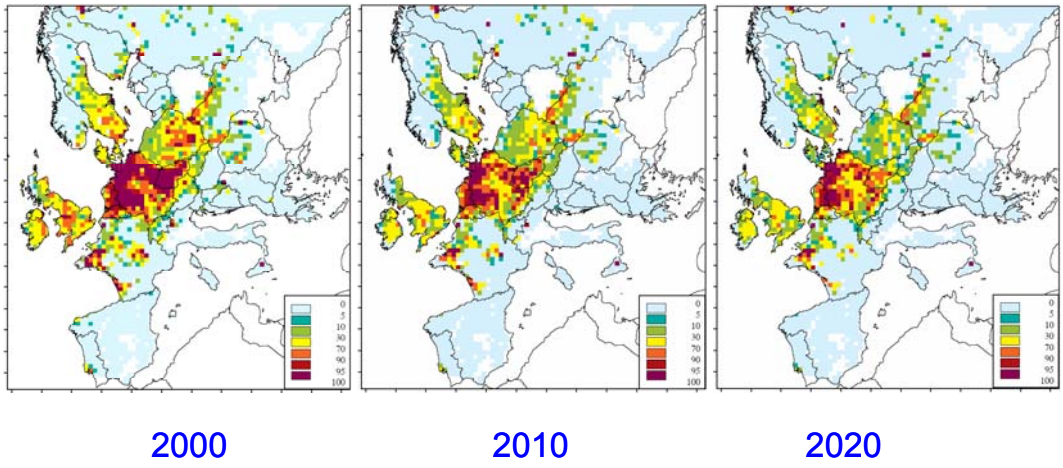

Figure 5.19: Percentage of forest area receiving acid deposition above the critical loads for the baseline emissions for 2000, 2010 and 2020. Results averaged from the calculations for 1999 and 2003 meteorological conditions, using ecosystem-specific deposition for forests. Critical loads data base of 2003.

5.5 Conclusions

This report presents a first perspective on the likely future development of emissions and air quality in Europe in absence of further legal measures to control emissions. While this assessment brings together for the first time a wide range of updated information on economic development, energy policies, emission inventories, atmospheric dispersion and impacts of air pollution, it has to be considered as provisional since information in all these fields needs further refinement and validation.

Of particular urgency is the further improvement and validation of emission estimates for the countries that are not included in the Clean Air For Europe (CAFE) program of the Commission of the European Union.

However, despite the large number of outstanding improvements in detail, the overall picture at the European scale as presented in this report is unlikely to change dramatically. Thus, a preliminary conclusion would suggest that the full implementation of the present legislation on emission controls will lead to significant reduction of emissions in the future. However, these improvements are not likely to fully eliminate all negative impacts of air pollution within the time period analysed in this report.

Acknowledgement

The development of the baseline emission and air quality projection for the Member States of the European Union was financially supported by the Commission of the European Union. The results for the EU Member States presented in this report reflect the status of the draft CAFE baseline scenario as of May 2004.

6. References

Amann, M. et al. (2004) Modelling of health impacts of fine particles. International Institute for Applied Systems Analysis. http://www.iiasa.ac.at/rains/review/review-healthpm.pdf

Amann, M., Cofala, J., Heyes, C., Klimont, Z., Schöpp, W., Jonson, J.-E., Simpson, D. and Tarrasón, L. (2004) An initial outlook into the future development of fine particulate matter in Europe. In: *Transboundary particulate matter in Europe. Status report 4/2004.* Kjeller, Norwegian Institute for Air Research. pp. 93-120.

Andersson-Sköld, Y. and Simpson, D. (2001) Secondary organic aerosol formation in Northern Europe: a model study. *J. Geophys. Res.*, *106D:* 7357-7374.

Ansari, A.S. and Pandis, S.N. (2000) Water absorption by secondary organic aerosol and its effect on inorganic aerosol behaviour. *Environ. Sci. Tech.*, *34*, 71–77.

Bardouki, H., Liakakou, H., Economou, C., Sciare, J., Smolík, J., Ždímal, V., Eleftheriadis, K., Lazaridis, M. and Mihalopoulos, N. (2003) Chemical composition of size resolved atmospheric aerosols in the eastern Mediterranean during summer and winter. *Atmos. Environ., 37,* 195-208.

CEC (2003) European energy and transport. Trends to 2030. Luxembourg, European Commission, Directorate General for Energy and Transport (KO-AC-02-001-EN-C).

CEPMEIP (2002) The co-ordinated European programme on particulate matter emission inventories, projections and guidance. http://www.air.sk/tno/cepmeip/

COPERT (2003) Computer programme to calculate emissions from road transport, version III. http://vergina.eng.auth.gr/mech/lat/copert/copert3f.htm

EMEP (2004) Transboundary acidification, eutrophication and ground level ozone in Europe. Oslo, Norwegian Meteorological Institute (EMEP Status Report 1/2004).

EMEP/CCC (2003) Transboundary particulate matter in Europe. Ed. by M. Kahnert and L. Tarrasón. Kjeller, Norwegian Institute for Air Research (EMEP Report 4/2003).

Fagerli, H., Simpson, D. and Aas, W. (2003) Model performance for sulphur and nitrogen compounds for the period 1980 to 2000, 2003. In: *Transboundary acidification, eutrophication and ground level ozone in Europe. EMEP status report 1/2003, Part II Unified EMEP model performance*. Oslo, Norwegian Meteorological Institute. pp. 1–66.

Fagerli, H. (2004) Air concentrations and depositions of acidifying and eutrophying components, status 2002. In: *Transboundary acidification, eutrophication and ground level ozone in Europe. Status report 1/2004*. Oslo, Norwegian Meteorological Institute.

Gelencsér, A., Hoffer, A., Kiss, G., Tombacs, E., Kurdi, R. and Becze, L. (2003) In-situ formation of light-absorbibg organic matter in cloud water. *J. Atmos. Chem.*, *45*, 45–54.

Hjellbrekke, A.-G. (2004) Data Report 2002. Acidifying and eutrophying compounds. Kjeller, Norwegian Institute for Air Research (EMEP/CCC-Report 1/2004).

Hoffer, A. and Kiss, G. and Blazsó, M. and Gelencsér, A. (2004) Chemical characterization of humic-like substances (HULIS) formed from a lignin-type precursor in model cloud water. *Geophys. Res. Lett.*, *31:* doi10.1029/2003GL018962.

Jang, M., Czoschke, N.M., Kee, S. and Kamens, R.M. (2002) Heterogeneous atmospheric aerosol production by acid-catalyzed particle-phase reactions. *Science*, *298*, 814-817.

Kahnert, M. (ed.) (2003) Measurements of particulate matter: Status report 2003. Kjeller, Norwegian Institute for Air Research (EMEP/CCC-Report 5/2003).

Kalberer, M., Paulsen, D., Sax, M., Steinbacher, M., Dommen, J., Prevot, A.S.H., Fisseha, R., Weingartner, V., Frankevich, E., Zenobi, R. and Baltensperger, U. (2004) Identification of polymers as major components of atmospheric organic aerosols. *Science*, *303*, 1659–1662.

Kamens, R., Jang, M., Chien, C.J. and Leach, K. (1999) Aerosol formation from the reaction of α-pinene and ozone using a gas-phase kinetics-aerosol partitioning model. *Environ. Sci. Tech.*, *33*, 1430–1438.

Kamens, R.M. and Jaoui, M. (2001) Modeling aerosol formation from α-pinene + NO_x in the presence of natural sunlight using gas-phase kinetics and gas-particle partitioning theory. *Environ. Sci. Tech.*, *35*, 1394–1405.

Kulmala, M., Vehkamäki, H., Petäjä, T., Dal Maso, M., Lauri, A., Kerminer, V.-M., Birmili, W. and McMurry, P.H. (2004) Formation and growth rates of ultrafine atmospheric particles: a review of observations. *J. Aerosol Sci., 35,* 143-176.

Kupiainen, K. and Klimont, Z. (2004) The primary emissions of submicron and carbonaceous particles in Europe and potential for their control. IIASA interim report, in preparation.

Limbeck, A., Kulmala, M. and Puxbaum, H. (2003) Secondary organic aerosol formation in the atmosphere via heterogeneous reaction of gaseous isoprene on acidic particles. *Geophys. Res. Lett.*, 30:doi10.1029/2003GL017738.

McDow, S.R. and Huntzicker, J.J. (1990) Vapor adsorption artifact in the sampling of organic aerosol: face velocity effects. *Atmos. Environ.*, *24A,* 2563-2571.

Metzger, S., Dentener, F., Pandis, S. and Lelieveld, J. (2002) Gas/Aerosol Partitioning 1: A computationally efficient model. *J. Geophys. Res., 107D:* 10.1029/2001JD001102.

Millan, M.M., Salvador, R., Mantilla, E. and Kallos, G. (1997) Photo-oxidant dynamics in the Mediterranean basin in summer: results from European research projects. *J. Geophys. Res., 102,* 8811-8823.

Odum, J.R., Hoffmann, T., Bowman, F., Collins, D., Flagan, R.C. and Seinfeld, J.H. (1997) Gas/particle partitioning and secondary aerosol formation. *Environ. Sci. Tech.*, *30*, 2580–2585.

Pankow, J.F. (1994a) An absorption model of the gas/aerosol partitioning involved in the formation of secondary organic aerosol. *Atmos. Environ.*, *28,* 189–193.

Pankow, J.F. (1994b) An absorption model of gas/particle partitioning of organic compounds in the atmosphere. *Atmos. Environ.*, *28,* 185–188.

Pope, C.A., Burnett, R., Thun, M.J., Calle, E.E., Krewski, D., Ito, K. and Thurston, G.D. (2002) Lung Cancer, Cardiopulmonary Mortality and Long-term Exposure to Fine Particulate Air Pollution. *J. American Medical Assoc., 287,* 1132-1141.

Pun, B.K., Wu, S.Y., Seigneur, C., Seinfeld, J.H., Griffin, R.J. and Pandis, A.N. (2003) Uncertainties in modeling secondary organic aerosols: Three-dimensional modeling studies in Nashville/Western Tennessee. *Environ. Sci. Tech.*, *37*, 3647–3661.

Putaud, J.-P., Raes, F, Van Dingenen, R., Brüggemann, E., Faccini, M.-C., Decesari, S., Fuzzi, S., Gehrig, R., Hüglin, S., Laj, P., Lorbeer, G., Maenhaut, W., Mihalopoulos, N., Müller, K., Querol, X., Rodriguez, S., Schneider, J., Spindler, G., ten Brink, H., Tørseth, K. and Wiedensohler, A. (2004) A European aerosol phenomenology – 2: chemical characteristics of particulate matter at kerbside, urban, rural, and background sites in Europe. *Atmos. Environ., 38*, 2579-2595.

Rau, J.A. (1989) Composition and size distribution of residential wood smoke particles. *Aerosol Sci. Techn.*, *10*, 181-192.

Rodriguez, S., Querol, X., Alastuey, A. and Mantilla, E. (2002) Origin of high summer PM_{10} and TSP concentrations at rural sites in Eastern Spain. *Atmos. Environ., 36,* 3101-3112.

Rodríguez, S., Querol, X., Alastuey, A. and Plana, F. (2002) Sources and processes affecting levels and composition of atmospheric aerosol the western Mediterranean. *J. Geophys. Res., 107, D24,* 4777, doi:10.1029/2001JD001488.

Schauer, J.J., Kleemand, M.J., Cass, G.R. and Simoneit, B.D.T. (2001) Measurements of emissions from air pollution sources. 3. c_1-c_{29} organic compounds from fireplace combustion of wood. *Environ. Sci. Tech.*, *35*, 1716-1728.

Schöpp, W., Amann, M., Cofala, J., Heyes, C. and Klimont, Z. (1999) Integrated assessment of European air pollution emission control strategies. *Environ. Modeling Software, 14,* 1-9.

Simpson, D., Fagerli, H., Jonson, J.E., Tsyro, S., Wind, P. and Tuovinen, J.-P. (2003a) Transboundary acidification, eutrophication and ground level ozone in Europe. Part I. Unified EMEP model description. Oslo, Norwegian Meteorological Institute (EMEP/MSC-W Status report 1/2003 Part I). http://www.emep.int

Simpson, D., Fagerli, H., Solberg, S. and Aas, W. (2003b) Photo-oxidants. In: *Transboundary acidification, eutrophication and ground level ozone in Europe. EMEP Status Report 1/2003, Part II Unified EMEP Model Performance*. Oslo, Norwegian Meteorological Institute. pp. 67–104.

Simpson, D., Guenther, A., Hewitt, C.N. and Steinbrecher, R. (1995) Biogenic emissions in Europe 1.Estimates and uncertainties. *J. Geophys. Res., 100*, 22875-22890.

Smolík, J., Ždímal, V., Schwarz, J., Lazaridis, M., Havránek, V., Eleftheriadis, K., Mihalopoulos, N., Bryant, C. and Colbeck, I. (2003) Size resolved mass concentration and elemental composition of atmospheric aerosols over the Eastern Mediterranean Area. *Atmos. Chem. Phys., 3,* 2207-2216.

Szidat, S., Jenk, H.W., Gäggler, T.M., Synal, H.-A., Fisseha, R., Baltensperger, U., Kalberer, M., Samburova, V., Reimann, S., Kasper-Giebl, A. and Hajdas, I. (2004) Radiocarbon (^{14}C)-deduced biogenic and anthropogenic contributions to organic carbon (OC) of urban aerosols from Zürich, Switzerland. *Atmos. Environ.*, *38*, 4035–4044.

Tsyro, S. (2004) To what extent aerosol water can explain the discrepancy between model calculated and gravimetric PM_{10} and $PM_{2.5}$. Submitted to *Atmos. Chem. Phys*.

Tunved, P., Hansson, H.-C., Kulmala, M., Aalto, P., Viisanen, Y., Karlsson, H., Kristensson, A., Swietlicki, E., Dal Maso, M., Ström, J. and Komppula, M. (2003) One year boundary layer aerosol size distribution data from five Nordic background stations. *Atmos. Chem. Phys., 3, 2183-2205.*

Turpin, B.J., Huntzicker, J.J. and Hering, S.V. (1994) Investigation of organic aerosol sampling artefacts in the Los Angeles basin. *Atmos. Environ*., *28*, 3061-3071.

UN/ECE (1997) Energy balances for Europe and North America, 1992-2010. Geneva, United Nations Economic Commission for Europe.

UN/ECE (2004) Mapping critical levels for vegetation. Geneva, Working Group on Effects, United Nations Economic Commission for Europe.

Vestreng, V. (2003) Review and revision. Emission data reported to CLRTAP. MSC-W Status Report 2003. Oslo, Norwegian Meteorological Institute (EMEP/MSC-W Technical report 1/2003).

Vestreng, V., Adams, M. and Goodwin, J. (2004) Inventory Review 2004. Emission data reported to CLRTAP and under the NEC Directive. EMEP/EEA Joint Review Report. Oslo, Norwegian Meteorological Institute (EMEP/MSC-W Technical report 1/2004).

Williams, D.J., Milne, J.W., Quigley, S.M., Roberts, R.B. and Kimberlee, M.C. (1989) Particulate emissions from in-use motor vehicles. II Diesel vehicles. *Atmos. Environ*., *23*, 2647-2661.

Yttri, K.E. and Tørseth, K.(2002) Chemical characterisation and mass concentration of ambient aerosol at the EMEP site in Birkenes (Southern Norway) - A one-year study. In: *Measurements of particulate matter. Status report 2002.* Ed. by M. Kahnert. Kjeller, Norwegian Institute for Air Research (EMEP/CCC Report 4/2002). pp. 20-25. http://www.emep.int

Zappoli, S., Andracchio, A., Fuzzi, S., Facchini, M.C., Gelencser, A., Kiss, G., Krivacsy, Z., Molnar, A., Meszaros, E., Hansson, H.-C., Rosman, K. and Zebuhr, Y. (1999) Inorganic, organic and macromolecular components of fine aerosol in different areas of Europe in relation to their water solubility. *Atmos. Environ., 33,* 2733-2743.

Appendix A

Tables with national emission totals

Table A.1: National total emission trends.
Emissions of sulphur dioxide (1980, 1990, 2000-2000, 2010 & 2020) used for modelling at the MSC-W (Gg of SO_2 per year)[1].

Area/Year	1980	1990	2000	2001	2002	2010	2010 CP	2020	2020 CP
Albania	72	72	58	58	**58**	**30**	30	**31**	31
Armenia	141	72	8.4	4.4	**7.5**	**4**	4	**4**	4
Austria	**360**	**80**	**35**	**38**	**36**	**30**	29	**28**	26
Azerbaijan	15	15	15	15	15	**15**	15	**15**	15
Belarus	740	637	143	151	**143**	**350**	350	**296**	296
Belgium	828	362	165	160	**153**	**105**	101	**97**	92
Bosnia and Herzegovina	482	482	419	419	**419**	**411**	411	**380**	380
Bulgaria	2050	2008	982	**940**	**940**	**979**	961	**828**	651
Croatia	150	180	58	58	**58**	**69**	69	**65**	65
Cyprus	28	46	50	48	**51**	**18**	18	**10**	10
Czech Republic	2257	1881	264	251	**237**	**126**	119	**70**	57
Denmark	452	**177**	**29**	**26**	**25**	**18**	18	**14**	14
Estonia	287	252	95	92	**88**	**44**	35	**11**	9,2
Finland	584	260	74	85	82	**63**	60	**62**	58
France	**3214**	**1326**	**627**	**570**	**537**	**404**	374	**339**	317
Georgia	230	248	**6**	**6**	**6**	**9**	9	**9**	9
Germany	7514	**5326**	**636**	**643**	**611**	**450**	427	**426**	363
Greece	400	493	483	485	**485**	**165**	150	**110**	103
Hungary	1633	1010	486	400	**359**	**262**	231	**95**	95
Iceland	18	24	27	27	**27**	**29**	29	**29**	29
Ireland	222	186	131	**126**	**96**	**34**	30	**20**	20
Italy	**3440**	**1748**	**752**	**709**	**709**	**366**	337	**298**	291
Kazakhstan	289	289	237	237	**237**	**237**	237	**237**	237
Latvia	96	**96**	**16**	13	**12**	**11**	10	**9**	7,4
Lithuania	311	222	43	49	**43**	**33**	32	**25**	23
Luxembourg	24	15	3	3	**3**	**3**	2,7	**2**	2,1
Netherlands	490	**191**	**77**	**76**	**71**	**68**	67	**70**	68
Norway	136	52	27	25	**22**	**23**	22	**22**	20
Poland	4100	3210	1511	1564	**1564**	**1045**	962	**722**	572
Portugal	*253*	***229***	***220***	***200***	***205***	**103**	101	**87**	84
Republic of Moldova	308	265	13	12	**15**	**117**	117	**102**	102
Romania	1055	1311	912	912	**912**	**669**	492	**405**	182
Russian Federation	7323	4671	1997	**2031**	**2130**	**2470**	2470	**2019**	2019
Serbia and Montenegro	406	508	387	394	**382**	**277**	277	**168**	168
Slovakia	780	542	124	129	**102**	**54**	52	**38**	31
Slovenia	234	196	99	68	**71**	**22**	22	**19**	16
Spain	2913	***2098***	***1488***	***1433***	***1507***	**411**	392	**353**	336
Sweden	491	106	**55**	57	**58**	**61**	60	**62**	59
Switzerland	116	42	19	21	**19**	**16**	16	**14**	13
TFYR of Macedonia	107	107	105	137	**166**	**82**	82	**72**	72
Turkey	1030	1590	2112	2112	**2112**	**1821**	1821	**1821**	1821
Ukraine	3849	2783	1129	1230	**1329**	**1146**	1146	**842**	842
United Kingdom	**4852**	**3721**	**1189**	**1115**	**1002**	**364**	362	**224**	198
North Africa	413	413	413	413	**413**	**413**	413	**413**	413
Remaining Asiatic areas	854	854	854	854	**854**	**854**	805	**854**	805
Baltic Sea	228	228	228	228	**228**	**228**	228	**228**	228
Black Sea	57	57	57	57	**57**	**57**	57	**57**	57
Mediterranean Sea	1189	1189	1189	1189	**1189**	**1189**	1189	**1189**	1189
North Sea	454	454	454	454	**454**	**454**	454	**454**	454
Remaining N-E Atlantic Ocean	901	901	901	901	**901**	**901**	901	**901**	901
Natural marine emissions	743	743	743	743	**743**	**743**	743	**743**	743
Volcanic emissions	2144	2607	2000	2000	**2000**	**2000**	2000	**2000**	2000
TOTAL	61262	46575	24146	23968	23944	19853	19339	17389	16598

[1] All years except 2010 and 2020: Reported values with white background, expert estimates in grey. Values in bold differ from reporting in 2003. Values in italic are reported values modified for modelling purposes by MSC-W. Projections (Base Line Scenario) provide by IIASA (April 2004) in grey boxes. Reported values or extrapolations in white.

Table A.2: National total emission trends.
Emissions of nitrogen oxides (1980, 1990, 2000-2000, 2010 & 2020) used for modelling at the MSC-W (Gg of NO_2 per year)[1].

Area/Year	1980	1990	2000	2001	2002	2010	2010 CP	2020	2020 CP
Albania	24	24	29	29	**29**	**27**	27	**34**	34
Armenia	15	46	10	13	**13**	**13**	13	**13**	13
Austria	246	212	190	196	**204**	**157**	156	**123**	119
Azerbaijan	**43**	**43**	**43**	43	**43**	**43**	43	**43**	43
Belarus	234	285	135	135	**137**	**266**	266	**285**	285
Belgium	442	334	329	292	**284**	**227**	222	**196**	188
Bosnia and Herzegovina	79	**79**	55	55	**55**	**53**	53	**56**	56
Bulgaria	416	361	**184**	**188**	**188**	**141**	139	**105**	97
Croatia	60	88	77	77	**77**	**91**	91	**101**	101
Cyprus	13	18	23	18	**22**	**22**	23	**19**	20
Czech Republic	937	544	321	332	**318**	**187**	182	**117**	102
Denmark	**307**	**283**	**208**	**203**	**200**	**146**	143	**105**	103
Estonia	70	68	41	38	**40**	**28**	27	**16**	14
Finland	295	300	236	222	**208**	**150**	147	**1124**	111
France	**2024**	1897	**1431**	**1395**	**1352**	**1051**	1015	**812**	772
Georgia	121	130	**42**	**44**	**44**	**30**	30	**30**	30
Germany	3334	**2845**	**1639**	**1566**	**1499**	**1176**	1155	**906**	874
Greece	306	290	321	331	**331**	**274**	267	**227**	222
Hungary	273	238	185	185	**180**	**132**	128	**92**	85
Iceland	21	26	28	28	**28**	**30**	30	**30**	30
Ireland	73	118	125	**132**	**125**	**93**	88	**61**	59
Italy	**1585**	**1919**	**1360**	**1317**	**1317**	**980**	965	**669**	657
Kazakhstan	89	89	50	50	**50**	**50**	50	**50**	50
Latvia	**83**	**83**	**38**	**41**	**41**	**30**	29	**18**	15
Lithuania	152	158	48	55	**51**	**41**	40	**29**	27
Luxembourg	23	23	17	17	**17**	**27**	27	**18**	17
Netherlands	583	**579**	**423**	**413**	**406**	**327**	323	**259**	253
Norway	191	224	224	220	**213**	**204**	203	**189**	188
Poland	1229	1280	838	805	**805**	**616**	585	**393**	365
Portugal	*158*	**222**	**248**	**243**	**265**	**233**	230	**167**	162
Republic of Moldova	115	100	27	23	**25**	**62**	62	**60**	60
Romania	523	546	319	319	**319**	**269**	248	**193**	171
Russian Federation	3634	3600	2357	2462	**2566**	**2500**	2500	**2782**	2781
Serbia and Montenegro	192	211	158	158	**158**	**168**	168	**173**	173
Slovakia	197	216	**107**	106	**102**	**65**	63	**52**	46
Slovenia	51	63	58	**57**	**58**	**39**	39	**28**	25
Spain	1068	***1206***	***1333***	***1305***	***1339***	**924**	901	**668**	643
Sweden	404	**324**	**250**	**247**	**242**	**193**	190	**150**	145
Switzerland	170	154	96	98	**94**	**74**	73	**59**	58
TFYR of Macedonia	39	**39**	30	32	**37**	**37**	37	**40**	40
Turkey	364	644	951	951	951	**2044**	951	**951**	951
Ukraine	1145	1097	561	583	**587**	**587**	1157	**588**	1223
United Kingdom	**2580**	**2771**	**1718**	**1647**	**1582**	**1113**	1098	**803**	766
North Africa	96	96	96	96	**96**	**96**	96	**96**	96
Remaining Asiatic areas	169	169	169	169	**169**	**169**	79	**169**	79
Baltic Sea	352	352	352	352	**352**	**352**	352	**352**	352
Black Sea	86	86	86	86	**86**	**86**	86	**86**	86
Mediterranean Sea	1639	1639	1639	1639	**1639**	**1639**	1639	**1639**	1639
North Sea	648	648	648	648	**648**	**648**	648	**648**	648
Remaining N-E Atlantic	1266	1266	1266	1266	**1266**	**1266**	1266	**1266**	1266
Natural marine	0	0	0	0	**0**	**0**		**0**	
Volcanic emissions	0	0	0	0	0	**0**		**0**	
TOTAL	28164	28033	21119	20927	20858	19176	18348	17090	16342

[1] All years except 2010 and 2020: Reported values with white background, expert estimates in grey. Values in bold differ from reporting in 2003. Values in italic are reported values modified for modelling purposes by MSC-W. Projections (Base Line Scenario) provide by IIASA (April 2004) in grey boxes. Reported values or extrapolations in white.

Table A.3: National total emission trends.
Emissions of ammonia (1980, 1990, 2000-2000, 2010 & 2020) used for modelling at the MSC-W (Gg of NH3 per year)[1].

Area/Year	1980	1990	2000	2001	2002	2010	2010 CP	2020	2020 CP
Albania	32	32	32	32	**32**	**26**	26	**26**	26
Armenia	25	25	15	14	**12**	**25**	25	**25**	25
Austria	**52**	**57**	54	54	**53**	**56**	56	**54**	54
Azerbaijan	25	25	25	25	**25**	**25**	25	**25**	25
Belarus	142	142	142	137	**128**	**147**	147	**147**	147
Belgium	89	99	81	**85**	**83**	**79**	79	**76**	76
Bosnia and	31	31	23	23	**23**	**17**	17	**17**	17
Bulgaria	144	144	56	**56**	**56**	**124**	124	**124**	124
Croatia	37	37	23	23	**23**	**33**	33	**33**	33
Cyprus	8,5	8,5	8,5	8,5	**6,6**	**6**	6,3	**6**	6,4
Czech Republic	156	156	74	77	72	**63**	63	**64**	64
Denmark	**138**	133	**105**	**104**	**101**	**93**	93	**91**	91
Estonia	24	24	8,8	9	**9,1**	**11**	11	**12**	12
Finland	39	38	33	33	**33**	**38**	38	**37**	36
France	795	779	784	**786**	**778**	**732**	732	**701**	701
Georgia	97	97	97	97	**97**	**97**	97	**97**	97
Germany	835	**735**	**602**	**614**	**614**	**624**	623	**606**	604
Greece	79	79	73	73	**73**	**54**	54	**52**	52
Hungary	157	124	71	66	**65**	**83**	83	**85**	85
Iceland	3	3	3	3	**3**	**3**	3	**3**	3
Ireland	112	112	122	**123**	**119**	**131**	131	**123**	123
Italy	**441**	**428**	**429**	**442**	**442**	**421**	421	**402**	401
Kazakhstan	18	18	18	18	**18**	**18**	18	**18**	18
Latvia	**38**	**38**	**10**	**11**	**11**	**14**	14	**16**	16
Lithuania	**85**	**84**	**25**	**50**	**51**	**55**	55	**57**	57
Luxembourg	7	7	7,2	7	**7**	**4**	4,3	**4**	3,9
Netherlands	234	232	152	**142**	**136**	**154**	154	**150**	149
Norway	**20**	**20**	**23**	**23**	**22**	**27**	27	**27**	27
Poland	550	508	322	**328**	**328**	**328**	328	**335**	333
Portugal	***96***	***96***	***92***	***92***	***93***	**69**	69	**67**	67
Republic of Moldova	53	49	25	26	**27**	**45**	45	**44**	44
Romania	340	300	221	221	**221**	**285**	285	**285**	285
Russian Federation	1189	1191	650	625	**600**	**835**	835	**833**	834
Serbia and Montenegro	90	90	79	79	**79**	**69**	69	**69**	69
Slovakia	63	63	30	28	**29**	**32**	32	**33**	32
Slovenia	24	24	19	19	**19**	**20**	20	**20**	20
Spain	285	***327***	***386***	***380***	***379***	**382**	382	**370**	370
Sweden	54	54	**58**	**55**	**55**	**51**	51	**48**	48
Switzerland	77	72	68	68	**67**	**63**	63	**61**	60
TFYR of Macedonia	17	17	16	16	**16**	**15**	15	**15**	15
Turkey	321	321	321	321	**321**	**321**	321	**321**	321
Ukraine	729	729	358	378	**378**	**324**	619	**270**	619
United Kingdom	361	**361**	**311**	**306**	**296**	**320**	320	**307**	306
North Africa	235	235	235	235	235	**235**	235	**235**	235
Remaining Asiatic	278	278	278	278	278	**278**	278	**278**	278
Baltic Sea	0	0	0	0	0	**0**		**0**	
Black Sea	0	0	0	0	0	**0**		**0**	
Mediterranean Sea	0	0	0	0	0	**0**		**0**	
North Sea	0	0	0	0	0	**0**		**0**	
Remaining N-E Atlantic	0	0	0	0	0	**0**		**0**	
Natural marine	0	0	0	0	0	**0**		**0**	
Volcanic emissions	0	0	0	0	0	**0**		**0**	
TOTAL	8627	8423	6566	6590	6513	6832	7124	6669	7010

[1] All years except 2010 and 2020: Reported values with white background, expert estimates in grey. Values in bold differ from reporting in 2003. Values in italic are reported values modified for modelling purposes by MSC-W. Projections (Base Line Scenario) provide by IIASA (April 2004) in grey boxes. Reported values or extrapolations in white.

Table A.4: National total emission trends.
Emissions of non-methane volatile organic compounds (1980, 1990, 2000-2000, 2010 & 2020) used for modelling at the MSC-W (Gg of NMVOC per year)[1].

Area/Year	1980	1990	2000	2001	2002	2010	2010 CP	2020	2020 CP
Albania	31	31	34	34	**34**	**35**	35	**40**	40
Armenia	26	81	16	28	**14**	**28**	28	**28**	28
Austria	**437**	**298**	**190**	**195**	**193**	**164**	165	**157**	157
Azerbaijan	**9**	**9**	**9**	**9**	**9**	**9**	9	**9**	9
Belarus	549	533	225	215	**229**	**250**	250	**258**	258
Belgium	274	274	233	**276**	**264**	**173**	172	**175**	175
Bosnia and Herzegovina	51	51	42	42	**42**	**44**	44	**51**	51
Bulgaria	309	217	120	123	**123**	**118**	118	**90**	89
Croatia	105	105	80	80	**80**	**104**	104	**107**	107
Cyprus	**14**	**14**	**14**	14	**16**	**3**	3,4	**3**	3
Czech Republic	275	441	227	220	**203**	**150**	150	**137**	136
Denmark	**194**	**164**	**132**	**126**	**124**	**86**	86	**81**	81
Estonia	81	88	34	33	**38**	**34**	34	**29**	29
Finland	210	224	161	157	**151**	**130**	130	**106**	106
France	**2734**	**2499**	**1719**	**1648**	**1542**	**1024**	1026	**937**	936
Georgia	46	46	**28**	**29**	**29**	**19**	19	**19**	19
Germany	3224	**3591**	**1700**	**1595**	**1478**	**1141**	1140	**867**	868
Greece	255	255	305	268	**268**	**180**	180	**166**	165
Hungary	215	205	173	166	**155**	**83**	83	**72**	72
Iceland	7,7	13	10	10	**10**	**7**	6,6	**7**	6,6
Ireland	111	111	90	**87**	**81**	**72**	72	**70**	70
Italy	**2032**	2041	**1557**	**1467**	**1467**	**971**	970	**732**	732
Kazakhstan	89	89	50	50	**50**	**50**	50	**50**	50
Latvia	**152**	**152**	**81**	**85**	**89**	**24**	24	**14**	14
Lithuania	100	108	61	71	**72**	**42**	49	**38**	38
Luxembourg	15	19	15	15	**15**	**11**	11	**12**	12
Netherlands	579	**490**	**266**	**250**	**243**	**237**	237	**242**	241
Norway	173	294	**380**	**391**	**345**	**299**	299	**147**	146
Poland	1036	831	599	576	**576**	**453**	452	**417**	411
Portugal	189	**255**	**271**	**266**	**271**	**298**	298	**258**	258
Republic of Moldova	105	157	21	**25**	**28**	**38**	38	**38**	38
Romania	829	772	638	638	**638**	**369**	370	**287**	287
Russian Federation	3410	3668	2450	**2614**	**2777**	**2643**	2644	**2915**	2915
Serbia and Montenegro	142	142	129	129	**129**	**140**	140	**144**	144
Slovakia	**252**	**252**	**85**	**88**	**87**	**62**	62	**63**	63
Slovenia	39	44	40	**49**	**49**	**33**	33	**25**	25
Spain	1392	***1591***	***1496***	***1477***	***1459***	**832**	833	**794**	795
Sweden	**528**	**503**	**306**	**297**	**295**	**176**	175	**168**	167
Switzerland	323	279	159	145	**143**	**102**	101	**96**	96
TFYR of Macedonia	19	19	17	17	**17**	**31**	31	**36**	36
Turkey	359	463	726	726	**726**	**1935**	726	**726**	726
Ukraine	1626	1369	271	269	**282**	**282**	672	**282**	781
United Kingdom	**2100**	**2419**	**1364**	**1265**	**1186**	**902**	901	**863**	862
North Africa	96	96	96	96	**96**	**96**	96	**96**	96
Remaining Asiatic areas	204	204	204	204	**204**	**204**	186	**204**	186
Baltic Sea	8	8	8	8	**8**	**8**	8	**8**	8
Black Sea	2	2	2	2	**2**	**2**	2	**2**	2
Mediterranean Sea	34	34	34	34	**34**	**34**	34	**34**	34
North Sea	15	15	15	15	**15**	**15**	1	**15**	1
Remaining N-E Atlantic	25	25	25	25	**25**	**25**	25	**25**	25
Natural marine	0	0	0	0	**0**	**0**		**0**	
Volcanic emissions	0	0	0	0	**0**	**0**		**0**	
TOTAL	25030	24603	16907	16648	16410	14168	13323	12140	12595

[1] All years except 2010 and 2020: Reported values with white background, expert estimates in grey. Values in bold differ from reporting in 2003. Values in italic are reported values modified for modelling purposes by MSC-W. Projections (Base Line Scenario) provide by IIASA (April 2004) in grey boxes. Reported values or extrapolations in white.

Table A.5: National total emission trends. Emissions of carbon monoxide (1980, 1990, 2000-2000, 2010 & 2020) used for modelling at the MSC-W (Gg of CO per year)[1].

Area/Year	1980	1990	2000	2001	2002	2010	2010 CP	2020	2020 CP
Albania	84	84	102	102	**102**	**160**	160	**196**	196
Armenia	405	304	110	104	**106**	**104**	104	**104**	104
Austria	**1786**	**1249**	**833**	**837**	**812**	**727**	727	**695**	695
Azerbaijan	293	293	293	293	**293**	**293**	293	**293**	293
Belarus	1654	1722	718	711	**712**	**837**	837	**951**	951
Belgium	1285	1285	1100	1006	**1019**	**306**	306	**286**	286
Bosnia and Herzegovina	277	277	193	193	**193**	**160**	160	**203**	203
Bulgaria	997	891	667	**619**	**619**	**568**	568	**393**	393
Croatia	655	655	402	402	**402**	**480**	480	**514**	514
Cyprus	46	63	81	85	**83**	**85**	85	**85**	85
Czech Republic	894	1257	648	649	**546**	**475**	475	**438**	438
Denmark	**1036**	**745**	**602**	**603**	**577**	**358**	358	**309**	309
Estonia	400	434	202	177	**178**	**126**	126	**105**	105
Finland	660	559	526	605	**600**	**644**	644	**602**	602
France	**15810**	**10947**	**6624**	**6261**	**5954**	**4795**	4795	**4576**	4576
Georgia	648	526	**216**	**218**	**218**	**222**	222	**222**	222
Germany	14046	**11212**	**4925**	**4573**	**4311**	**1036**	4245	**967**	4000
Greece	1298	1298	1531	1366	**1366**	**1240**	1237	**1120**	1120
Hungary	1019	997	633	592	**620**	**492**	492	**487**	487
Iceland	44	58	40	40	**40**	**19**	19	**19**	19
Ireland	401	401	280	270	**254**	**204**	204	**192**	192
Italy	**7164**	**7146**	**5221**	**4965**	**4965**	**365**	3651	**309**	3085
Kazakhstan	*410*	*410*	*279*	*279*	***279***	***279***	279	***279***	279
Latvia	**752**	**752**	**364**	**381**	**378**	**185**	185	**133**	133
Lithuania	541	519	282	229	**224**	**228**	228	**155**	156
Luxembourg	193	175	49	49	**49**	**42**	42	**37**	37
Netherlands	1530	1128	**699**	**673**	**653**	**622**	623	**678**	678
Norway	**878**	867	**571**	**560**	**530**	**1552**	1552	**1542**	1542
Poland	7406	7406	3463	3528	**3528**	**2863**	2863	**3068**	3068
Portugal	***745***	***745***	***675***	***638***	***644***	**1794**	1794	**1810**	1810
Republic of Moldova	394	453	**102**	**104**	**107**	**192**	192	**199**	199
Romania	3245	3186	2325	2325	**2325**	**1034**	1034	**845**	845
Russian Federation	13520	13329	10811	**11164**	**11517**	**9805**	9806	**7924**	7924
Serbia and Montenegro	672	739	553	553	**553**	**573**	573	**639**	639
Slovakia	491	**493**	**300**	**300**	**297**	**240**	240	**231**	231
Slovenia	68	81	68	**93**	**89**	**199**	199	**203**	203
Spain	3494	3702	2774	**2743**	**2623**	**3362**	3362	**3176**	3176
Sweden	**1202**	**1202**	**838**	**796**	**766**	**624**	624	**598**	598
Switzerland	1280	673	394	**374**	**383**	**346**	346	**331**	331
TFYR of Macedonia	77	77	77	76	**81**	**214**	214	**248**	248
Turkey	2934	3585	3778	3778	**3778**	**3778**	3778	**3778**	3778
Ukraine	9832	8141	2708	2744	**2780**	**3055**	3055	**3824**	3824
United Kingdom	7669	**7417**	**3928**	**3636**	**3238**	**1924**	1924	**1810**	1810
North Africa	336	336	336	336	336	**336**	336	**336**	336
Remaining Asiatic areas	449	449	449	449	449	**131**	131	**131**	131
Baltic Sea	29	29	29	29	29	**15**	15	**15**	15
Black Sea	8	8	8	8	8	**8**	8	**8**	8
Mediterranean Sea	139	139	139	139	139	**2,5**	3	**2,5**	3
North Sea	59	59	59	59	59	**91**	91	**91**	91
Remaining N-E Atlantic	111	111	111	111	111	**133**	133	**133**	133
Natural marine	0	0	0	0	0	**0**		**0**	
Volcanic emissions	0	0	0	0	0	**0**		**0**	
TOTAL	109364	98613	62114	60824	59922	**47324**	58064	**45291**	51105

[1] All years except 2010 and 2020: Reported values with white background, expert estimates in grey. Values in bold differ from reporting in 2003. Values in italic are reported values modified for modelling purposes by MSC-W. Projections (Base Line Scenario) provide by IIASA (April 2004) in grey boxes. Reported values or extrapolations in white.

Table A.6: National total emission trends. Emissions of Particulate Matter (1980, 1990, 2000-2000, 2010 & 2020) used for modelling at the MSC-W (Gg of $PM_{2.5}$ per year)[1].

Area/Year	1999	2000	2001	2002	2010	2010 CP	2020	2020 CP
Albania	**6**	**6**	**6**	**6**	**5**	5,3	**6**	5,7
Armenia	**5**	**5**	**5**	**5**	5	5,1	5	5,1
Austria	**25**	**25**	**26**	**26**	**29**	30	**25**	25
Azerbaijan	**19**	19	19	19	19	19	19	19
Belarus	**36**	**36**	**36**	**36**	**33**	33	**28**	28
Belgium	**36**	36	**37**	**34**	**24**	24	**21**	20
Bosnia and	**20**	**20**	**20**	**20**	**17**	17	**16**	16
Bulgaria	**56**	**56**	**56**	**56**	**46**	45	**38**	36
Croatia	**18**	**18**	**18**	**18**	**14**	14	**14**	14
Cyprus	**3**	**3**	**3**	**3**	**3**	2,8	**3**	3,1
Czech Republic	**55**	**55**	**55**	**55**	**34**	33	**23**	20
Denmark	**15**	**15**	**15**	**14**	**18**	18	**15**	15
Estonia	**21**	**21**	**25**	**25**	**13**	13	**7**	5,8
Finland	**38**	38	38	**39**	**31**	31	**26**	26
France	**307**	**290**	**288**	**275**	**196**	196	**161**	156
Georgia	**8**	**8**	**8**	**8**	8	7,6	8	7,6
Germany	**166**	**166**	**166**	**166**	**132**	129	**117**	110
Greece	**50**	**50**	**50**	**50**	**50**	48	**44**	42
Hungary	**20**	26	24	**24**	**26**	26	**24**	21
Iceland	**3**	3	3	3	3	2,7	3	2,7
Ireland	**13**	**13**	**12**	**11**	**11**	10	**8**	8,3
Italy	**202**	**202**	**202**	**202**	**126**	125	**93**	92
Kazakhstan	**NA**	**NA**	**NA**	**NA**	**NA**		**NA**	
Latvia	**2,9**	**2,9**	**3,1**	**3,1**	**6**	5,8	**4**	4
Lithuania	**17**	**17**	**17**	**17**	**14**	14	**12**	11
Luxembourg	**3**	**3**	**3**	**3**	**2**	2,5	**2**	2,2
Netherlands	**37**	**31**	**29**	**28**	**29**	29	**25**	25
Norway	**59**	**60**	**59**	**55**	**43**	43	**40**	40
Poland	**135**	135	142	**142**	**146**	145	**104**	98
Portugal	**45**	**45**	**45**	**45**	**38**	38	**36**	37
Republic of Moldova	**22**	**22**	**22**	**22**	**21**	21	**14**	14
Romania	**104**	**104**	**104**	**104**	**83**	76	**67**	56
Russian Federation	**876**	**876**	**876**	**876**	**857**	856	**868**	868
Serbia and	**44**	**44**	**44**	**44**	**39**	39	**41**	41
Slovakia	**18**	**18**	**16**	**16**	**14**	13	**13**	12
Slovenia	**15**	**15**	**15**	**15**	**10**	10	**7**	6
Spain	***147***	***147***	***148***	***145***	**107**	106	**86**	84
Sweden	**46**	**44**	**45**	**45**	**21**	21	**17**	17
Switzerland	**10**	**10**	**10**	**10**	**7**	7,4	**6**	6,3
TFYR of Macedonia	**9**	**9**	**9**	**9**	**8**	7,9	**8**	7,6
Turkey	223	223	223	223	223	223	223	223
Ukraine	**310**	**310**	**310**	**310**	**269**	268	**282**	282
United Kingdom	**115**	**102**	**102**	**93**	**81**	81	**65**	62
North Africa		**NA**	**NA**	**NA**	**NA**		**NA**	
Remaining Asiatic		**NA**	**NA**	**NA**	**NA**		**NA**	
Baltic Sea		**NA**	**NA**	**NA**	**NA**	4	**NA**	6,7
Black Sea		**NA**	**NA**	**NA**	**NA**	0,8	**NA**	0,8
Mediterranean Sea		**NA**	**NA**	**NA**	**NA**	0,7	**NA**	1,1
North Sea		**NA**	**NA**	**NA**	**NA**	25	**NA**	41
Remaining N-E Atlantic		**NA**	**NA**	**NA**	**NA**	36	**NA**	60
Natural marine		**NA**	**NA**	**NA**	**NA**		**NA**	
Volcanic emissions		**NA**	**NA**	**NA**	**NA**		**NA**	
Totals	3360	3329	3334	3300	2861	2904	2624	2682

[1] All years except 2010 and 2020: Reported values with white background, expert estimates in grey. Values in bold differ from reporting in 2003. Values in italic are reported values modified for modelling purposes by MSC-W. Projections (Base Line Scenario) provide by IIASA (April 2004) in grey boxes. Reported values or extrapolations in white.

Table A.7: National total emission trends.
Emissions of Particulate Matter (1999-2002, 2010 & 2020) used for modelling at the MSC-W (Gg of PM_{10} per year)[1].

Area/Year	1999	2000	2001	2002	2010	2010 CP	2020	2020 CP
Albania	8	8	8	8	6	6,3	7	6,9
Armenia	7	7	7	7	7	7,3	7	7,3
Austria	39	38	40	41	42	42	37	37
Azerbaijan	30	30	30	30	30	30	30	30
Belarus	51	51	51	51	44	44	36	36
Belgium	65	65	66	64	43	42	40	38
Bosnia and Herzegovina	47	47	47	47	36	36	33	33
Bulgaria	90	90	90	90	76	75	66	60
Croatia	27	27	27	27	19	19	20	20
Cyprus	5	5	5	5	5	4,7	5	5,1
Czech Republic	83	83	83	83	53	51	37	33
Denmark	22	22	23	22	28	28	24	24
Estonia	41	41	35	35	18	18	9	8
Finland	48	48	54	55	37	37	33	32
France	556	535	531	518	274	272	248	232
Georgia	12	12	12	12	12	12	12	12
Germany	254	254	254	254	217	212	204	191
Greece	66	66	66	66	68	65	62	58
Hungary	46	47	45	43	38	37	37	32
Iceland	3	3	3	3	3	3,1	3	3,1
Ireland	14	14	17	15	17	17	14	14
Italy	264	264	264	264	176	174	144	141
Kazakhstan	NA	NA	NA	NA	NA		NA	
Latvia	4,22	4,22	4,19	4,21	8	7,5	6	5,5
Lithuania	20	20	20	20	18	18	15	14
Luxembourg	4	4	4	4	4	3,5	3	3,3
Netherlands	63	49	46	45	52	52	48	48
Norway	65	66	65	62	48	48	45	45
Poland	282	282	303	299	206	202	155	145
Portugal	58	58	58	58	48	48	47	47
Republic of Moldova	39	39	39	39	36	36	22	22
Romania	151	151	151	151	122	107	102	77
Russian Federation	1352	1352	1352	1352	1353	1353	1337	1337
Serbia and Montenegro	89	89	89	89	73	73	78	78
Slovakia	25	25	25	25	22	21	20	19
Slovenia	21	21	21	21	14	13	11	8
Spain	*213*	*213*	*213*	*217*	157	155	138	133
Sweden	67	66	66	67	31	30	27	26
Switzerland	26	26	24	15	13	13	12	12
TFYR of Macedonia	20	20	20	20	15	15	14	14
Turkey	420	420	420	420	420	420	420	420
Ukraine	499	499	499	499	430	430	443	443
United Kingdom	199	179	180	161	135	134	116	109
North Africa	NA	NA	NA	NA	NA		NA	
Remaining Asiatic areas	NA	NA	NA	NA	NA		NA	
Baltic Sea	NA	NA	NA	NA	NA	4,3	NA	7,1
Black Sea	NA	NA	NA	NA	NA	1,5	NA	1,5
Mediterranean Sea	NA	NA	NA	NA	NA	0,7	NA	1,2
North Sea	NA	NA	NA	NA	NA	26	NA	43
Remaining N-E Atlantic	NA	NA	NA	NA	NA	38	NA	63
Natural marine	NA	NA	NA	NA	NA		NA	
Volcanic emissions	NA	NA	NA	NA	NA		NA	
Totals	8395	5340	5357	5308	4454	4481	4167	4176

[1] All years except 2010 and 2020: Reported values with white background, expert estimates in grey. Values in bold differ from reporting in 2003. Values in italic are reported values modified for modelling purposes by MSC-W. Projections (Base Line Scenario) provide by IIASA (April 2004) in grey boxes. Reported values or extrapolations in white.

Appendix B

Daily time-series of elemental carbon, and daily time-series of number concentrations

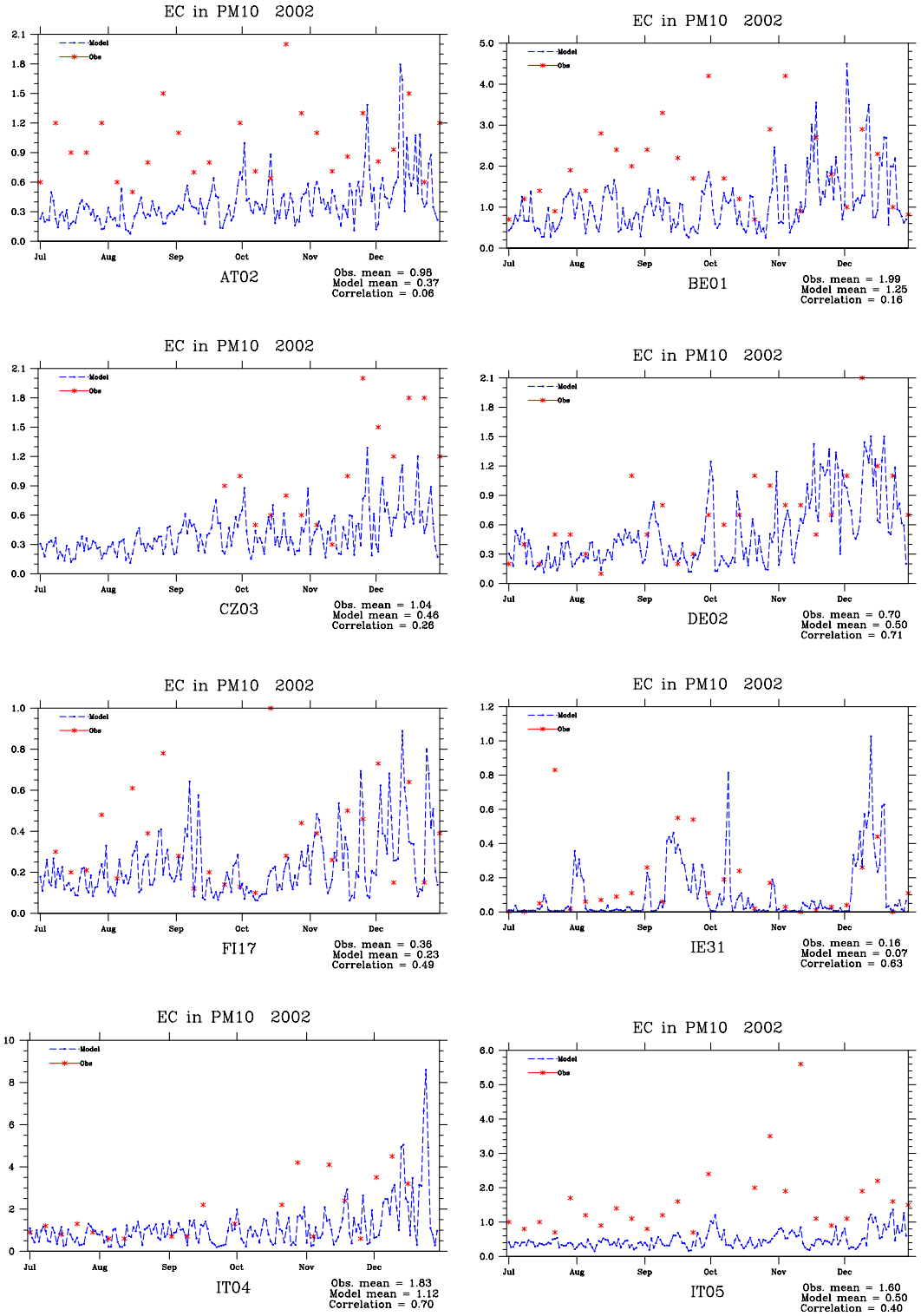

Figure A.1: Daily time-series of calculated (blue line) and measured (red stars) concentrations of elemental carbon (measurements from NILU OC/EC campaign).

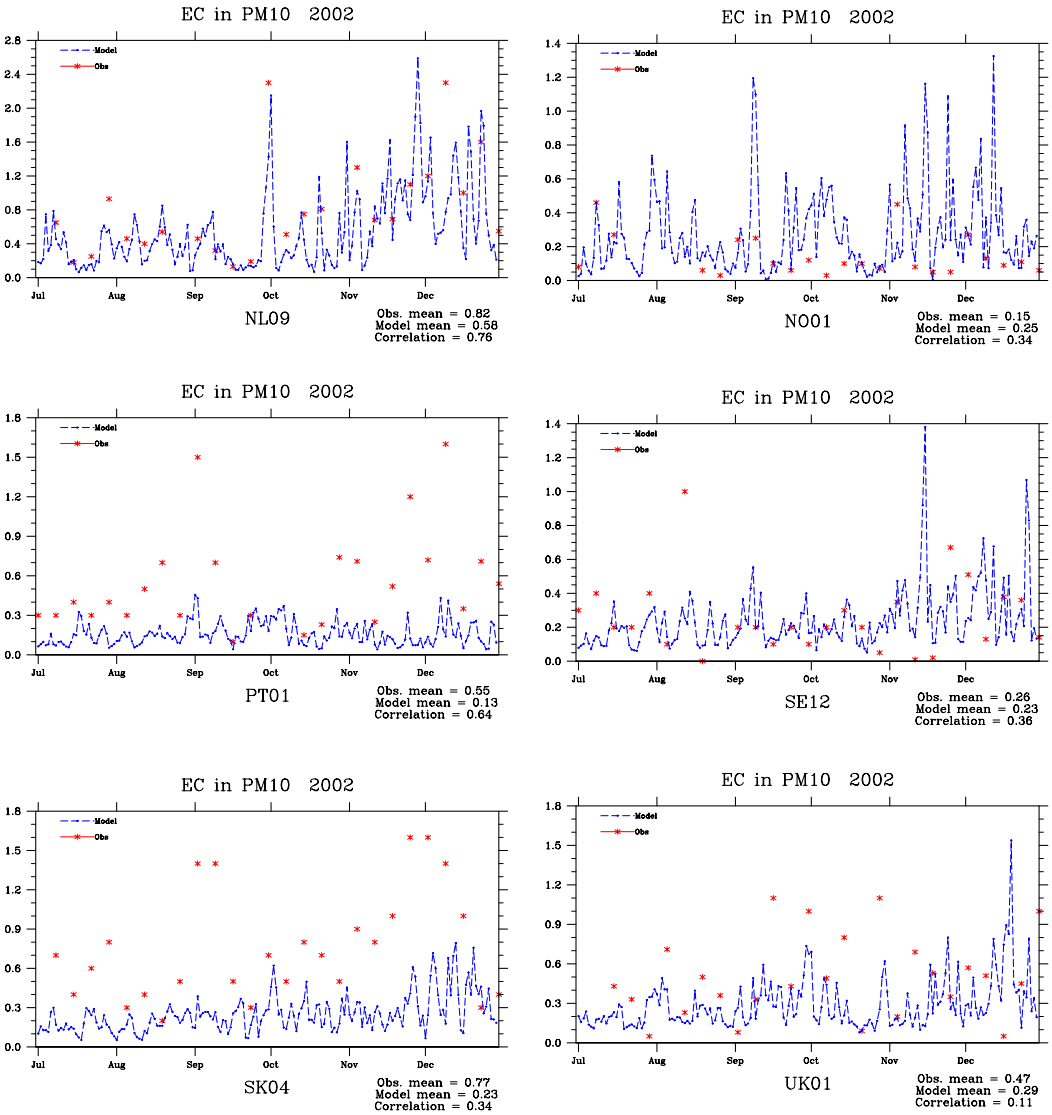

Figure A.1 (continued):

Daily time-series of calculated (blue line) and measured (red stars) concentrations of elemental carbon (measurements from NILU OC/EC campaign).

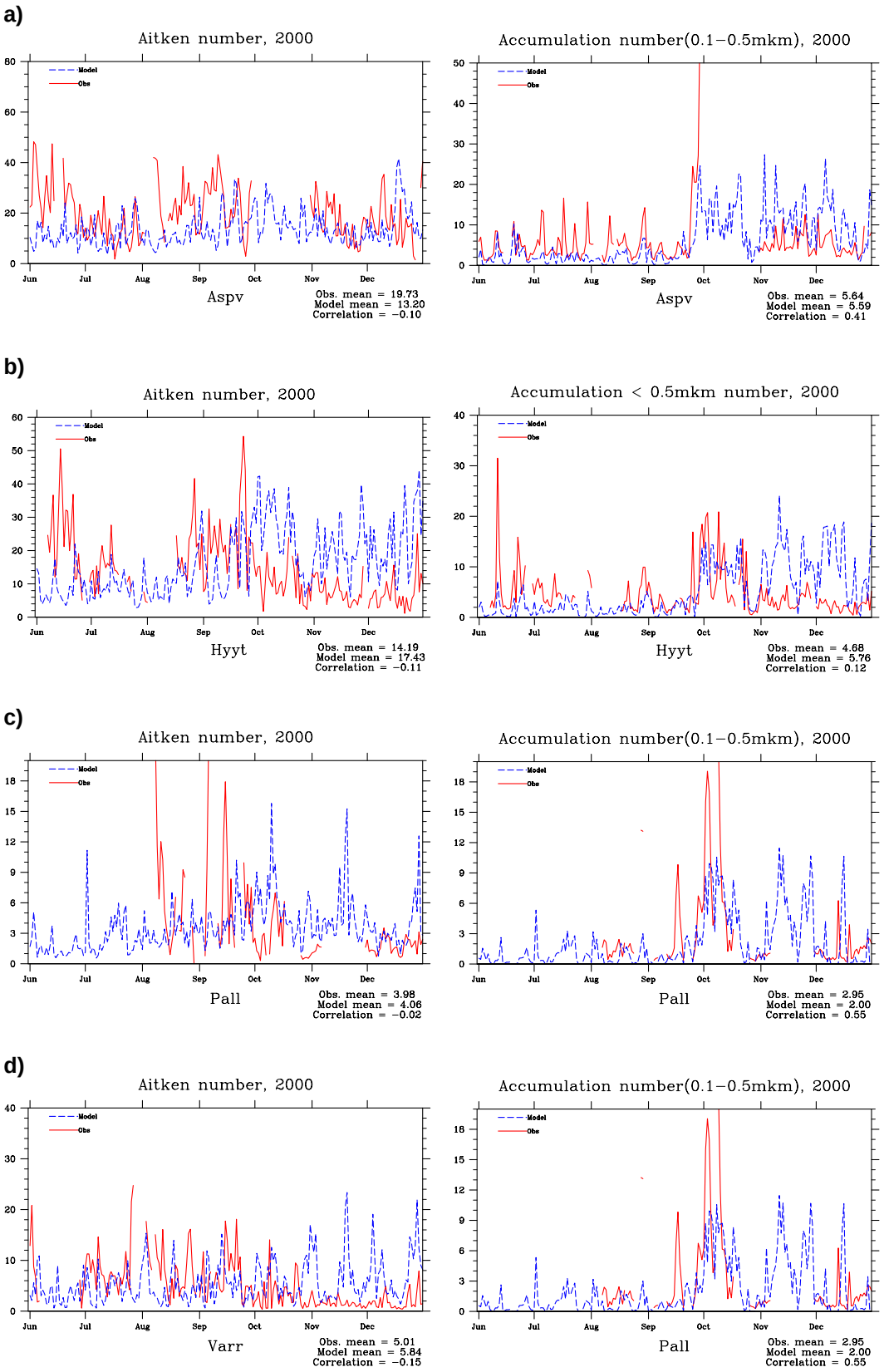

Figure A.2: Daily time-series of the number concentrations of Aitken and accumulation particles for June-December 2000 at: a) Aspvreten, b) Hyytiälä, c) Pallas and d) Värriö.

Appendix C

Daily timeseries of PM_{10} and $PM_{2.5}$

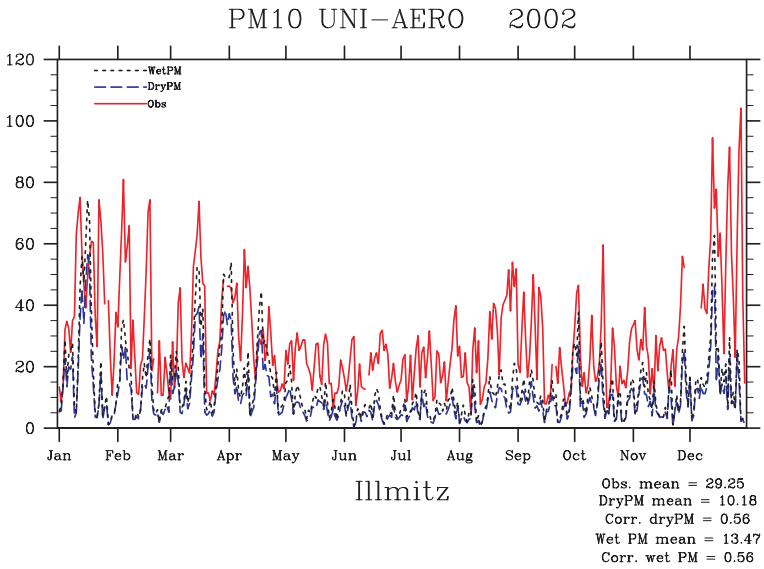
PM10 UNI–AERO 2002
WetPM
DryPM
Obs
120
100
80
60
40
20
0
Jan Feb Mar Apr May Jun Jul Aug Sep Oct Nov Dec
Illmitz
Obs. mean = 29.25
DryPM mean = 10.18
Corr. dryPM = 0.56
Wet PM mean = 13.47
Corr. wet PM = 0.56

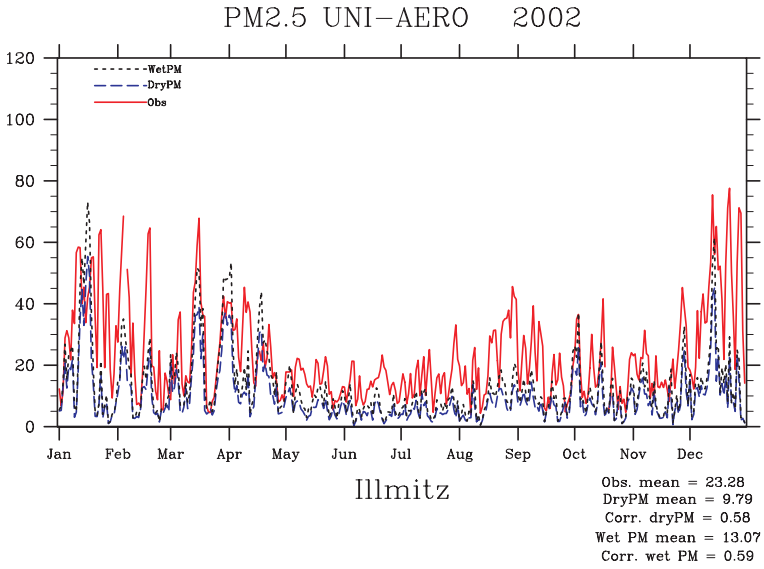
PM2.5 UNI–AERO 2002
WetPM
DryPM
Obs
120
100
80
60
40
20
0
Jan Feb Mar Apr May Jun Jul Aug Sep Oct Nov Dec
Illmitz
Obs. mean = 23.28
DryPM mean = 9.79
Corr. dryPM = 0.58
Wet PM mean = 13.07
Corr. wet PM = 0.59

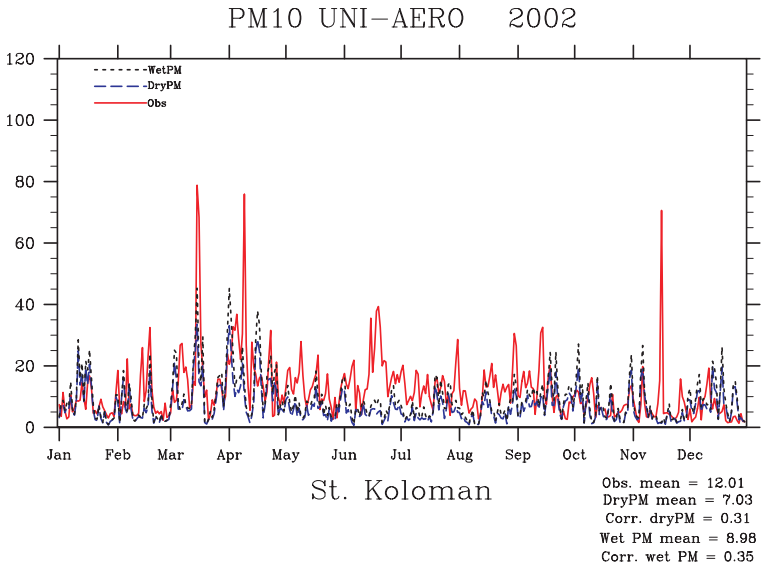
PM10 UNI–AERO 2002
WetPM
DryPM
Obs
120
100
80
60
40
20
0
Jan Feb Mar Apr May Jun Jul Aug Sep Oct Nov Dec
St. Koloman
Obs. mean = 12.01
DryPM mean = 7.03
Corr. dryPM = 0.31
Wet PM mean = 8.98
Corr. wet PM = 0.35

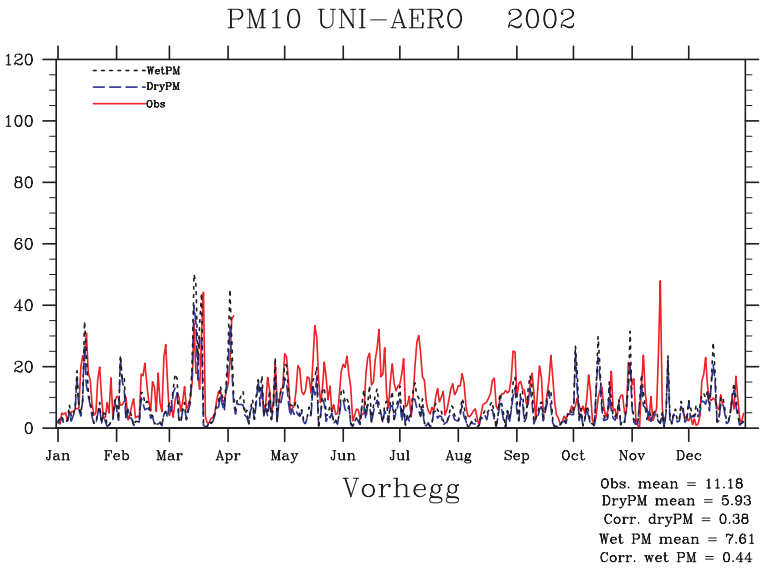
PM10 UNI-AERO 2002
WetPM
DryPM
Obs
120
100
80
60
40
20
0
Jan
Feb
Mar
Apr
May
Jun
Jul
Aug
Sep
Oct
Nov
Dec
Vorhegg
Obs. mean = 11.18
DryPM mean = 5.93
Corr. dryPM = 0.38
Wet PM mean = 7.61
Corr. wet PM = 0.44

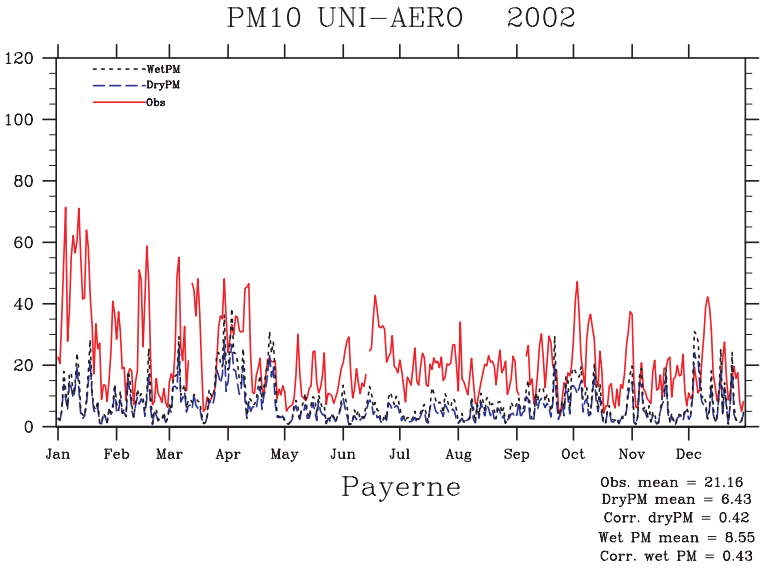
PM10 UNI-AERO 2002
WetPM
DryPM
Obs
120
100
80
60
40
20
0
Jan
Feb
Mar
Apr
May
Jun
Jul
Aug
Sep
Oct
Nov
Dec
Payerne
Obs. mean = 21.16
DryPM mean = 6.43
Corr. dryPM = 0.42
Wet PM mean = 8.55
Corr. wet PM = 0.43

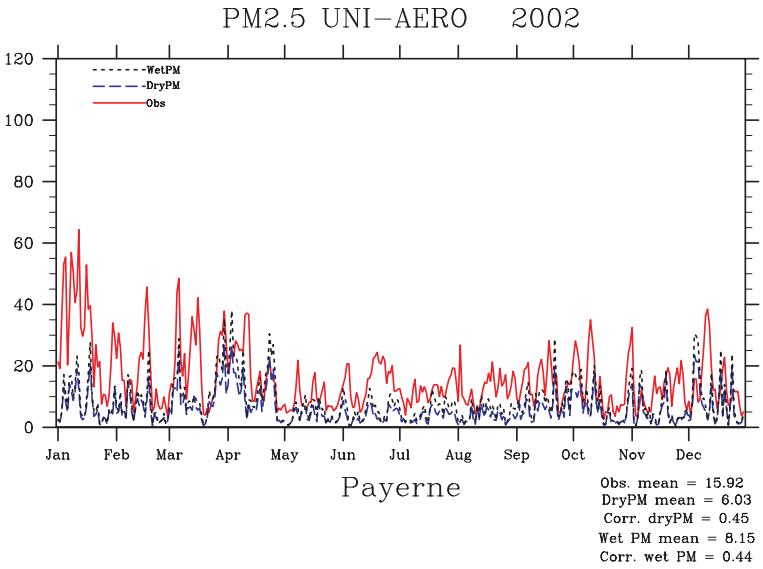
PM2.5 UNI-AERO 2002
WetPM
DryPM
Obs
120
100
80
60
40
20
0
Jan
Feb
Mar
Apr
May
Jun
Jul
Aug
Sep
Oct
Nov
Dec
Payerne
Obs. mean = 15.92
DryPM mean = 6.03
Corr. dryPM = 0.45
Wet PM mean = 8.15
Corr. wet PM = 0.44

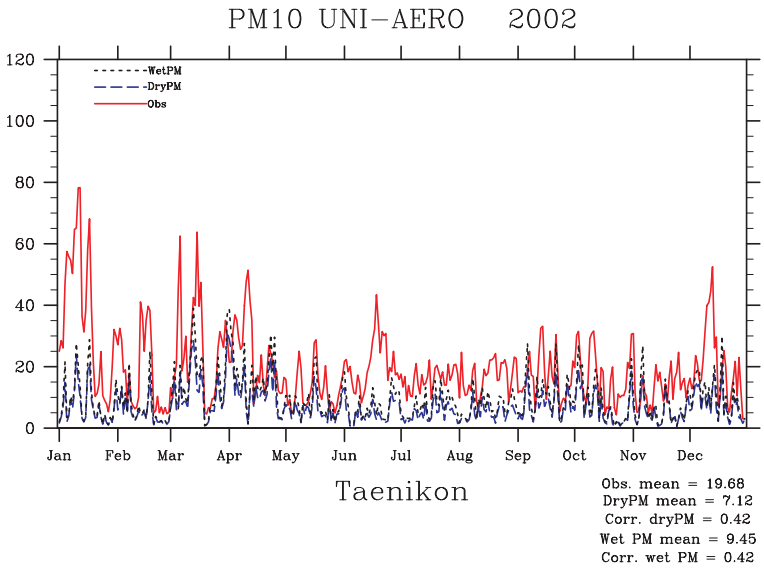
PM10 UNI–AERO 2002
WetPM
DryPM
Obs
120
100
80
60
40
20
0
Jan Feb Mar Apr May Jun Jul Aug Sep Oct Nov Dec
Taenikon
Obs. mean = 19.68
DryPM mean = 7.12
Corr. dryPM = 0.42
Wet PM mean = 9.45
Corr. wet PM = 0.42

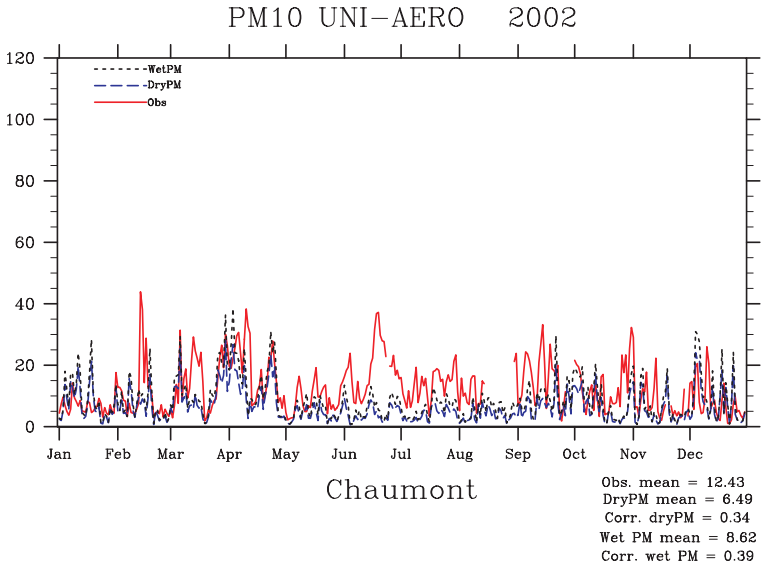
PM10 UNI–AERO 2002
WetPM
DryPM
Obs
120
100
80
60
40
20
0
Jan Feb Mar Apr May Jun Jul Aug Sep Oct Nov Dec
Chaumont
Obs. mean = 12.43
DryPM mean = 6.49
Corr. dryPM = 0.34
Wet PM mean = 8.62
Corr. wet PM = 0.39

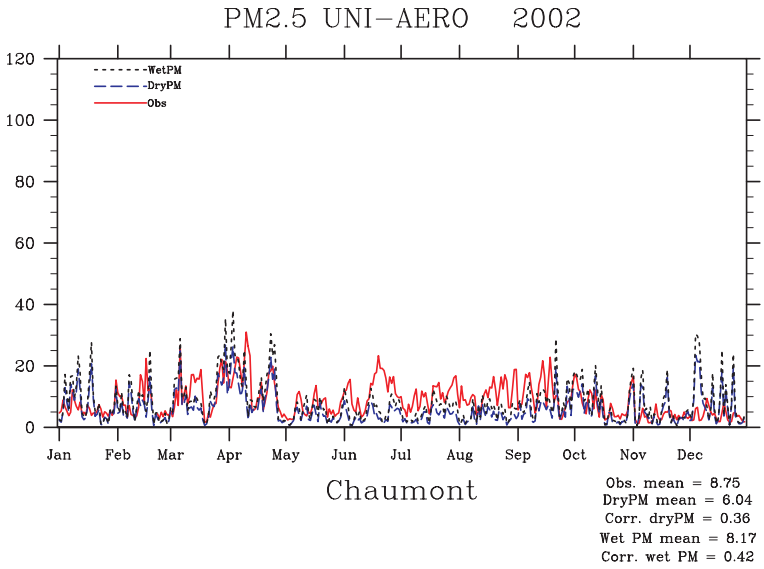
PM2.5 UNI–AERO 2002
WetPM
DryPM
Obs
120
100
80
60
40
20
0
Jan Feb Mar Apr May Jun Jul Aug Sep Oct Nov Dec
Chaumont
Obs. mean = 8.75
DryPM mean = 6.04
Corr. dryPM = 0.36
Wet PM mean = 8.17
Corr. wet PM = 0.42

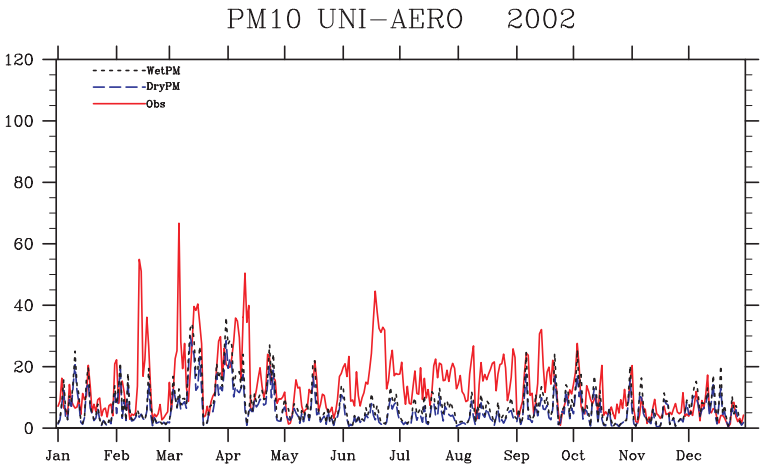

Rigi

Obs. mean = 13.24
DryPM mean = 5.83
Corr. dryPM = 0.34
Wet PM mean = 7.64
Corr. wet PM = 0.38

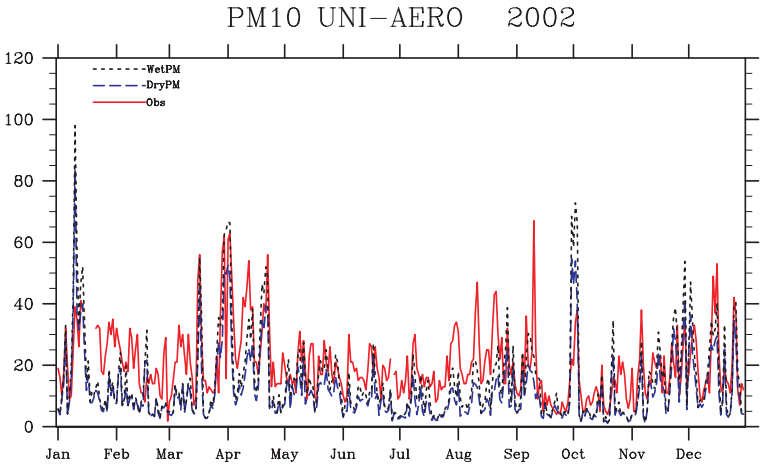

Westerland/Wenningsted

Obs. mean = 20.20
DryPM mean = 11.80
Corr. dryPM = 0.62
Wet PM mean = 15.30
Corr. wet PM = 0.63

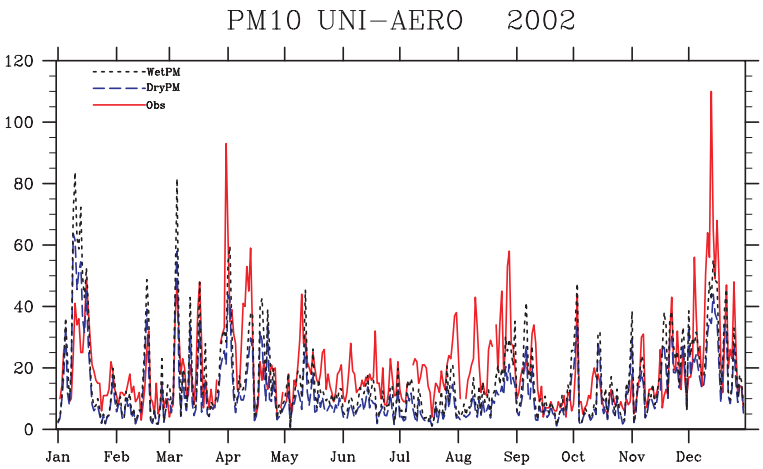

Langenbr☆gge/Waldhof

Obs. mean = 19.54
DryPM mean = 12.28
Corr. dryPM = 0.60
Wet PM mean = 16.43
Corr. wet PM = 0.61

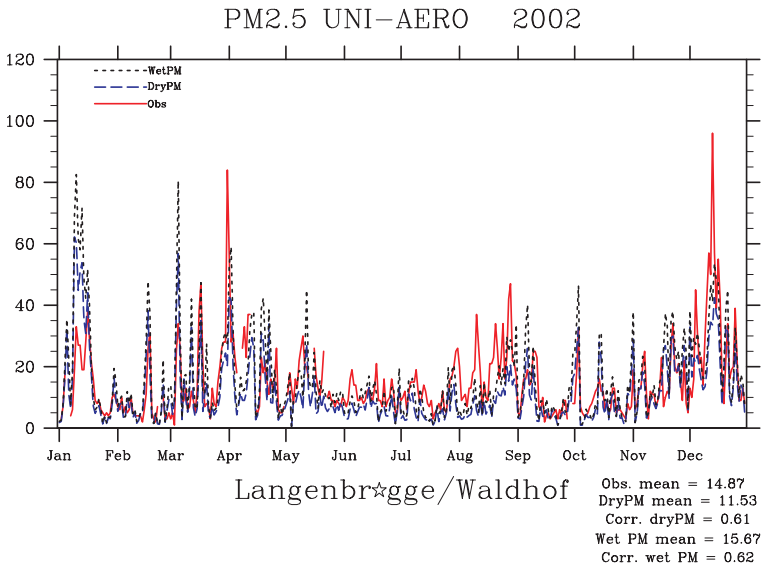
PM2.5 UNI–AERO 2002
WetPM
DryPM
Obs
120
100
80
60
40
20
0
Jan Feb Mar Apr May Jun Jul Aug Sep Oct Nov Dec
Langenbrʊgge/Waldhof
Obs. mean = 14.87
DryPM mean = 11.53
Corr. dryPM = 0.61
Wet PM mean = 15.67
Corr. wet PM = 0.62

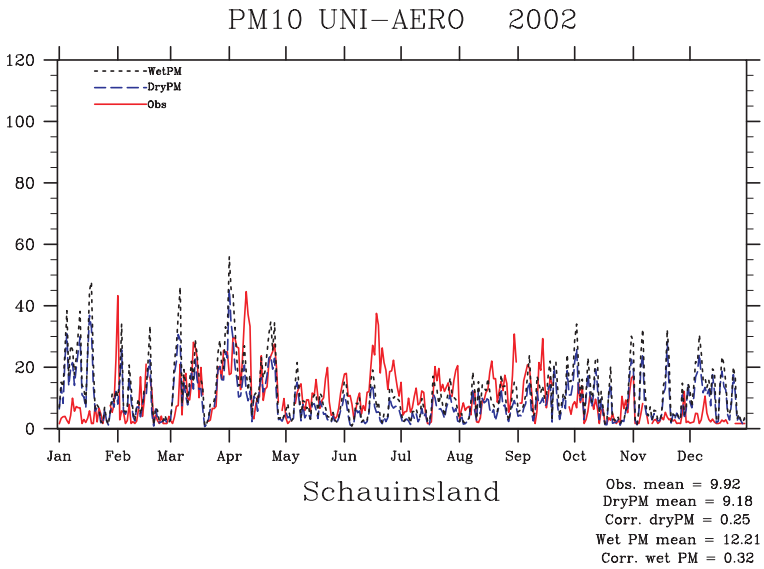
PM10 UNI–AERO 2002
WetPM
DryPM
Obs
120
100
80
60
40
20
0
Jan Feb Mar Apr May Jun Jul Aug Sep Oct Nov Dec
Schauinsland
Obs. mean = 9.92
DryPM mean = 9.18
Corr. dryPM = 0.25
Wet PM mean = 12.21
Corr. wet PM = 0.32

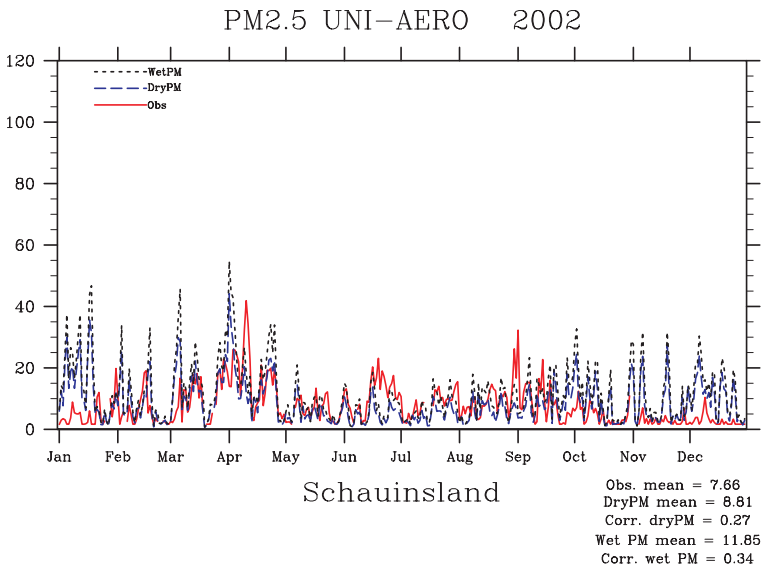
PM2.5 UNI–AERO 2002
WetPM
DryPM
Obs
120
100
80
60
40
20
0
Jan Feb Mar Apr May Jun Jul Aug Sep Oct Nov Dec
Schauinsland
Obs. mean = 7.66
DryPM mean = 8.81
Corr. dryPM = 0.27
Wet PM mean = 11.85
Corr. wet PM = 0.34

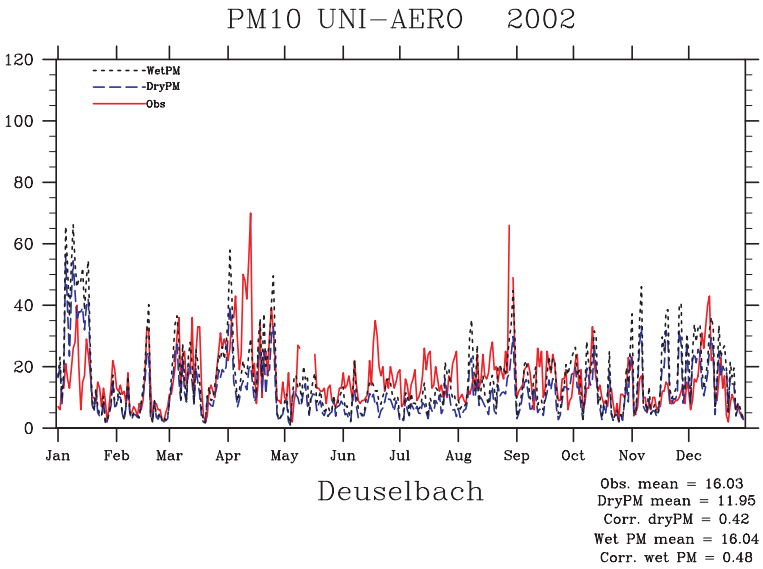
PM10 UNI-AERO 2002
WetPM
DryPM
Obs
120
100
80
60
40
20
0
Jan
Feb
Mar
Apr
May
Jun
Jul
Aug
Sep
Oct
Nov
Dec
Deuselbach
Obs. mean = 16.03
DryPM mean = 11.95
Corr. dryPM = 0.42
Wet PM mean = 16.04
Corr. wet PM = 0.48

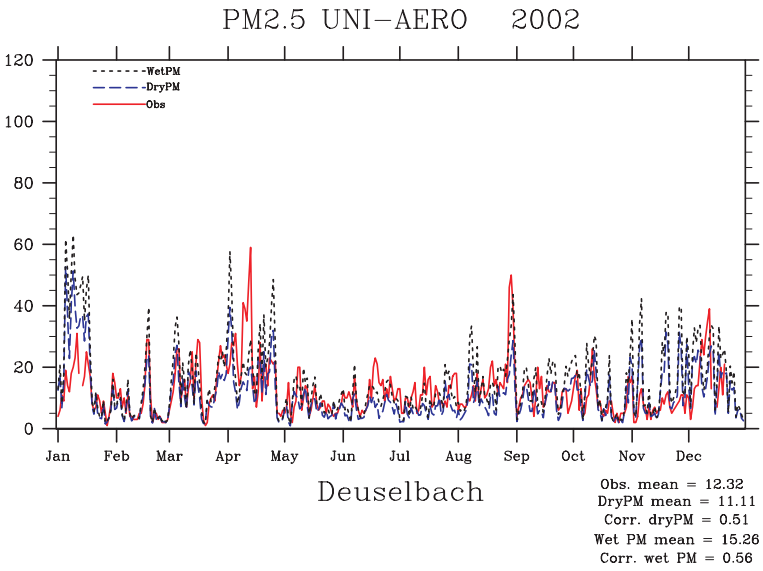
PM2.5 UNI-AERO 2002
WetPM
DryPM
Obs
120
100
80
60
40
20
0
Jan
Feb
Mar
Apr
May
Jun
Jul
Aug
Sep
Oct
Nov
Dec
Deuselbach
Obs. mean = 12.32
DryPM mean = 11.11
Corr. dryPM = 0.51
Wet PM mean = 15.26
Corr. wet PM = 0.56

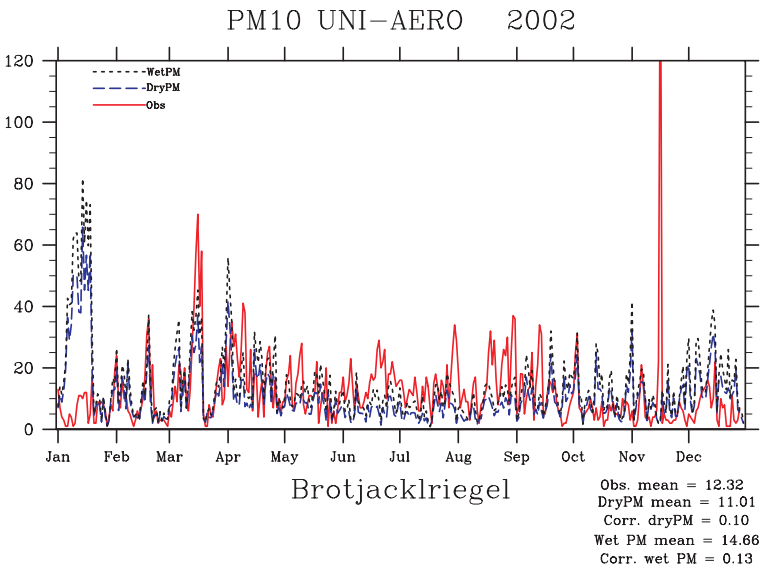
PM10 UNI-AERO 2002
WetPM
DryPM
Obs
120
100
80
60
40
20
0
Jan
Feb
Mar
Apr
May
Jun
Jul
Aug
Sep
Oct
Nov
Dec
Brotjacklriegel
Obs. mean = 12.32
DryPM mean = 11.01
Corr. dryPM = 0.10
Wet PM mean = 14.66
Corr. wet PM = 0.13

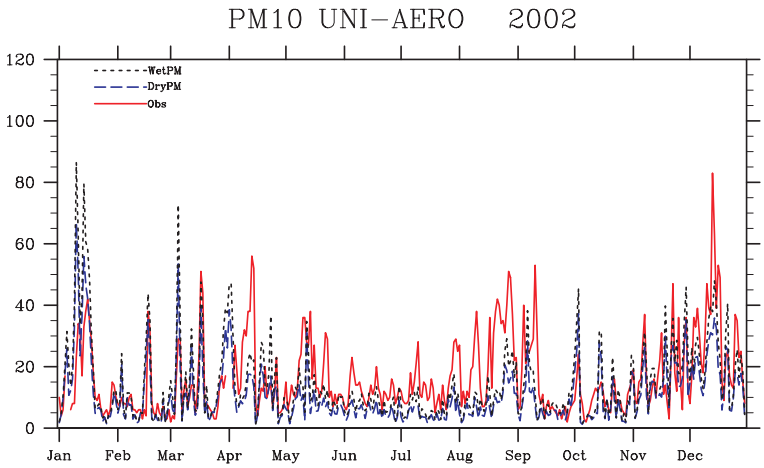

Neuglobsow

Obs. mean = 16.41
DryPM mean = 10.62
Corr. dryPM = 0.55
Wet PM mean = 14.12
Corr. wet PM = 0.57

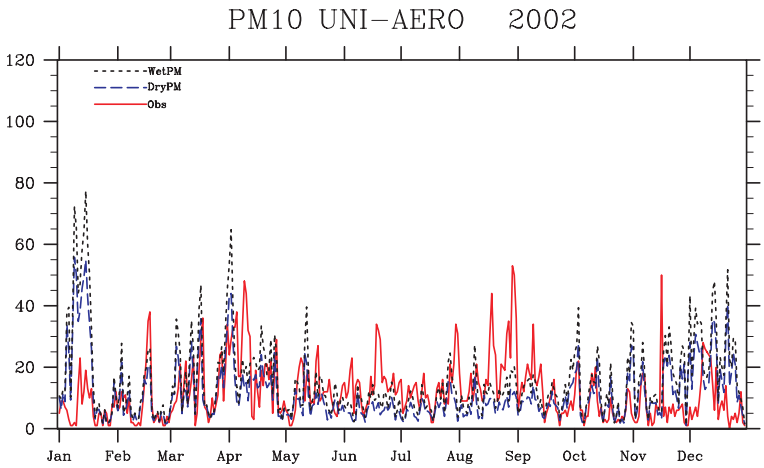

Schm☆cke

Obs. mean = 11.98
DryPM mean = 11.51
Corr. dryPM = 0.18
Wet PM mean = 15.39
Corr. wet PM = 0.22

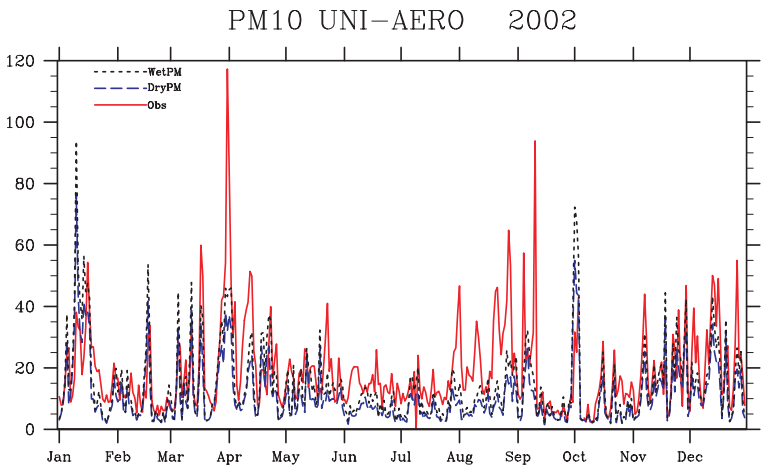

Zingst

Obs. mean = 18.85
DryPM mean = 11.00
Corr. dryPM = 0.57
Wet PM mean = 14.44
Corr. wet PM = 0.59

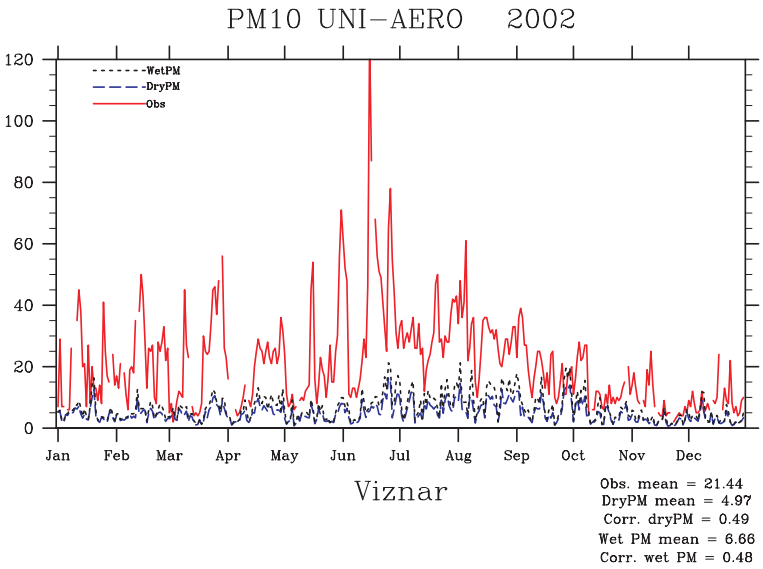
PM10 UNI-AERO 2002
WetPM
DryPM
Obs
120
100
80
60
40
20
0
Jan Feb Mar Apr May Jun Jul Aug Sep Oct Nov Dec
Viznar
Obs. mean = 21.44
DryPM mean = 4.97
Corr. dryPM = 0.49
Wet PM mean = 6.66
Corr. wet PM = 0.48

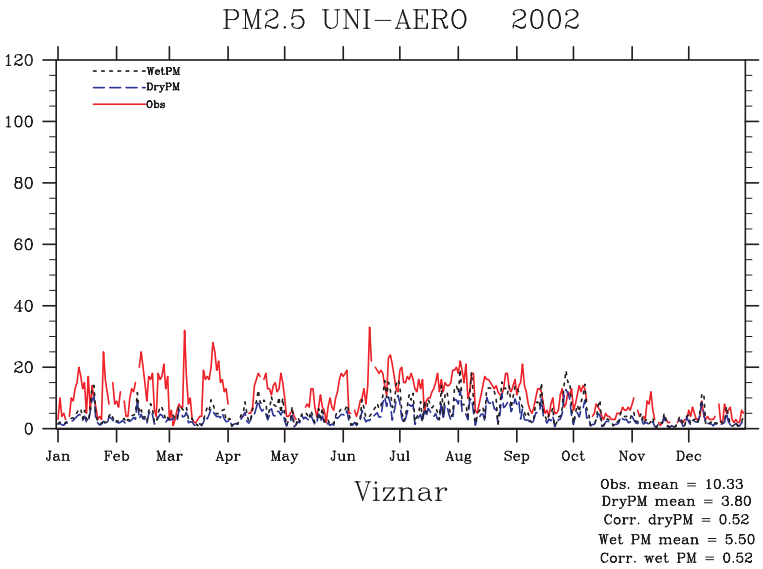
PM2.5 UNI-AERO 2002
WetPM
DryPM
Obs
120
100
80
60
40
20
0
Jan Feb Mar Apr May Jun Jul Aug Sep Oct Nov Dec
Viznar
Obs. mean = 10.33
DryPM mean = 3.80
Corr. dryPM = 0.52
Wet PM mean = 5.50
Corr. wet PM = 0.52

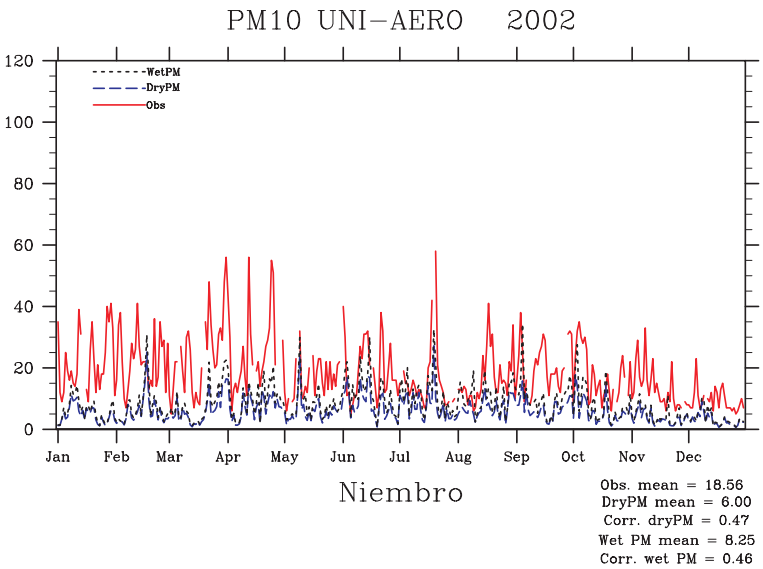
PM10 UNI-AERO 2002
WetPM
DryPM
Obs
120
100
80
60
40
20
0
Jan Feb Mar Apr May Jun Jul Aug Sep Oct Nov Dec
Niembro
Obs. mean = 18.56
DryPM mean = 6.00
Corr. dryPM = 0.47
Wet PM mean = 8.25
Corr. wet PM = 0.46

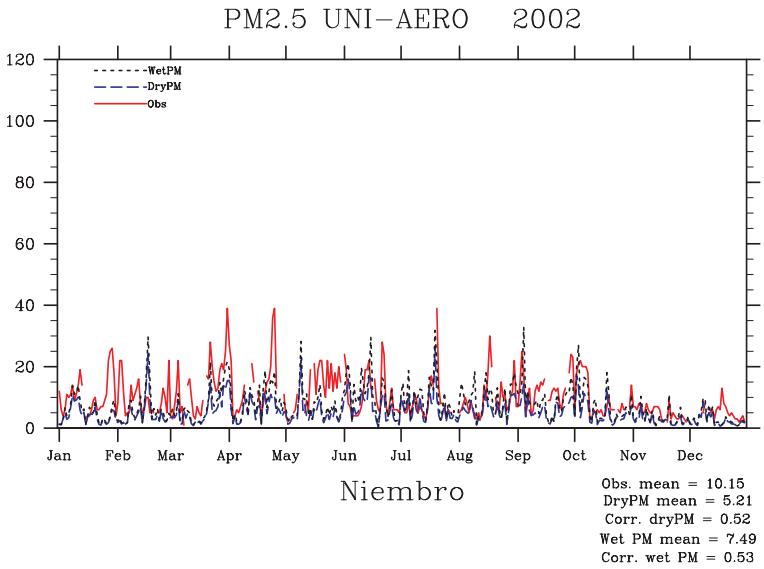
PM2.5 UNI–AERO 2002
WetPM
DryPM
Obs
120
100
80
60
40
20
0
Jan Feb Mar Apr May Jun Jul Aug Sep Oct Nov Dec
Niembro
Obs. mean = 10.15
DryPM mean = 5.21
Corr. dryPM = 0.52
Wet PM mean = 7.49
Corr. wet PM = 0.53

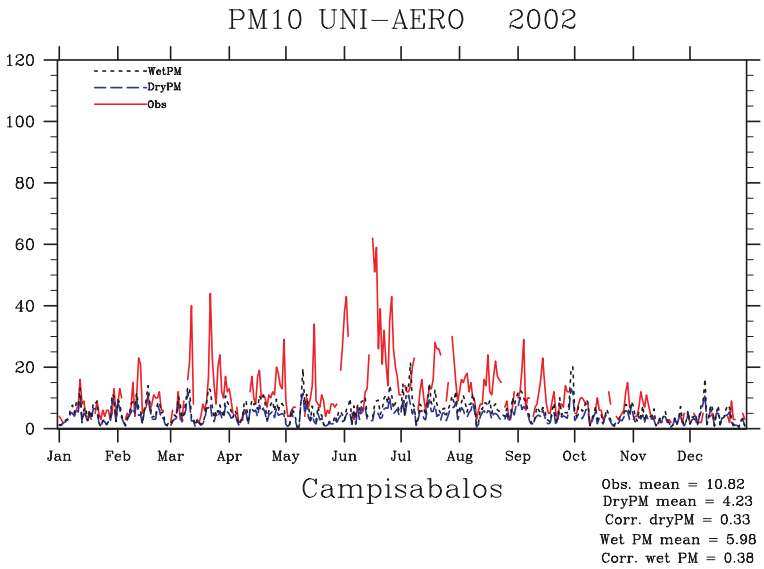
PM10 UNI–AERO 2002
WetPM
DryPM
Obs
120
100
80
60
40
20
0
Jan Feb Mar Apr May Jun Jul Aug Sep Oct Nov Dec
Campisabalos
Obs. mean = 10.82
DryPM mean = 4.23
Corr. dryPM = 0.33
Wet PM mean = 5.98
Corr. wet PM = 0.38

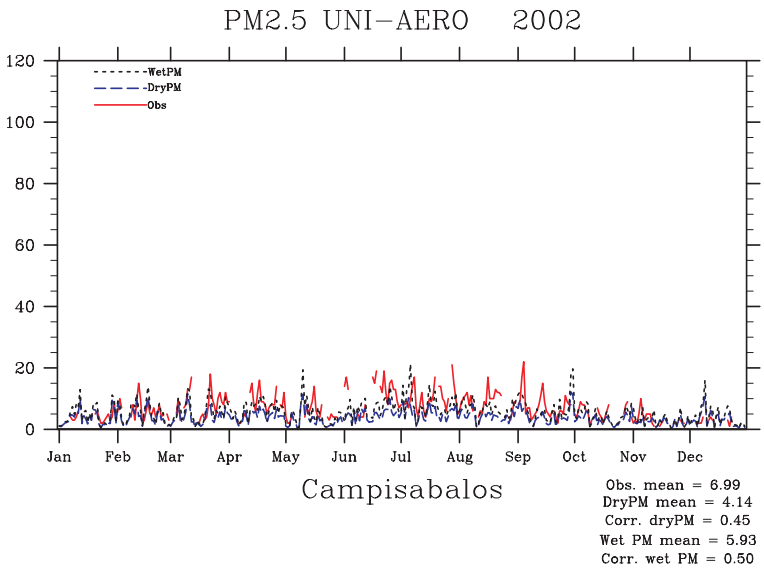
PM2.5 UNI–AERO 2002
WetPM
DryPM
Obs
120
100
80
60
40
20
0
Jan Feb Mar Apr May Jun Jul Aug Sep Oct Nov Dec
Campisabalos
Obs. mean = 6.99
DryPM mean = 4.14
Corr. dryPM = 0.45
Wet PM mean = 5.93
Corr. wet PM = 0.50

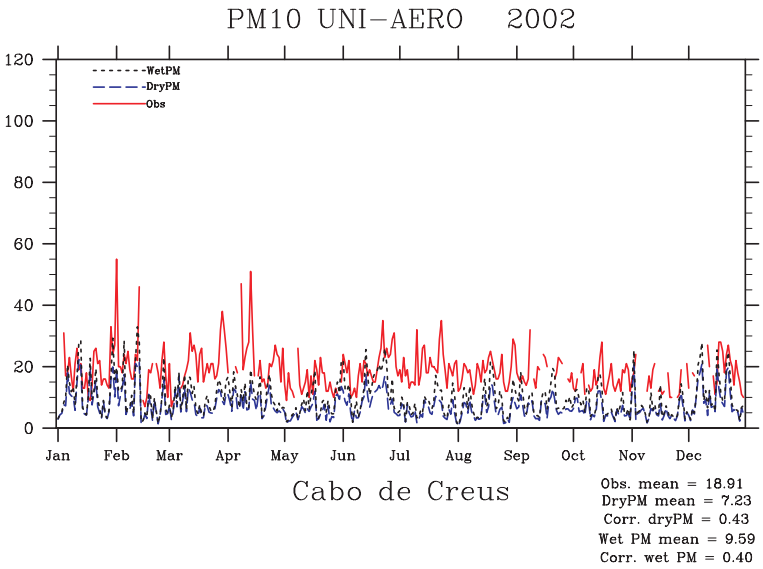
PM10 UNI-AERO 2002
WetPM
DryPM
Obs
120
100
80
60
40
20
0
Jan
Feb
Mar
Apr
May
Jun
Jul
Aug
Sep
Oct
Nov
Dec
Cabo de Creus
Obs. mean = 18.91
DryPM mean = 7.23
Corr. dryPM = 0.43
Wet PM mean = 9.59
Corr. wet PM = 0.40

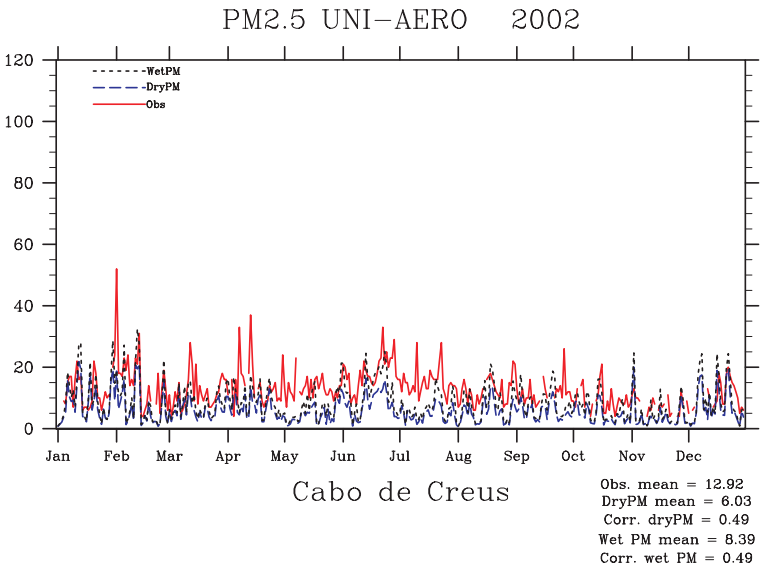
PM2.5 UNI-AERO 2002
WetPM
DryPM
Obs
120
100
80
60
40
20
0
Jan
Feb
Mar
Apr
May
Jun
Jul
Aug
Sep
Oct
Nov
Dec
Cabo de Creus
Obs. mean = 12.92
DryPM mean = 6.03
Corr. dryPM = 0.49
Wet PM mean = 8.39
Corr. wet PM = 0.49

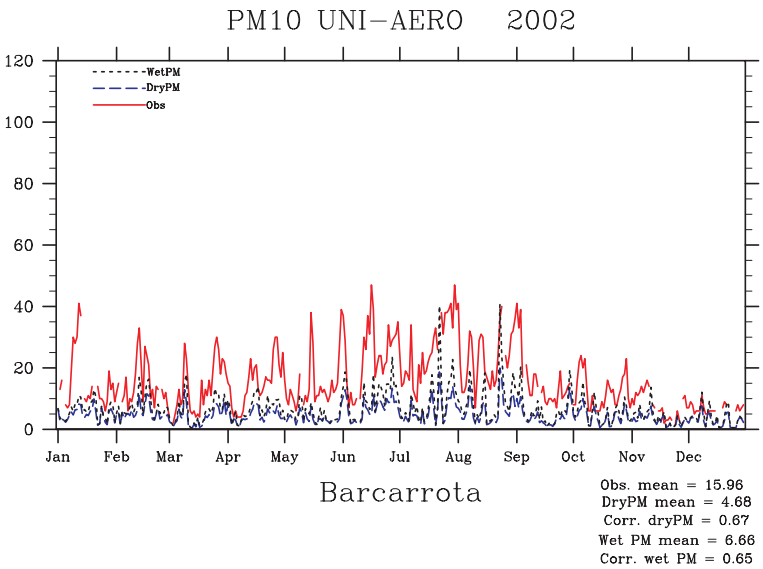
PM10 UNI-AERO 2002
WetPM
DryPM
Obs
120
100
80
60
40
20
0
Jan
Feb
Mar
Apr
May
Jun
Jul
Aug
Sep
Oct
Nov
Dec
Barcarrota
Obs. mean = 15.96
DryPM mean = 4.68
Corr. dryPM = 0.67
Wet PM mean = 6.66
Corr. wet PM = 0.65

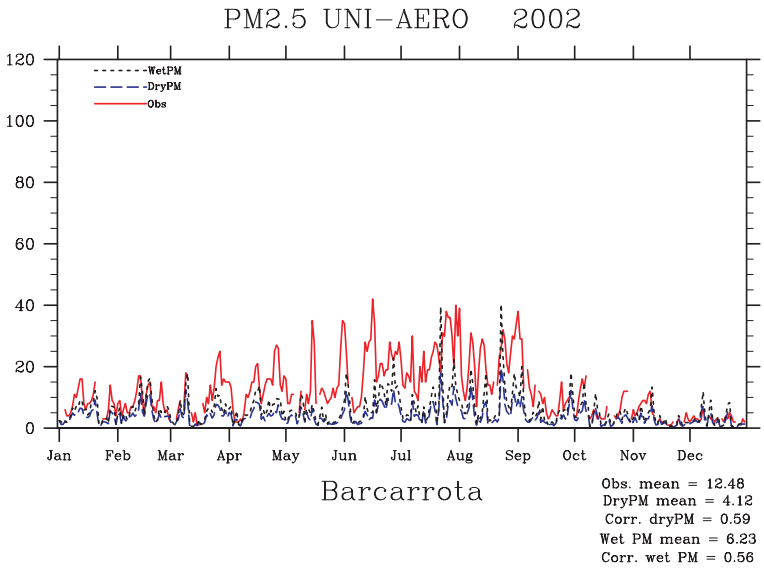
PM2.5 UNI–AERO 2002
WetPM
DryPM
Obs
120
100
80
60
40
20
0
Jan Feb Mar Apr May Jun Jul Aug Sep Oct Nov Dec
Barcarrota
Obs. mean = 12.48
DryPM mean = 4.12
Corr. dryPM = 0.59
Wet PM mean = 6.23
Corr. wet PM = 0.56

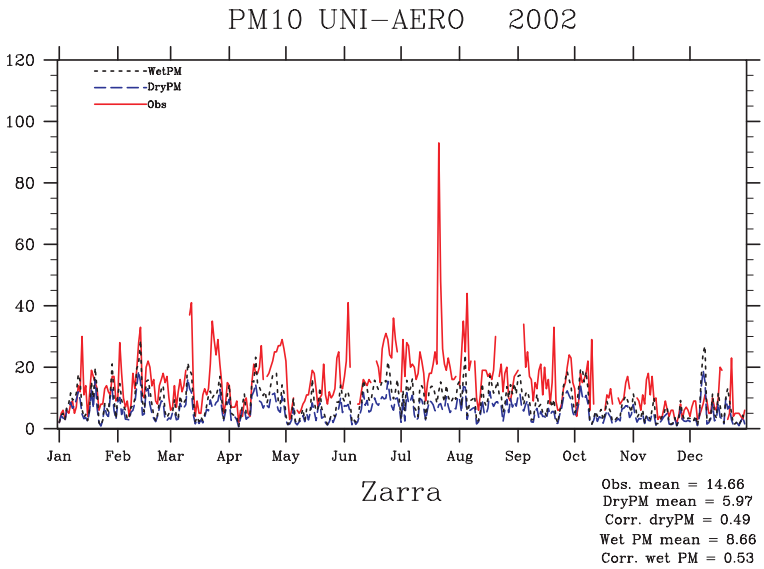
PM10 UNI–AERO 2002
WetPM
DryPM
Obs
120
100
80
60
40
20
0
Jan Feb Mar Apr May Jun Jul Aug Sep Oct Nov Dec
Zarra
Obs. mean = 14.66
DryPM mean = 5.97
Corr. dryPM = 0.49
Wet PM mean = 8.66
Corr. wet PM = 0.53

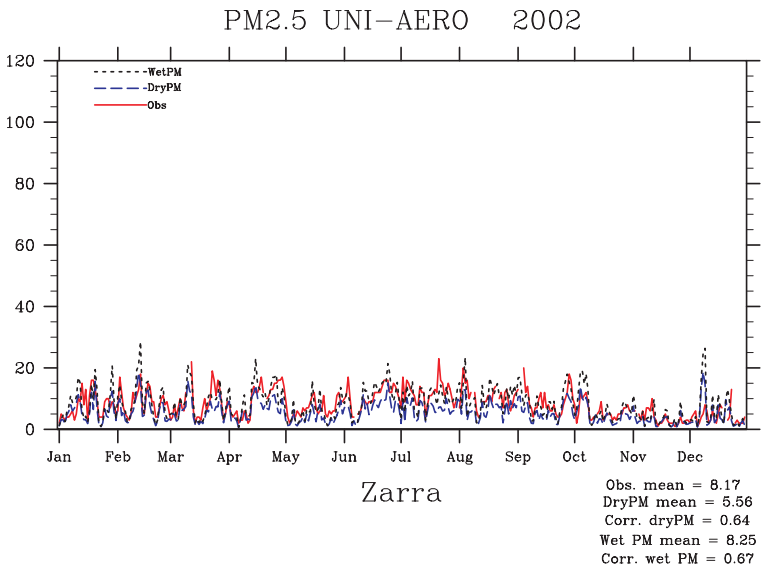
PM2.5 UNI–AERO 2002
WetPM
DryPM
Obs
120
100
80
60
40
20
0
Jan Feb Mar Apr May Jun Jul Aug Sep Oct Nov Dec
Zarra
Obs. mean = 8.17
DryPM mean = 5.56
Corr. dryPM = 0.64
Wet PM mean = 8.25
Corr. wet PM = 0.67

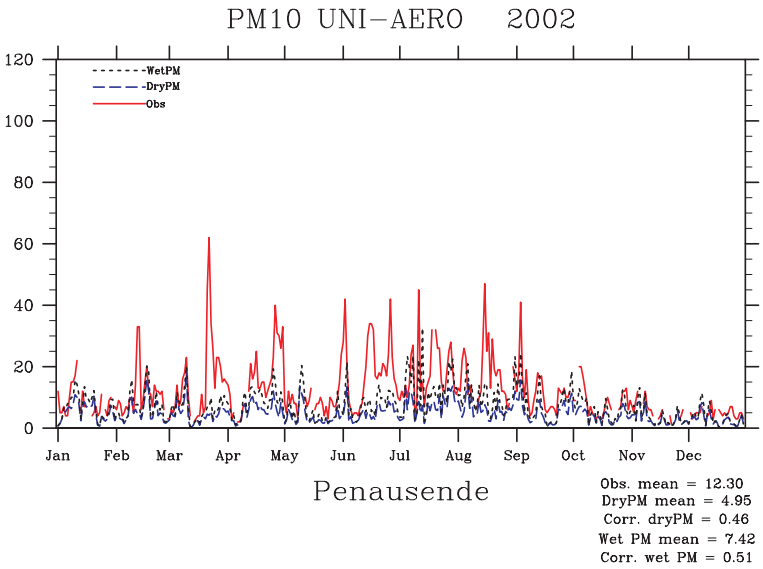
PM10 UNI-AERO 2002
WetPM
DryPM
Obs
120
100
80
60
40
20
0
Jan
Feb
Mar
Apr
May
Jun
Jul
Aug
Sep
Oct
Nov
Dec
Penausende
Obs. mean = 12.30
DryPM mean = 4.95
Corr. dryPM = 0.46
Wet PM mean = 7.42
Corr. wet PM = 0.51

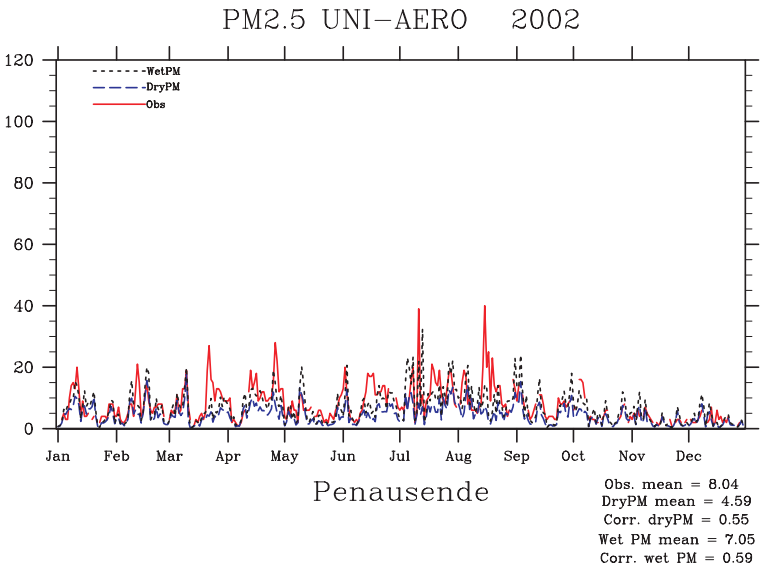
PM2.5 UNI-AERO 2002
WetPM
DryPM
Obs
120
100
80
60
40
20
0
Jan
Feb
Mar
Apr
May
Jun
Jul
Aug
Sep
Oct
Nov
Dec
Penausende
Obs. mean = 8.04
DryPM mean = 4.59
Corr. dryPM = 0.55
Wet PM mean = 7.05
Corr. wet PM = 0.59

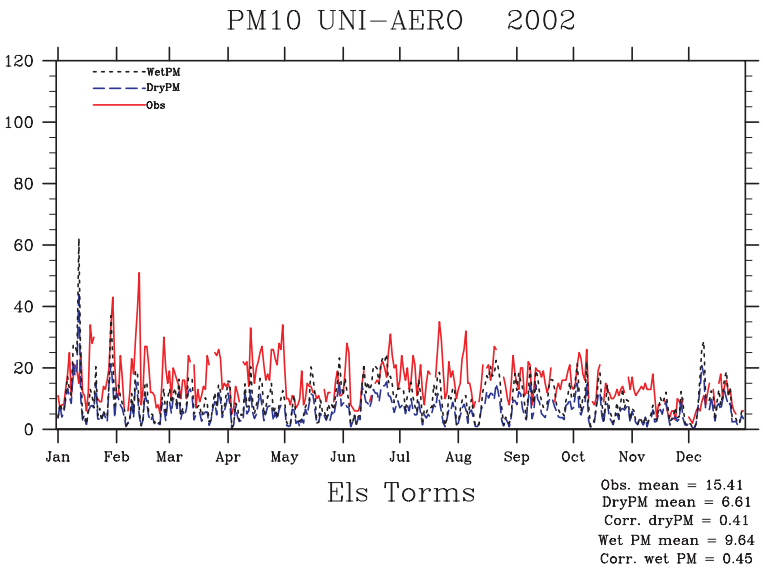
PM10 UNI-AERO 2002
WetPM
DryPM
Obs
120
100
80
60
40
20
0
Jan
Feb
Mar
Apr
May
Jun
Jul
Aug
Sep
Oct
Nov
Dec
Els Torms
Obs. mean = 15.41
DryPM mean = 6.61
Corr. dryPM = 0.41
Wet PM mean = 9.64
Corr. wet PM = 0.45

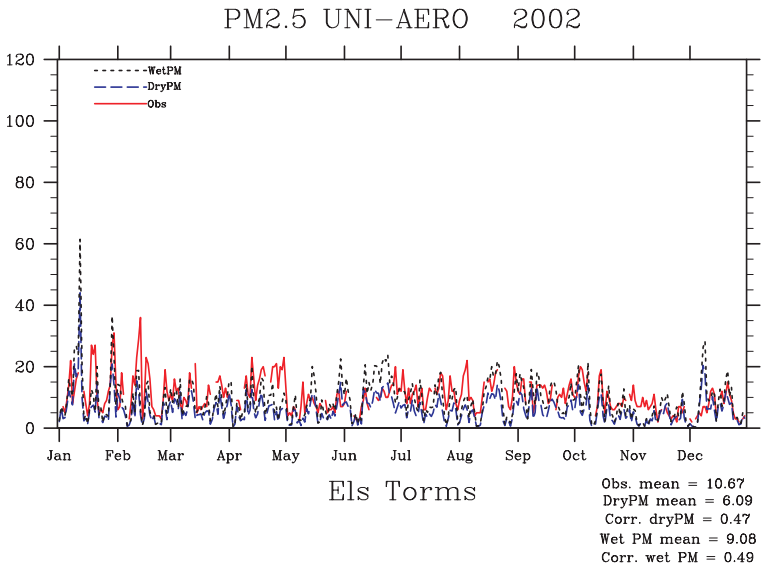
PM2.5 UNI–AERO 2002
WetPM
DryPM
Obs
120
100
80
60
40
20
0
Jan Feb Mar Apr May Jun Jul Aug Sep Oct Nov Dec
Els Torms
Obs. mean = 10.67
DryPM mean = 6.09
Corr. dryPM = 0.47
Wet PM mean = 9.08
Corr. wet PM = 0.49

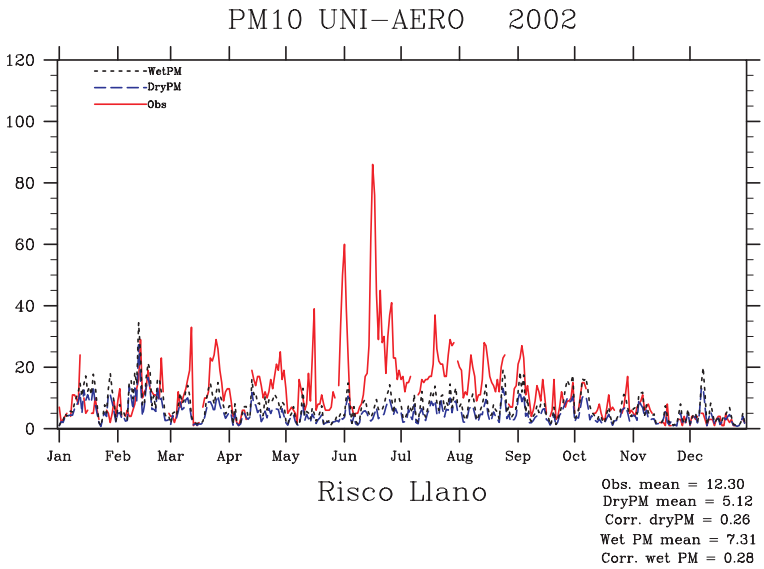
PM10 UNI–AERO 2002
WetPM
DryPM
Obs
120
100
80
60
40
20
0
Jan Feb Mar Apr May Jun Jul Aug Sep Oct Nov Dec
Risco Llano
Obs. mean = 12.30
DryPM mean = 5.12
Corr. dryPM = 0.26
Wet PM mean = 7.31
Corr. wet PM = 0.28

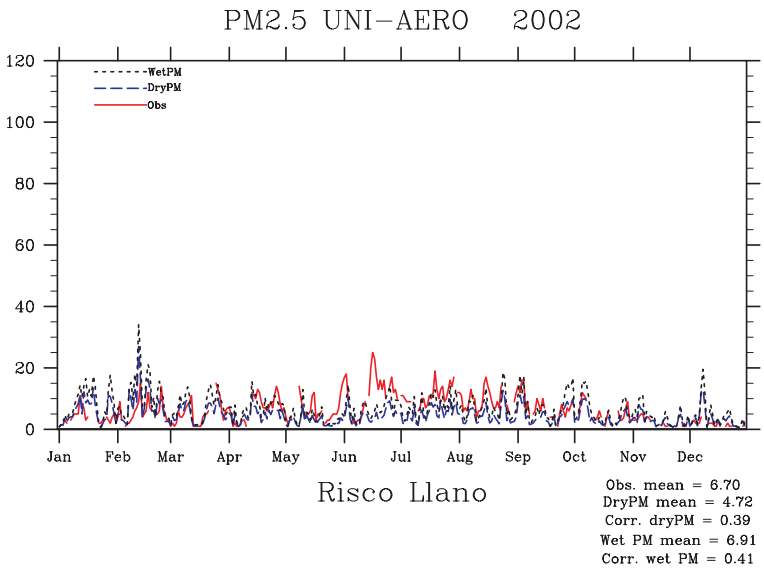
PM2.5 UNI–AERO 2002
WetPM
DryPM
Obs
120
100
80
60
40
20
0
Jan Feb Mar Apr May Jun Jul Aug Sep Oct Nov Dec
Risco Llano
Obs. mean = 6.70
DryPM mean = 4.72
Corr. dryPM = 0.39
Wet PM mean = 6.91
Corr. wet PM = 0.41

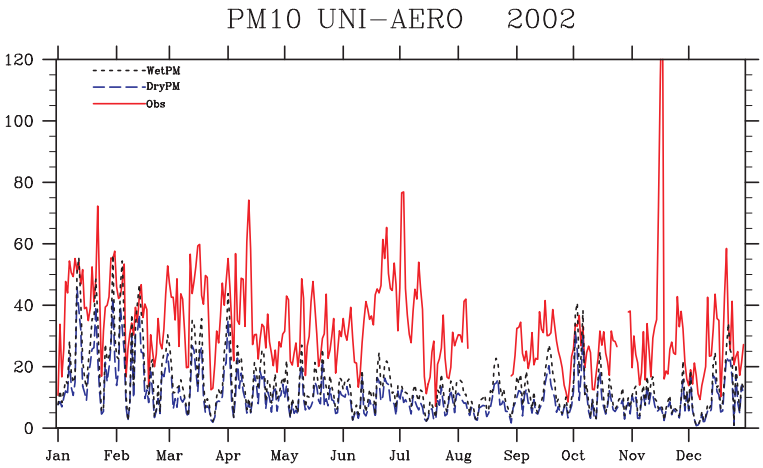

Montelibretti

Obs. mean = 33.27
DryPM mean = 11.11
Corr. dryPM = 0.38
Wet PM mean = 14.69
Corr. wet PM = 0.40

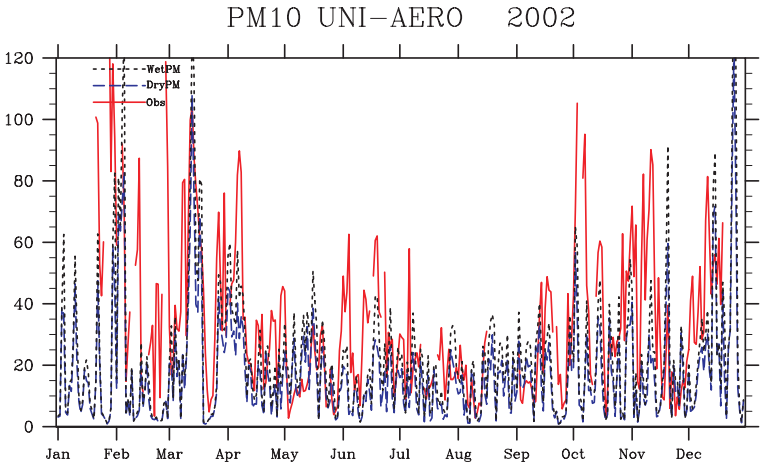

Ispra

Obs. mean = 34.48
DryPM mean = 16.98
Corr. dryPM = 0.47
Wet PM mean = 22.17
Corr. wet PM = 0.47

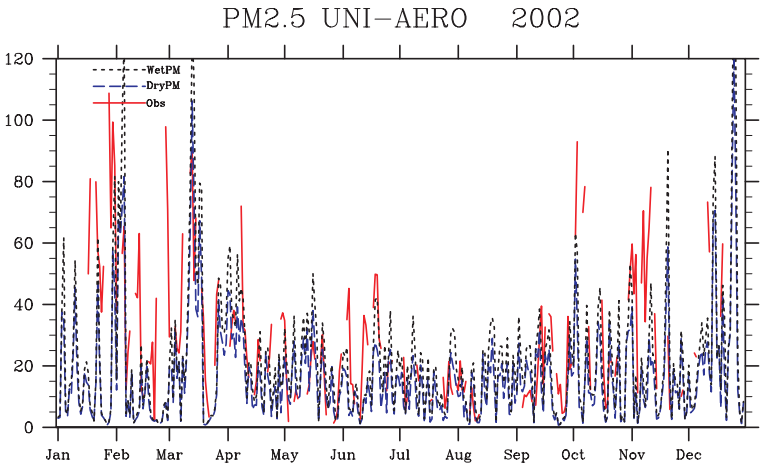

Ispra

Obs. mean = 29.39
DryPM mean = 16.22
Corr. dryPM = 0.44
Wet PM mean = 21.58
Corr. wet PM = 0.43

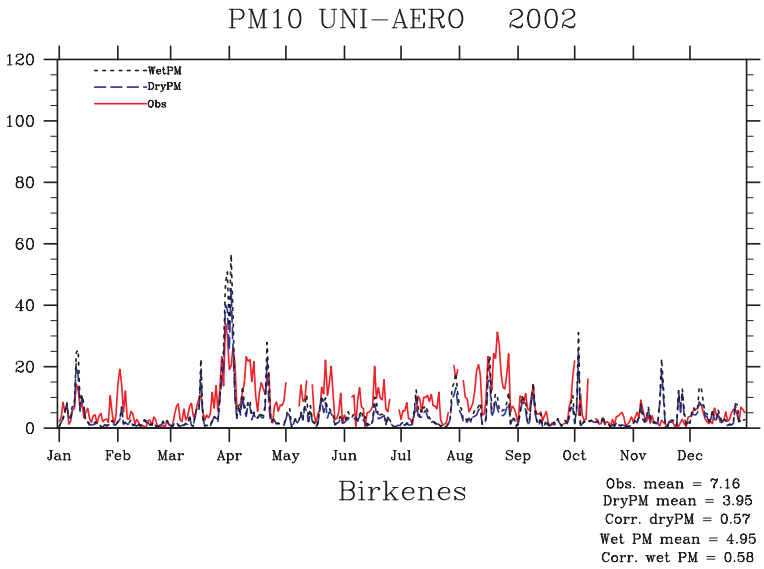
PM10 UNI–AERO 2002
WetPM
DryPM
Obs
120
100
80
60
40
20
0
Jan
Feb
Mar
Apr
May
Jun
Jul
Aug
Sep
Oct
Nov
Dec
Birkenes
Obs. mean = 7.16
DryPM mean = 3.95
Corr. dryPM = 0.57
Wet PM mean = 4.95
Corr. wet PM = 0.58

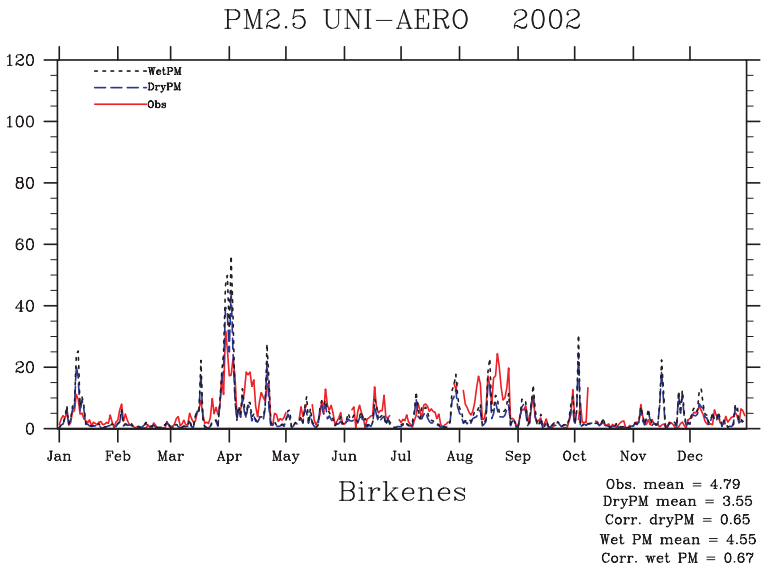
PM2.5 UNI–AERO 2002
WetPM
DryPM
Obs
120
100
80
60
40
20
0
Jan
Feb
Mar
Apr
May
Jun
Jul
Aug
Sep
Oct
Nov
Dec
Birkenes
Obs. mean = 4.79
DryPM mean = 3.55
Corr. dryPM = 0.65
Wet PM mean = 4.55
Corr. wet PM = 0.67

emep

Chemical Co-ordinating Centre of EMEP
Norwegian Institute for Air Research
P.O. Box 100, N-2027 Kjeller, Norway

Produksjon: www.kursiv.no

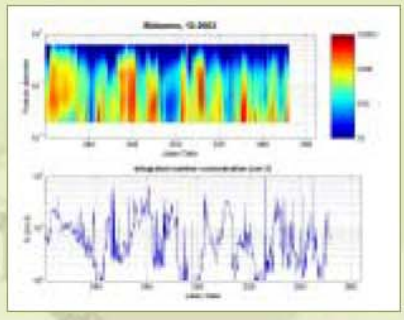

ccc
Norwegian Institute
for Air Research (NILU)
P.O. Box 100
N-2027 Kjeller
Norway
Phone: +47 63 89 81 58
Fax: +47 63 89 80 50
E-mail: kjetil.torseth@nilu.no
Internet: www.nilu.no

ciam
International Institute for
Applied Systems Analysis
(IIASA)
A-2361 Laxenburg
Austria
Phone: +43 2236 80 70
Fax: +43 2236 71 31
E-mail: amann@iiasa.ac.at
Internet: www.iiasa.ac.at

msc-e
Meteorological Synthesizing
Centre - East
ul. Arhitektor Vlasov, 51,
Moscow, 117393
Russia
Phone +7 095 128 90 98
Fax +7 095 125 24 09
E-mail: msce@msceast.org
Internet: www.msceast.org

msc-w
Norwegian Meteorological
Institute (met.no)
P.O. Box 43 Blindern
N-0313 OSLO
Norway
Phone: +47 22 96 30 00
Fax: +47 22 96 30 50
E-mail: emep.mscw@met.no
Internet: www.emep.int